European Commission

JRC TECHNICAL REPORTS

Evaluation of low-cost sensors for air pollution monitoring

Effect of gaseous interfering compounds and meteorological conditions

Spinelle, L., Gerboles, M., Kotsev, A. and Signorini, M.

2017

Joint Research Centre

EUR 28601 EN

Contact information
Name: Michel Gerboles
Address: Via E. Fermi, TP 120, I -21027 Ispra (VA)
Email: michel.gerboles@ec.europa.eu
Tel.: +39 033-278-5652

JRC Science Hub
https://ec.europa.eu/jrc

JRC106095

EUR 28601 EN

PDF ISBN 978-92-79-68830-0 ISSN 1831-9424 doi:10.2760/548327

Luxembourg: Publications Office of the European Union, 2017

How to cite this report: Spinelle, L., Gerboles, M., Kotsev, A. and Signorini, M., *Evaluation of low-cost sensors for air pollution monitoring - Effect of gaseous interfering compounds and meteorological conditions*, EUR 28601 EN, doi:10.2760/548327.

Contents

Authors

Laurent Spinelle, Air and Climate Unit, Joint Research Centre, European Commission, 21027 Ispra, Italy, Telephone: +39 0332 78 9572, laurent.spinelle@ec.europa.eu

Michel Gerboles, Air and Climate Unit, Joint Research Centre, European Commission, 21027 Ispra, Italy, Telephone: +39 0332 78 5652, michel.gerboles@ec.europa.eu

Alexander Kotsev, Digital Economy Unit, Joint Research Centre, European Commission 21027 Ispra, Italy, Telephone: +39 0332 78 9069, alexander.kotsev@ec.europa.eu

and Marco Signorini, Liberaintentio S.r.l, 21046 Malnate, Italy, marco.signorini@liberaintentio.com

Acknowledgements

The authors wish to thank Dr. Annette Borowiak and Dr. Julian Wilson of the Air and Climate Unit, Directorate for Energy, Transport and Climate of the Joint Research Centre for the English language revision of the report.

Abstract

In this report the performances of low-cost sensors for air pollution monitoring are evaluated in order to give guidance to users on which parameters to take into account when performing field calibration of these sensors prior to using them to monitor air pollution.

In particular, the effects of gaseous interfering compounds and meteorological conditions on four low cost sensors selected to be mounted on the AirSensEUR platform are characterised. The selected sensors are of the electrochemical type, as they are less power consuming and they have been shown, in previous studies, to give fastest response times and to suffer less from gaseous interference than metal-oxide sensors.

Ten set of four sensors for ozone (Membrapor O3/M-5), nitrogen dioxide (Alphasense NO2-B43F), carbon monoxide (Membrapor CO/MF-200) and nitrogen monoxide (Alphasense NO-B4) were evaluated under controlled conditions in a laboratory exposure chamber. The tests allow the evaluation of the interference from gaseous compounds together with the effect of relative humidity, temperature and pressure variations.

In general, each sensor was found to be highly linear when measuring its target gaseous species. Concerning gaseous interference, only the ozone sensors showed a high interference (> 75%) to nitrogen dioxide. The ozone filter of the NO2-B43F appears to be effective. The sensitivity of the CO and NO sensors was sufficient to be able to detect concentration levels expected at ambient gaseous concentrations. However, the interference of NO to the CO/MF-200 was found relevant at high NO and low CO values. The cross-sensitivity (CO and NO on O_3 and NO_2 sensors and vice-versa) was found low or not significant for each type of sensor.

The meteorological evaluation showed that the four types of sensor behave similarly concerning the temperature interference. In fact both sensors showed a quadratic response with the increase of the temperature. Relative humidity was only found relevant for the two Alphasense sensors (NO2-B43F and NO-B4) with linear sensitivity associated with a clear hysteresis effect. Ambient pressure, however, was found to be relevant only for the two Membrapor sensors (O3/M-5 and CO/MF-200).

Finally, the good reproducibility between sensors for the majority of effects including sensitivity to gas concentration and to meteorological variables with relative standard deviations of less than 10 % suggests that satisfactory calibration of sensors could be achieved without the need of a full characterisation of each sensor. By using calibration coefficients equal to the averages of the effects given in this report, a reasonable calibration function could be established. This result is promising, supporting future increased use of sensors for low cost for air pollution monitoring both by expert institutes and citizen science projects.

1 Introduction

Ten sets of four sensors were characterised in the Joint Research Centre exposure chamber under controlled conditions. Each set consisted of Alphasense sensors, NO2-B43F and NO-B4, used in 3 electrode mode, without correction of the channel OP2, and Membrapor sensors, O3/M-5 and CO/MF-200. The sensors were purchased from AlphaSense and Membrapor. The part number of each sensor is given in Table 1. The sensors were configured using the parameters given in Table 2. After the JRC laboratory testing the sensor systems were delivered to the European institutes, named in the left column of table 1.

Table 1: Part number of tested sensors

	NO2-B43F	CO/MF-200	O3/M-5	NO-B4
NILU	202830057	16173144	16184060	160830131
KNMI	202830058	16173149	16184063	160830130
52NORTH	202830044	16173148	16184062	160830129
INERIS	202830056	16173141	16184061	160830119
VMM	202830054	16173143	16159571	160830127
VITO	202830046	16173142	16159174	160830122
RICARDO	202830047	16173151	16159570	160830123
GEONOVUM	202830052	16173146	16159569	160830126
AirParif	202830045	16173150	16159572	160830121
RIVM	202830055	16173145	16159573	160830128

The sensors were plugged into 10 AirSensEUR shields that provide digital values (DigitalReading) between 0 and 65535 (2^{16} corresponding to the 16-bit analogue to digital conversion used in the shield). The digital values were converted to voltages (V) according to the configuration parameters (see Table 2) using Equation 1. RefAD was set so that 2RefAD exceeds the range of expected sensor voltages product of the Sensitivity of the sensor, Expected Range of pollutants, and Amplifier (up to 350 kOhm). Equation 2 gives the range of expected voltages for a CO/MF-200 measuring between 0 and 10 ppm of CO.

$$V = (\text{'Ref-'} - RefAD) + DigitalReading\ 2RefAD/(2^{16}) \quad \text{Equation 1}$$

$$Range = Sensitivity\ CO\ Gain = 500_{nA/ppm}\ 10_{ppm}\ 350_{k\Omega} = 1.75\ V \quad \text{Equation 2}$$

Figure 1 below shows the typical behaviour of the sensors and illustrates how to set the sensors' configuration.

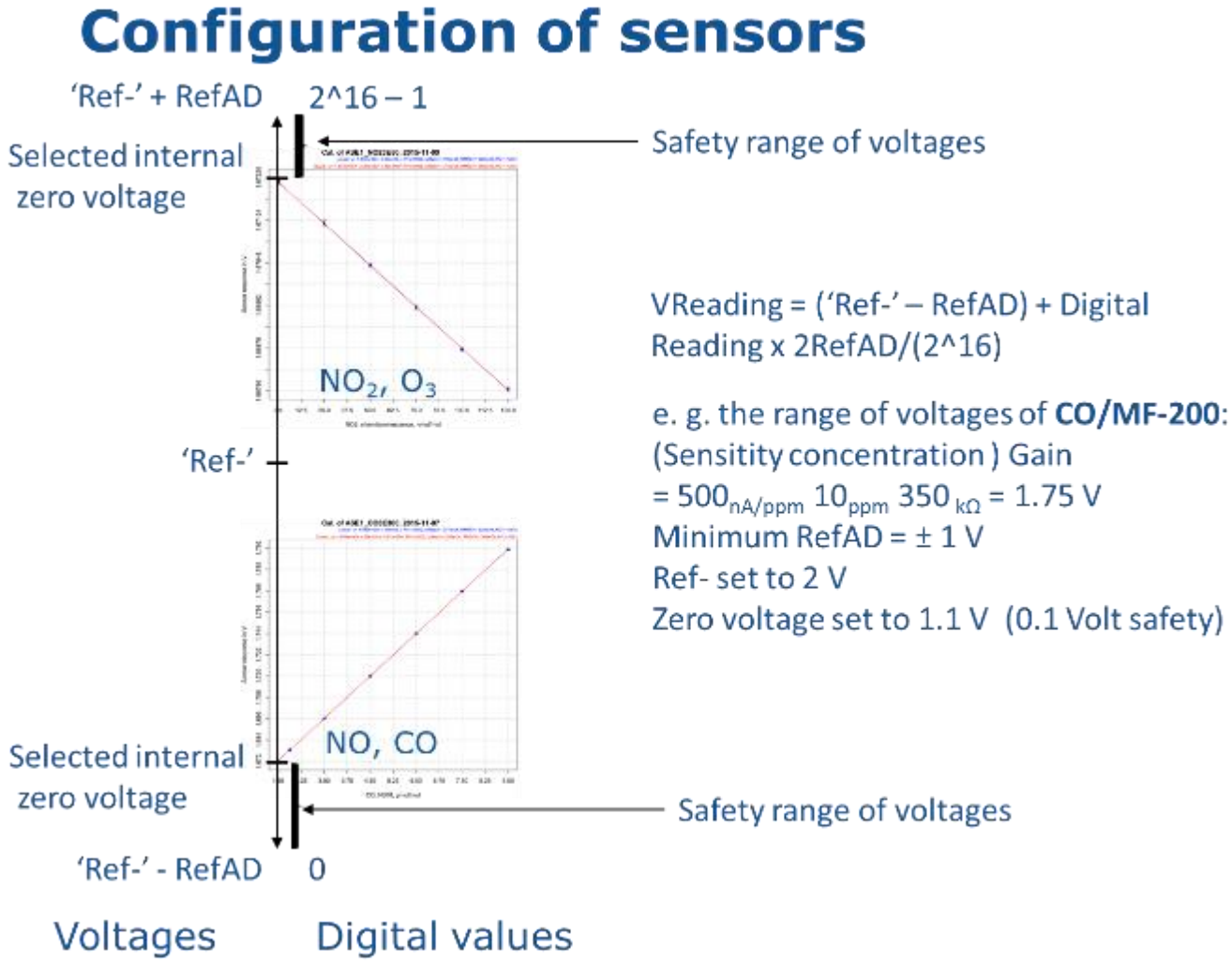

Figure 1: Configuration of sensors

In all figures and tables, the variable names corresponding to the tested sensors are coded as: number_Institute_Sensor

- 1_NILU_NO2-B43F, 1_NILU_CO/MF-200, 1_NILU_O3/M-5, 1_NILU_NO-B4_P1
- 2_KNMI_NO2-B43F, 2_KNMI_CO/MF-200, 2_KNMI_O3/M-5, 2_KNMI_NO-B4_P1
- 3_52North_NO2-B43F, 3_52North_CO/MF-200, 3_52North_O3/M-5, 3_52North_NO-B4_P1
- 4_INERIS_NO2-B43F, 4_INERIS_CO/MF-200, 4_INERIS_O3/M-5, 4_INERIS_NO-B4_P1
- 5_VMM_NO2-B43F, 5_VMM_CO/MF-200, 5_VMM_O3/M-5, 5_VMM_NO-B4_P1
- 6_VITO_NO2-B43F, 6_VITO_CO/MF-200, 6_VITO_O3/M-5, 6_VITO_NO-B4_P1
- 7_AEA_NO2-B43F, 7_AEA_CO/MF-200, 7_AEA_O3/M-5, 7_AEA_NO-B4_P1)
- 8_GeonoVum_NO2-B43F,8_GeonoVum_CO/MF-200,8_GeonoVum_O3/M-5,8_GeonoVum_NO-B4_P1
- 9_AIRPARIF_NO2-B43F,9_AIRPARIF_CO/MF-200,9_AIRPARIF_O3/M-5,9_AIRPARIF_NO-B4_P1
- 10_RIVM_NO2-B43F, 10_RIVM_CO/MF-200, 10_RIVM_O3/M-5, 10_RIVM_NO-B4_P1

Table 2: Configuration parameters chosen for each sensors of the AirSensEUR shield

	Sensor 1	Sensor 2	Sensor 3	Sensor 4	Temperature	Humidity	Pressure
	NO2-B43F channel OP1	CO/MF-200	O3/M-5	NO-B4 channel OP1			
Gain[1]	350 kOhm	350 kOhm	350 kOhm	350 kOhm	N/A	N/A	N/A
RLoad	50 Ohm	10 Ohm	33 Ohm	50 Ohm	N/A	N/A	N/A
Reference Voltage source	External	External	External	External	N/A	N/A	N/A
Internal Zero	50 %	67 %	50 %	50 %	N/A	N/A	N/A
Bias Polarity	Positive or negative	Positive or negative	Positive or negative	Positive	N/A	N/A	N/A
Bias Percentage	0 %	0%	0 %	12 %	N/A	N/A	N/A
Shorting FET	Disabled	Disabled	Disabled	Disabled	N/A	N/A	N/A
Working Mode	3-lead amp cell	3-lead amp cell	3-lead amp cell	3-lead amp cell	N/A	N/A	N/A
Ref -	1.7 V	2 V	1.7 V	1.7 V	N/A	N/A	N/A
Ref AD	±0.5 V	±1 V	±0.5 V	±1 V	N/A	N/A	N/A
Ref AFE	4.3 V	1.642 V	4.3 V	1.663 V	N/A	N/A	N/A
Gain	x 2	x 1	x 2	x 1	N/A	N/A	N/A
Sample Rate Prescaler	11 ticks	11 ticks	11 ticks	11 ticks	11 ticks	11 ticks	25 ticks
IIR1 Coefficient	1/4	1/4	1/4	1/4	1/4	1/4	1/4
IIR2 Coefficient	1/8	1/8	1/8	1/8	1/8	1/8	1/8
Decimation	Every 5 samples	Every 5 samples	Every 5 samples	Every 5 samples	Every 5 samples	Every 5 samples	Every 5 samples
Moving Average Window Size	30 samples	30 samples	30 samples	30 samples	30 samples	30 samples	30 samples

2 Set-up of Experiments

Experiments were designed to calibrate the sensors for use in outdoor ambient air. All calibration functions were established by plotting sensor response versus reference values of gaseous compounds, temperature, pressure or relative humidity. Each step lasted for 120 minutes once the reference values of gaseous concentration levels, temperature and humidity were reached and stable. The mean values of the last 60 minutes are plotted, except for the relative humidity test, whose steps lasted for 30 minutes.

The tests were carried out in the exposure chamber of the Joint Research Centre. Details of the experimental setup are given in Annex 1. The sensors were placed in the chamber following the scheme of Figure 2.

[1] Amplifier Gain: A_{CL} = 1+Rf/Rg = 1 + 350 000/100 = 3501

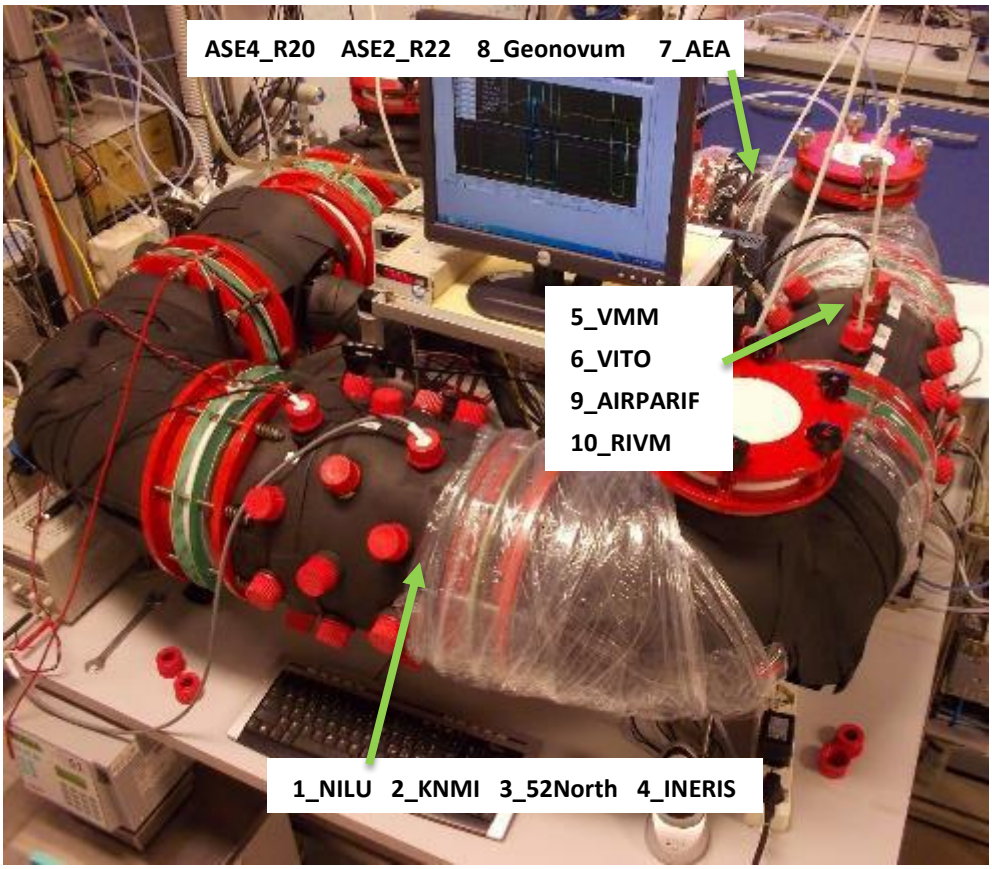

Figure 2: Position of AirSensEUR shields in the exposure chamber

For each sensor, a linear calibration was plotted to transform sensor readings into air pollutant levels. The experiments were carried out without bias from any gaseous interfering compound and at the mean temperature and relative humidity (22°C and 60 % relative humidity respectively). The full scale of the gas compounds were set to 120 ppb for O_3, 150 ppb for NO_2 and NO and 9 ppm for CO. Temperature and relative humidity, which affect the sensor responses, were kept under control (± 1°C and ± 0.5% respectively) during tests, while it was not possible to control atmospheric pressure. Generally one compound was tested at a time, thus if for example O_3 was tested, NO_2, NO and CO were maintained either at zero or at a constant levels.

3 Effects of O_3 and NO on sensors (2016-05-18)

In this experiment, we evaluated the effect of NO and O_3 on the four sensor models. This experiment gives the initial calibration of O3/M-5 and NO-B4 sensors, the O_3 cross-sensitivity on the NO-B4 sensor, the NO cross-sensitivity on the O3/M-5 sensor and the O_3 and NO cross sensitivities on the NO2_B43F and CO/MF-200 sensors.

Table 3 below gives the reference values of all monitored parameters during the stable phase of the experiment. It includes one ramp of O_3 concentrations between 0 and 120 ppb followed by one ramp of NO concentrations between 0 and 150 ppb while the other parameters remain pretty constant during all experiments with a slight NO_2 increase during the NO experiment (about 2 %). Humidity was completely constant, temperature changed about 0.2ºC, while the ambient pressure, which is not regulated, changed about 8 hPa.

Figure 3 shows the time series plot for all reference parameters. One can notice that the experiment was stopped due to a malfunction of the whole system on the 2016-05-20 between 04:00 and 06:00. Some disturbances appear on the gaseous lines. However, they did not affect the data treatment as the whole system waits until complete stability of all parameters for 90 minutes before starting another step of the experiment. The slight increase in SO_2 during the NO calibration corresponds to a well-known NO interference on

SO_2 fluorescence analysers. No SO_2 was injected in the chamber during this test. Conversely, the slight increase in NO_2 (about 2 %) is likely to be caused by in-situ oxidation of NO into NO_2. This NO_2 increase could not be avoided.

Table 3: Reference values of all steps of experiments started on 2016-05-18.

Begin	End	O3, ppb	NO2, ppb	NO, ppb	CO, ppm	SO2, ppb	Temp., °C	RH, %	Pressure, hPa	Wind_Speed, m/s
2016-05-18 20:54	2016-05-18 21:53	0.9	0.1	0.2	0.341	-0.1	22.0	60.0	995	3.8
2016-05-19 00:06	2016-05-19 01:05	30.2	0.1	0.1	0.338	-0.1	21.9	60.0	994	3.8
2016-05-19 10:28	2016-05-19 11:27	60.0	0.0	0.1	0.356	-0.1	21.8	60.0	991	3.8
2016-05-19 12:06	2016-05-19 13:05	90.0	0.1	0.1	0.343	-0.1	21.8	60.0	990	3.8
2016-05-19 16:56	2016-05-19 17:55	120.0	0.1	0.1	0.357	-0.1	21.8	60.0	990	3.8
2016-05-19 21:01	2016-05-19 22:00	1.5	0.3	1.0	0.340	-0.1	21.9	60.0	993	3.8
2016-05-19 22:55	2016-05-19 23:54	0.5	2.5	25.0	0.344	-0.0	21.9	60.0	995	3.8
2016-05-20 07:15	2016-05-20 08:14	0.4	2.8	50.0	0.335	0.1	21.8	60.0	997	2.5
2016-05-20 09:04	2016-05-20 10:03	0.3	3.1	75.0	0.344	0.2	21.8	60.0	998	2.5
2016-05-20 10:51	2016-05-20 11:50	0.3	3.2	100.0	0.342	0.4	21.8	60.0	998	2.5
2016-05-20 12:41	2016-05-20 13:40	0.3	3.8	150.0	0.346	0.6	21.9	60.0	998	2.5

Table 4 shows the mean effect of the two compounds NO and O_3 (sensor readings in volt versus reference values in ppb or ppm) on the 10 sensors of the four model types. It gives the sensor model types, the reference gaseous compounds, the intercepts in V (Interc. ± s) and slopes in V/ppb or V/ppm (slope ± s) of the linear lines, the probability that the intercepts and slopes are different from 0 (any value > 0.05 indicates that these variables are significantly different from 0), the coefficients of determination (R^2), the root mean square errors (RMSE) in V calculated using the residual degrees of freedom and the lack of fit in ppb or ppm of the linear model calculated for the x axis u(lof). The standard deviations of the intercepts and slopes are computed using the results of the 10 sensors. Since a few outliers are evidenced later, more accurate values of these are given in the following tables.

Table 4: Effect of NO and O3 on sensor readings, experimental results of 2016-05-18*. P(Interc.) and P(Slope) give the probability that the intercept and the slope are equal to zero.*

Sensors	Compounds	Interc.	P(Interc.)	Slope	P(Slope)	R^2	RMSE	u(lof)
COMF200	NO	1.12793 ± 0.00427	0.000	-0.00002871 ± 0.00000462	0.006	0.8993	0.00022	13.5
COMF200	O3	1.12207 ± 0.00495	0.000	0.00004243 ± 0.00001567	0.615	0.1013	0.00349	137.4
NO2B43F	NO	2.14701 ± 0.00311	0.000	0.00000211 ± 0.00001437	0.048	0.6679	0.00010	9999.0
NO2B43F	O3	2.14410 ± 0.01287	0.000	0.00001563 ± 0.00007134	0.027	0.8849	0.00029	9999.0
NOB4_P1	NO	0.84113 ± 0.00106	0.000	0.00013984 ± 0.00000369	0.000	0.9981	0.00013	9999.0
NOB4_P1	O3	0.84541 ± 0.00542	0.000	-0.00003803 ± 0.00003357	0.114	0.6965	0.00048	10002.2
O3/M-5	NO	2.14759 ± 0.00345	0.000	-0.00000408 ± 0.00000523	0.021	0.8020	0.00007	9999.0
O3/M-5	O3	2.14895 ± 0.00336	0.000	-0.00036698 ± 0.00001760	0.000	0.9995	0.00013	9999.0

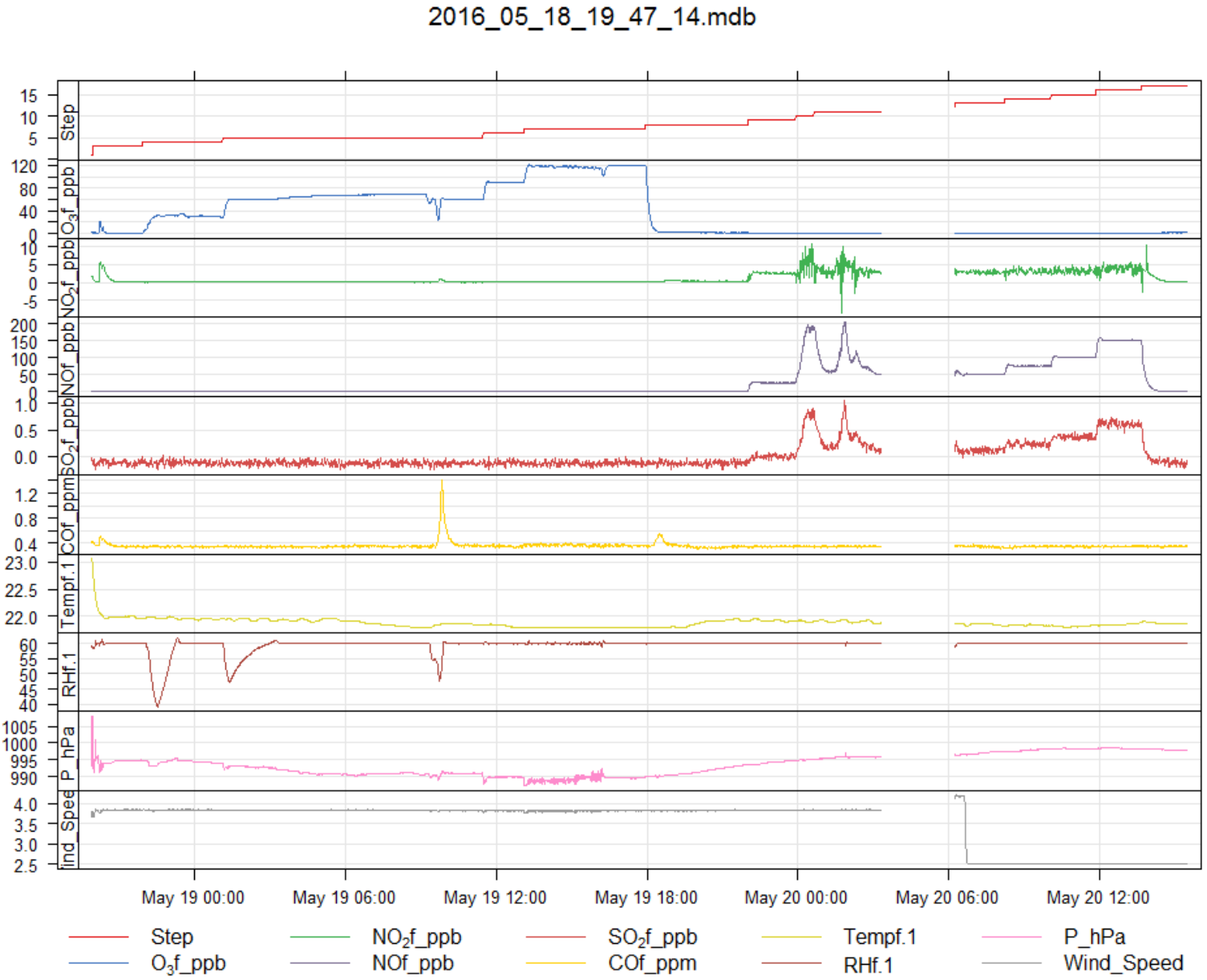

Figure 3: Time series plot of the reference parameters for the experiment started on 2016-05-18

The O3/M-5 and NO-B4 sensors show a linear relationship for O_3 and NO, respectively, with coefficient of determination (R^2) over 0.998. The slopes and intercept of the linear lines are always significantly different from zero. The intercept values are nearly equal to the zero values set in the configuration (see Table 2). One can notice 2 cross-sensitivities:

- NO on CO/MF-200 sensors with R^2 = 0.8974 and a slope of -0.00002771 V/ppm whose probability not to be zero is very low (0.2%). The extent of this interference has to be compared with the slope of the calibration of the CO/MF-200 in the next paragraph;
- O_3 on NO2-B43F sensors with R^2 = 0.8346 and a slope of -0.00000941 V/ppm significantly different from zero. The extent of this interference has to be compared with the slope of the calibration of the NO2-B43F in the next paragraph.

3.1 Scatter plots of effects of O_3 and NO

3.1.1 NO2-B43F sensor

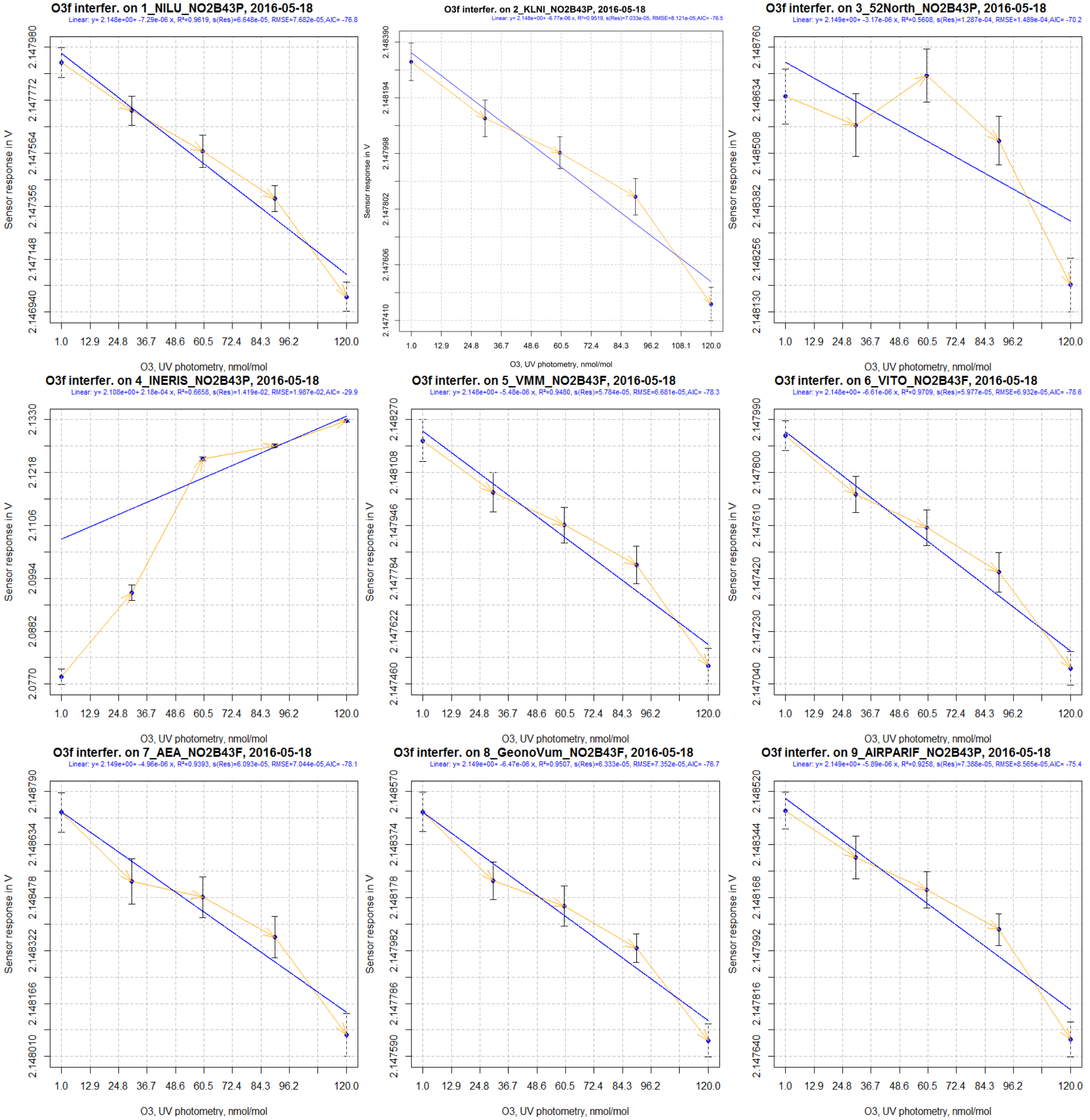

Figure 4: O_3 cross-sensitivity on NO2-B43F

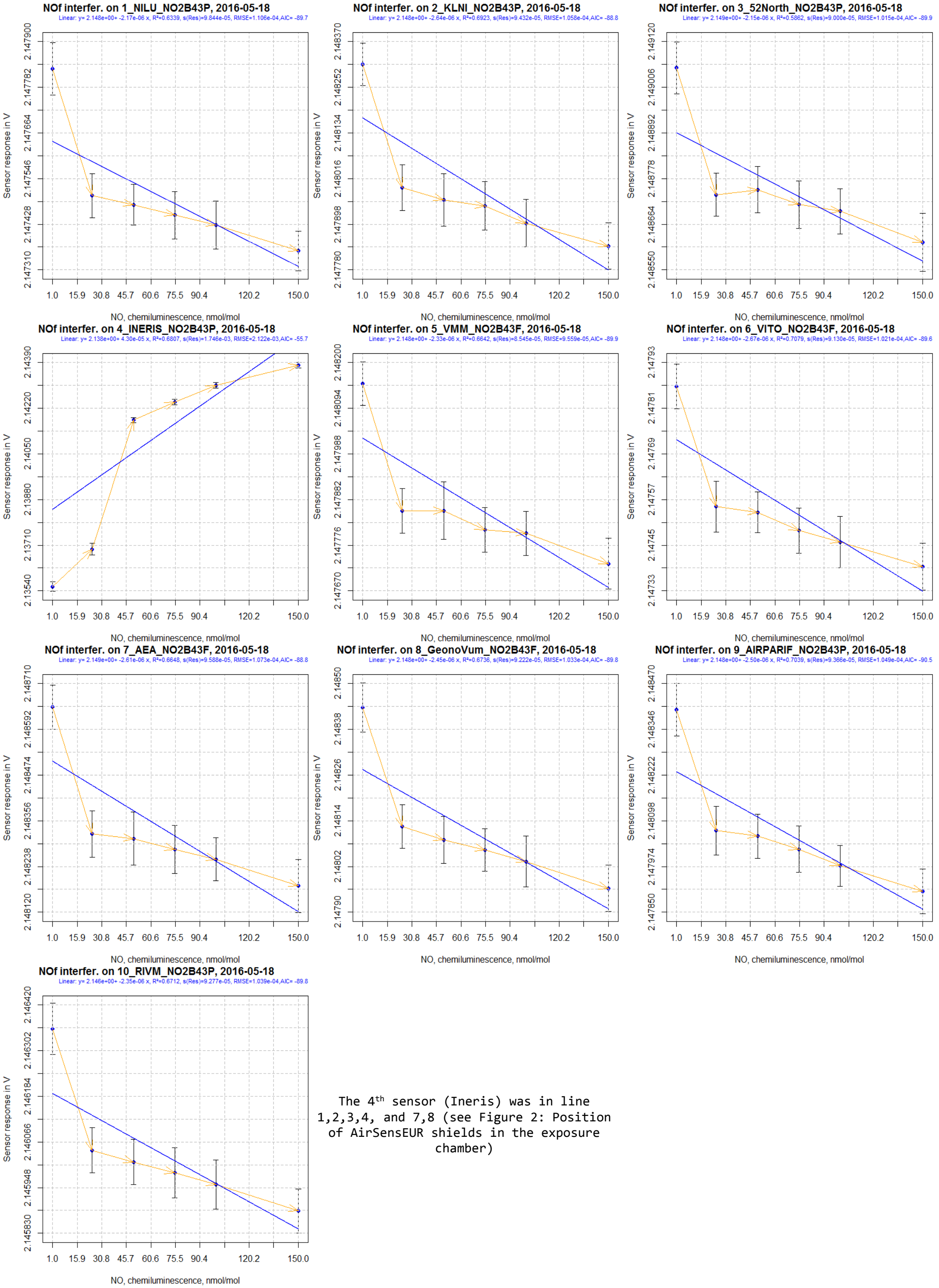

The 4th sensor (Ineris) was in line 1,2,3,4, and 7,8 (see Figure 2: Position of AirSensEUR shields in the exposure chamber)

Figure 5: NO cross-sensitivity on NO2-B43F

3.1.2 CO/MF-200 sensor

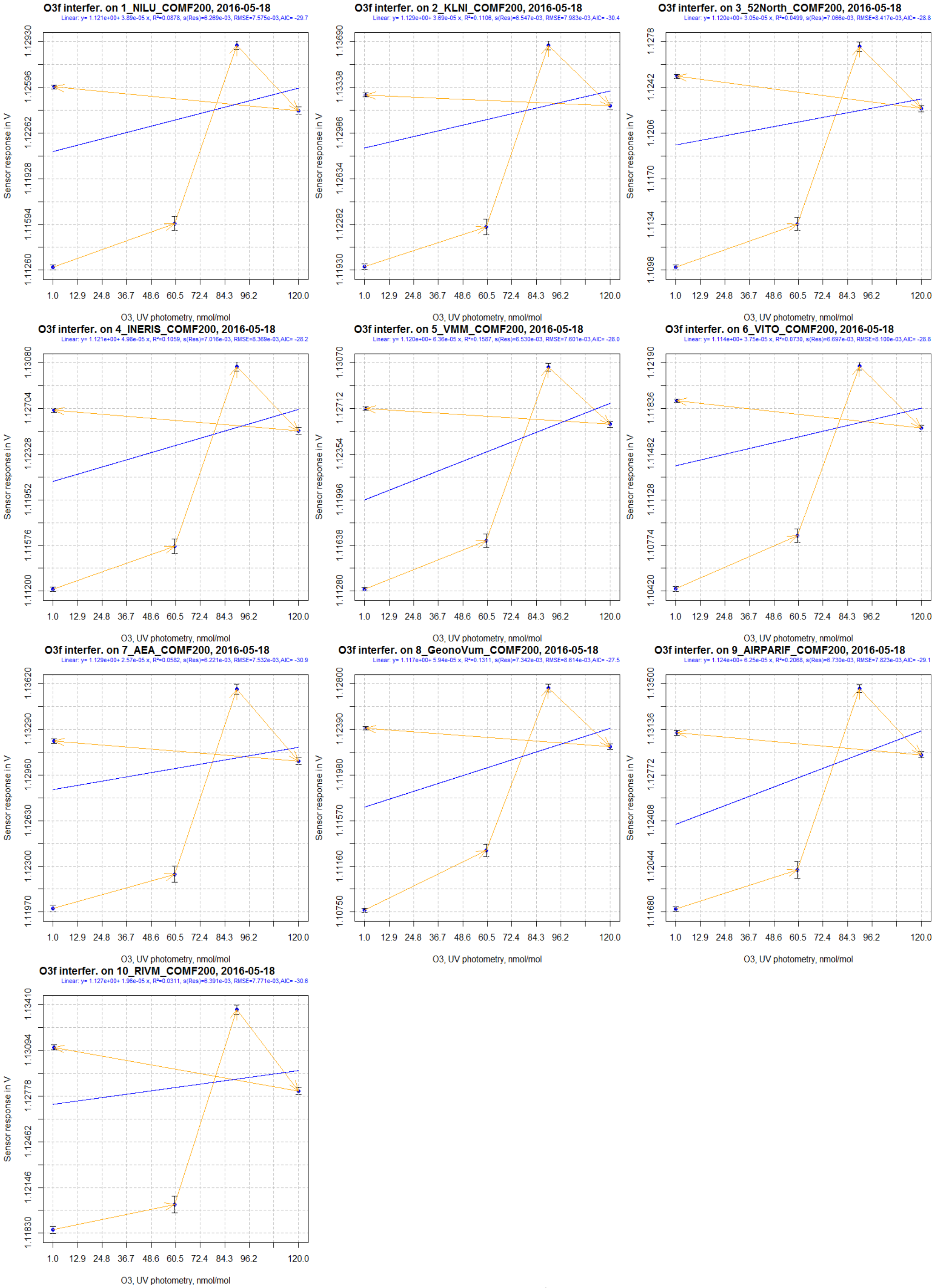

Figure 6 O_3 cross-sensitivity on CO/MF-200

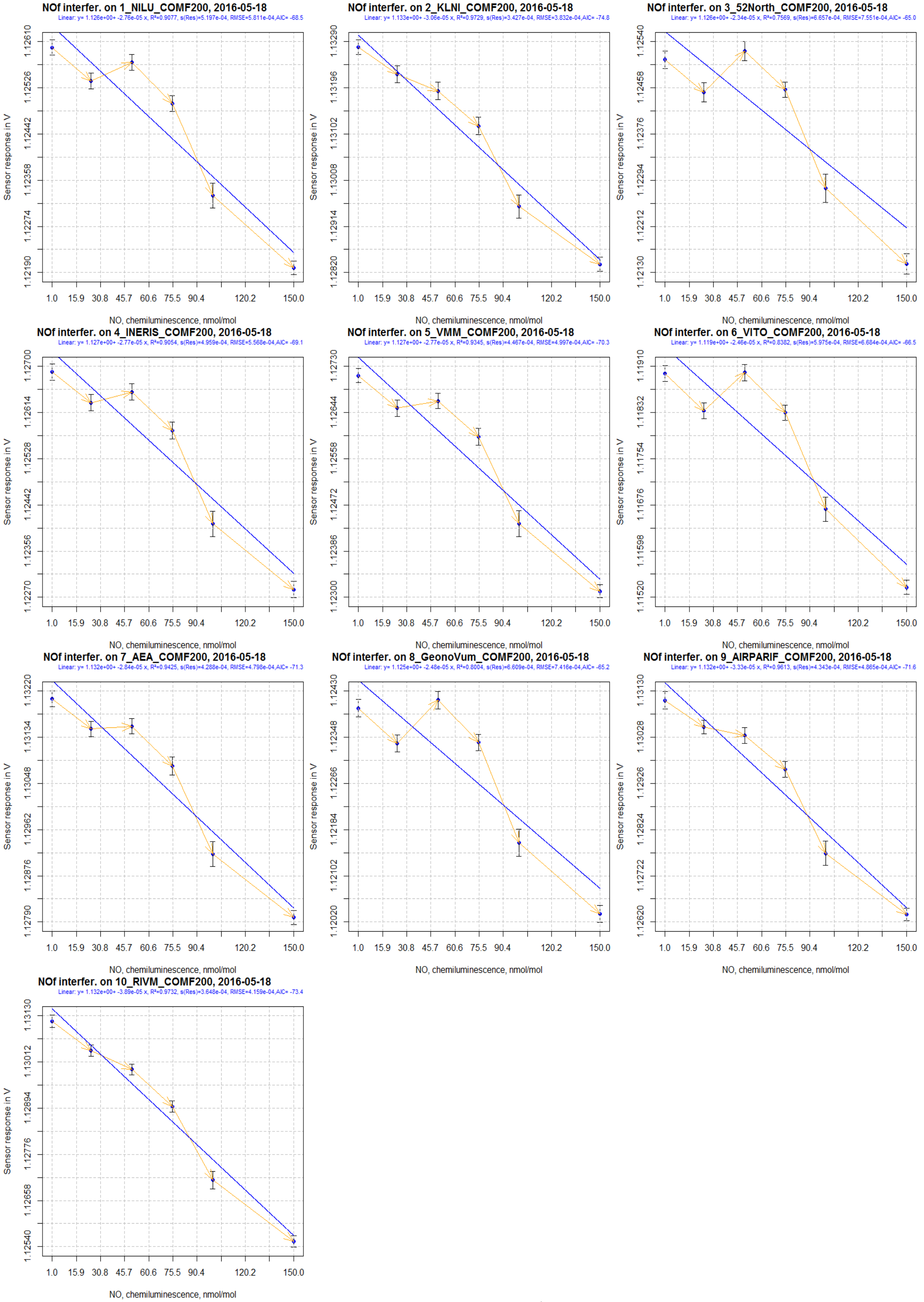

Figure 7: NO cross-sensitivity on CO/MF-200

3.1.3 O3/M-5 sensor

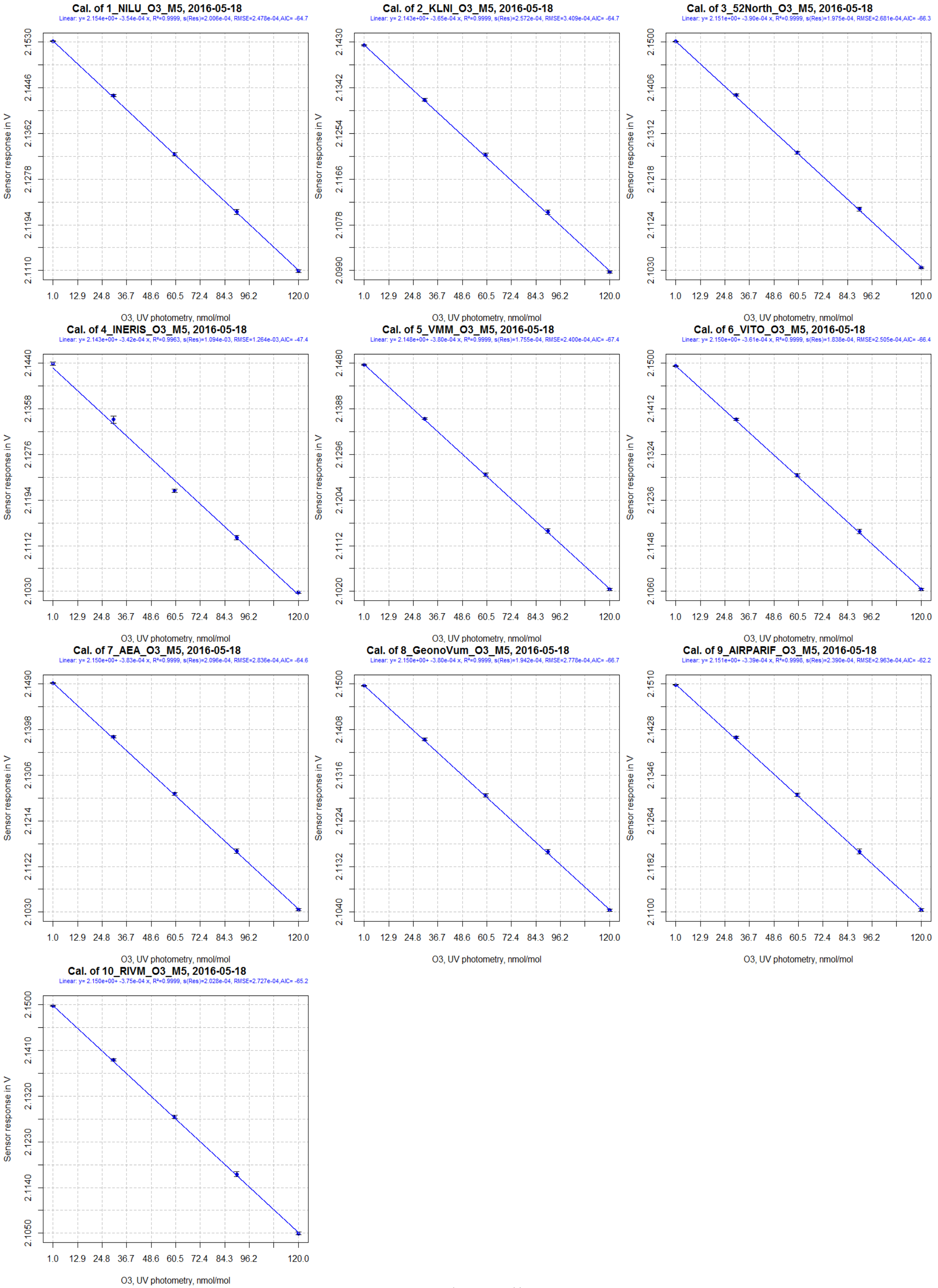

Figure 8: O3/M-5, O_3 calibration

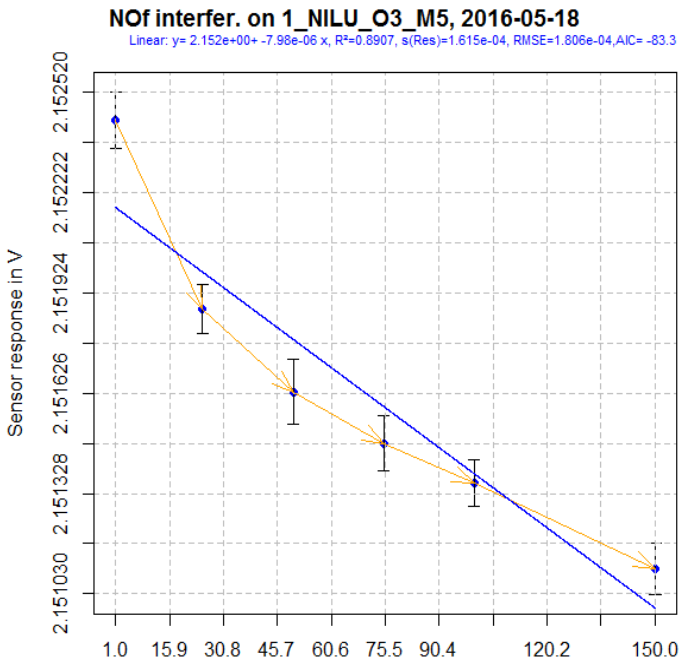

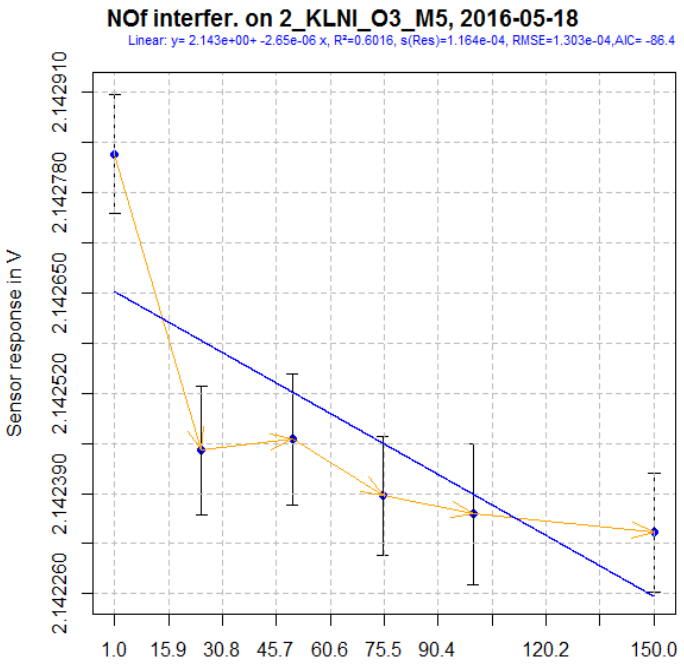

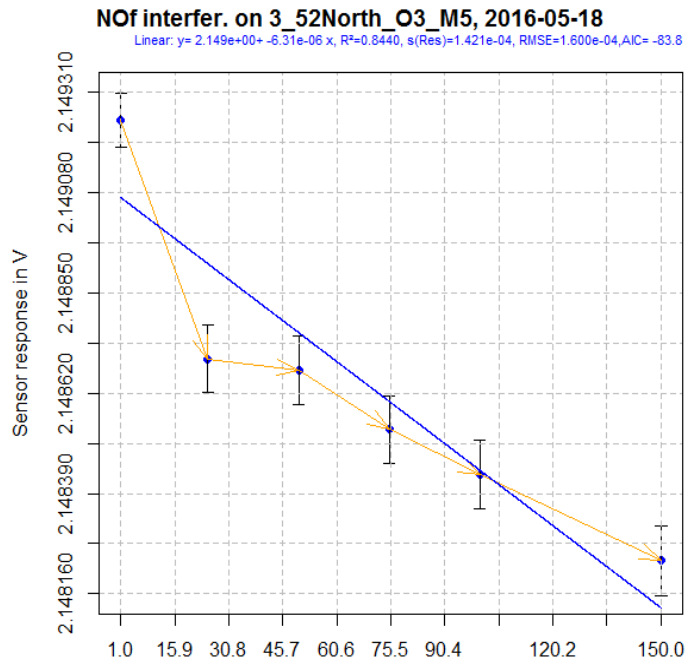

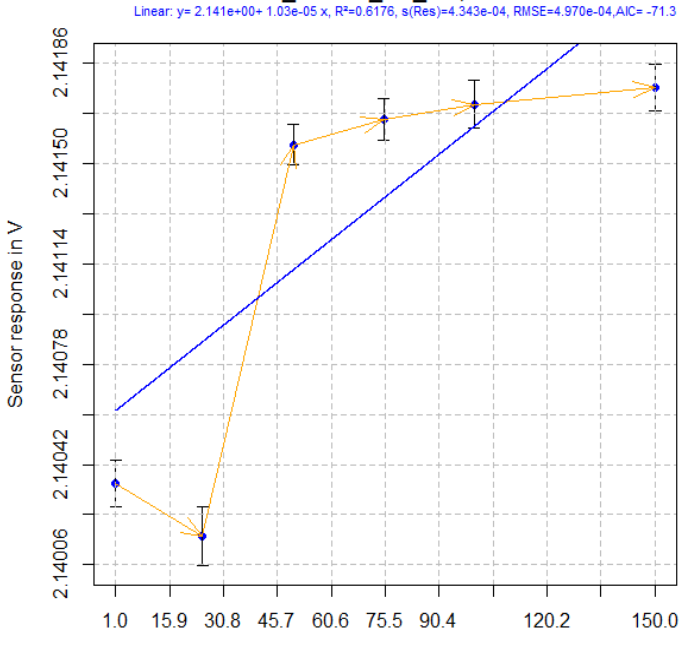

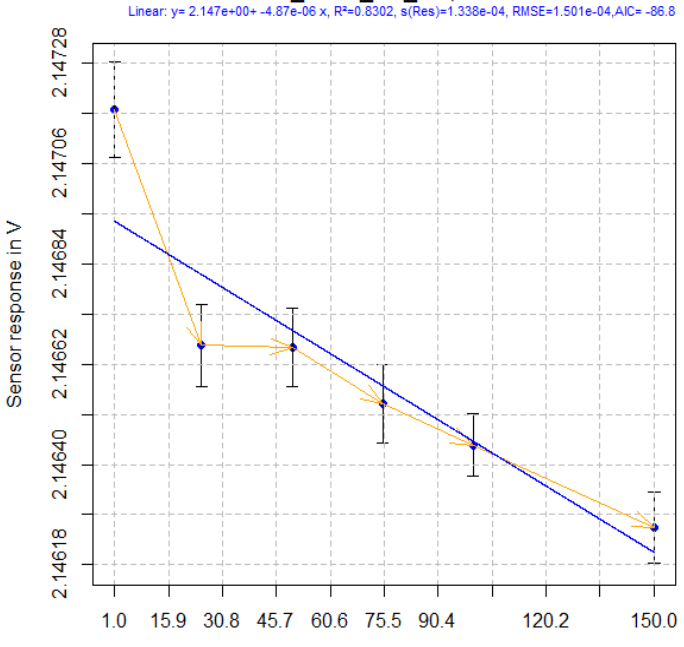

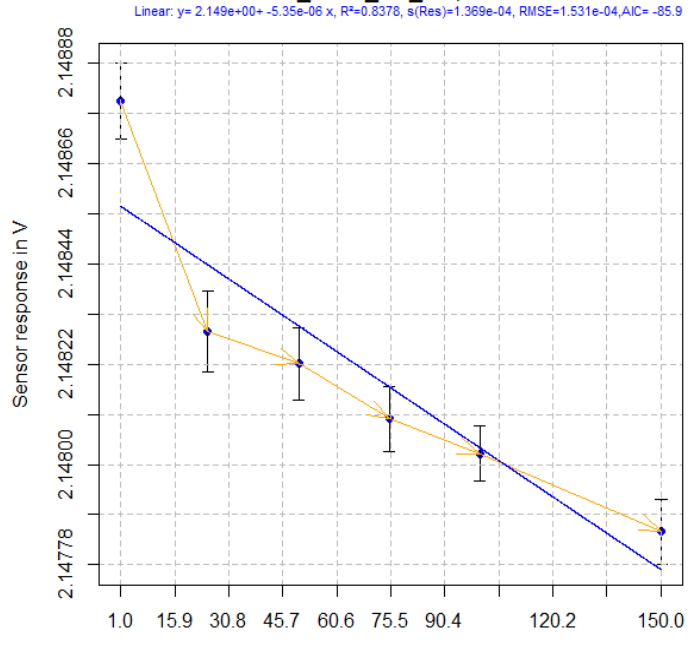

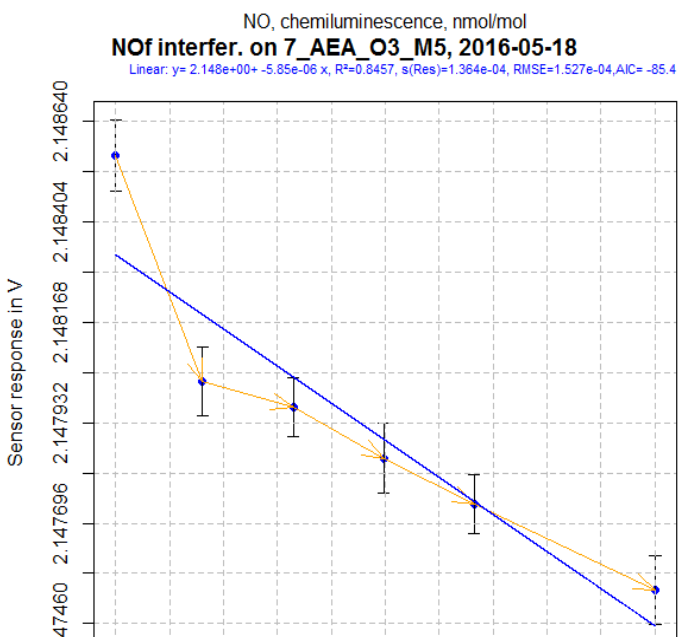

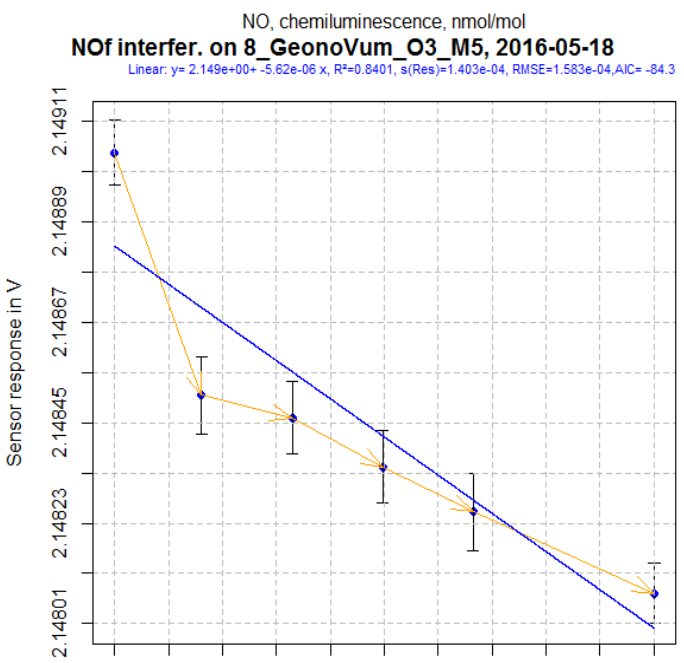

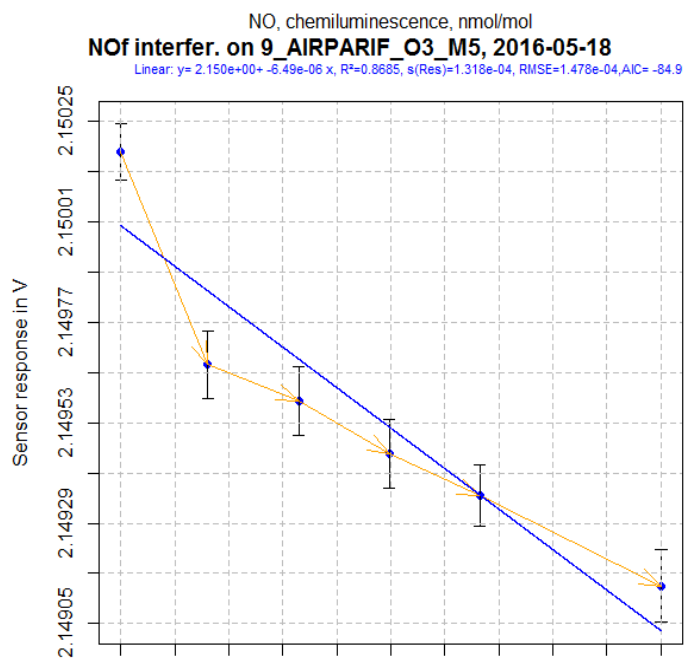

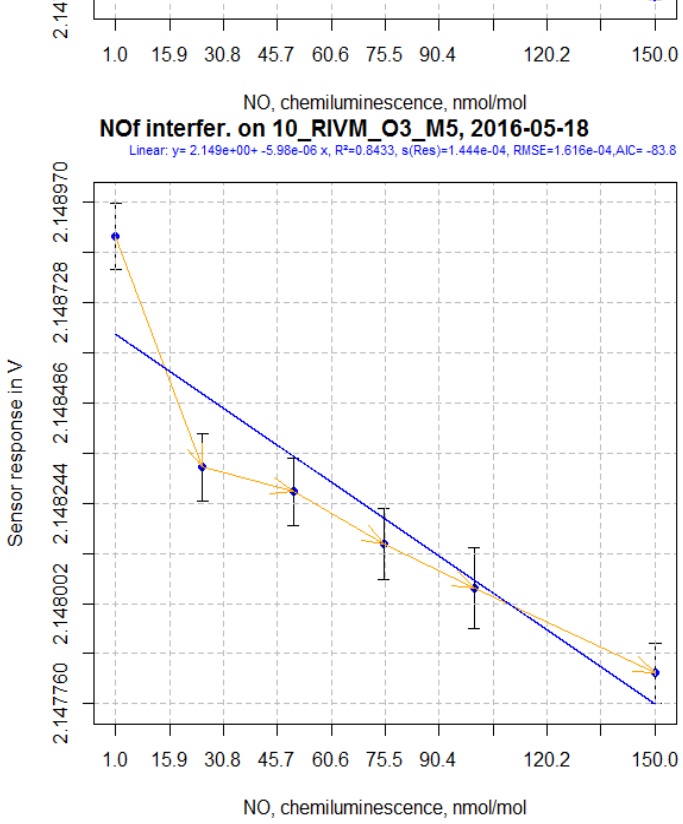

Figure 9: NO cross-sensitivity on O3/M-5

3.1.4 NO-B4 sensor

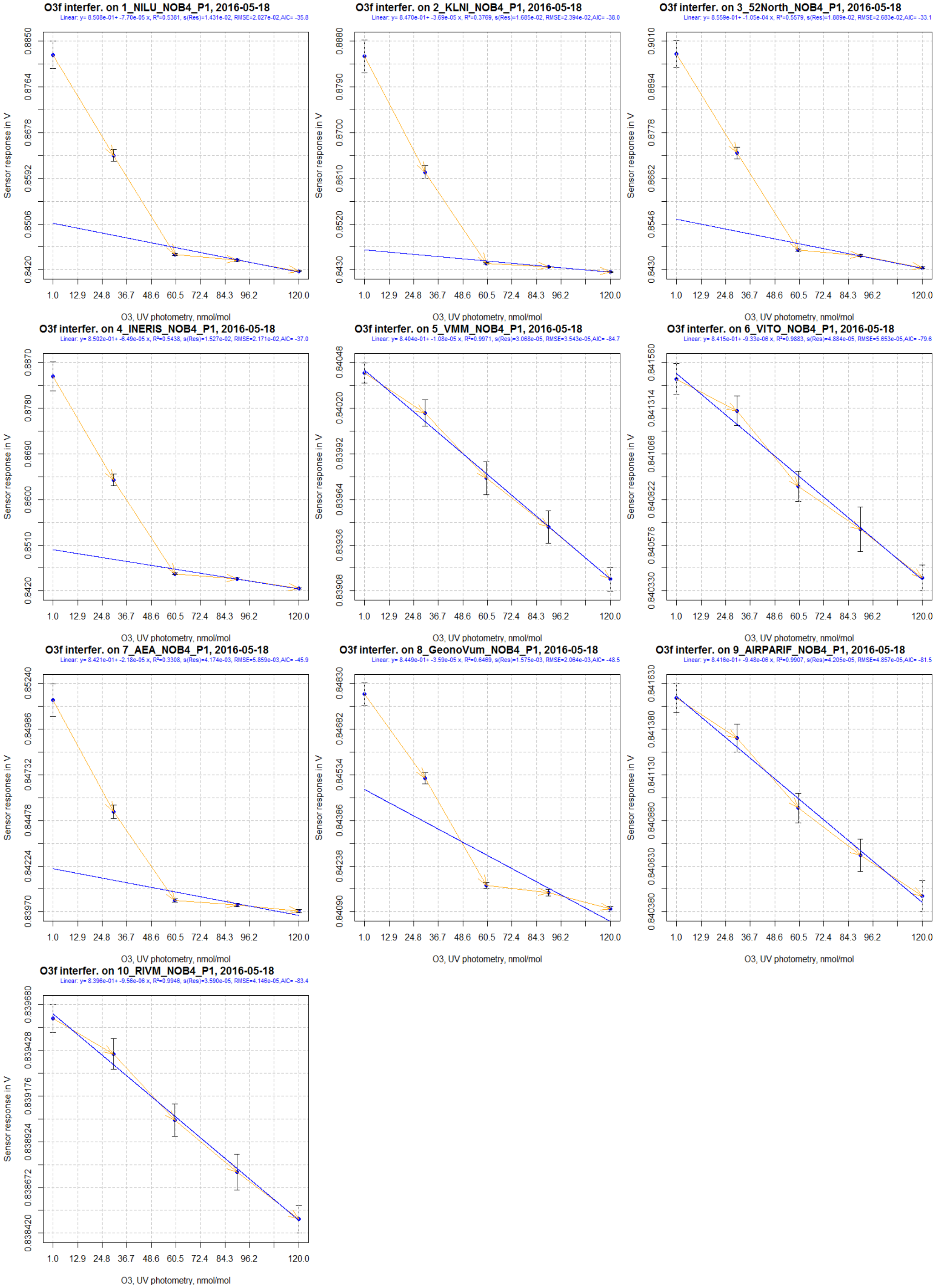

Figure 10: O_3 cross-sensitivity on NO-B4

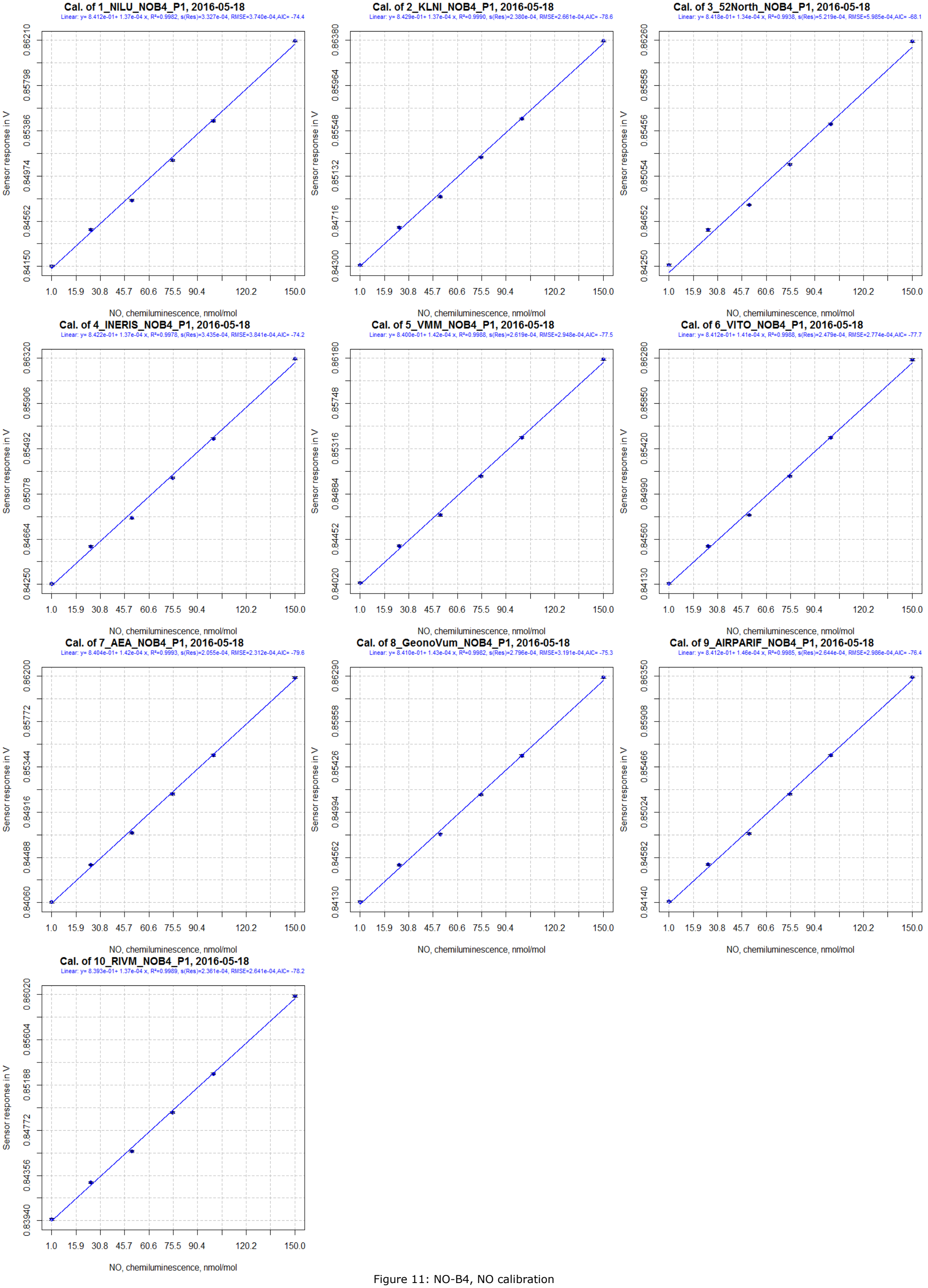

Figure 11: NO-B4, NO calibration

3.1.5 Selection of data steps within the experiment

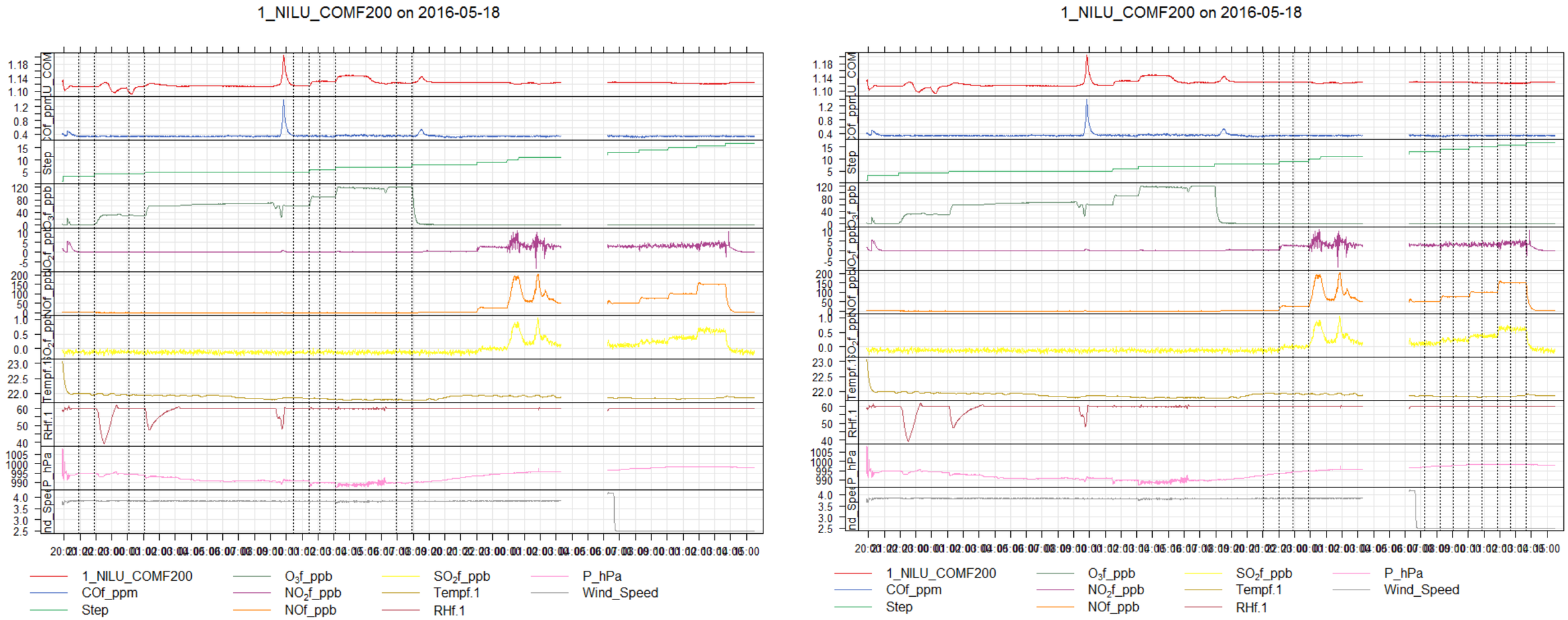

Figure 12: Selection of the O_3 steps (up) and NO steps (below) for the evaluation the Membrapor CO-MF200 sensors. For the step at 30 ppb of O_3 the sensor reading appears to be unstable while all available measured parameters appear to be almost stable (O_3, NO_2, NO, SO_2, temperature, humidity and pressure).

3.2 NO and O_3 tabulated results

The following tables give the effect of both compounds on each set of 10 sensors (sensor readings in volt versus reference values in ppb or ppm) to estimate the scattering of sensor readings (see rows labelled Means and relative standard deviation, RSD). The tables give the sensor model types, the intercepts in V (Interc. ± s) and slopes in V/ppb or V/ppm (slope ± s) of the linear lines, the probability that the intercepts and slopes are different from 0 (any value > 0.05 indicates that these variables are significantly different from 0), the coefficients of determination (R^2), the root mean square errors (RMSE) in V calculated using the residual degrees of freedom and the lack of fit in ppb of the linear lines calculated for the x axis u(lof). Figure 4 to Figure 11 gives the scatterplots of the experiments, sensor readings versus reference values.

3.2.1 NO2-B43F sensor

3.2.1.1 Effect of NO

The NO2-B43F sensors clearly show an NO cross-sensitivity. The slopes of linear lines are highly significant, with RSD of the slopes of 8.0 % and mean slope value of -0.0000024 ± 0.0000002 V/ppb (see Figure 5 which shows the scatter plot of the sensor values against NO concentration levels). The fourth sensor (INERIS) is clearly an outlier. It shows a different behaviour from the other sensors due to a malfunction during the tests. The sensor was thus discarded for data treatment.

Table 5: Effect of NO on 10 NO2-B43F sensors (sensor readings in volt versus reference values in ppb or ppm), experimental results of 2016-05-18. 4_INERIS_NO2-B43F is discarded for computing the means, mean SDs and RSDs

Sensors	Interc.	P(Interc.)	Slope	P(Slope)	R^2	RMSE	u(lof)
1_NILU_NO2B43P	2.14764 ± 0.00007	0	-0.0000022 ± 0.0000008	0.058	0.6339	4.117e-05	9999
2_KNMI_NO2B43P	2.14818 ± 0.00007	0	-0.0000026 ± 0.0000009	0.04	0.6923	4.468e-05	9999
3_52North_NO2B43P	2.14889 ± 0.00007	0	-0.0000022 ± 0.0000009	0.076	0.5862	4.067e-05	9999
4_INERIS_NO2B43P	2.13840 ± 0.00136	0	0.0000430 ± 0.0000147	0.043	0.6807	0.00064987	9999
5_VMM_NO2B43F	2.14803 ± 0.00007	0	-0.0000023 ± 0.0000008	0.048	0.6642	4.042e-05	9999
6_VITO_NO2B43F	2.14773 ± 0.00007	0	-0.0000027 ± 0.0000009	0.036	0.7079	4.176e-05	9999
7_AEA_NO2B43F	2.14851 ± 0.00007	0	-0.0000026 ± 0.0000009	0.048	0.6648	4.462e-05	9999
8_GeonoVum_NO2B43F	2.14828 ± 0.00007	0	-0.0000024 ± 0.0000008	0.045	0.6736	4.125e-05	9999
9_AIRPARIF_NO2B43P	2.14823 ± 0.00007	0	-0.0000025 ± 0.0000008	0.037	0.7039	3.878e-05	9999
10_RIVM_NO2B43P	2.14619 ± 0.00007	0	-0.0000023 ± 0.0000008	0.046	0.6712	4.101e-05	9999
Means	2.14796 ± 0.00077		-0.0000024 ± 0.0000002		0.6664	0.0000416	9999.0
RSD	0.000		0.080				

3.2.1.2 Effect of O_3

The NO2-B43F sensors clearly show an O_3 cross-sensitivity. The slopes of linear lines are highly significant. The O_3 effect shows significant scattering with RSD of the slopes of 22.5% and mean slope value of -0.0000058 ± 0.0000013 V/ppb.

The NO_2 sensor of the fourth shield (INERIS) did not work during this test while the NO_2 sensor of the tenth shield (RIVM) was also considered as an outlier (Dixon's test gives Q=2 >> Qcritic=0.49). Thus for this experiment, the fourth and tenth sensors were discarded for data treatment.

Table 6: Effect of O_3 on 10 NO2-B43F sensors (sensor readings in volt versus reference values in ppb or ppm), experimental results of 2016-05-18. 4_INERIS_NO2-B43F is discarded for computing the means, mean SDs and RSDs

Sensors	Interc.	P(Interc.)	Slope	P(Slope)	R^2	RMSE	u(lof)
1_NILU_NO2B43P	2.14796 ± 0.00006	0	-0.0000073 ± 0.0000008	0.003	0.9619	3.532e-05	9999
2_KNMI_NO2B43P	2.14836 ± 0.00007	0	-0.0000068 ± 0.0000009	0.005	0.9519	3.639e-05	9999
3_52North_NO2B43P	2.14873 ± 0.00012	0	-0.0000032 ± 0.0000016	0.145	0.5608	6.784e-05	9999
4_INERIS_NO2B43P	2.10752 ± 0.00895	0	0.0002185 ± 0.0000894	0.092	0.6658	0.00250193	9999
5_VMM_NO2B43F	2.14824 ± 0.00006	0	-0.0000055 ± 0.0000007	0.005	0.948	3.04e-05	9999
6_VITO_NO2B43F	2.14795 ± 0.00005	0	-0.0000066 ± 0.0000007	0.002	0.9709	2.922e-05	9999
7_AEA_NO2B43F	2.14874 ± 0.00005	0	-0.0000050 ± 0.0000007	0.006	0.9393	3.096e-05	9999
8_GeonoVum_NO2B43F	2.14850 ± 0.00007	0	-0.0000065 ± 0.0000008	0.005	0.9507	3.52e-05	9999
9_AIRPARIF_NO2B43P	2.14850 ± 0.00007	0	-0.0000059 ± 0.0000010	0.009	0.9258	4.044e-05	9999
10_RIVM_NO2B43P	2.14649 ± 0.00011	0	-0.0000155 ± 0.0000015	0.002	0.9739	6.199e-05	9999
Means	2.14884 ± 0.00031		-0.0000058 ± 0.0000013		0.9012	0.0000382	9999
RSD	0.000		0.225				

3.2.2 CO/MF-200 sensor

3.2.2.1 Effect of NO

The CO/MF-200 sensors clearly show a NO cross-sensitivity. The intercepts and slopes of linear lines are highly significant. However, some scattering is observed with RSD of the slopes of the linear lines of 16.1% with mean slope value of -0.0000287 ± 0.0000046 V/ppb. Figure 7 shows the scatter plot of the CO/MF-200 sensors versus NO concentration levels.

Table 7: Effect of NO on 10 CO/MF-200 sensors (sensor readings in volt versus reference values in ppb), experimental results of 2016-05-18.

Sensors	Interc.	P(Interc.)	Slope	P(Slope)	R^2	RMSE	u(lof)
1_NILU_COMF200	1.12641 ± 0.00038	0	-0.0000277 ± 0.0000044	0.003	0.9077	0.00023604	14
2_KNMI_COMF200	1.13306 ± 0.00022	0	-0.0000306 ± 0.0000026	0	0.9729	0.00014026	9
3_52North_COMF200	1.12560 ± 0.00052	0	-0.0000234 ± 0.0000066	0.024	0.7569	0.00031639	20
4_INERIS_COMF200	1.12730 ± 0.00036	0	-0.0000277 ± 0.0000045	0.003	0.9054	0.00022607	13
5_VMM_COMF200	1.12749 ± 0.00032	0	-0.0000277 ± 0.0000037	0.002	0.9345	0.00020034	12
6_VITO_COMF200	1.11945 ± 0.00046	0	-0.0000246 ± 0.0000054	0.01	0.8382	0.00028043	18
7_AEA_COMF200	1.13242 ± 0.00030	0	-0.0000284 ± 0.0000035	0.001	0.9425	0.00018729	11
8_GeonoVum_COMF200	1.12452 ± 0.00051	0	-0.0000248 ± 0.0000062	0.016	0.8004	0.00031163	20
9_AIRPARIF_COMF200	1.13152 ± 0.00030	0	-0.0000333 ± 0.0000033	0.001	0.9613	0.00018006	10
10_RIVM_COMF200	1.13152 ± 0.00026	0	-0.0000389 ± 0.0000032	0	0.9732	0.00015806	8
Means	1.12793 ± 0.00427		-0.0000287 ± 0.0000046		0.8993	0.0002237	13.5
RSD	0.004		0.161				

3.2.2.2 Effect of O_3

The sensor signal for the step with O_3 at 30 ppb was found unstable (see Figure 12) although the measured ambient parameters were rather stable. Only a slight change of pressure can be observed. Furthermore such an instability of the sensor signal is not present for the test of NO_2 and O_3 together (see Figure 31) thus it is likely that the

instability of the sensor signal at 30 ppb is not repeatable. Therefore, we decided to drop the step with O_3 at 30 ppb from the data treatment (see Figure 6).

The CO/MF-200 sensors do not show a clear O_3 cross-sensitivity. The slope of the linear lines are not significantly different from zero (p>35 %). The R^2 are low. Figure 6 shows the lack of correlation between CO/MF-200 and O_3. In Table 8, the data treatment is performed with the second O_3 level at 1.5 ppb and without the O_3 level at 30 ppb (see values in Table 3). Figure 6 shows a bit of scattering in the sensor values (about 10 mV). This scattering might be a combination of the effect of CO (a change of 17 ppb results in a sensor signal of 1.4 mV), temperature (change of 0.2 ºC) and pressure (change of 5 hPa), the only parameters that changed during the experiment.

Table 8: Effect of O_3 on 10 CO/MF-200 sensors (sensor readings in volt versus reference values in ppb), experimental results of 2016-05-18.

Sensors	Interc.	P(Interc.)	Slope	P(Slope)	R^2	RMSE	u(lof)
1_NILU_COMF200	1.12124 ± 0.00339	0	0.0000389 ± 0.0000627	0.569	0.0877	0.002874	227
2_KNMI_COMF200	1.12868 ± 0.00332	0	0.0000369 ± 0.0000523	0.52	0.1106	0.002676	257
3_52North_COMF200	1.11963 ± 0.00384	0	0.0000305 ± 0.0000664	0.67	0.0499	0.003206	316
4_INERIS_COMF200	1.12099 ± 0.00383	0	0.0000498 ± 0.0000724	0.529	0.1058	0.003287	194
5_VMM_COMF200	1.11990 ± 0.00370	0	0.0000636 ± 0.0000732	0.434	0.1586	0.00323	132
6_VITO_COMF200	1.11389 ± 0.00368	0	0.0000375 ± 0.0000669	0.605	0.0729	0.003114	245
7_AEA_COMF200	1.12853 ± 0.00300	0	0.0000257 ± 0.0000517	0.645	0.0582	0.00251	338
8_GeonoVum_COMF200	1.11687 ± 0.00427	0	0.0000594 ± 0.0000765	0.481	0.1311	0.003602	159
9_AIRPARIF_COMF200	1.12373 ± 0.00380	0	0.0000625 ± 0.0000613	0.365	0.2067	0.003081	142
10_RIVM_COMF200	1.12719 ± 0.00324	0	0.0000196 ± 0.0000547	0.738	0.031	0.002666	461
Means	1.12206 ± 0.00495	0.000	0.0000424 ± 0.0000156	0.556	0.1013	0.0030246	247.1
RSD	0.004		0.369				

3.2.3 O3/M5 sensor

3.2.3.1 Effect of NO

The O3/M-5 sensors clearly show a NO cross-sensitivity. Both the intercepts and slopes of linear lines are highly significant. The slope shows some scattering with RSD of the slopes of 25.2% and mean slope value of -0.0000057 ± 0.0000014 V/ppb. The fourth sensor is clearly an outlier. Figure 9 shows that it behaved in a different way than the other sensors. The sensor was discarded for data treatment.

Table 9: Effect of NO on 10 O3/M-5 sensors (sensor readings in volt versus reference values in ppb or ppm), experimental results of 2016-05-18. The 4th sensor 4_INERIS_O3/M-5 is discarded for computing the means, mean SDs and RSDs.

Sensors	Interc.	P(Interc.)	Slope	P(Slope)	R^2	RMSE	u(lof)
1_NILU_O3/M-5	2.15219 ± 0.00012	0	-0.0000080 ± 0.0000014	0.005	0.8907	7.01e-05	22
2_KNMI_O3/M-5	2.14265 ± 0.00009	0	-0.0000026 ± 0.0000011	0.07	0.6016	5.456e-05	34
3_52North_O3/M-5	2.14908 ± 0.00011	0	-0.0000063 ± 0.0000014	0.01	0.844	6.775e-05	22
4_INERIS_O3/M-5	2.14060 ± 0.00033	0	0.0000103 ± 0.0000040	0.064	0.6176	0.00019046	401
5_VMM_O3/M-5	2.14694 ± 0.00010	0	-0.0000049 ± 0.0000011	0.011	0.8302	5.209e-05	24
6_VITO_O3/M-5	2.14857 ± 0.00011	0	-0.0000053 ± 0.0000012	0.01	0.8378	5.616e-05	20
7_AEA_O3/M-5	2.14833 ± 0.00010	0	-0.0000058 ± 0.0000012	0.009	0.8457	5.899e-05	20
8_GeonoVum_O3/M-5	2.14884 ± 0.00011	0	-0.0000056 ± 0.0000012	0.01	0.8401	6.5e-05	23
9_AIRPARIF_O3/M-5	2.15001 ± 0.00010	0	-0.0000065 ± 0.0000013	0.007	0.8685	6.179e-05	18
10_RIVM_O3/M-5	2.14866 ± 0.00011	0	-0.0000060 ± 0.0000013	0.01	0.8433	6.731e-05	20
Means	2.14836 ± 0.00257		-0.0000057 ± 0.0000014		0.8224	0.0000615	
RSD	0.001		0.252				

3.2.3.2 Ozone calibration

The O3/M-5 sensors have a linear responses when calibrating against O_3. The slopes of linear lines are highly significant. The scattering of these parameters are low with RSD of 0.1 % for the intercepts (2.14853 ± 0.00367) and 4.8 % for the slopes (-0.0003670 ± 0.0000176) suggesting that the sensor could be used without previous calibration against O_3 (see Figure 8). The fourth sensor gives a slightly lower sensitivity than other sensors. However, it was not discarded for data treatment since other sensors (sensor 9 and 1) had a similar slope.

Table 10: O_3 calibration of 10 O3/M-5 sensors (sensor readings in volt versus reference values in ppb or ppm), experimental results of 2016-05-18.

Sensors	Interc.	P(Interc.)	Slope	P(Slope)	R^2	RMSE	u(lof)
1_NILU_O3/M-5	2.15356 ± 0.00009	0	-0.0003541 ± 0.0000023	0	0.9999	8.164e-05	2
2_KNMI_O3/M-5	2.14279 ± 0.00009	0	-0.0003652 ± 0.0000021	0	0.9999	8.194e-05	2
3_52North_O3/M-5	2.15054 ± 0.00006	0	-0.0003901 ± 0.0000018	0	0.9999	5.797e-05	2
4_INERIS_O3/M-5	2.14348 ± 0.00105	0	-0.0003424 ± 0.0000121	0	0.9963	0.00057731	6
5_VMM_O3/M-5	2.14813 ± 0.00008	0	-0.0003800 ± 0.0000016	0	0.9999	6.812e-05	2
6_VITO_O3/M-5	2.14985 ± 0.00009	0	-0.0003612 ± 0.0000018	0	0.9999	7.385e-05	2
7_AEA_O3/M-5	2.14959 ± 0.00009	0	-0.0003829 ± 0.0000021	0	0.9999	8.092e-05	2
8_GeonoVum_O3/M-5	2.15007 ± 0.00008	0	-0.0003797 ± 0.0000016	0	0.9999	6.79e-05	2
9_AIRPARIF_O3/M-5	2.15126 ± 0.00012	0	-0.0003388 ± 0.0000029	0	0.9998	0.0001029	2
10_RIVM_O3/M-5	2.15021 ± 0.00008	0	-0.0003754 ± 0.0000020	0	0.9999	7.243e-05	2
Means	2.14895 ± 0.00336		-0.0003670 ± 0.0000176		0.9995	0.0001265	
RSD	0.002		0.048				

3.2.4 NO-B4 sensor

3.2.4.1 NO calibration

The NO-B4_P1 sensor have highly linear responses when calibrating against NO. Both the intercept and slope of linear lines are highly significant. The scattering of these parameters are low with RSD of 0.1 % for the intercepts (0.84113 ± 0.00106) and 2.6 % for the slopes

(0.0001398 ± 0.0000037) suggesting that the sensor could be used without previous calibration against NO. Figure 11 shows the scatter plots of calibration.

Table 11: NO calibration of 10 NO-B4_P1 sensors (sensor readings in volt versus reference values in ppb or ppm), experimental results of 2016-05-18.

Sensors	Interc.	P(Interc.)	Slope	P(Slope)	R^2	RMSE	u(lof)
1_NILU_NOB4_P1	0.84119 ± 0.00024	0	0.0001371 ± 0.0000029	0	0.9982	0.00014836	9999
2_KNMI_NOB4_P1	0.84290 ± 0.00017	0	0.0001375 ± 0.0000022	0	0.999	0.00010468	9999
3_52North_NOB4_P1	0.84184 ± 0.00044	0	0.0001344 ± 0.0000053	0	0.9938	0.00024634	9999
4_INERIS_NOB4_P1	0.84224 ± 0.00026	0	0.0001371 ± 0.0000032	0	0.9978	0.00014988	9999
5_VMM_NOB4_P1	0.84004 ± 0.00020	0	0.0001424 ± 0.0000025	0	0.9988	0.00011378	9999
6_VITO_NOB4_P1	0.84117 ± 0.00018	0	0.0001413 ± 0.0000025	0	0.9988	0.00011106	9999
7_AEA_NOB4_P1	0.84042 ± 0.00016	0	0.0001420 ± 0.0000019	0	0.9993	9.563e-05	9999
8_GeonoVum_NOB4_P1	0.84103 ± 0.00022	0	0.0001431 ± 0.0000030	0	0.9982	0.00013464	9999
9_AIRPARIF_NOB4_P1	0.84119 ± 0.00022	0	0.0001463 ± 0.0000028	0	0.9985	0.00012497	9999
10_RIVM_NOB4_P1	0.83925 ± 0.00018	0	0.0001372 ± 0.0000022	0	0.9989	0.00010757	9999
Means	0.84113 ± 0.00106		0.0001398 ± 0.0000037		0.9981	0.0001337	9999.0
RSD	0.001		0.026				

3.2.4.2 Effect of O_3

The results on the effect of O_3 on NO-B4_P1 sensors are surprising. There are clearly two groups: sensors 5, 6, 9 and 10 show a clear O_3 cross-sensitivity towards -0.0000100 V/ppb while sensors 1, 2, 3, 4 and 7 show a low correlation with more scattering and a larger effect (range of about 40 mV) (see Figure 10).

We did not find the reason for this behaviour while it is rather repeatable within the two groups. Based on this experiment we cannot conclude further on the effect of O_3 on NO-B4 sensors. However, in another test with NO_2 and O_3 together we confirmed that the correct O_3 sensitivity is the one at 0.0000100 V/ppb (see Table 12). We think that the questionable results with high sensitivity (20x) might be caused by a mistake in the exposure chamber data acquisition system. Another possibility would be the interference of 2 PID sensors with UV lamps placed near by sensors 5, 6, 9 and 10, altering the air composition around the sensors.

The sensors 1, 2, 3, 4, 7 and 8 were discarded from the averaging of Table 12. The NO-B4 sensors clearly show an O_3 cross-sensitivity. The slope of the linear lines are significant with scattering: RSD of the slopes of the linear lines 6.7% with mean slope value of -0.0000098 ± 0.0000007 V/ppb.

Table 12: Effect of O_3 on 10 NO-B4_P1 sensors (sensor readings in volt), experimental results of 2016-05-18.

Sensors	Interc.	P(Interc.)	Slope	P(Slope)	R^2	RMSE	u(lof)
1_NILU_NO-B4_P1	0.86301 ± 0.00940	0.000	-0.0001987 ± 0.0001401	0.229	0.3345	0.015193	
2_KNMI_NO-B4_P1	0.86405 ± 0.00960	0.000	-0.0002099 ± 0.0001430	0.216	0.3498	0.01551	
3_52North_NO-B4_P1	0.87170 ± 0.01266	0.000	-0.0002607 ± 0.0001887	0.239	0.3231	0.020455	
4_INERIS_NO-B4_P1	0.86415 ± 0.00956	0.000	-0.0002046 ± 0.0001425	0.224	0.3402	0.015447	
5_VMM_NO-B4_P1	0.84041 ± 0.00003	0.000	-0.0000104 ± 0.0000005	0.000	0.9918	5.1e-05	
6_VITO_NO-B4_P1	0.84147 ± 0.00004	0.000	-0.0000089 ± 0.0000006	0.000	0.9834	6.3e-05	
7_AEA_NO-B4_P1	0.84601 ± 0.00250	0.000	-0.0000611 ± 0.0000372	0.176	0.4031	0.004032	
8_GeonoVum_NO-B4_P1	0.84495 ± 0.00154	0.000	-0.0000359 ± 0.0000229	0.193	0.3799	0.002488	
9_AIRPARIF_NO-B4_P1	0.84155 ± 0.00003	0.000	-0.0000093 ± 0.0000004	0.000	0.9918	4.6e-05	
10_RIVM_NO-B4_P1	0.83960 ± 0.00003	0.000	-0.0000092 ± 0.0000005	0.000	0.9881	5.5e-05	
Means	0.84079 ± 0.00093		-0.0000098 ± 0.0000007		0.9927	0.000021	
RSD	0.001		0.067				

4 Effects of CO and NO_2 individually and NO_2 + O_3 together on sensor readings (2016-05-20)

This experiment gives the first CO calibration of CO/MF-200 sensors, and the first NO_2 calibration of NO2-B43F sensors, the NO_2 cross-sensitivity of the CO/MF-200 sensor, the CO cross-sensitivity of the NO2-B43F sensor and the cross sensitivities of CO and NO_2 on NO-B4 and O3/M-5 sensors. The effect of NO_2 and O_3 together is also evaluated for the four sensors.

Table 13 below gives the reference values of all monitored parameters during the stable steps of the experiment. It includes a ramp of CO concentrations between 0.6 and 9 ppm followed with a ramp of NO_2 concentrations between 0 and 100 ppb and a last experiment with both NO_2 (from 0 to 150 ppb) and O_3 (from 0 to 90 ppb) while the other parameters were kept nearly constant during the whole experiment.

Figure 13 shows the time series plot for all reference parameters. One can notice that the experiment stopped because of a malfunctioning of the whole system on 2016-05-21 between 18:00 and 21:00. Some disturbances appear on the lines. However, they did not affect the data treatment since the whole system waits for complete stability of all parameters (except pressure) and runs the step for 90 min before starting another step of the experiment. The slight increase of NO (about 2 %) is likely to have been caused by a reduction or photo-dissociation of NO_2 into NO. This NO increase could not be avoided.

Table 13: Reference values of all steps of experiments started on 2016-05-20.

Begin	End	O3, ppb	NO2, ppb	NO, ppb	CO, ppm	SO2, ppb	Temp., °C	RH, %	Pressure, hPa	Wind_Speed, m/s
2016-05-20 19:25	2016-05-20 20:24	1.9	4.5	1.5	2.197	-0.1	22.0	60.0	998	2.5
2016-05-21 02:00	2016-05-21 02:59	1.5	0.0	0.2	0.558	-0.1	22.0	60.0	1000	2.5
2016-05-21 03:38	2016-05-21 04:37	1.4	0.1	0.2	3.000	-0.1	22.0	60.0	1001	2.5
2016-05-21 07:40	2016-05-21 08:39	1.7	-0.0	0.1	5.998	-0.1	22.0	60.0	1001	2.5
2016-05-21 09:49	2016-05-21 10:48	1.8	-0.0	0.1	8.999	-0.1	22.0	60.0	1002	2.5
2016-05-21 12:10	2016-05-21 13:09	2.0	1.0	0.5	0.403	-0.1	22.0	60.0	1001	2.5
2016-05-21 15:26	2016-05-21 16:25	2.1	50.0	2.6	0.382	-0.1	22.0	60.0	999	2.5
2016-05-21 17:07	2016-05-21 18:06	2.1	100.0	3.0	0.374	-0.1	22.0	60.0	999	2.5
2016-05-21 22:08	2016-05-21 23:07	1.7	75.0	1.9	0.349	-0.1	22.1	60.0	1000	2.5
2016-05-22 00:16	2016-05-22 01:15	1.4	25.0	0.9	0.334	-0.1	22.0	60.0	1002	2.5
2016-05-22 02:07	2016-05-22 03:06	1.3	0.8	0.3	0.325	-0.1	22.0	60.0	1001	2.5
2016-05-22 04:08	2016-05-22 05:07	30.1	50.0	0.6	0.316	-0.1	22.0	60.0	1001	2.5
2016-05-22 09:19	2016-05-22 10:18	60.0	100.0	0.6	0.271	-0.1	22.1	60.0	999	2.5
2016-05-22 11:58	2016-05-22 12:57	90.0	150.0	0.6	0.253	-0.1	22.0	60.0	998	2.5

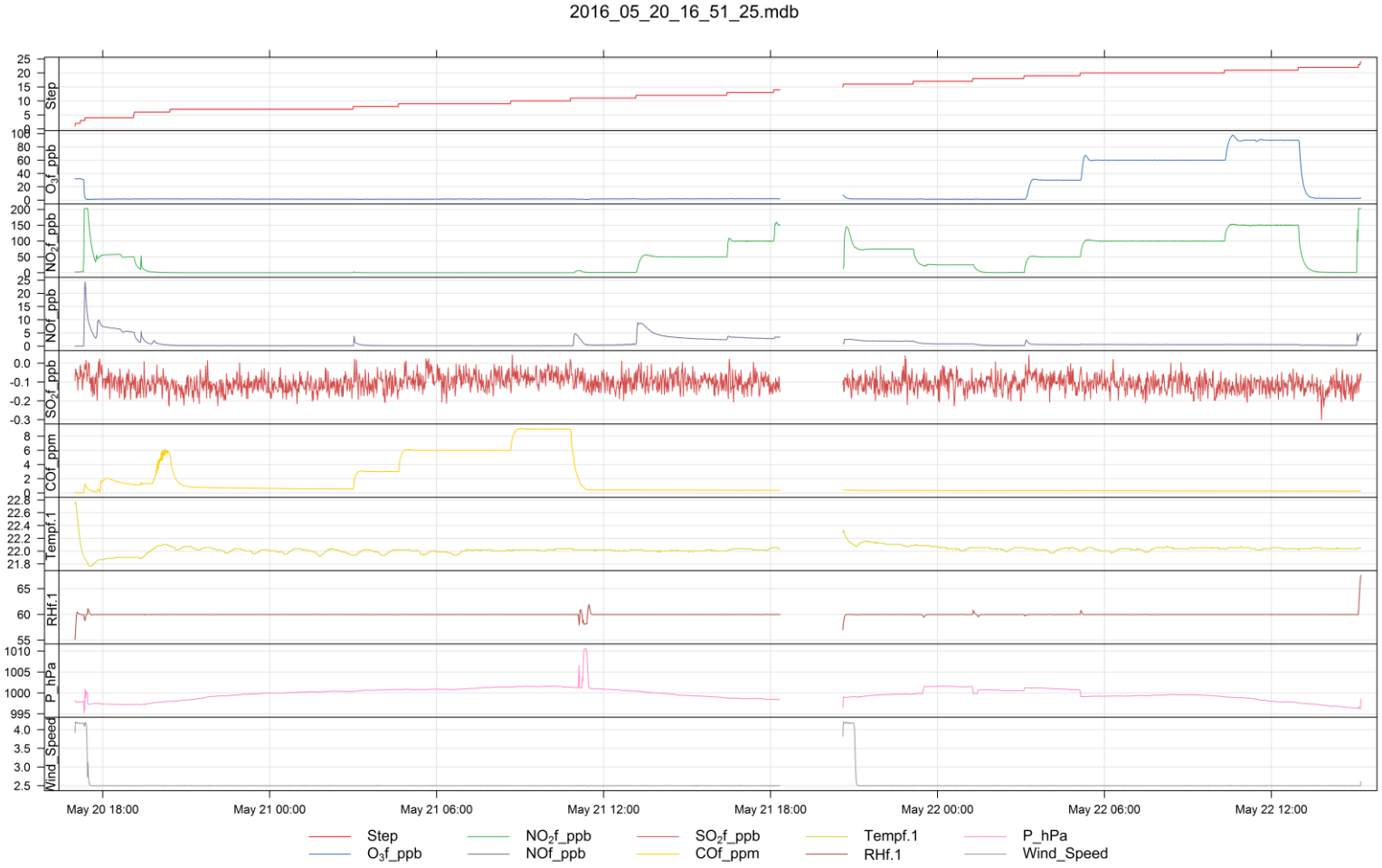

Figure 13: Time series plot of the reference parameters for the experiment started on 2016-05-20

Table 14 shows the mean effect of CO, NO_2 and NO_2/O_3 (sensor readings in volt versus reference values in ppb or ppm) on the 10 sensors of the four model types. The table gives the sensor model types, the reference gaseous compounds, the intercepts in V (Interc. ± s)

and slopes in V/ppb or V/ppm (slope ± s) of the linear lines, the probability that the intercepts and slopes are different from 0 (any value > 0.05 indicates that these variables are significantly different from 0), the coefficients of determination (R^2), the root mean square errors (RMSE) in V calculated using the residual degrees of freedom and the lack of fit in ppb or ppm of the linear model calculated for the x axis u(lof). The standard deviations of the intercepts and slopes are computed using the results of the 10 sensors. Since a few outliers were evidenced later, more accurate values are given in the following tables.

Table 14: Effect of CO, NO_2 and NO_2 + O_3 together on sensor readings, experimental results of 2016-05-20.

Sensors	Compounds	Interc.	P(Interc.)	Slope	P(Slope)	R^2	RMSE	u(lof)
CO/MF-200	CO	1.08358 ± 0.00343	0.000	0.08117327 ± 0.00623965	0.000	0.9997	0.00236	0.0
CO/MF-200	NO2	1.11826 ± 0.00393	0.000	0.00003385 ± 0.00001283	0.468	0.1581	0.00145	107.8
NO2-B43F	CO	2.14777 ± 0.00139	0.000	0.00002793 ± 0.00007547	0.213	0.6607	0.00001	2.8
NO2-B43F	NO2	2.14793 ± 0.00106	0.000	-0.00008553 ± 0.00000607	0.000	0.9888	0.00008	3.0
NO2-B43F	NO2+O3	2.14825 ± 0.00092	0.000	-0.00009016 ± 0.00000670*	0.002	0.9871	0.00018	2.9
NO-B4_P1	CO	0.84043 ± 0.00090	0.000	-0.00001017 ± 0.00000767	0.165	0.7345	0.00002	2.9
NO-B4_P1	NO2	0.84025 ± 0.00082	0.000	0.00000449 ± 0.00000039	0.053	0.6848	0.00014	20.2
NO-B4_P1	O3+NO2	0.84020 ± 0.00078	0.000	-0.00000720 ± 0.00000105+	0.010	0.9799	0.00005	4.4
O3/M-5	CO	2.14791 ± 0.00300	0.000	0.00010275 ± 0.00030785	0.236	0.6474	0.00004	3.5
O3/M-5	NO2	2.14805 ± 0.00318	0.000	-0.00028808 ± 0.00001039	0.000	0.9979	0.00020	2.1
O3/M-5	O3+NO2	2.14958 ± 0.00295	0.000	-0.00084333 ± 0.00003592**	0.000	0.9991	0.00054	2.0

(*) the slope is given for NO2-B43F versus NO2
(+)the slope is given for NO-B4 versus O3 as the NO-B4 sensor was shown not to be affected by NO2 cross-sensitivity
(**) the slope is given for O3/M-5 versus O3

The CO/MF-200 and NO2-B43F sensors show linear responses to CO and NO_2, respectively, with coefficient of determination (R^2) over 0.98 and slopes that are significantly different from zero. The intercept of the linear lines are significantly different from zero (P=0.000) for all tests. The intercept values are nearly equal to the Ref AFE multiplied by the Internal Zero values (2.15 V for NO2-B43F and O3/M-5, 1.1 V for CO/MF-200 and 0.84 V for NO-B4) set in the configuration (see Table 2). One can notice important cross-sensitivities:

- NO_2 on CO/MF-200 sensors with R^2 = 0. 468.
- NO_2 and CO on O3/M-5 with R^2 = 0.9979 and R^2 = 0.6474, respectively.
- NO_2 and CO on NO-B4 sensors with R^2 = 0. 6848 and R^2 = 0. 7345, respectively. We will show that the NO_2 effect is, in fact, an artefact due to little NO changes during the experiment.
- CO on NO2-B43F sensors with R^2 = 0. 6607.

The extent of these cross-sensitivities can be compared with the sensitivity of the calibration of the sensors in Table 45 to evaluate their importance.

4.1 Scatter plots of effects of CO, NO_2 and NO_2/O_3 together

4.1.1 NO2-B43F sensor

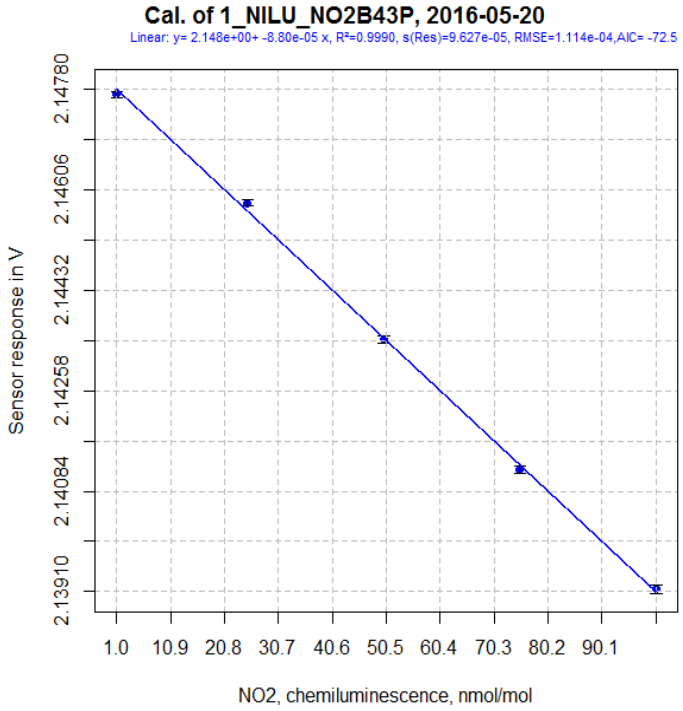

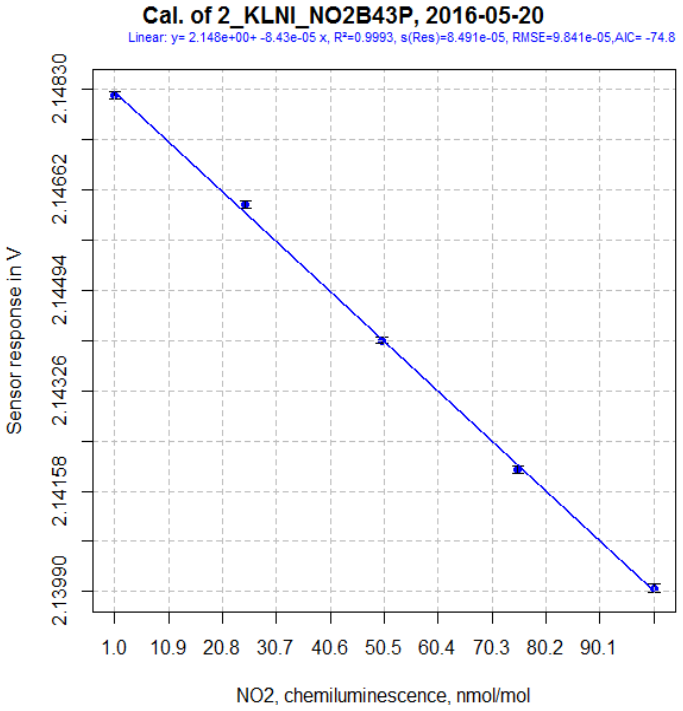

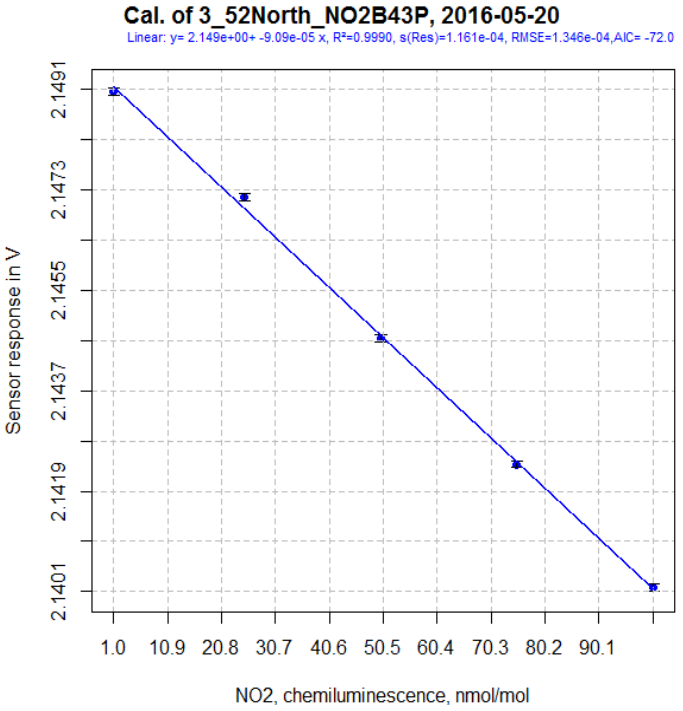

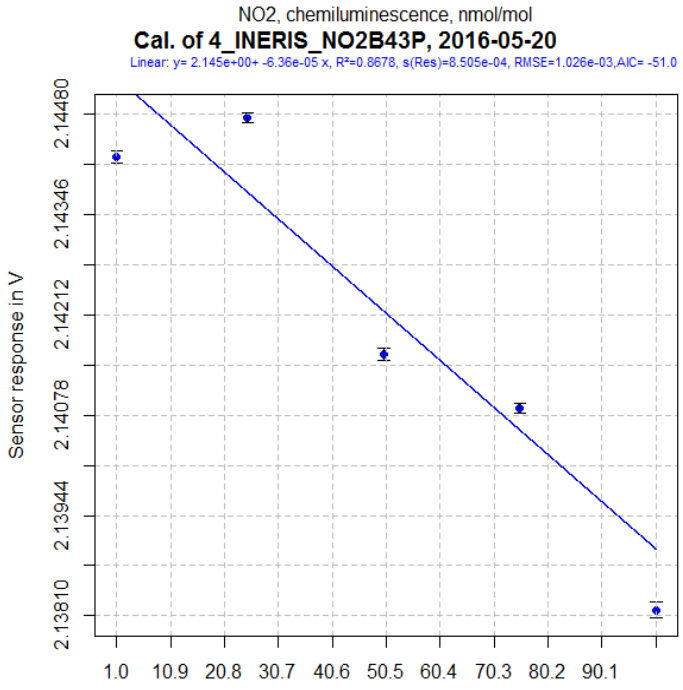

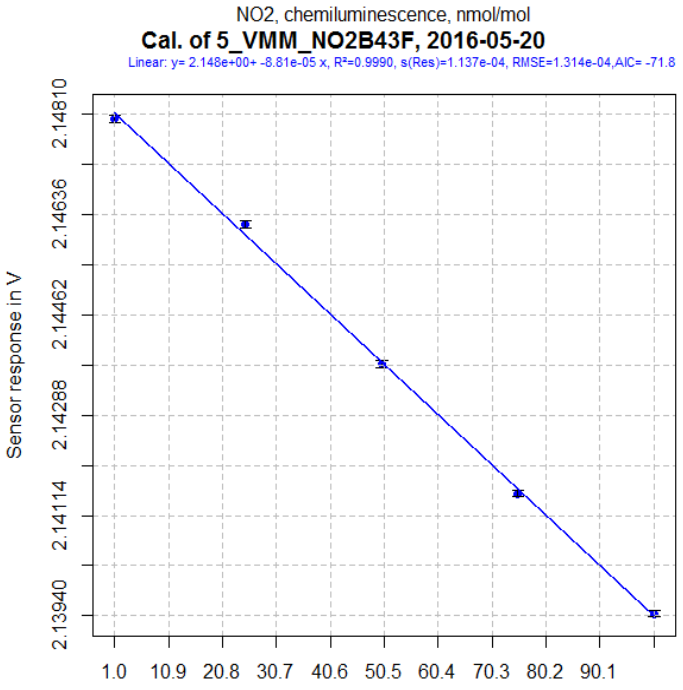

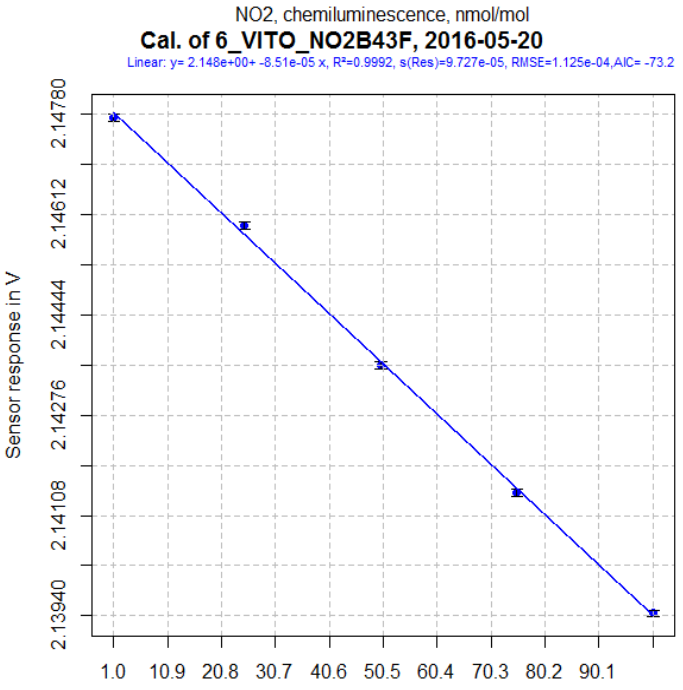

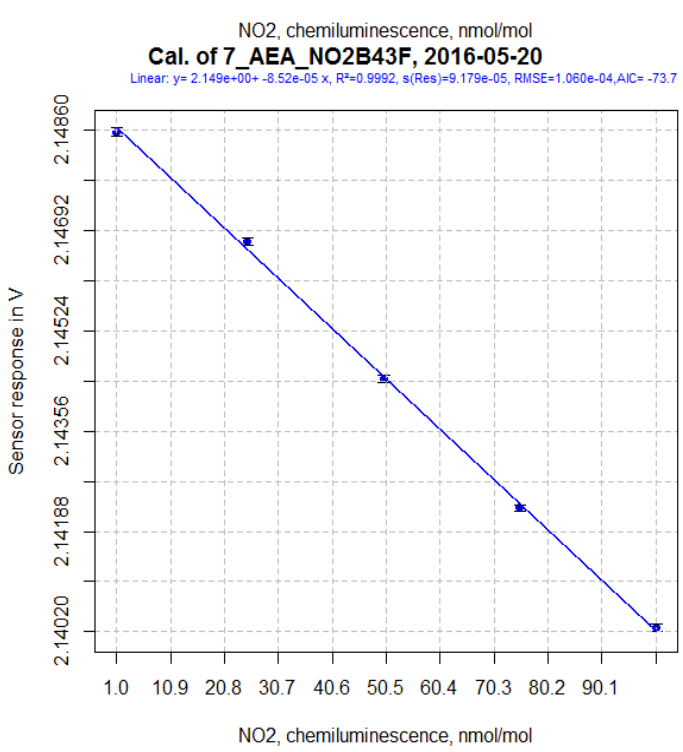

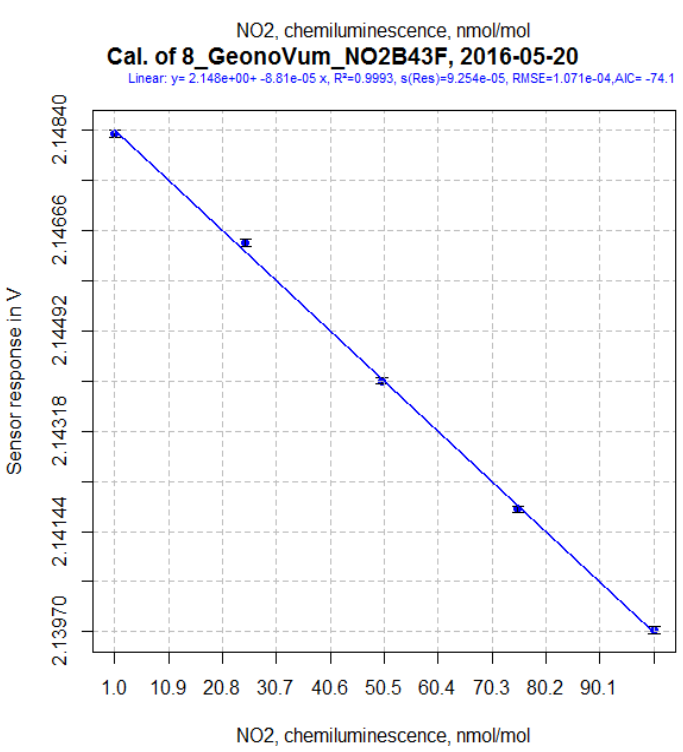

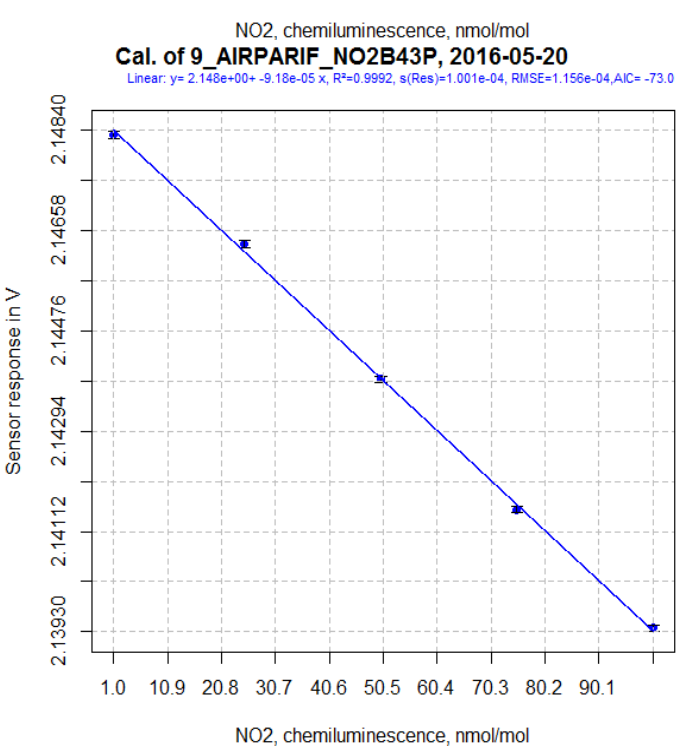

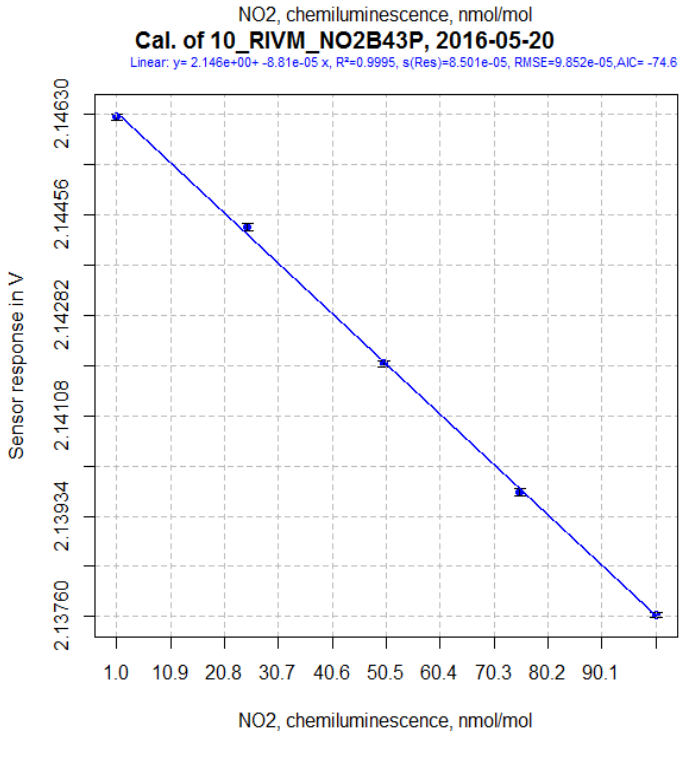

Figure 14: NO_2 calibration of NO2-B43F

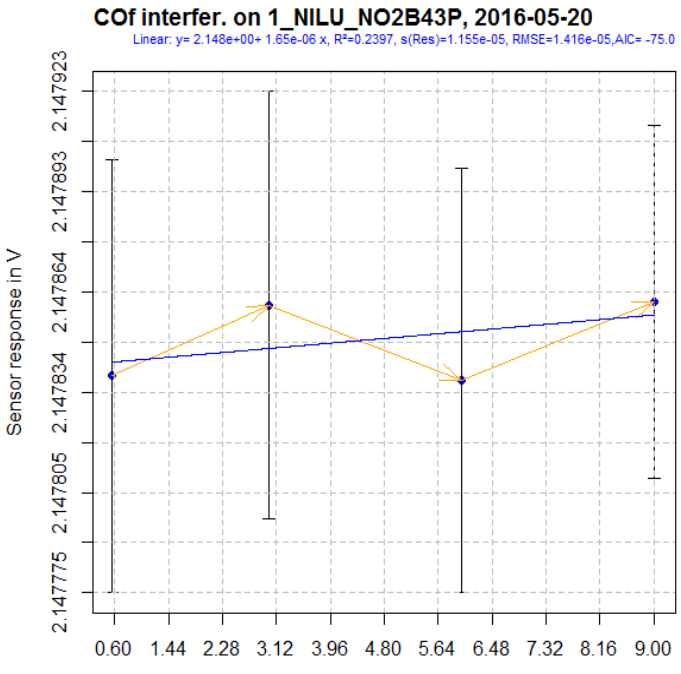

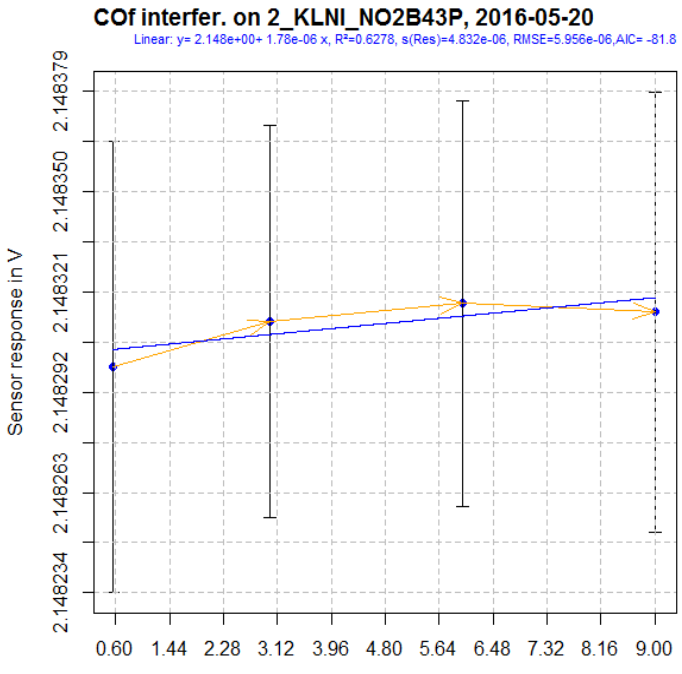

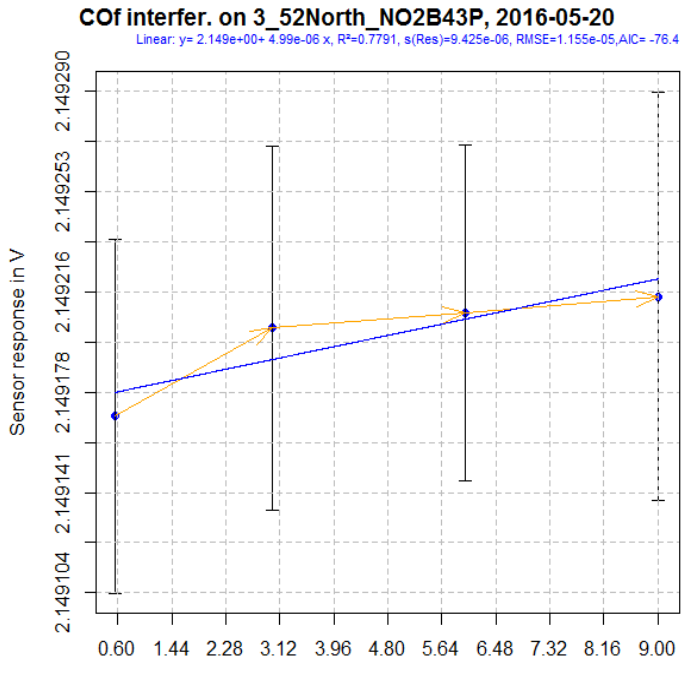

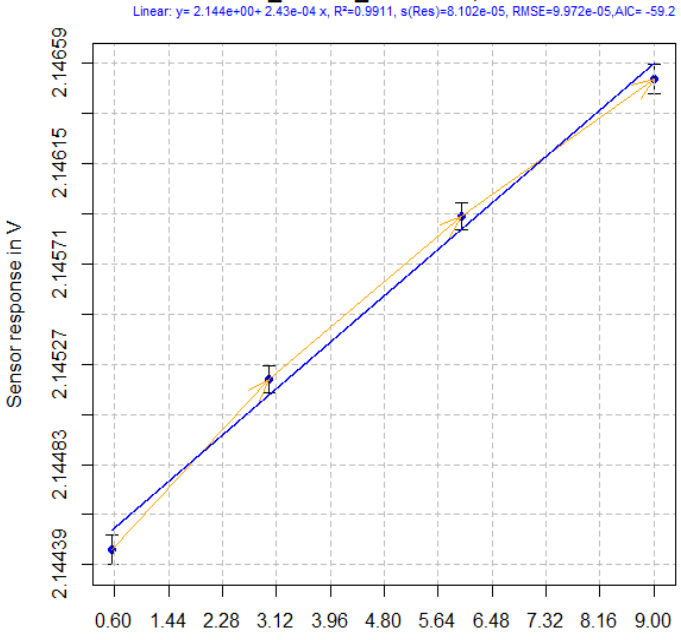

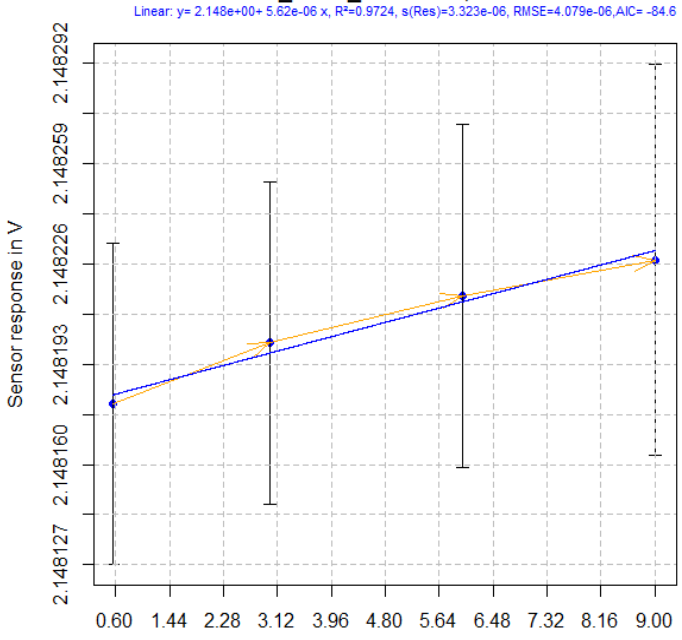

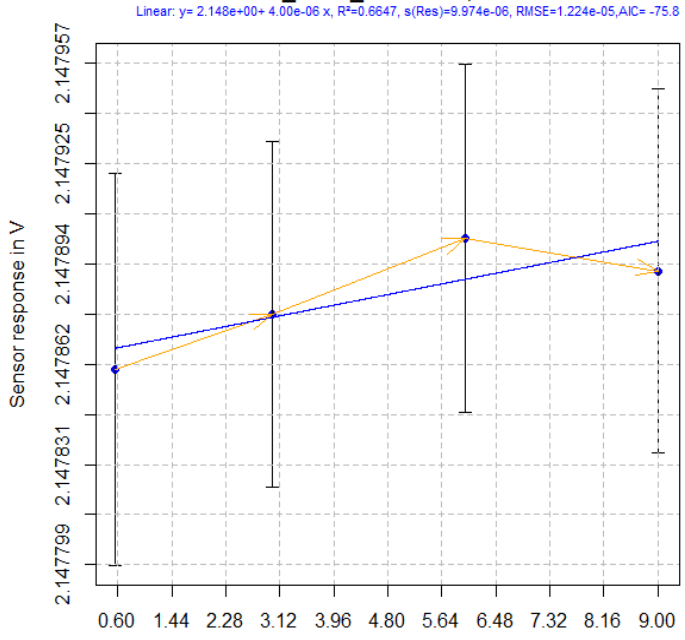

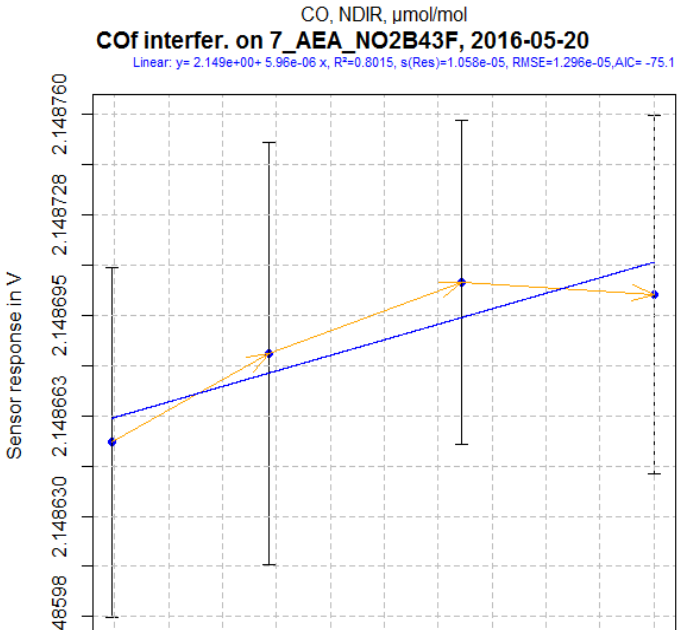

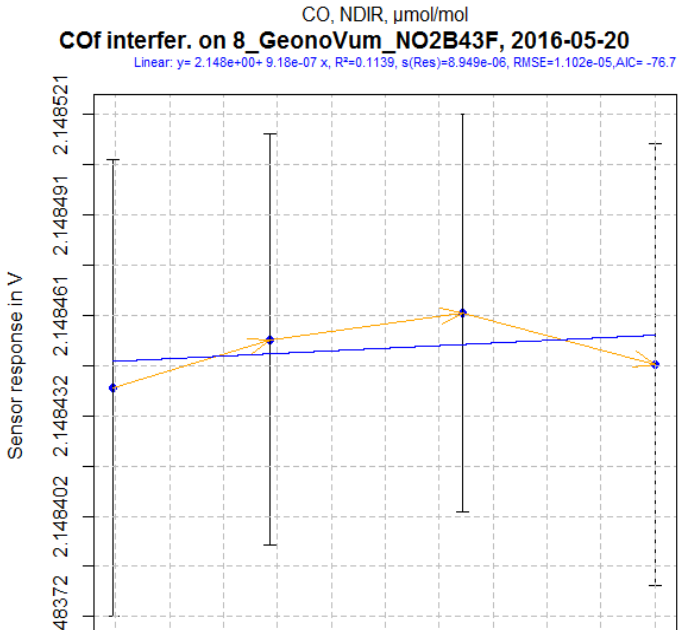

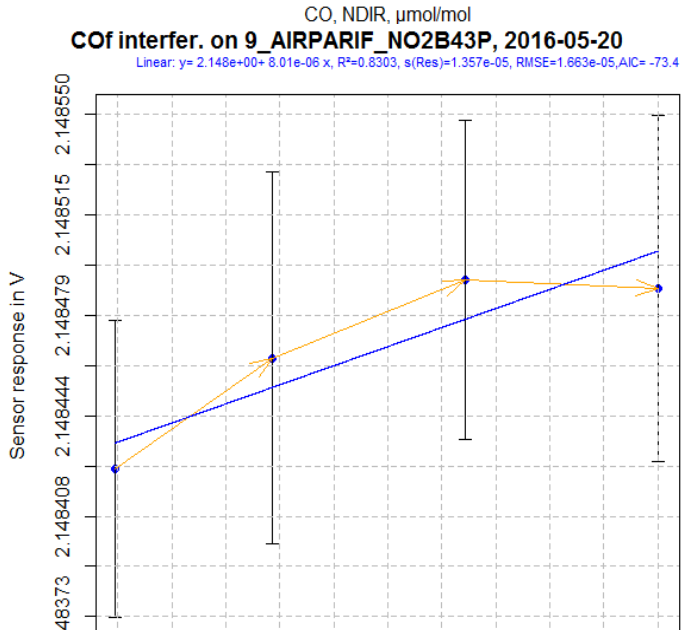

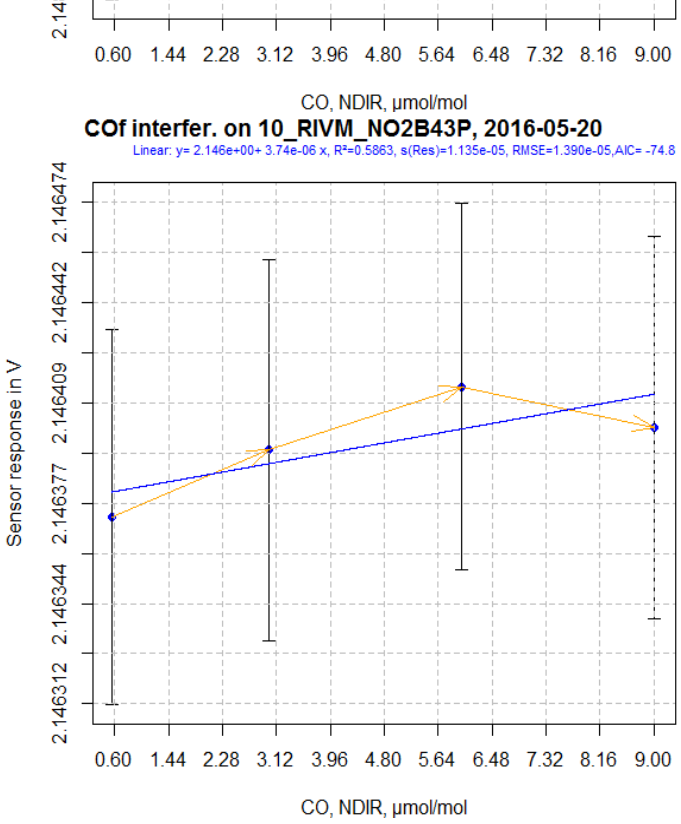

Figure 15: NO2-B43F, CO cross-sensitivity

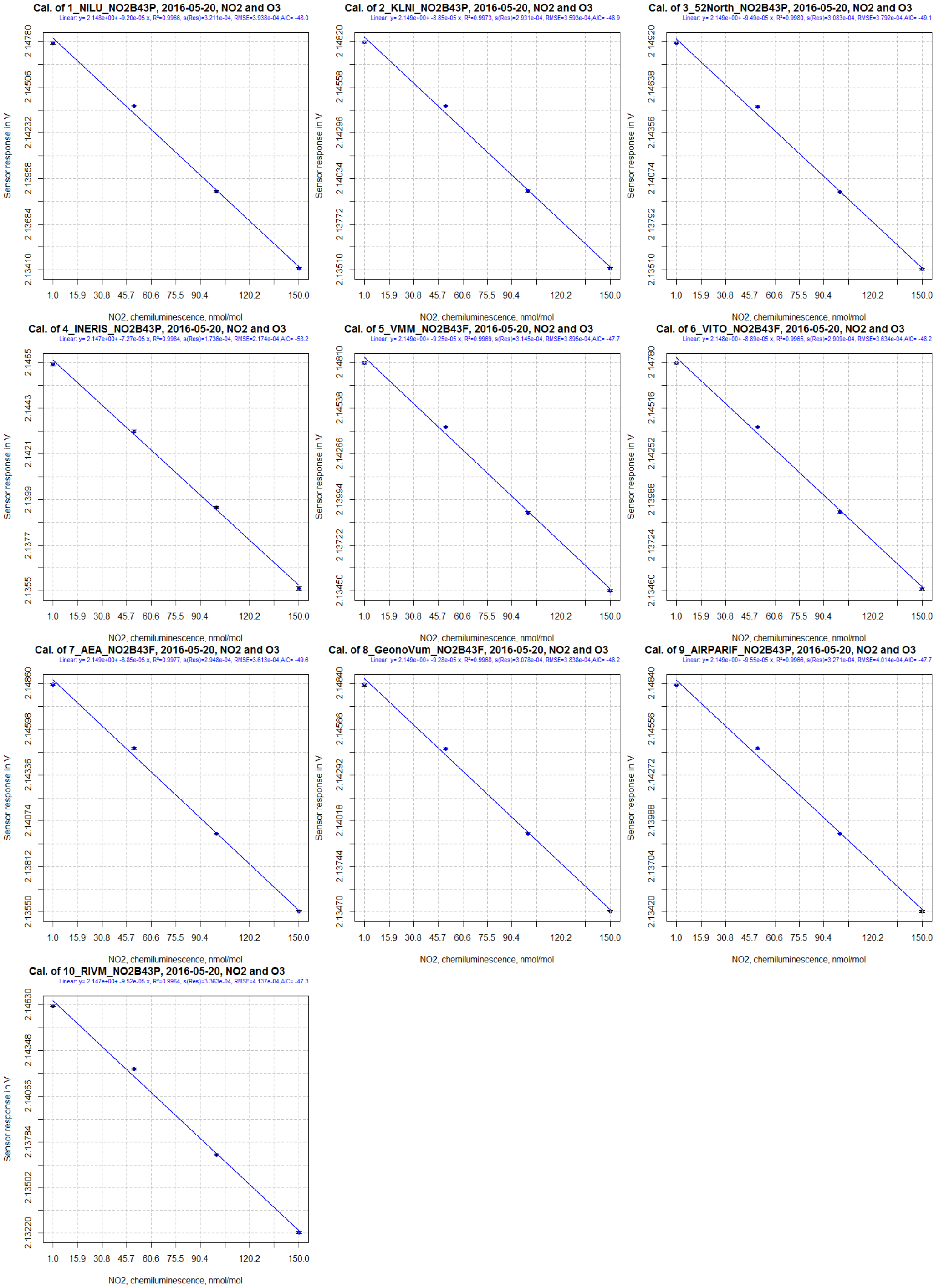

Figure 16: NO2-B43F versus NO_2, NO_2 (0-150 ppb) and O_3 (0-90 ppb) interference

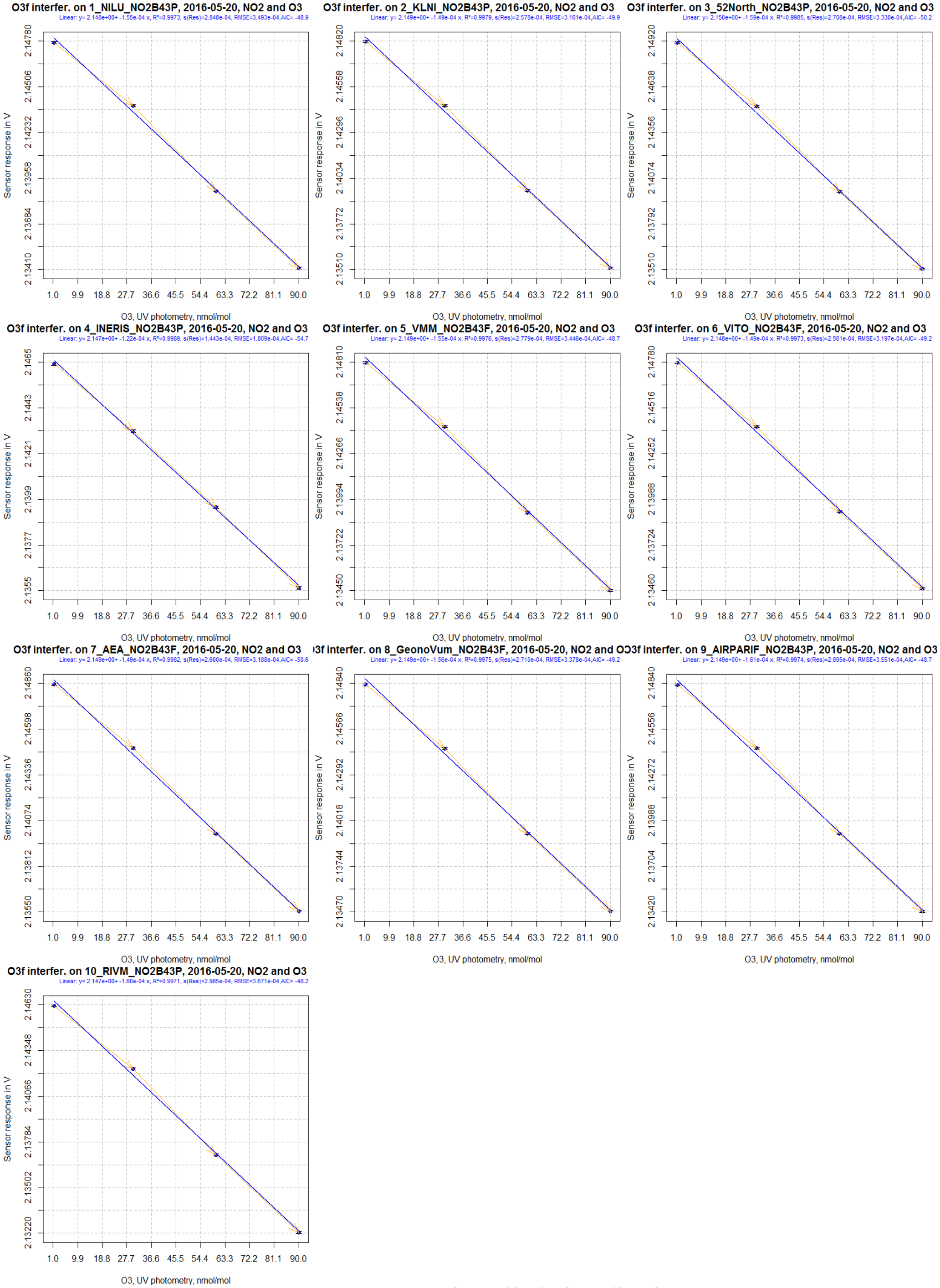

Figure 17: NO2-B43F versus O_3, NO_2 (0-150 ppb) and O_3 (0-90 ppb) interference

4.1.2 CO/MF-200 sensor

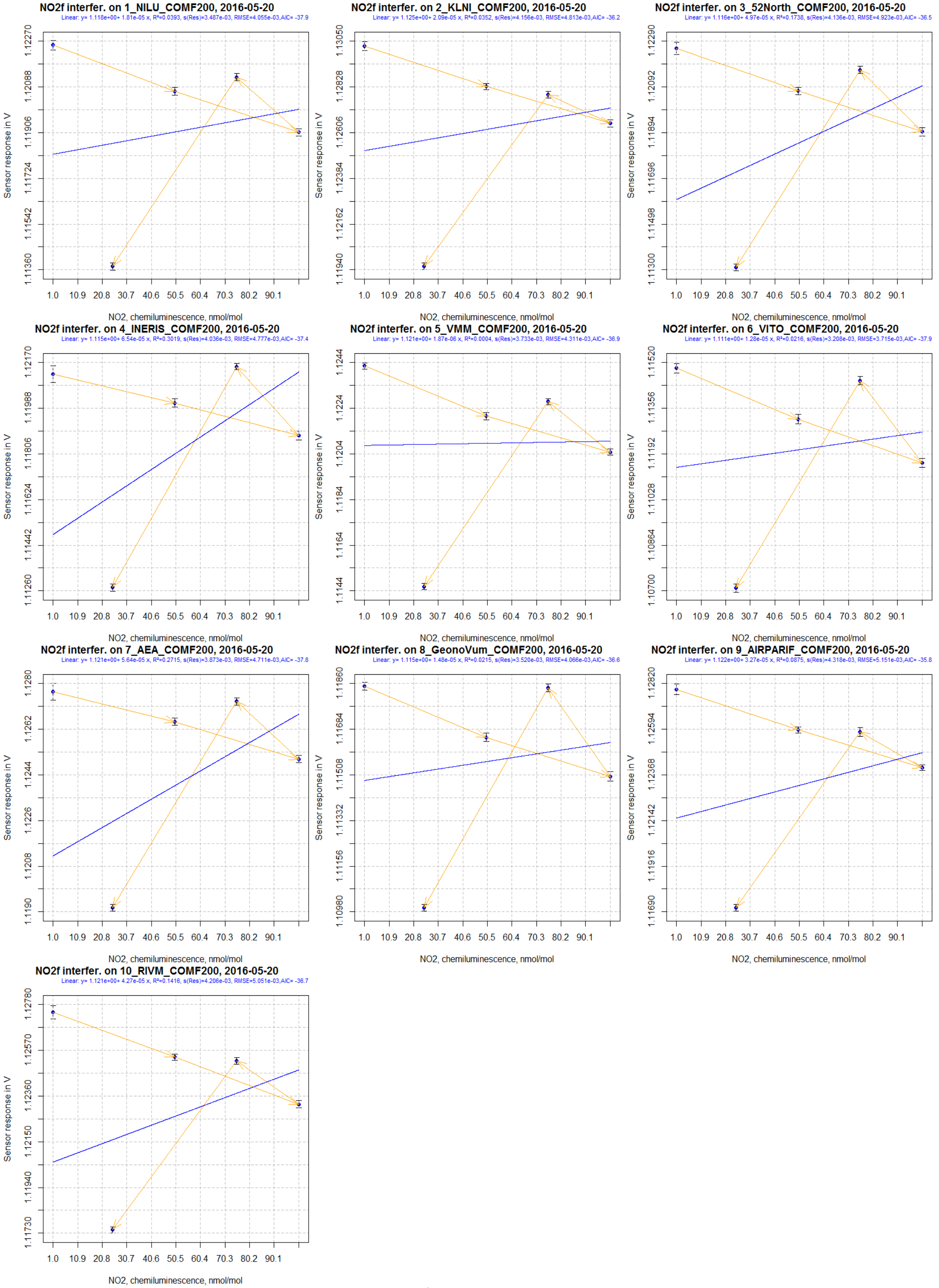

Figure 18: CO/MF-200, NO_2 cross-sensitivity

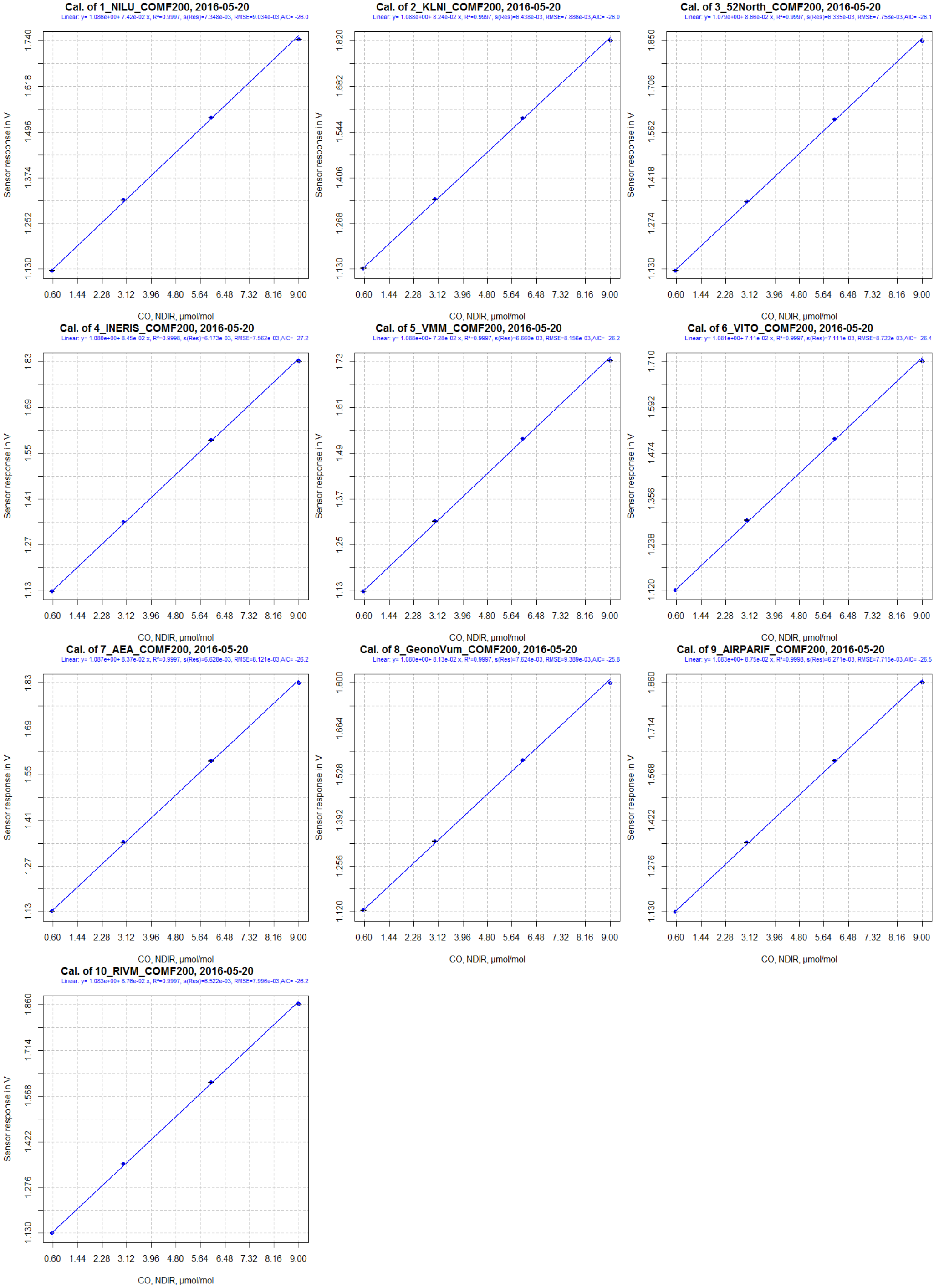

Figure 19: CO calibration of CO/MF-200

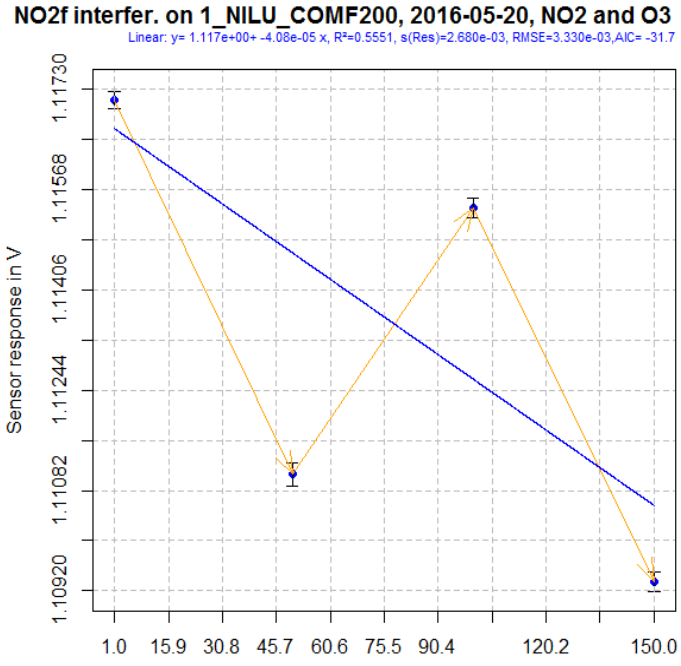

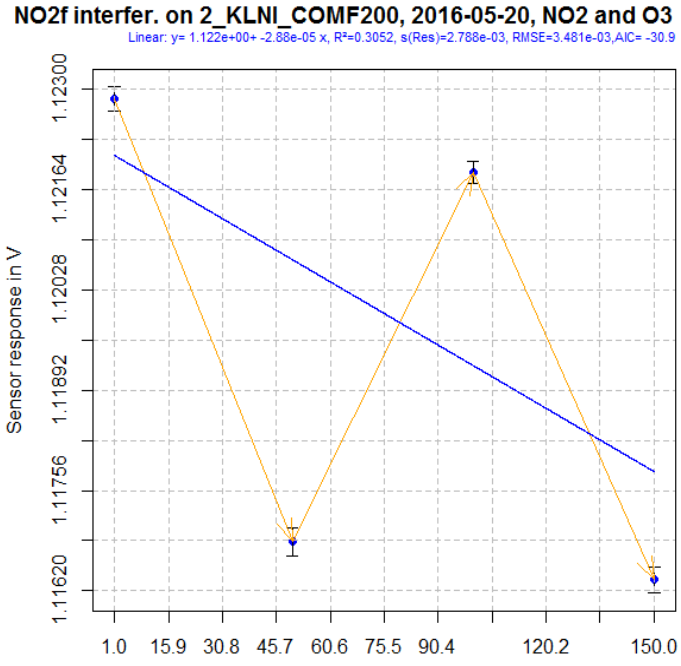

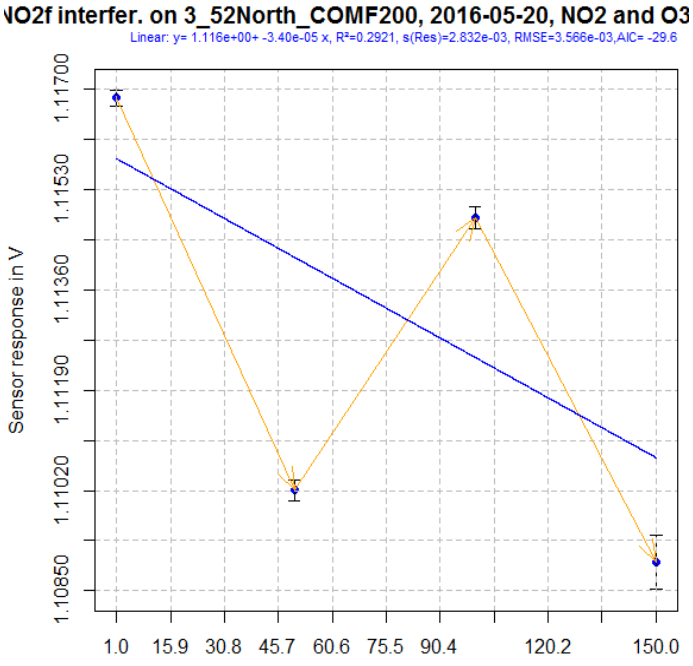

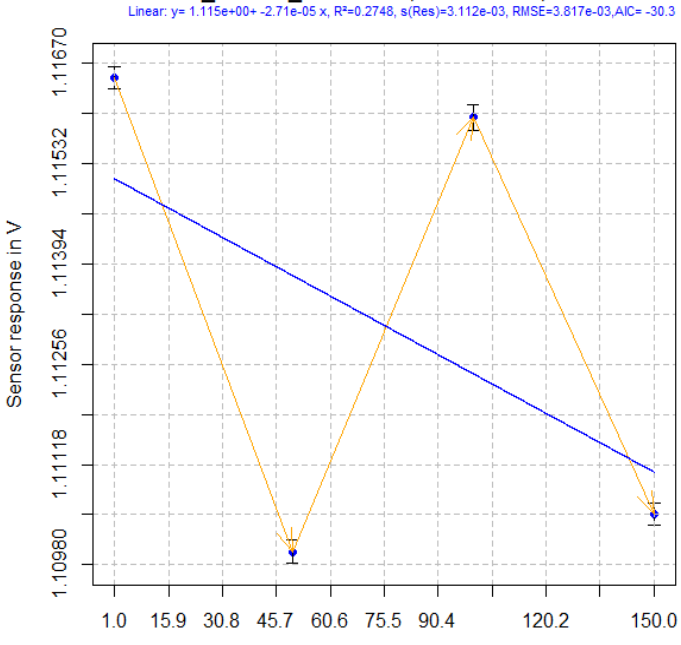

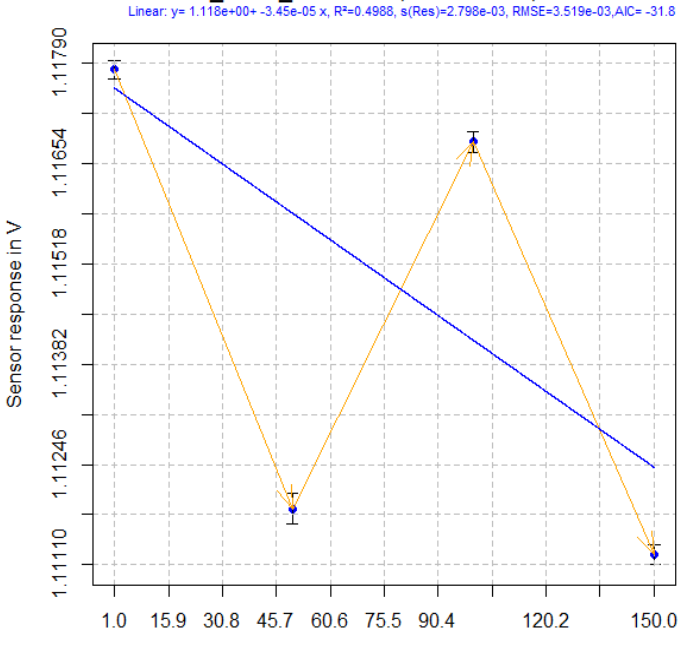

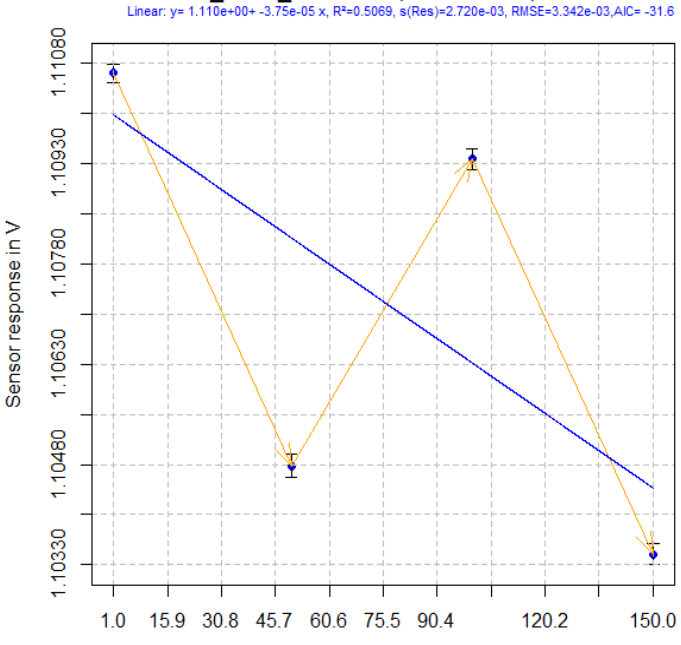

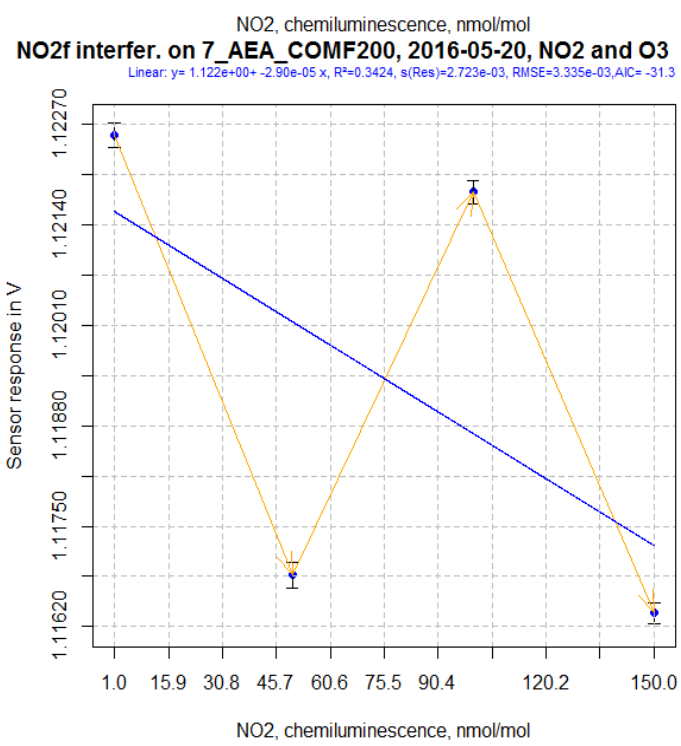

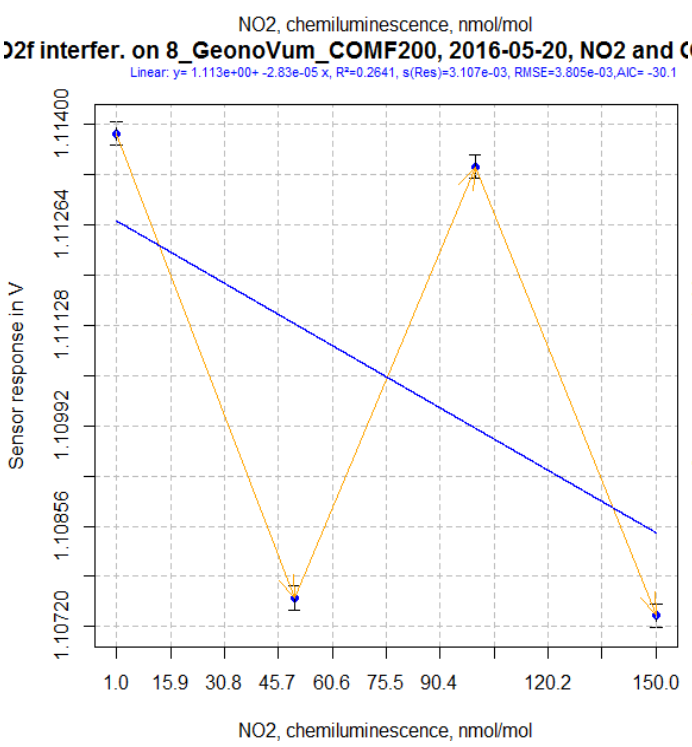

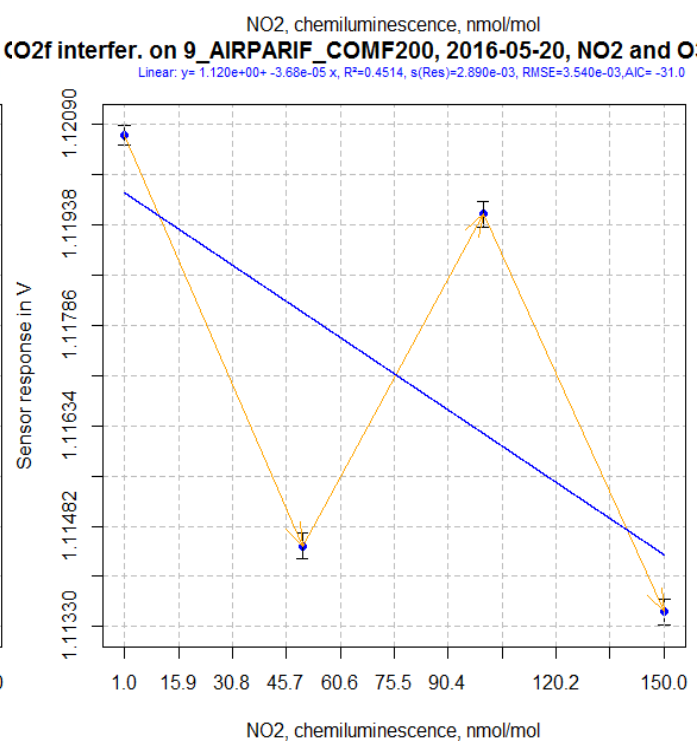

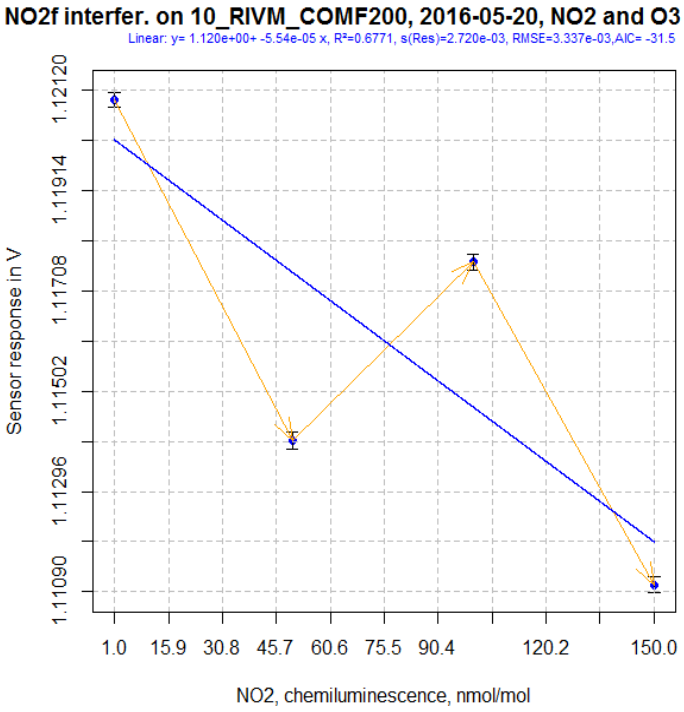

Figure 20: CO/MF-200 versus NO_2, NO_2 (0-150 ppb) and O_3 (0-90 ppb) interference

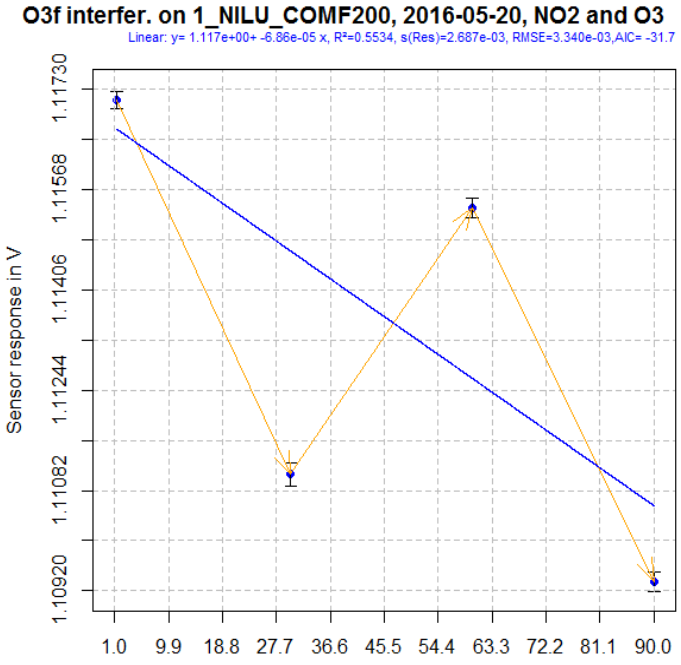

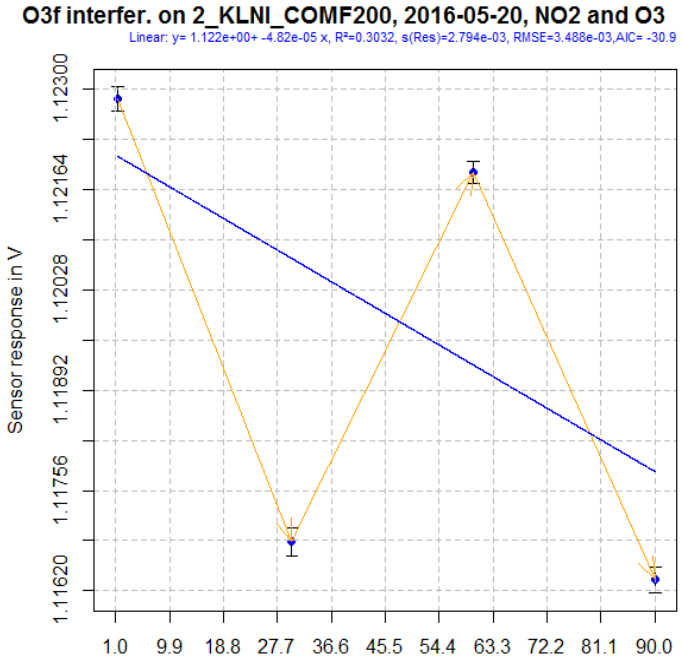

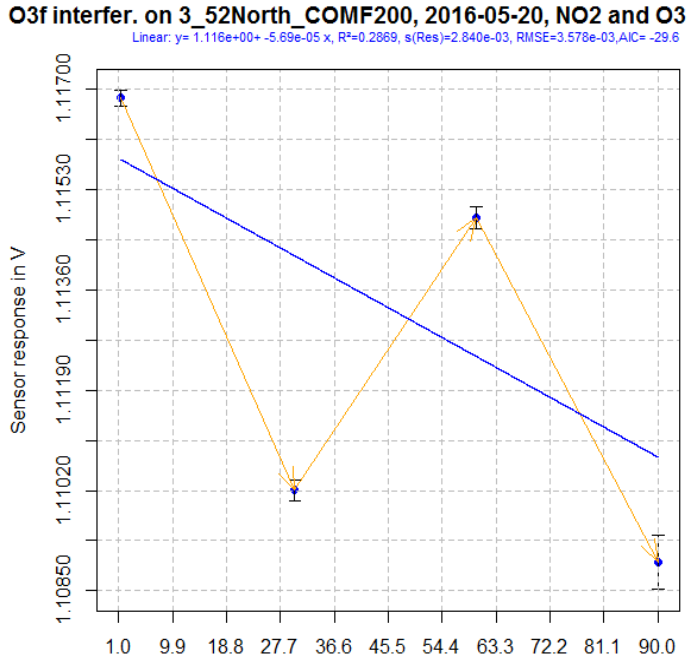

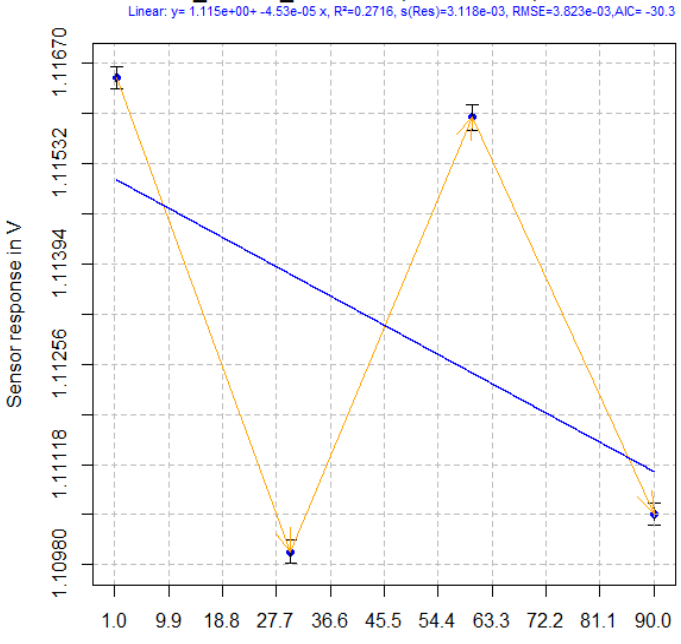

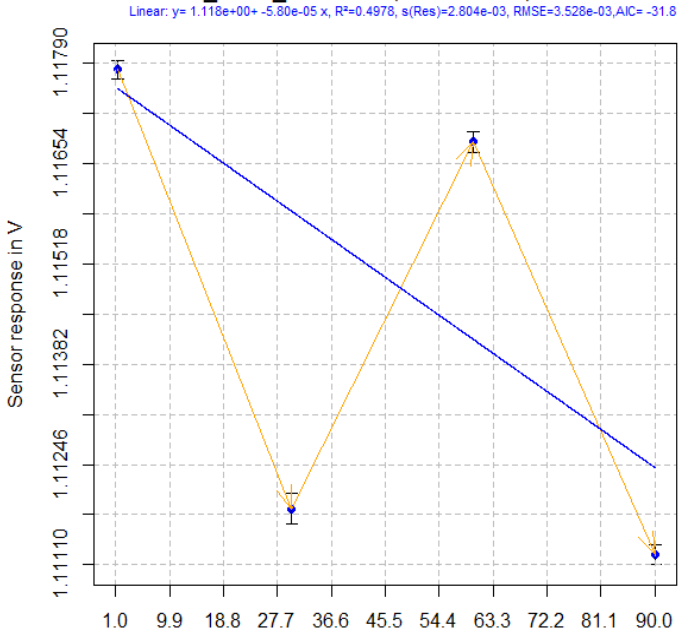

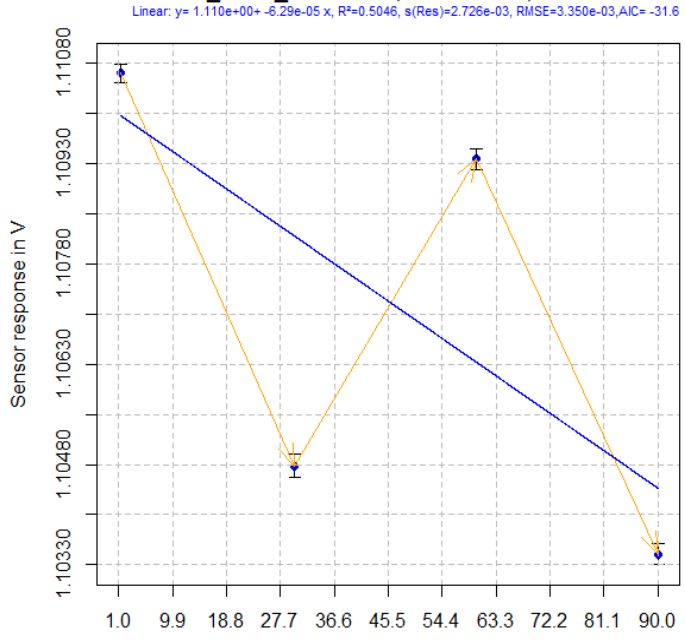

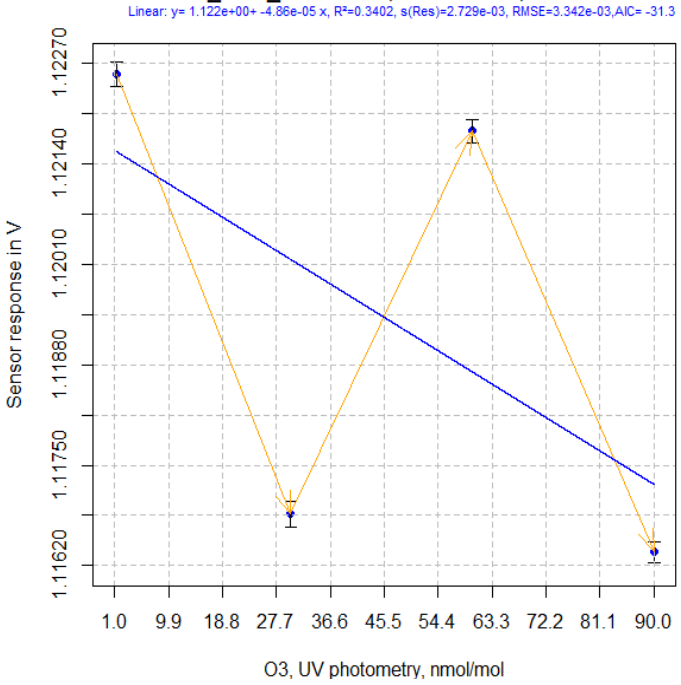

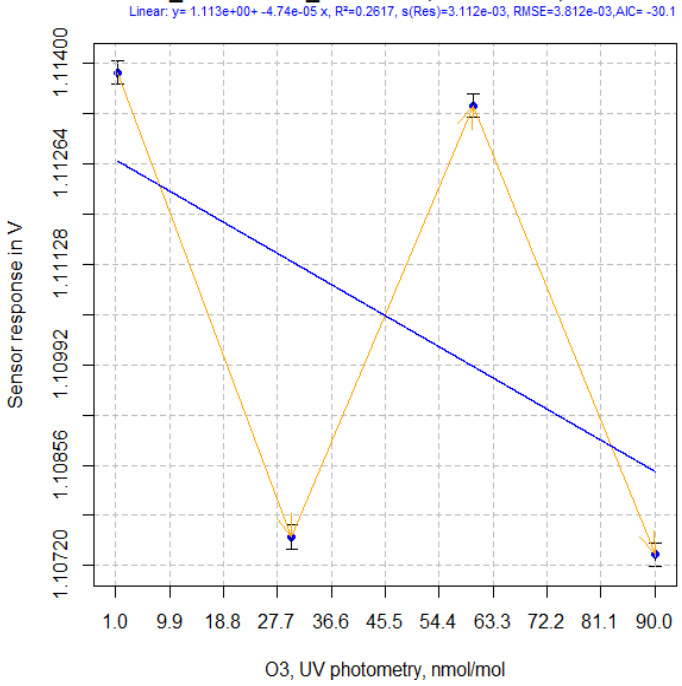

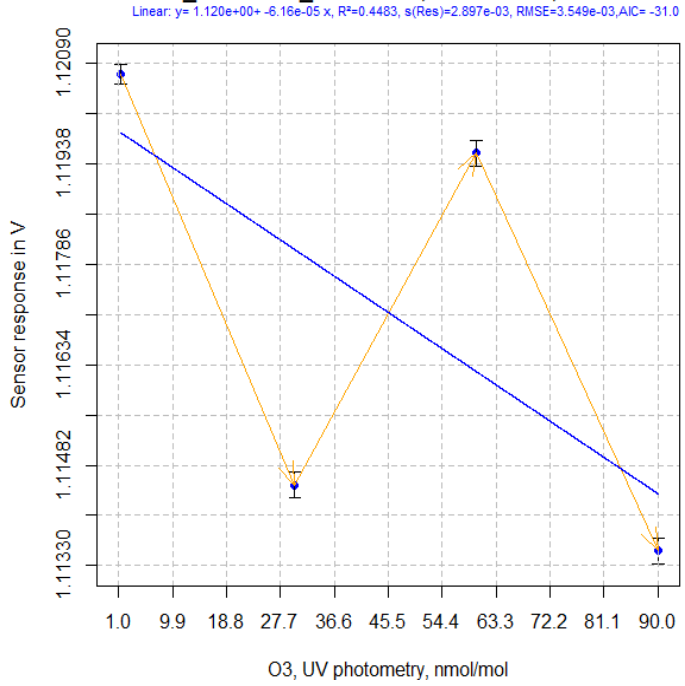

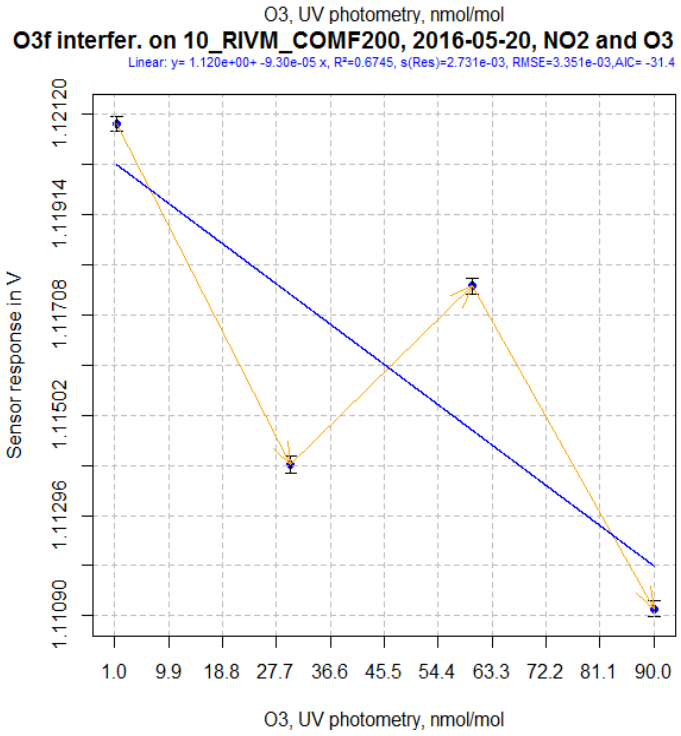

Figure 21: CO/MF-200 versus O_3, NO_2 (0-150 ppb) and O_3 (0-90 ppb) interference

4.1.3 O3/M-5 sensor

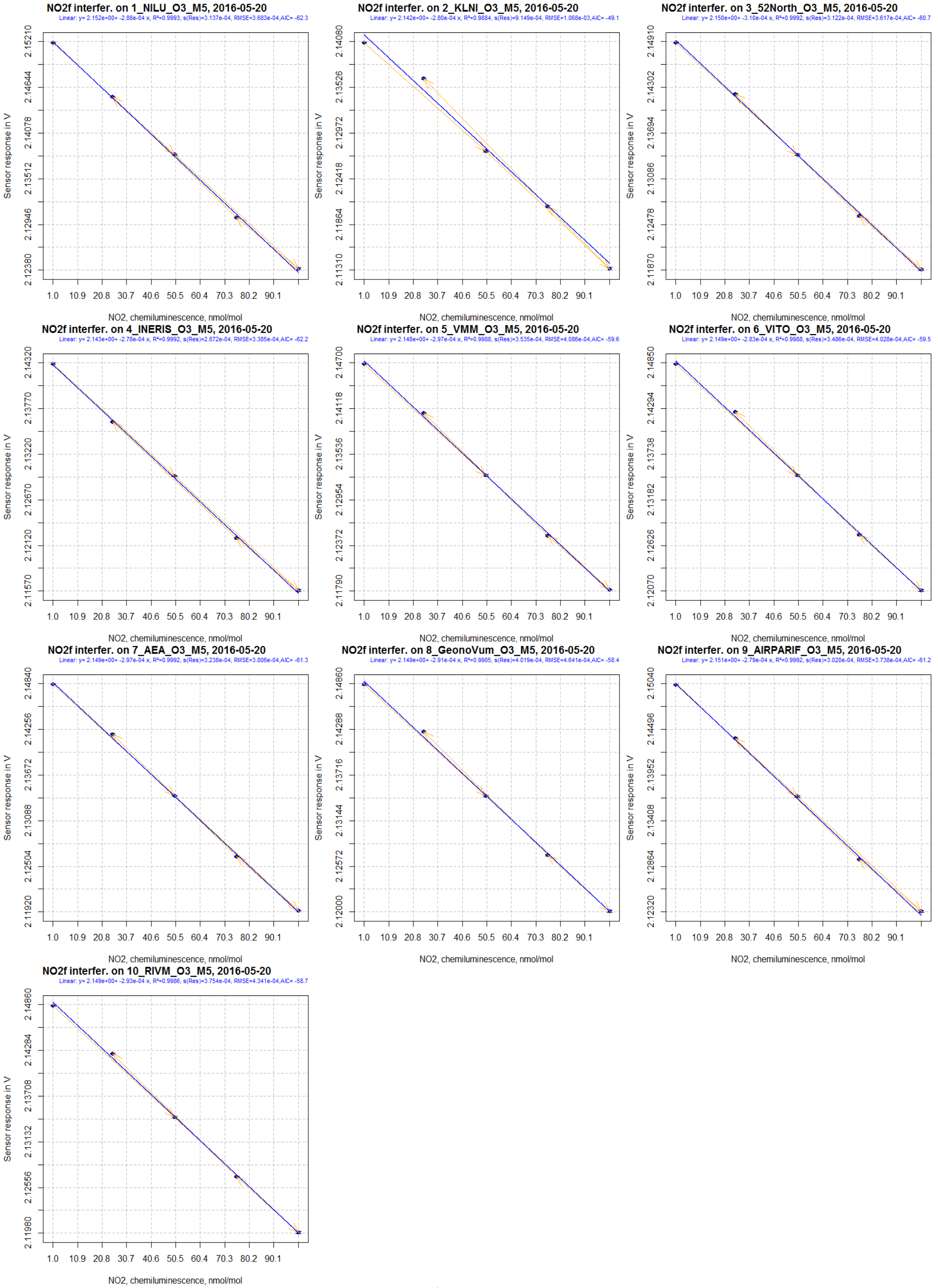

Figure 22: O3/M-5, NO_2 cross-sensitivity

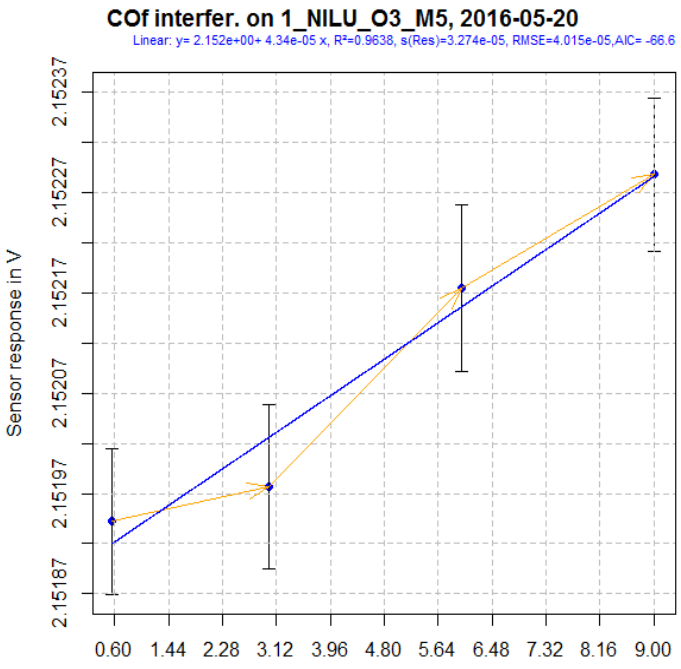

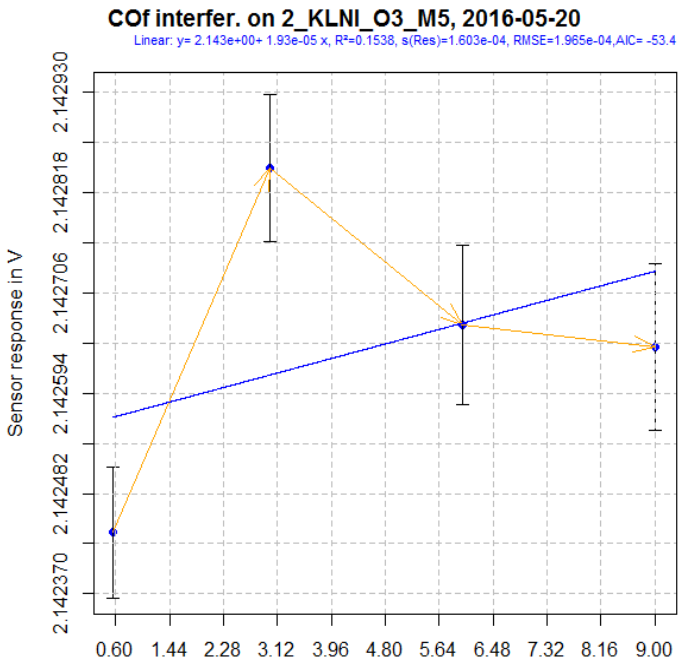

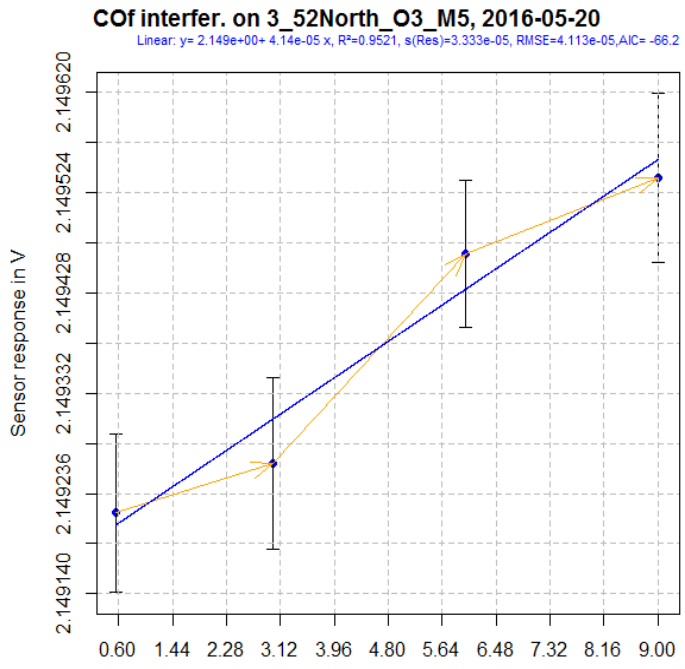

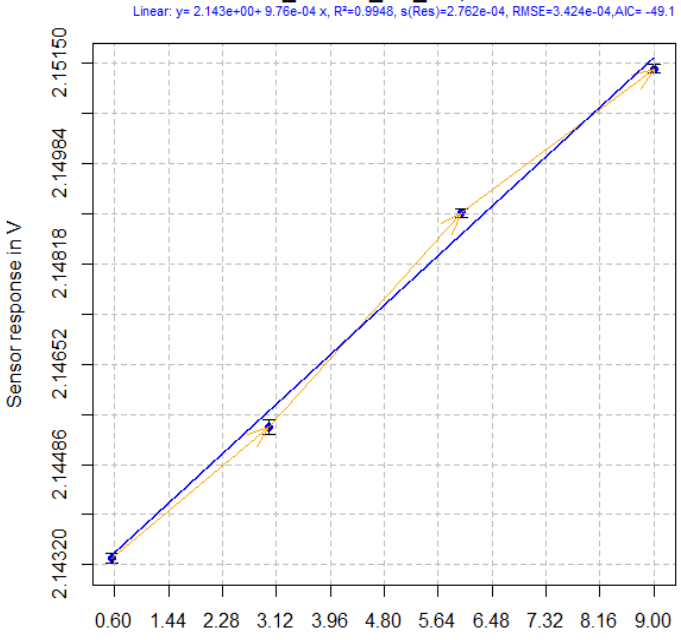

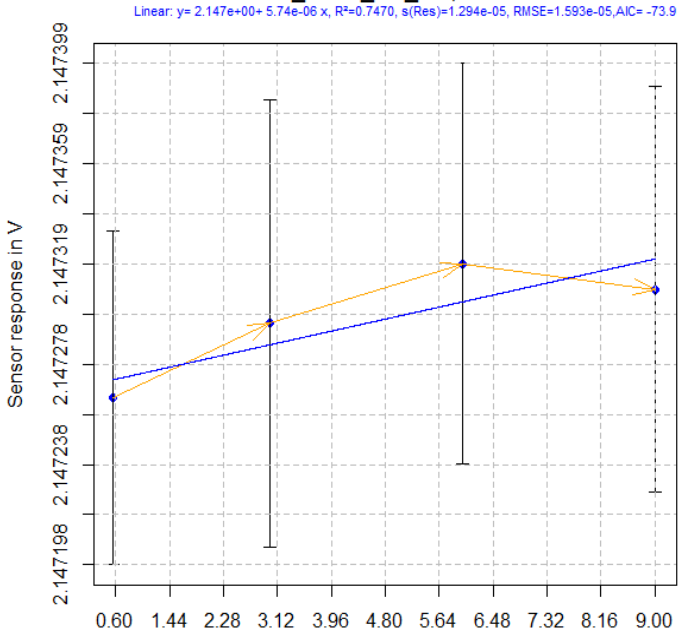

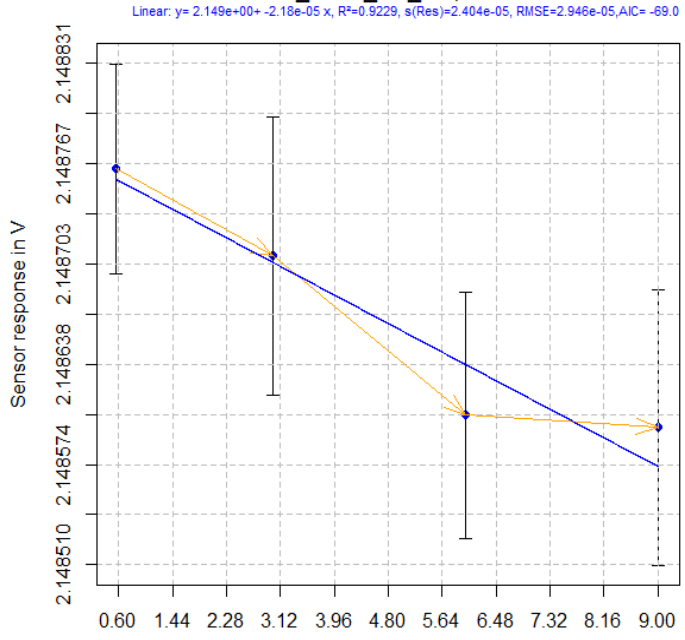

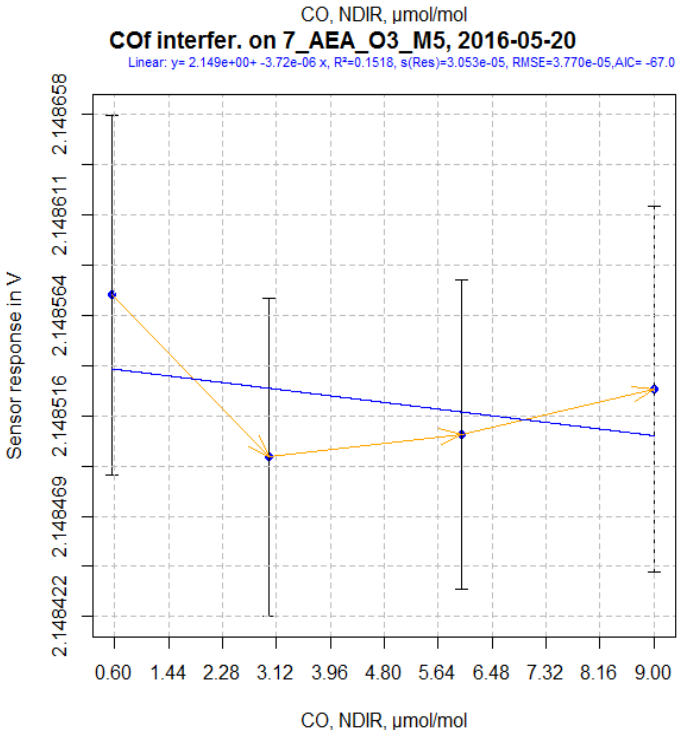

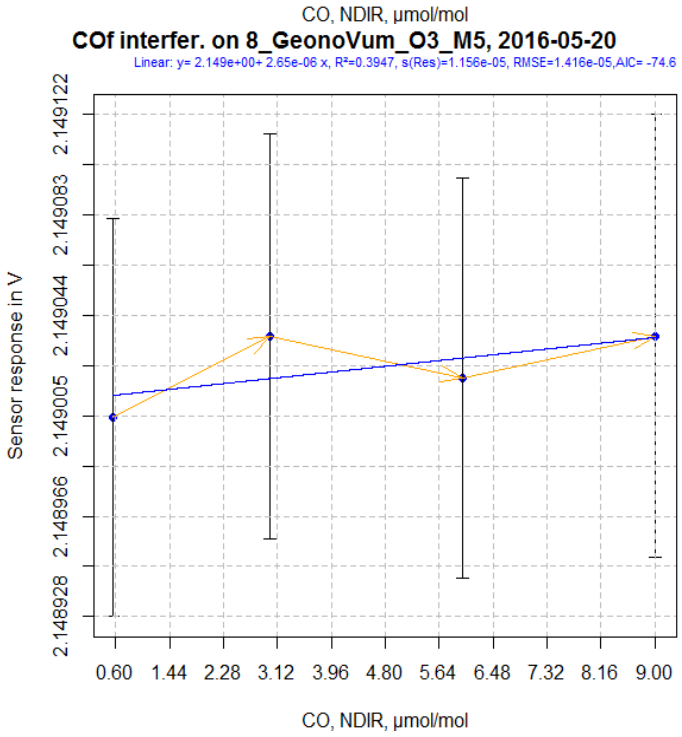

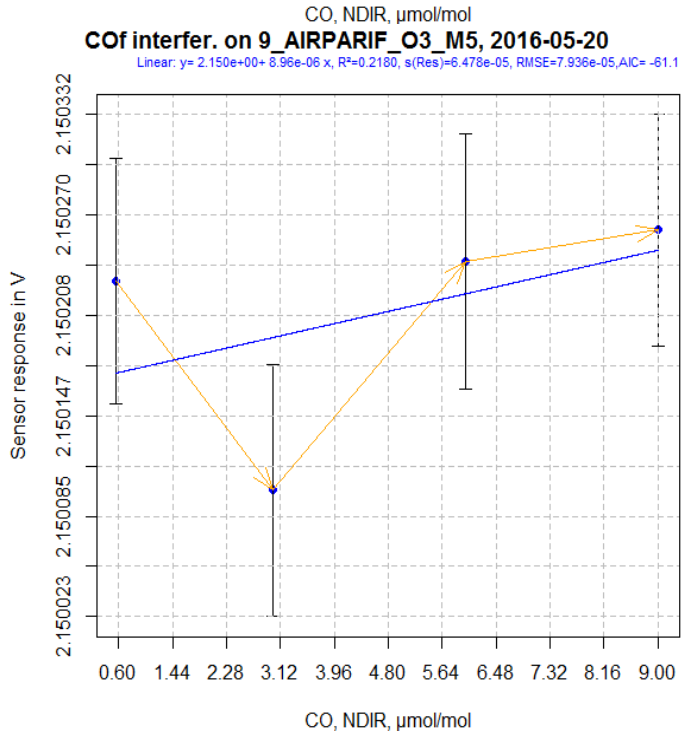

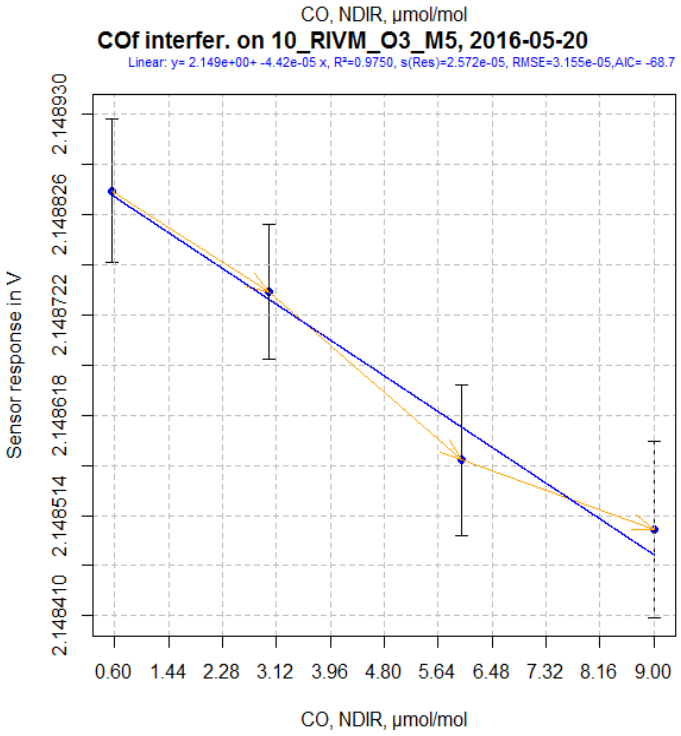

Figure 23: O3/M-5, CO cross-sensitivity

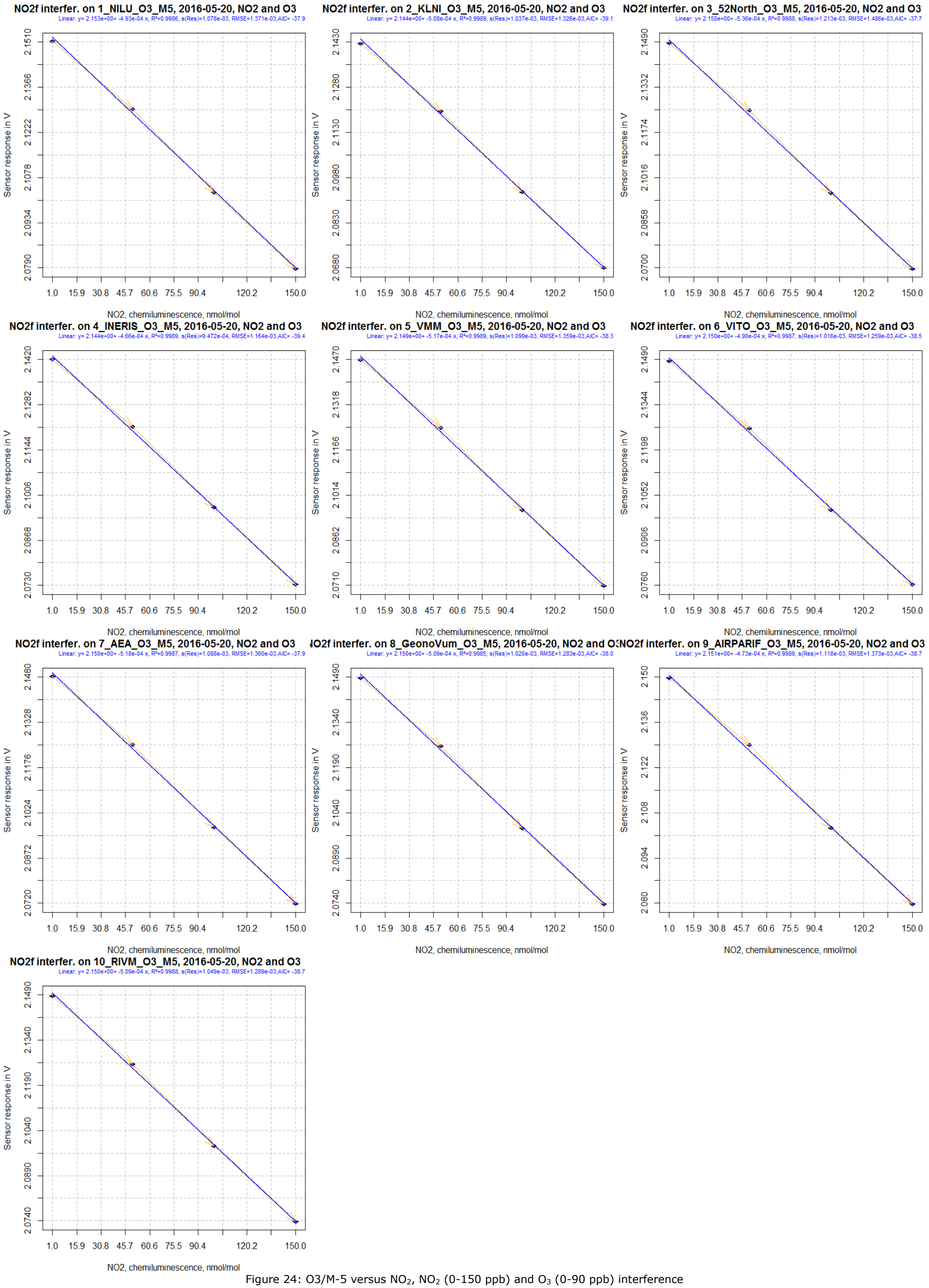

Figure 24: O3/M-5 versus NO_2, NO_2 (0-150 ppb) and O_3 (0-90 ppb) interference

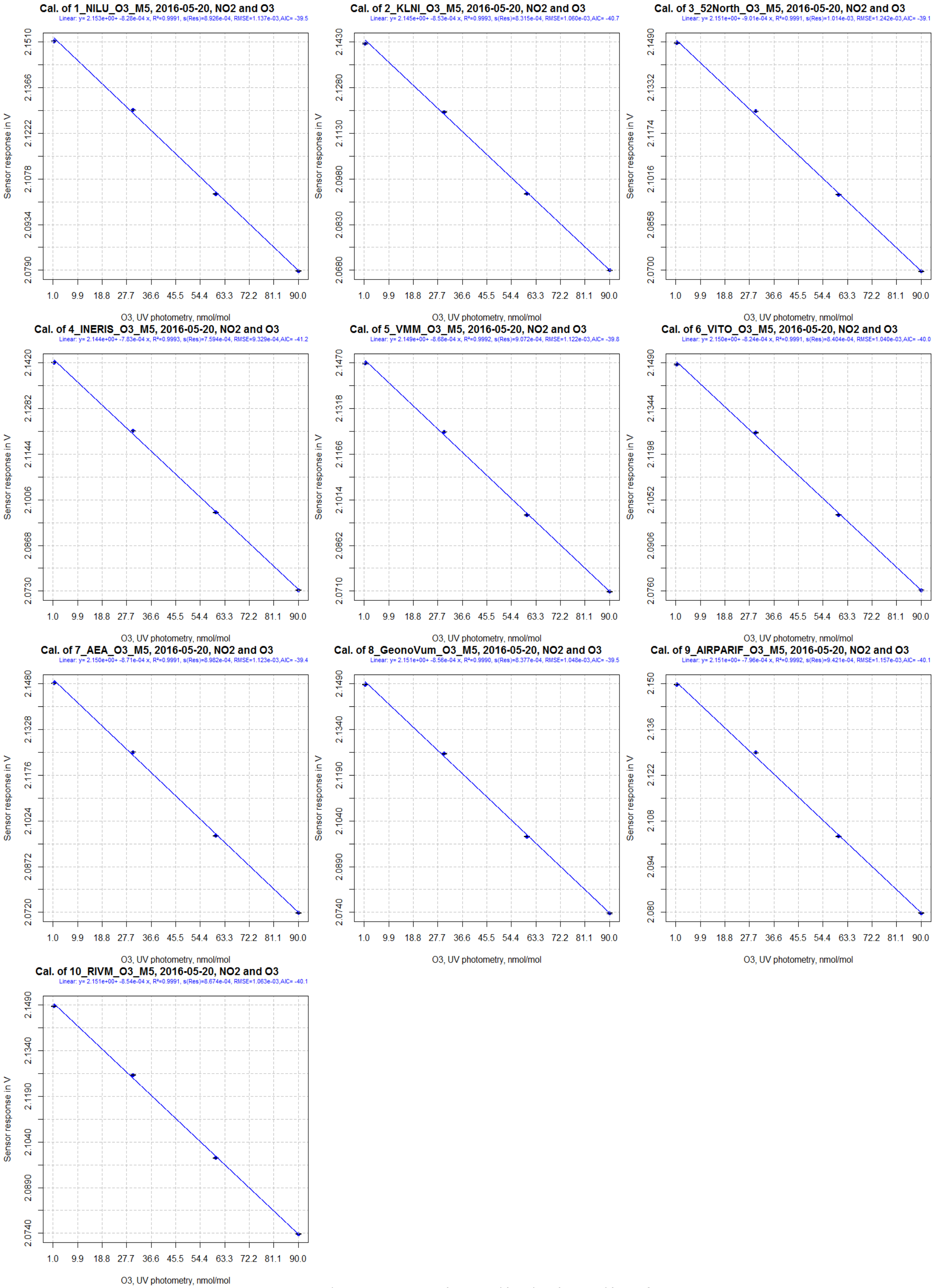

Figure 25: O3/M-5 versus O_3, NO_2 (0-150 ppb) and O_3 (0-90 ppb) interference

4.1.4 NO-B4 sensor

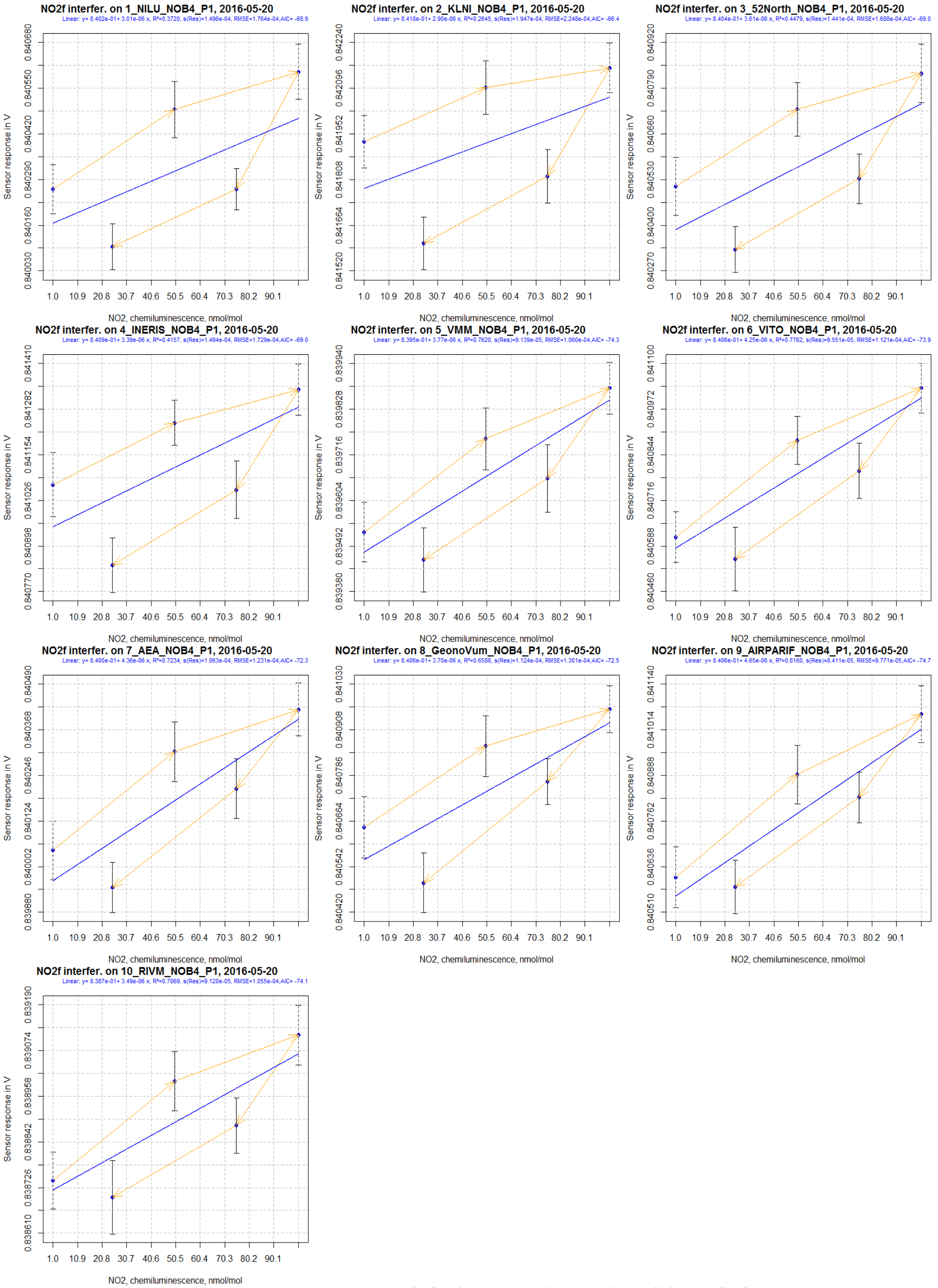

Figure 26: NO-B4, NO_2 cross-sensitivity (in fact the sensor signal correspond to small changes of NO)

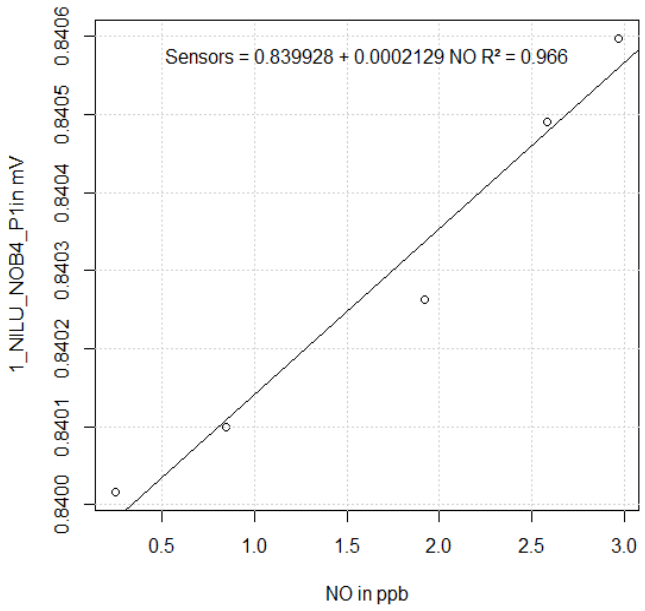

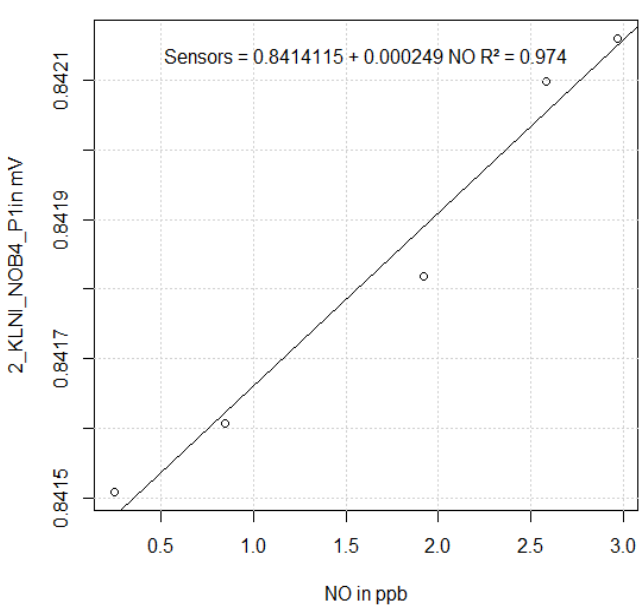

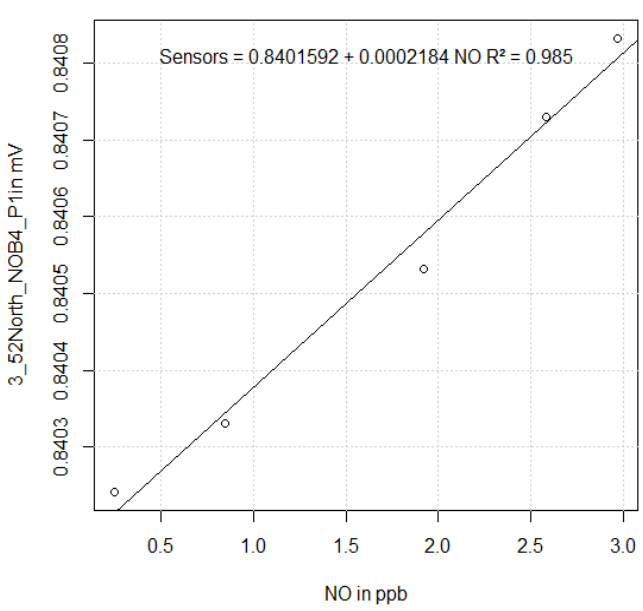

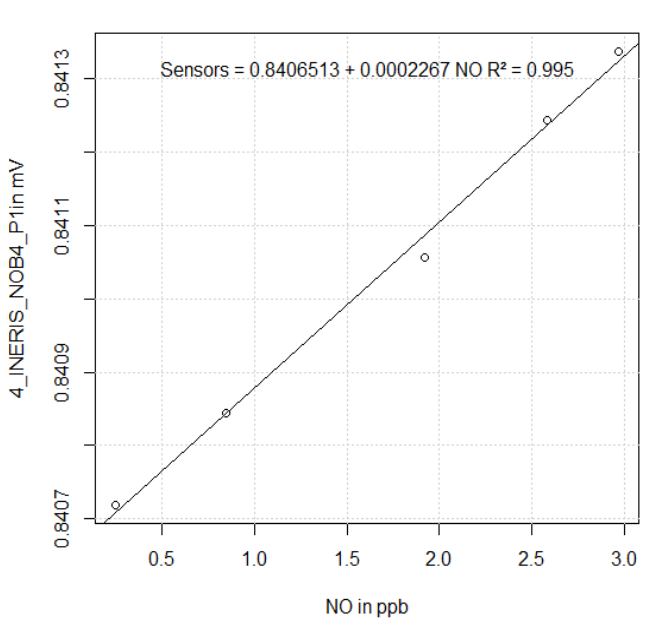

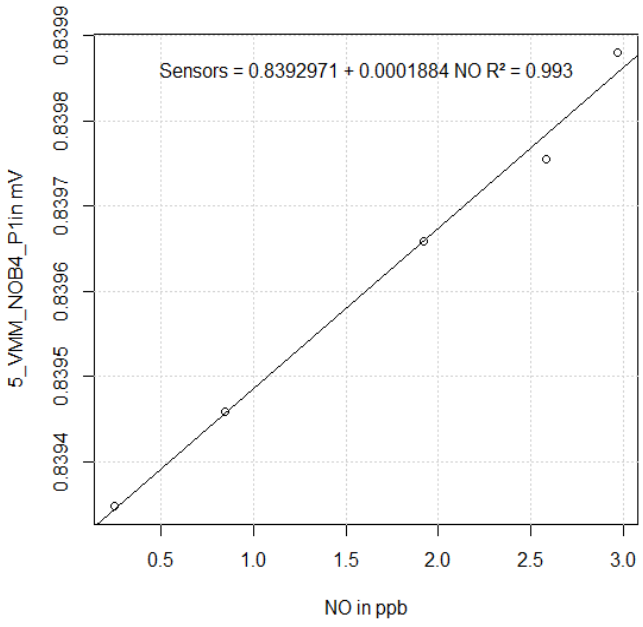

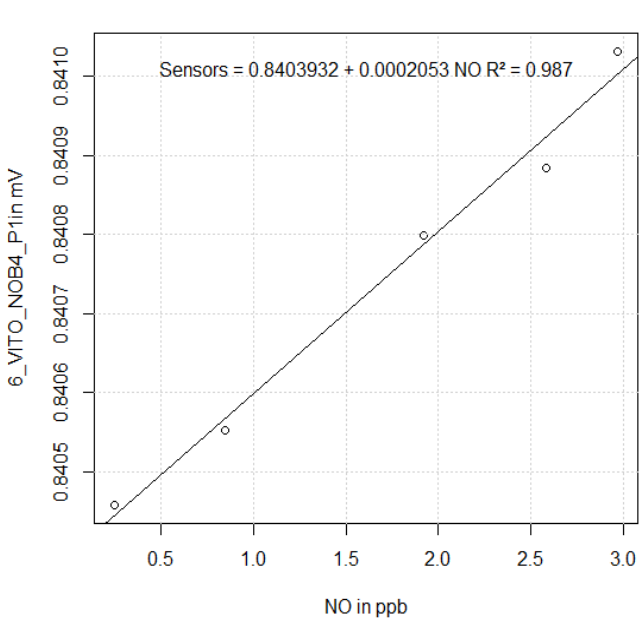

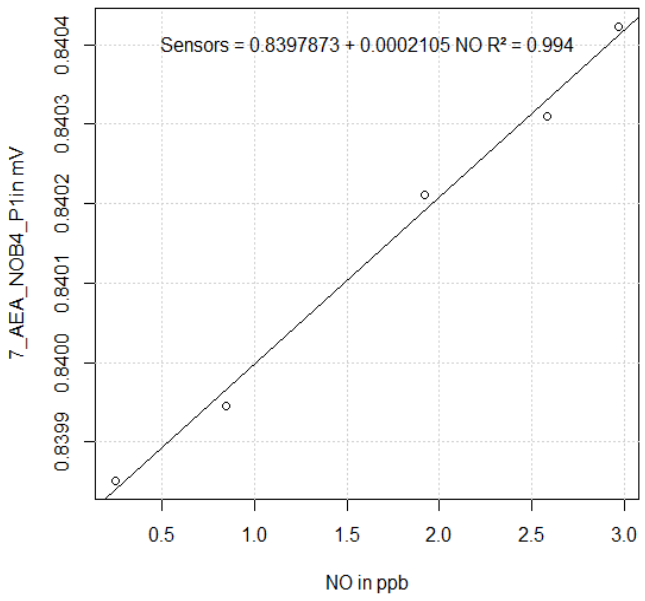

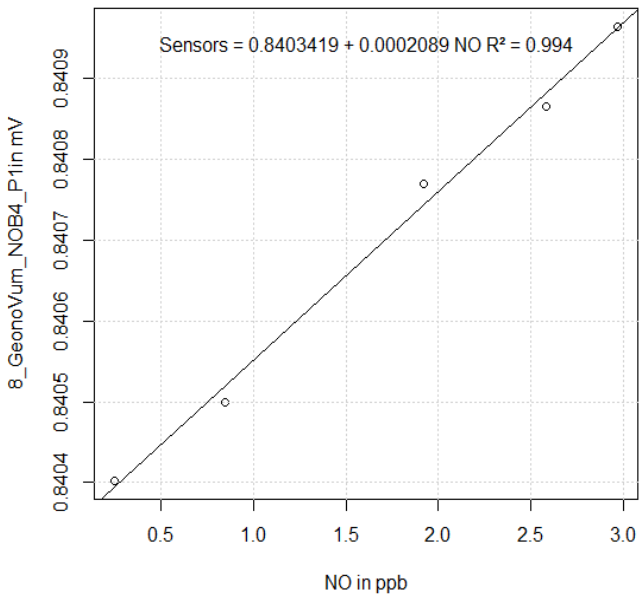

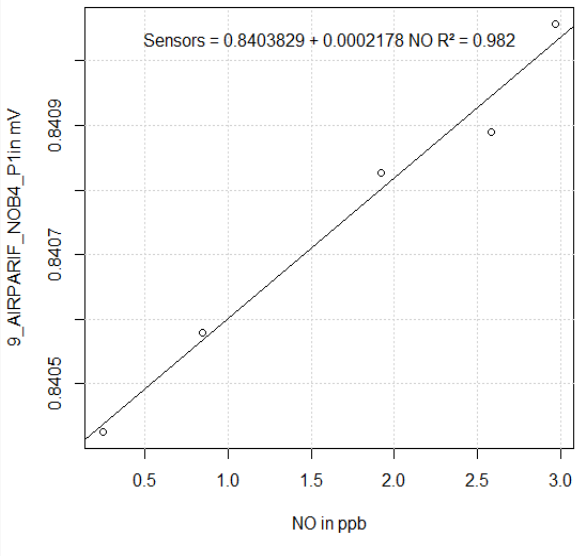

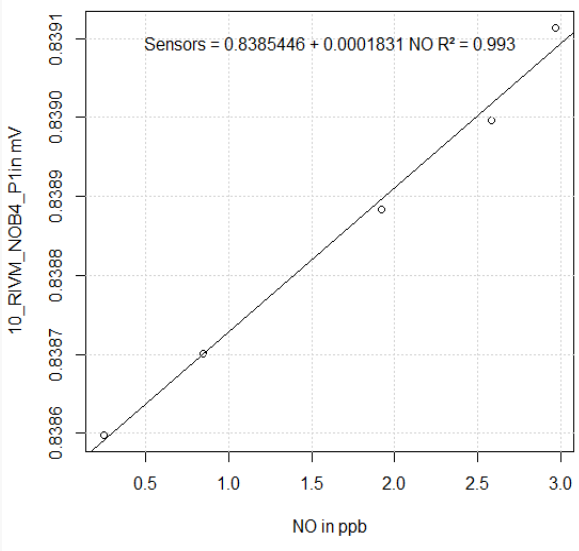

Figure 27: NO effect wrongly attributed to NO_2 on NO-B4 sensors

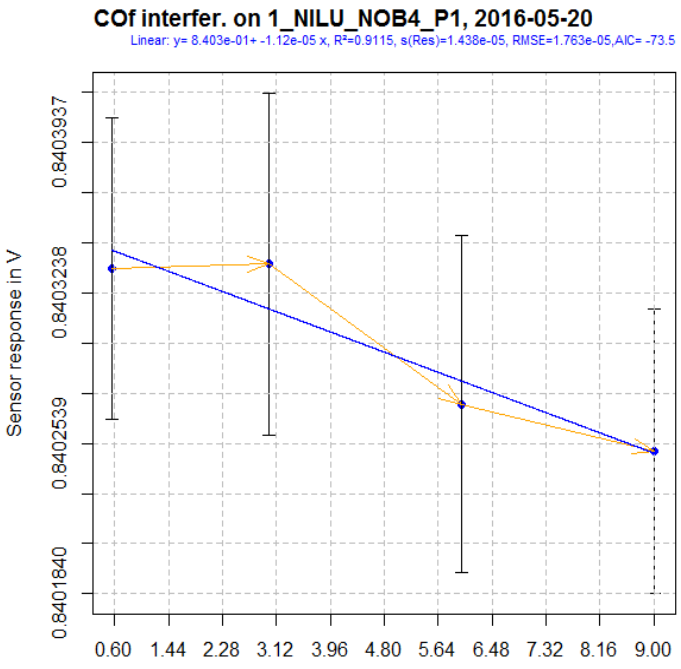

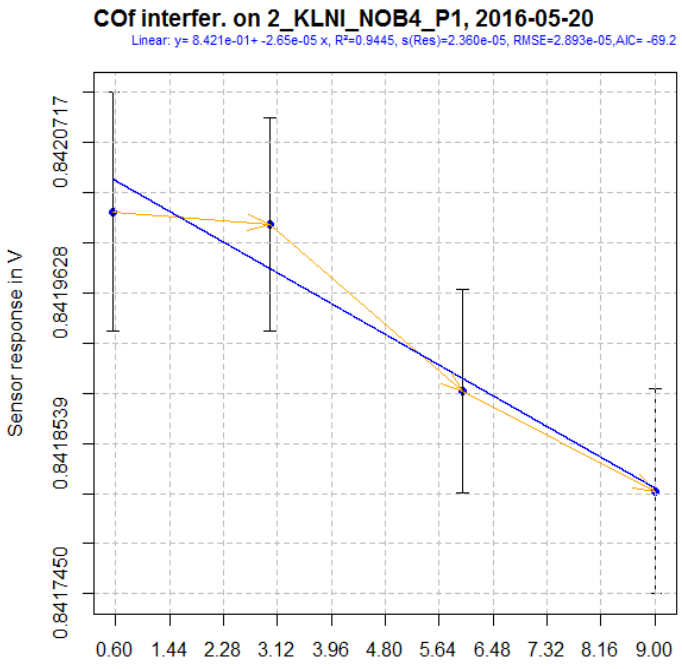

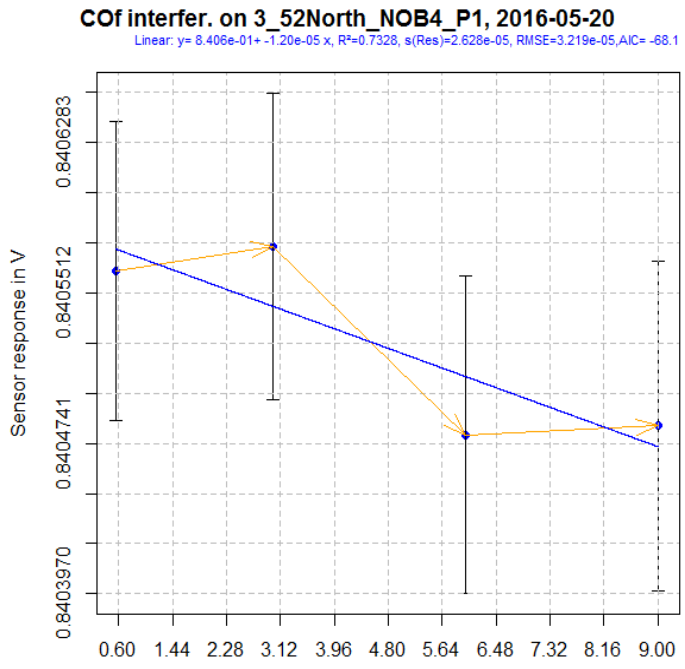

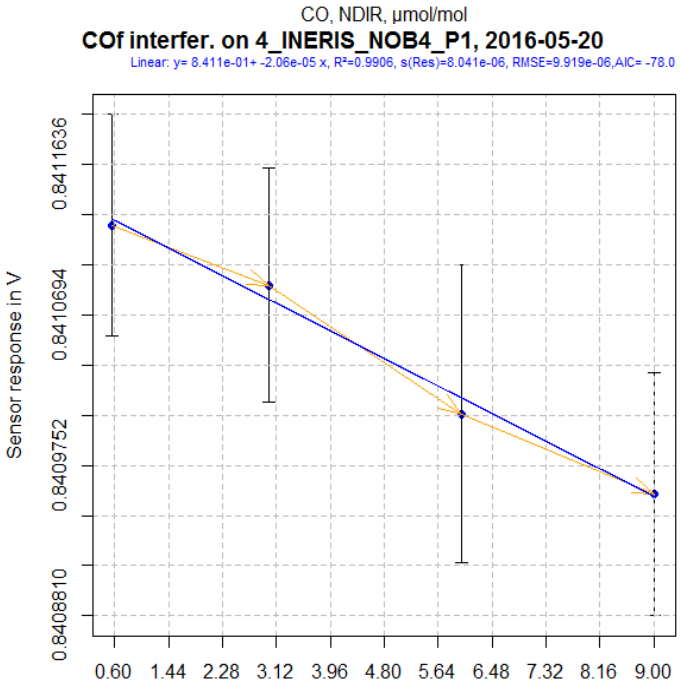

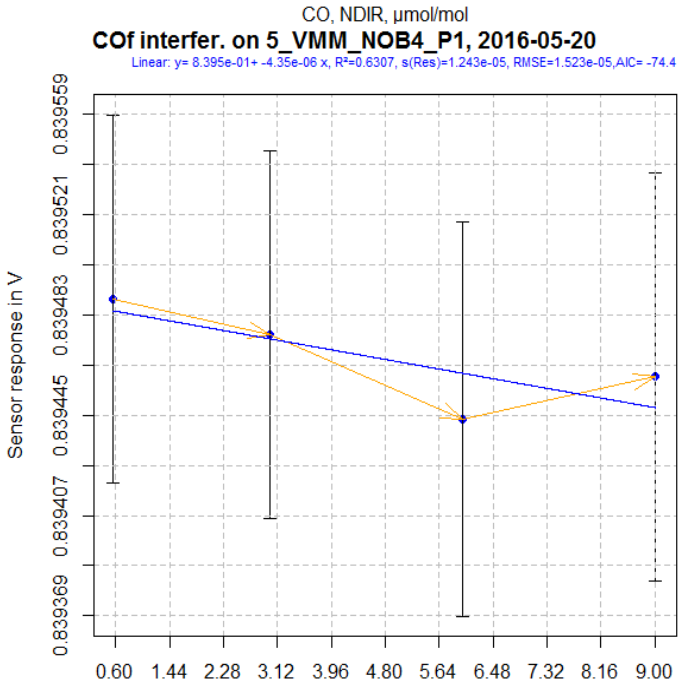

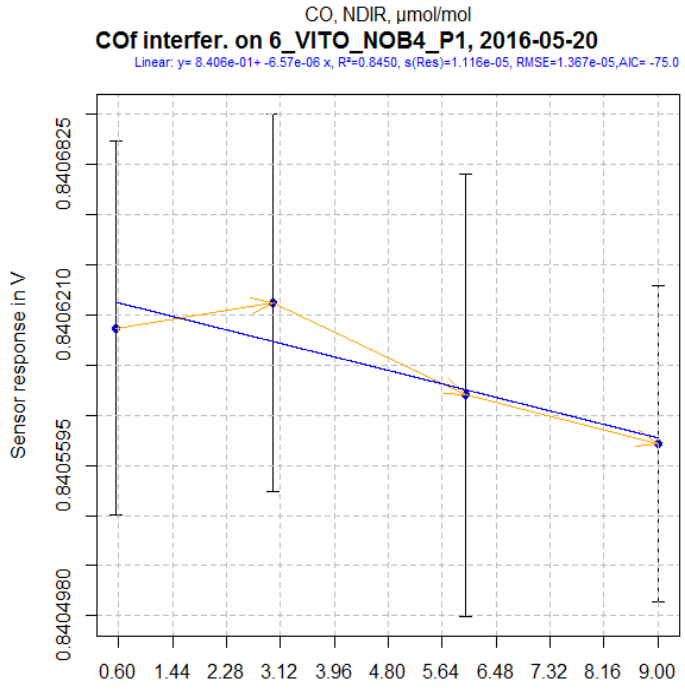

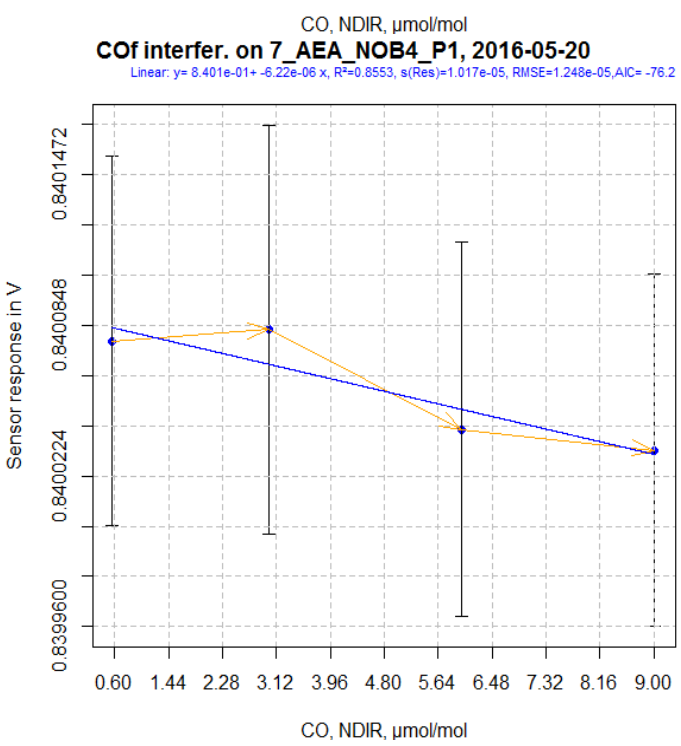

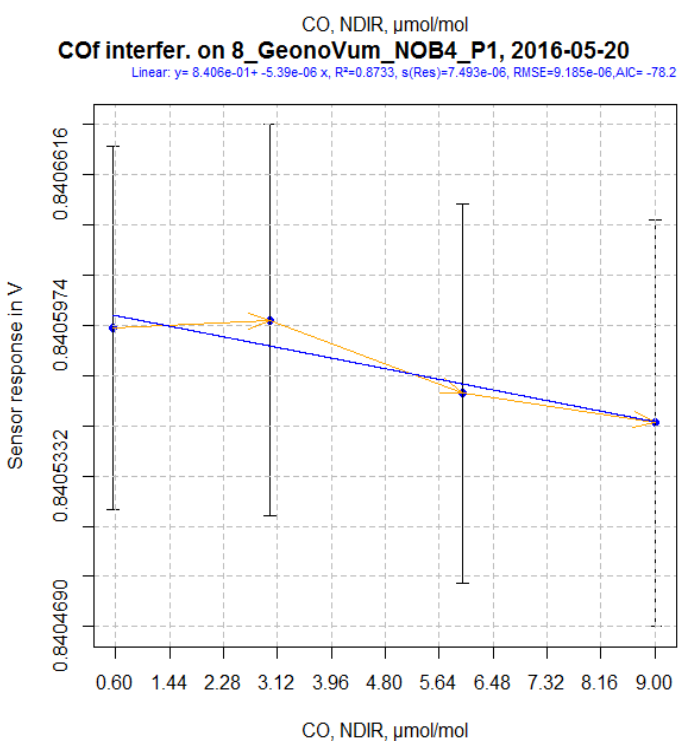

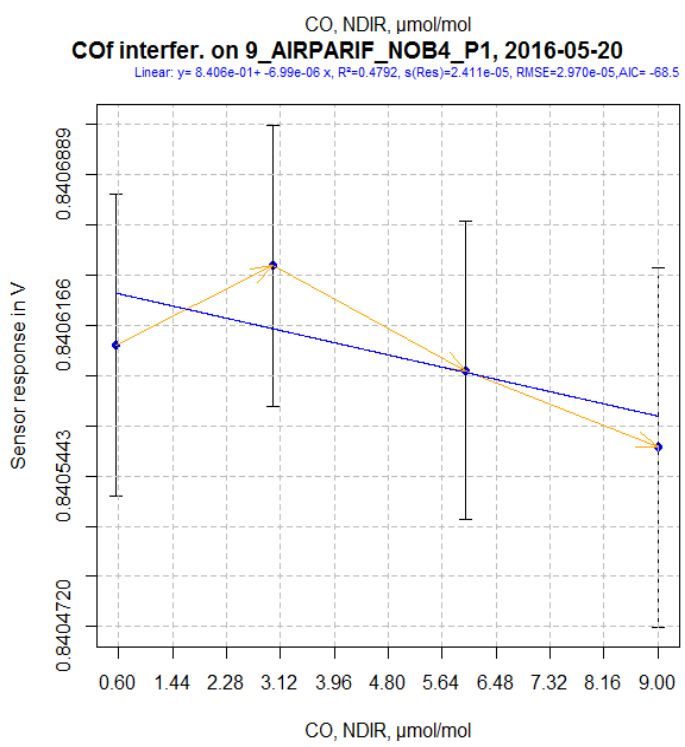

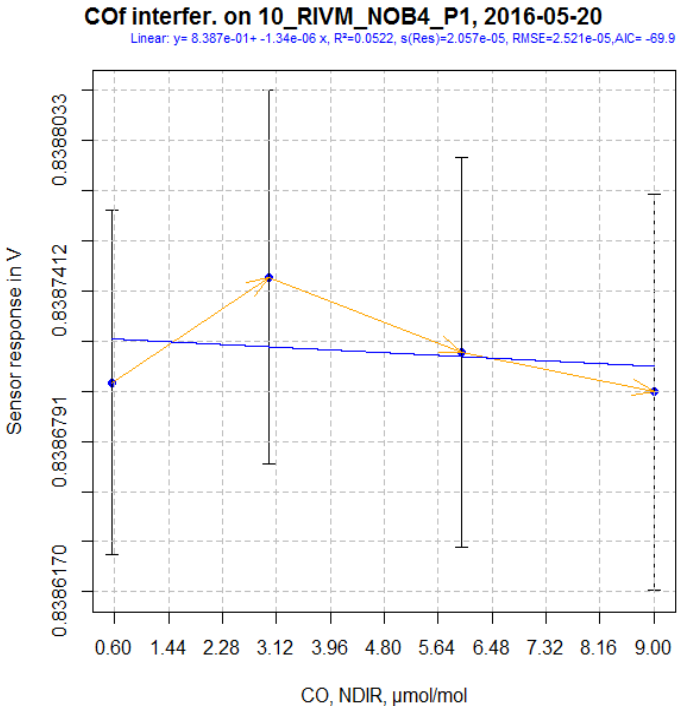

Figure 28: NO-B4, CO cross-sensitivity

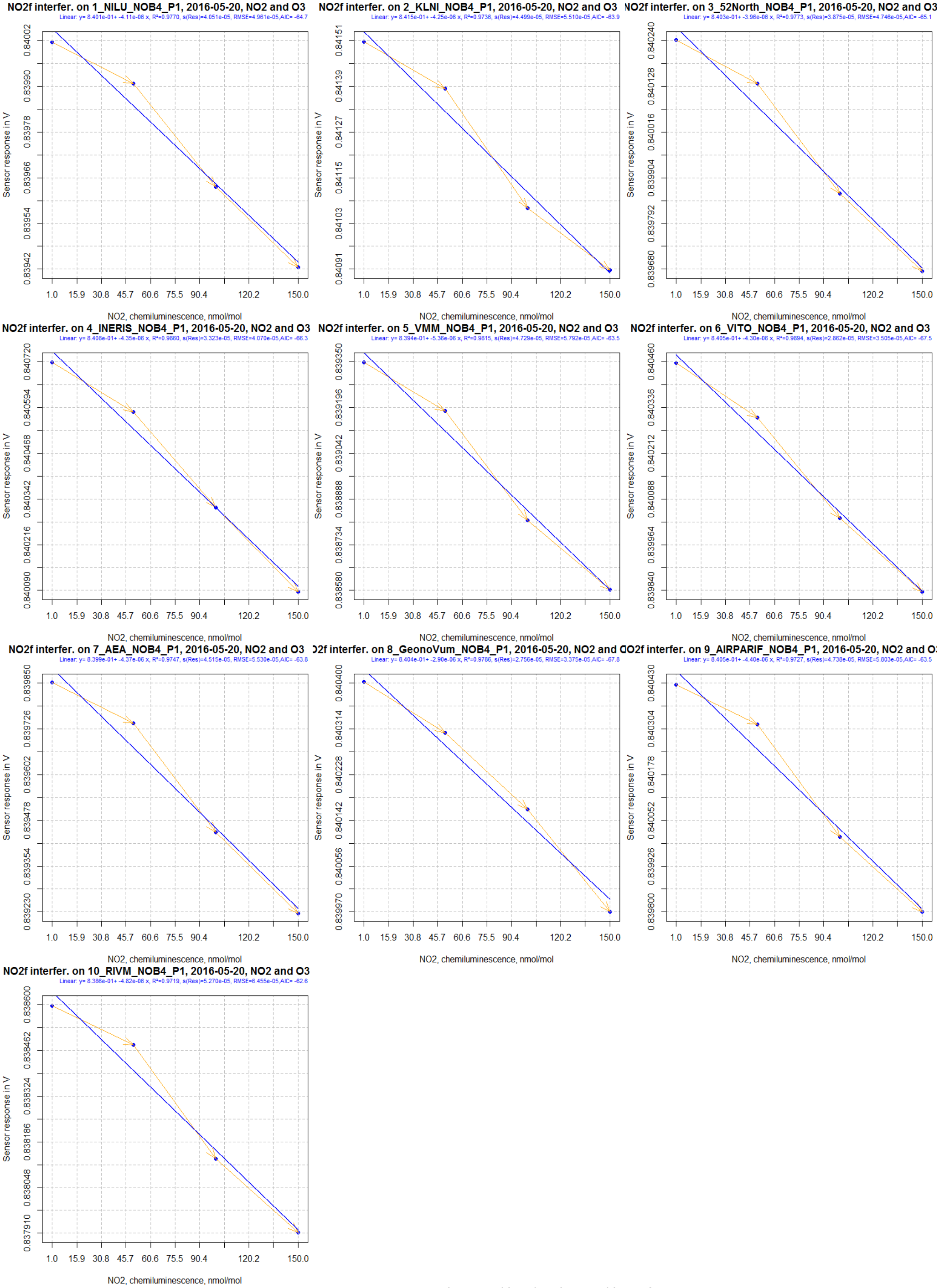

Figure 29: NO-B4 versus NO_2, NO_2 (0-150 ppb) and O_3 (0-90 ppb) interference

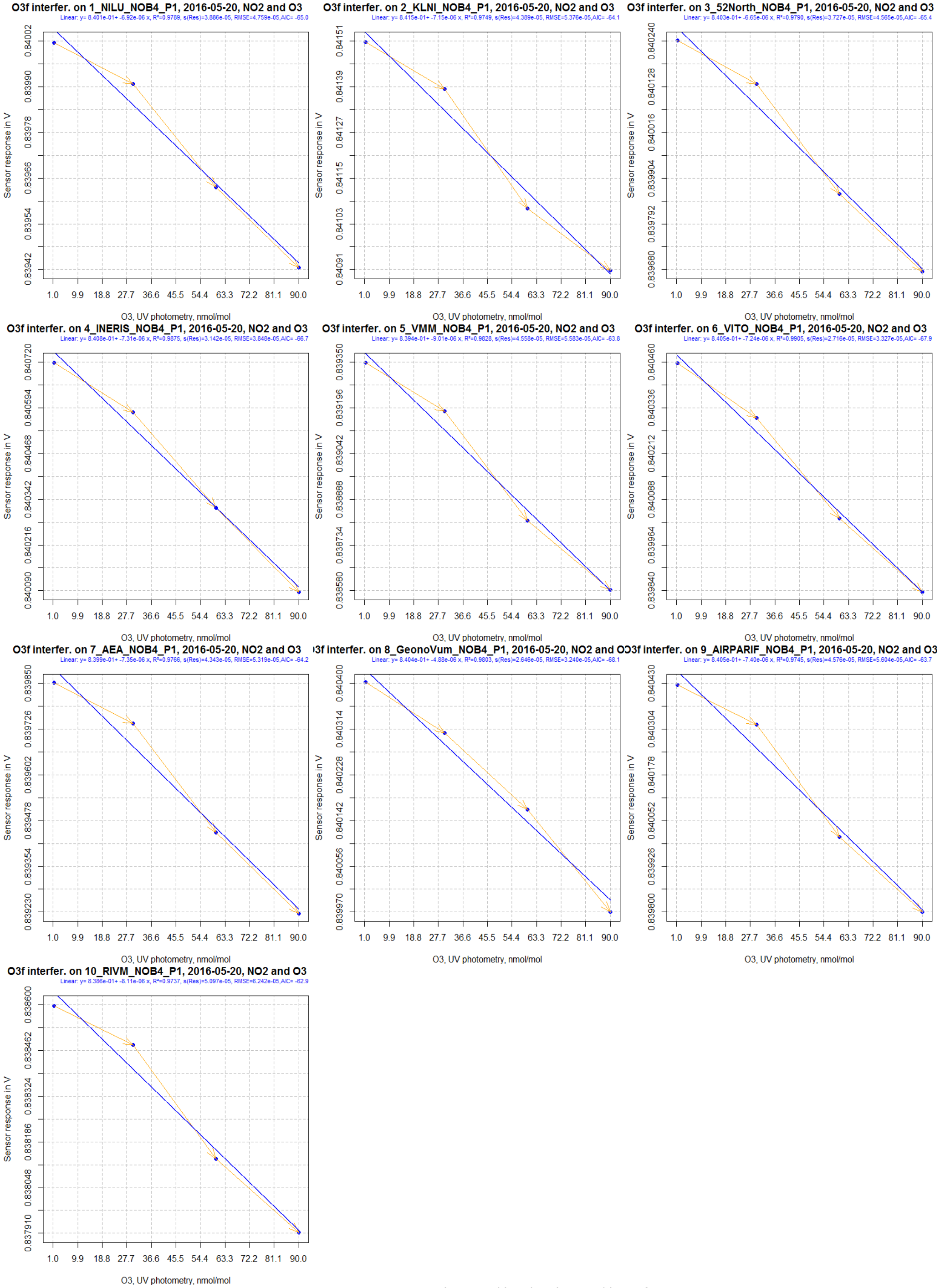

Figure 30: NO-B4 versus O_3, NO_2 (0-150 ppb) and O_3 (0-90 ppb) interference

4.1.5 Selection of data steps within the experiment

1_NILU_O_3_M5 on 2016-05-20, COf steps

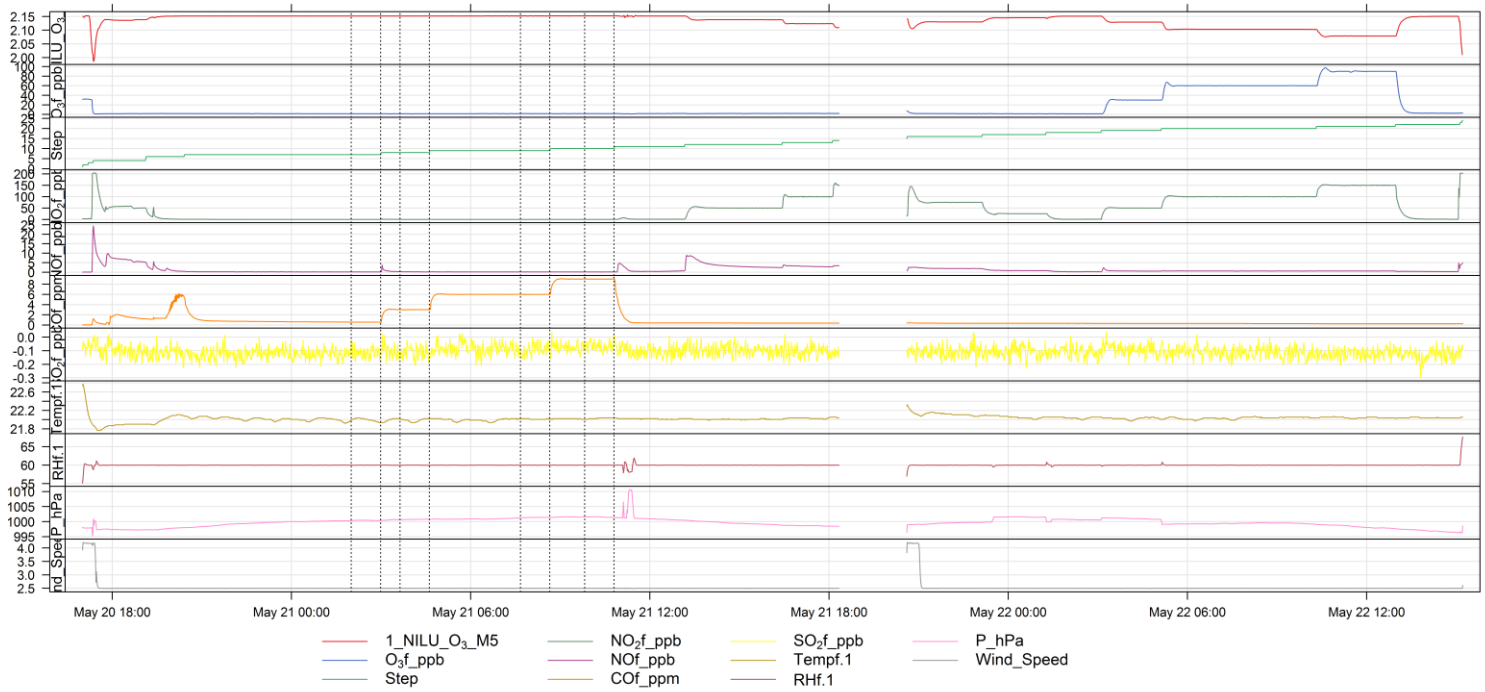

1_NILU_COMF200 on 2016-05-20, NO_2f steps

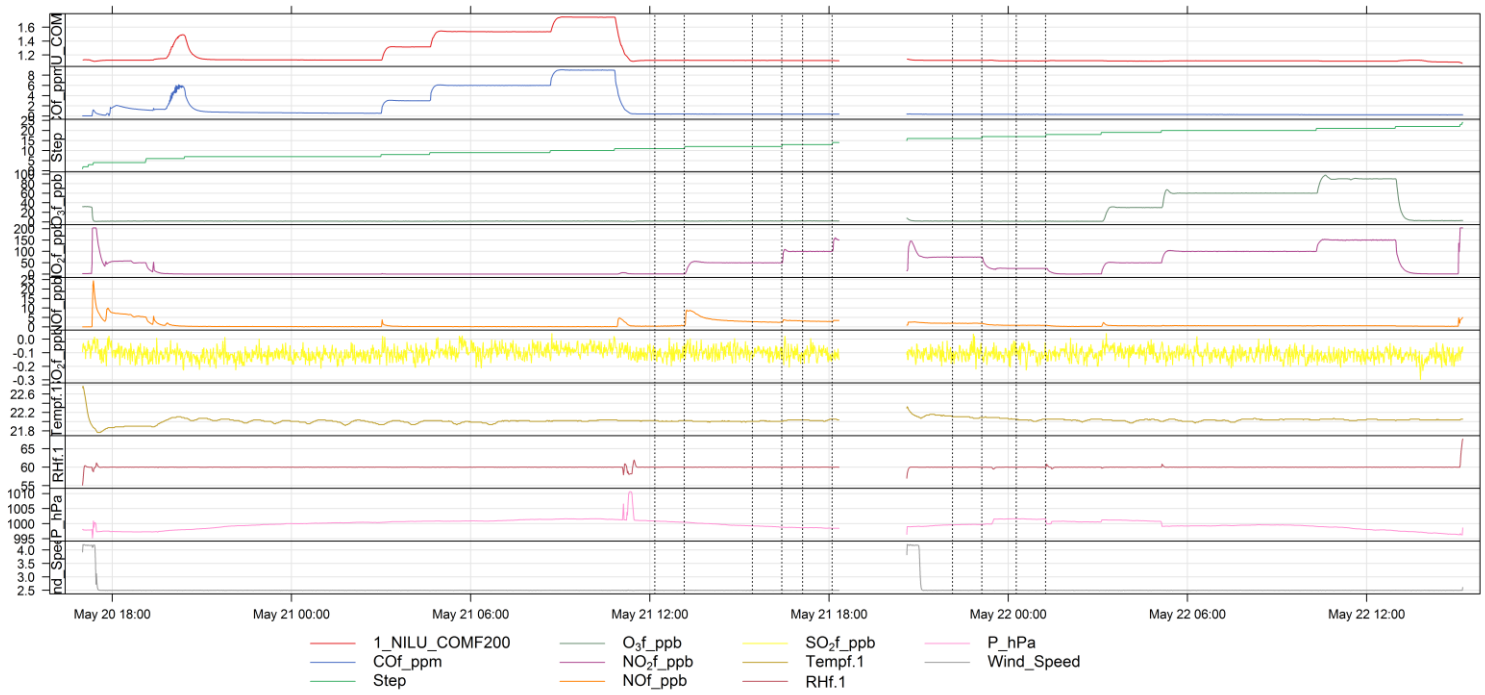

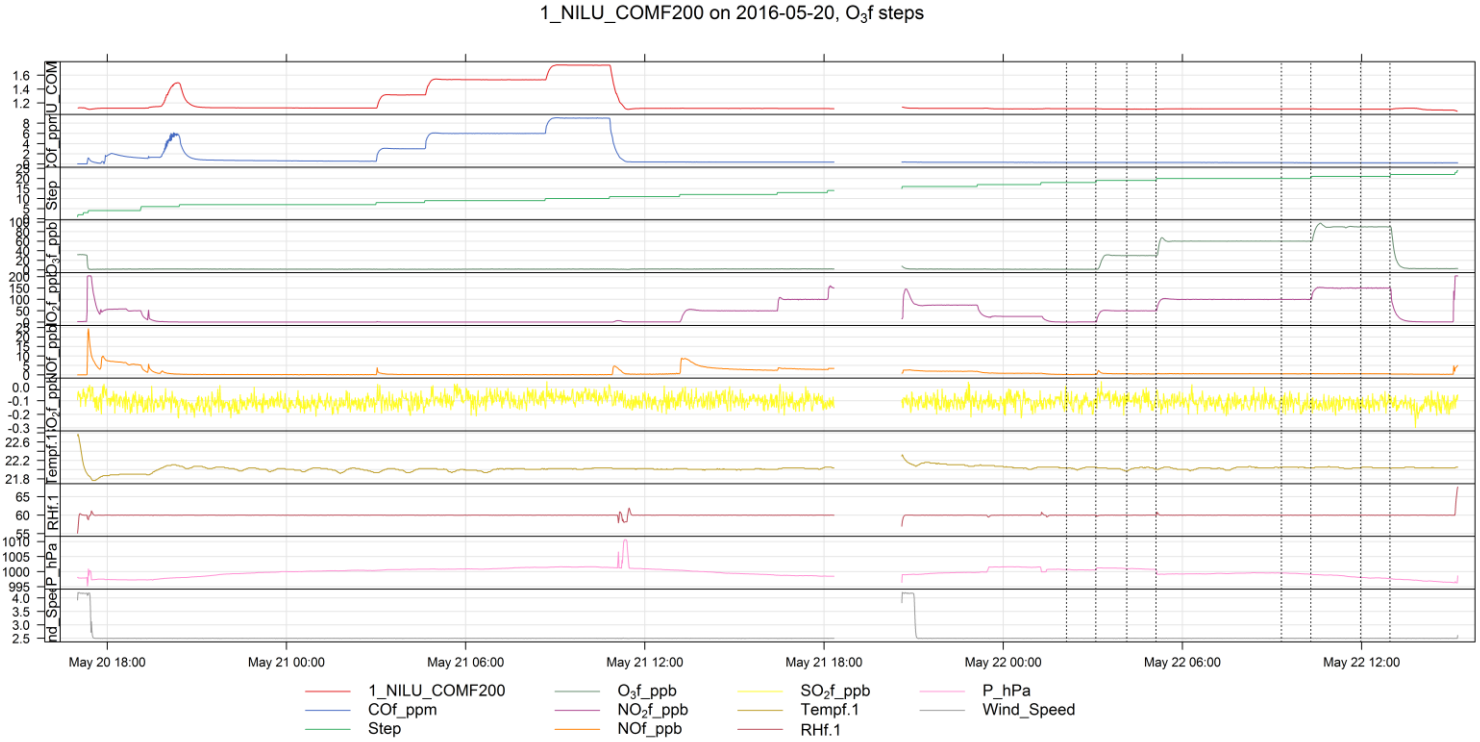

Figure 31: Selection of the CO steps (up), NO_2 steps (middle) and NO_2/O_3 steps (below) for the evaluation the Membrapor CO-MF200 sensors. For the step at 30 ppb of ozone the sensor reading appears to be unstable while all available measured parameters appear to be almost stable (O_3, NO_2, NO, SO_2, temperature, humidity and pressure).

4.2 CO, NO_2 and NO_2/O_3 together tests tabulated results

The following figures and tables give the effect of each compound on the set of 10 sensors (sensor readings in volt versus reference values in ppb or ppm) to estimate the scattering of sensor readings (see rows labelled Means and relative standard deviation (RSD). The tables give the sensor model types, the intercepts in V (Interc. ± s) and slopes in V/ppb or V/ppm (slope ± s) of the linear lines, the probability that the intercepts and slopes are different from 0 (any value > 0.05 indicates that these variables are significantly different from 0), the coefficients of determination (R^2), the root mean square errors (RMSE) in V calculated using the residual degrees of freedom and the lack of fit in ppb or ppm of the linear model calculated for the x axis u(lof). Figure 14 to Figure 30 give the scatterplots of the experiments, sensor readings versus reference values.

4.2.1 NO2-B4F sensor

4.2.1.1 Effect of CO

The NO2-B43F sensors show little CO cross-sensitivity. The slopes of linear lines are generally not significant. Moreover, the fourth sensor is clearly an outlier, Figure 15 shows that it behaved in a different way from the other sensors. The sensor was discarded for data treatment. Figure 15 also shows that the variations of sensor reading are well within the signal noise corresponding to the error bars.

Table 15: Effect of CO on 10 NO2-B43F sensors (sensor readings in volt), experimental results of 2016-05-20. 4_INERIS_NO2-B43F is discarded for computing the means, mean SDs and RSDs

Sensors	Interc.	P(Interc.)	Slope	P(Slope)	R^2	RMSE	u(lof)
1_NILU_NO2B43P	2.14784 ± 0.00001	0	0.0000016 ± 0.0000021	0.51	0.2397	6.79e-06	5
2_KNMI_NO2B43P	2.14830 ± 0.00001	0	0.0000018 ± 0.0000010	0.208	0.6278	2.94e-06	2
3_52North_NO2B43P	2.14918 ± 0.00001	0	0.0000050 ± 0.0000019	0.117	0.7791	5.72e-06	2
4_INERIS_NO2B43P	2.14441 ± 0.00009	0	0.0002426 ± 0.0000162	0.004	0.9911	4.945e-05	2
5_VMM_NO2B43F	2.14818 ± 0.00000	0	0.0000056 ± 0.0000007	0.014	0.9724	2.04e-06	2
6_VITO_NO2B43F	2.14787 ± 0.00001	0	0.0000040 ± 0.0000020	0.185	0.6647	6.16e-06	2
7_AEA_NO2B43F	2.14866 ± 0.00001	0	0.0000060 ± 0.0000021	0.105	0.8015	6.69e-06	2
8_GeonoVum_NO2B43F	2.14845 ± 0.00001	0	0.0000009 ± 0.0000018	0.662	0.1139	5.5e-06	6
9_AIRPARIF_NO2B43P	2.14843 ± 0.00001	0	0.0000080 ± 0.0000026	0.089	0.8303	8.27e-06	2
10_RIVM_NO2B43P	2.14638 ± 0.00001	0	0.0000037 ± 0.0000022	0.234	0.5863	7e-06	3
Means	2.14814 ± 0.00078		0.0000041 ± 0.0000023		0.6240	0.0000057	
RSD	0.000		0.572				

4.2.1.2 NO_2 calibration

The NO2-B43F sensors have highly linear responses when calibrating against NO_2. Both the intercepts and slopes of linear lines are highly significant and R^2 are over 0.999. The scattering of the slopes is low with RSD of 3 % (-0.0000877 ± 0.0000025) suggesting that the sensors could be used without previous calibration against NO_2. Figure 14 shows the scatter plot of the NO2-B43F sensors versus NO_2 concentration levels (sensor readings in volt versus reference values in ppb or ppm).

Table 16: NO_2 Calibration of 10 NO2-B43F sensors (sensor readings in volt), experimental results of 2016-05-20. 4_INERIS_NO2-B43F is discarded for computing the means, mean SDs and RSDs

Sensors	Interc.	P(Interc.)	Slope	P(Slope)	R^2	RMSE	**u(lof)**
1_NILU_NO2B43P	2.14789 ± 0.00009	0	-0.0000880 ± 0.0000016	0	0.999	5.373e-05	2
2_KNMI_NO2B43P	2.14834 ± 0.00007	0	-0.0000843 ± 0.0000013	0	0.9993	4.3e-05	2
3_52North_NO2B43P	2.14924 ± 0.00010	0	-0.0000909 ± 0.0000016	0	0.999	5.715e-05	2
4_INERIS_NO2B43P	2.14535 ± 0.00080	0	-0.0000636 ± 0.0000143	0.021	0.8678	0.00044892	12
5_VMM_NO2B43F	2.14821 ± 0.00010	0	-0.0000881 ± 0.0000016	0	0.999	5.816e-05	2
6_VITO_NO2B43F	2.14792 ± 0.00009	0	-0.0000851 ± 0.0000014	0	0.9992	5.071e-05	2
7_AEA_NO2B43F	2.14874 ± 0.00009	0	-0.0000852 ± 0.0000014	0	0.9992	4.804e-05	2
8_GeonoVum_NO2B43F	2.14849 ± 0.00008	0	-0.0000881 ± 0.0000014	0	0.9993	4.6e-05	2
9_AIRPARIF_NO2B43P	2.14849 ± 0.00009	0	-0.0000918 ± 0.0000015	0	0.9992	5.173e-05	2
10_RIVM_NO2B43P	2.14642 ± 0.00008	0	-0.0000881 ± 0.0000012	0	0.9995	4.376e-05	2
Means	2.14819 ± 0.00078		-0.0000877 ± 0.0000025		0.9992	0.0000503	
RSD	0.000		0.029				

4.2.1.3 Effect of NO_2 and O_3 together

In this experiment, the NO2-B43F sensors obviously show an O_3+NO_2 cross-sensitivity. The slopes of linear lines are highly significant.

Table 17: Effect of NO_2 (0-150 ppb) and O_3 (0-90 ppb) together on 10 NO2B43F sensors versus NO_2 (sensor readings in volt), experimental results of 2016-05-20.

Sensors	**Interc.**	**P(Interc.)**	**Slope**	**P(Slope)**	**R^2**	**RMSE**	**u(lof)**
1_NILU_NO2B43P	2.14810 ± 0.00034	0.000	-0.0000920 ± 0.0000038	0.002	0.9966	0.00019891	3
2_KNMI_NO2B43P	2.14854 ± 0.00031	0.000	-0.0000885 ± 0.0000033	0.001	0.9973	0.00017961	3
3_52North_NO2B43P	2.14945 ± 0.00030	0.000	-0.0000949 ± 0.0000030	0.001	0.998	0.00017279	3
4_INERIS_NO2B43P	2.14668 ± 0.00019	0.000	-0.0000727 ± 0.0000020	0.001	0.9984	0.00010276	2
5_VMM_NO2B43F	2.14850 ± 0.00034	0.000	-0.0000925 ± 0.0000036	0.002	0.9969	0.00020455	3
6_VITO_NO2B43F	2.14817 ± 0.00033	0.000	-0.0000889 ± 0.0000037	0.002	0.9965	0.00019322	3
7_AEA_NO2B43F	2.14890 ± 0.00030	0.000	-0.0000885 ± 0.0000030	0.001	0.9977	0.00016278	3
8_GeonoVum_NO2B43F	2.14878 ± 0.00035	0.000	-0.0000928 ± 0.0000037	0.002	0.9968	0.00019249	3
9_AIRPARIF_NO2B43P	2.14870 ± 0.00035	0.000	-0.0000955 ± 0.0000039	0.002	0.9966	0.00020698	3
10_RIVM_NO2B43P	2.14665 ± 0.00036	0.000	-0.0000952 ± 0.0000041	0.002	0.9964	0.0002185	3
Means	2.14842 ± 0.00078		-0.0000921 ± 0.0000029		0.9970	0.0001922	3.0
RSD	0.000		0.031				

This cross-sensitivity experiment shows a slight increase of the NO_2 sensitivity compared to the experiment performed only with NO_2: -0.0000921 ± 3.1 % V/ppb for NO_2 and O_3 together (Table 17) while the calibration with NO_2 alone gave -0.0000877 ± 2.9 % V/ppb of NO_2 (Table 16). The difference between the two values confirms the O_3 sensitivity of the sensor estimated previously: -0.0000877 + 90/150 x -0.0000058 = -0.0000912 V/ppb very similar to -0.0000921 V/ppb found in the current experiment. The small O_3 effect (about 6.6 % in sensitivity of NO_2) remains constant up to 90 ppb of O_3 with or without NO_2.

4.2.2 CO/MF-200 sensor

4.2.2.1 CO calibration

The CO/MF-200 sensors have highly linear responses when calibrating against CO. The slopes of linear lines are highly significant and R^2 are over 0.999. The scattering of the slopes is low with RSD of 7.7 % (0.0811733 ± 0.0062396) suggesting that the sensor could be used without previous calibration. Figure 19 shows the scatter plot of the CO/MF-200 sensors versus CO concentration levels.

Table 18: CO calibration of 10 CO/MF-200 sensors (sensor readings in volt), experimental results of 2016-05-20.

Sensors	**Interc.**	**P(Interc.)**	**Slope**	**P(Slope)**	**R^2**	**RMSE**	**u(lof)**
1_NILU_CO/MF-200	1.08628 ± 0.00338	0.000	0.0742149 ± 0.0009011	0.000	0.9997	0.00250428	0
2_KNMI_CO/MF-200	1.08836 ± 0.00347	0.000	0.0823661 ± 0.0009901	0.000	0.9997	0.00264042	0
3_52North_CO/MF-200	1.07891 ± 0.00326	0.000	0.0865903 ± 0.0009935	0.000	0.9997	0.00250808	0
4_INERIS_CO/MF-200	1.08021 ± 0.00228	0.000	0.0844994 ± 0.0009001	0.000	0.9998	0.00185149	0
5_VMM_CO/MF-200	1.08786 ± 0.00321	0.000	0.0727625 ± 0.0008687	0.000	0.9997	0.00244058	0
6_VITO_CO/MF-200	1.08137 ± 0.00300	0.000	0.0711284 ± 0.0008677	0.000	0.9997	0.00230042	0
7_AEA_CO/MF-200	1.08654 ± 0.00327	0.000	0.0837369 ± 0.0009690	0.000	0.9997	0.00250641	0
8_GeonoVum_CO/MF-200	1.08048 ± 0.00352	0.000	0.0812874 ± 0.0009537	0.000	0.9997	0.00261123	0
9_AIRPARIF_CO/MF-200	1.08316 ± 0.00268	0.000	0.0875351 ± 0.0009436	0.000	0.9998	0.00216534	0
10_RIVM_CO/MF-200	1.08263 ± 0.00259	0.000	0.0876116 ± 0.0010039	0.000	0.9997	0.00210758	0
Means	1.08358 ± 0.00343		0.0811733 ± 0.0062396		0.9997	0.0023636	
RSD	0.003		0.077				

4.2.2.2 Effect of NO_2

The CO/MF-200 sensors do not show any NO_2 cross-sensitivity. The slopes of the linear lines are not significantly different from zero (P> 25 %). The R^2 are low. Figure 18 also shows the lack of correlation between CO/MF-200 readings and NO_2.

Table 19: Effect of NO_2 on 10 CO/MF-200 sensors (sensor readings in volt), experimental results of 2016-05-20.

Sensors	Interc.	P(Interc.)	Slope	P(Slope)	R^2	RMSE	u(lof)
1_NILU_CO/MF-200	1.11766 ± 0.00210	0	0.0000250 ± 0.0000361	0.527	0.1069	0.0013403	112
2_KNMI_CO/MF-200	1.12413 ± 0.00263	0	0.0000350 ± 0.0000460	0.489	0.1266	0.00164055	101
3_52North_CO/MF-200	1.11645 ± 0.00228	0	0.0000434 ± 0.0000419	0.359	0.2115	0.00146028	81
4_INERIS_CO/MF-200	1.11569 ± 0.00227	0	0.0000532 ± 0.0000382	0.237	0.3259	0.00133004	60
5_VMM_CO/MF-200	1.11945 ± 0.00229	0	0.0000190 ± 0.0000408	0.666	0.0514	0.00155548	162
6_VITO_CO/MF-200	1.11106 ± 0.00195	0	0.0000177 ± 0.0000357	0.646	0.0581	0.00132296	143
7_AEA_CO/MF-200	1.12177 ± 0.00231	0	0.0000482 ± 0.0000376	0.27	0.2907	0.00130442	70
8_GeonoVum_CO/MF-200	1.11451 ± 0.00233	0	0.0000196 ± 0.0000441	0.68	0.047	0.00155555	149
9_AIRPARIF_CO/MF-200	1.12110 ± 0.00250	0	0.0000380 ± 0.0000417	0.415	0.1713	0.00156813	103
10_RIVM_CO/MF-200	1.12076 ± 0.00232	0	0.0000395 ± 0.0000406	0.386	0.1914	0.00141795	97
Means	1.11826 ± 0.00393		0.0000339 ± 0.0000128		0.1581	0.0014496	107.8
RSD	0.004		0.379				

4.2.2.3 Effect of NO_2 and O_3 together

As discussed in paragraph 3.2.2.2 and 4.2.2.2, the CO/MF-200 sensors do not show an O_3 and NO_2 cross-sensitivity. In both cases, the slope of the linear lines are not significant and the R^2 are low. Thus, it has been decided to not include results concerning the combined effect of NO_2 and O_3 on the CO/MF-200 sensors.

4.2.3 O3/M-5 sensor

4.2.3.1 Effect of CO

The O3/M-5 sensors show little or no CO cross-sensitivity. The slopes of linear lines are not generally significant and the interference is low and gives a low R^2. The fourth sensor 4_INERIS_O3/M-5 was discarded for computing the means, mean SDs and RSDs. Figure 23 also shows that the variations of sensor readings are generally within the signal noise corresponding to the error bars.

Table 20: Effect of CO on 10 O3/M-5 sensors (sensor readings in volt), experimental results of 2016-05-20.

Sensors	Interc.	P(Interc.)	Slope	P(Slope)	R^2	RMSE	u(lof)
1_NILU_O3/M-5	2.15190 ± 0.00003	0.000	0.0000434 ± 0.0000059	0.018	0.9638	1.954e-05	2
2_KNMI_O3/M-5	2.14256 ± 0.00016	0.000	0.0000193 ± 0.0000320	0.608	0.1538	0.00010129	7
3_52North_O3/M-5	2.14918 ± 0.00004	0.000	0.0000414 ± 0.0000066	0.024	0.9521	2.047e-05	2
4_INERIS_O3/M-5	2.14282 ± 0.00030	0.000	0.0009757 ± 0.0000499	0.003	0.9948	0.00016818	2
5_VMM_O3/M-5	2.14727 ± 0.00001	0.000	0.0000057 ± 0.0000024	0.136	0.747	7.79e-06	2
6_VITO_O3/M-5	2.14877 ± 0.00002	0.000	-0.0000218 ± 0.0000044	0.039	0.9229	1.433e-05	2
7_AEA_O3/M-5	2.14854 ± 0.00003	0.000	-0.0000037 ± 0.0000062	0.61	0.1518	1.852e-05	6
8_GeonoVum_O3/M-5	2.14901 ± 0.00001	0.000	0.0000026 ± 0.0000023	0.372	0.3947	7.2e-06	4
9_AIRPARIF_O3/M-5	2.15017 ± 0.00007	0.000	0.0000090 ± 0.0000120	0.533	0.218	3.9e-05	6
10_RIVM_O3/M-5	2.14887 ± 0.00003	0.000	-0.0000442 ± 0.0000050	0.013	0.975	1.495e-05	2
Means	2.14847 ± 0.00255		0.0000058 ± 0.0000279		0.609	0.00000270	
RSD	0.001		2.996				

4.2.3.2 Effect of NO_2

The O3/M-F sensors clearly show a NO_2 cross-sensitivity. The slopes of linear lines are highly significant. The effect shows little scattering with RSD of the slopes of the linear lines of 3.6 % with mean slope value of -0.0002881 ± 0.0000104 V/ppb. Figure 22 shows the scatter plot of the O3/M-5 sensors versus NO_2 concentration levels.

Table 21: Effect of NO_2 on 10 O3/M-5 sensors (sensor readings in volt), experimental results of 2016-05-20.

Sensors	Interc.	P(Interc.)	Slope	P(Slope)	R^2	RMSE	u(lof)
1_NILU_O3/M-5	2.15216 ± 0.00026	0.000	-0.0002855 ± 0.0000052	0.000	0.9987	0.00017281	2
2_KNMI_O3/M-5	2.14205 ± 0.00068	0.000	-0.0002820 ± 0.0000148	0.000	0.9891	0.00045792	3
3_52North_O3/M-5	2.14943 ± 0.00026	0.000	-0.0003082 ± 0.0000049	0.000	0.999	0.00017006	2
4_INERIS_O3/M-5	2.14293 ± 0.00028	0.000	-0.0002736 ± 0.0000051	0.000	0.9986	0.00017986	2
5_VMM_O3/M-5	2.14746 ± 0.00026	0.000	-0.0002952 ± 0.0000051	0.000	0.9988	0.0001702	2
6_VITO_O3/M-5	2.14895 ± 0.00024	0.000	-0.0002819 ± 0.0000048	0.000	0.9988	0.00016495	2
7_AEA_O3/M-5	2.14876 ± 0.00022	0.000	-0.0002954 ± 0.0000041	0.000	0.9992	0.00014416	2
8_GeonoVum_O3/M-5	2.14915 ± 0.00027	0.000	-0.0002905 ± 0.0000052	0.000	0.9987	0.00018066	2
9_AIRPARIF_O3/M-5	2.15048 ± 0.00026	0.000	-0.0002760 ± 0.0000046	0.000	0.9989	0.00016655	2
10_RIVM_O3/M-5	2.14913 ± 0.00028	0.000	-0.0002925 ± 0.0000053	0.000	0.9987	0.00018145	2
Means	2.14805 ± 0.00318		-0.0002881 ± 0.0000104		0.9979	0.0002154	
RSD	0.001		0.036				

4.2.3.3 Effect of NO_2 and O_3 together

The O3/M-5 sensor is affected by both NO_2 and O_3 as shown before (3.2.3.2 and 4.2.3.2). The slopes of linear lines are highly significant. This experiment gives the O_3 sensitivity adding the response of O_3 plus the response to NO_2: 0.0003628 + (150/90) * 0.0002881 = 0.0008430 very similar to the sensitivity found in the current experiment: -0.0008433 V/ppb (of equivalent O_3). Interestingly, the O3/M-5 sensor reading is an addition of the single effects of NO_2 and O_3 on this sensor.

Table 22: Effect of NO_2 (0-150 ppb) and O_3 (0-90 ppb) together on 10 O3/M-5 sensors versus O_3 (sensor readings in), experimental results of 2016-05-20.

Sensors	Interc.	P(Interc.)	Slope	P(Slope)	R^2	RMSE	u(lof)
1_NILU_O3/M-5	2.15342 ± 0.00101	0.000	-0.0008279 ± 0.0000181	0.000	0.9991	0.00057066	2
2_KNMI_O3/M-5	2.14482 ± 0.00095	0.000	-0.0008529 ± 0.0000163	0.000	0.9993	0.00048246	2
3_52North_O3/M-5	2.15077 ± 0.00109	0.000	-0.0009007 ± 0.0000186	0.000	0.9991	0.00060494	2
4_INERIS_O3/M-5	2.14396 ± 0.00083	0.000	-0.0007825 ± 0.0000146	0.000	0.9993	0.00046839	2
5_VMM_O3/M-5	2.14902 ± 0.00101	0.000	-0.0008680 ± 0.0000171	0.000	0.9992	0.00055374	2
6_VITO_O3/M-5	2.15046 ± 0.00095	0.000	-0.0008240 ± 0.0000175	0.000	0.9991	0.00054175	2
7_AEA_O3/M-5	2.15037 ± 0.00101	0.000	-0.0008709 ± 0.0000183	0.000	0.9991	0.0005804	2
8_GeonoVum_O3/M-5	2.15086 ± 0.00098	0.000	-0.0008562 ± 0.0000194	0.001	0.999	0.00056299	2
9_AIRPARIF_O3/M-5	2.15148 ± 0.00094	0.000	-0.0007957 ± 0.0000157	0	0.9992	0.00053674	2
10_RIVM_O3/M-5	2.15062 ± 0.00101	0.000	-0.0008545 ± 0.0000178	0	0.9991	0.00052856	2
Means	2.14958 ± 0.00295		-0.0008433 ± 0.0000359		0.9991	0.0005431	2.0
RSD	0.001		0.043				

4.2.4 NO-B4 sensor

4.2.4.1 Effect of CO

The NO-B4_P1 sensors show little CO cross-sensitivity. The slopes of linear lines are sometimes significant but the interference is low, the effect shows a lot of random noise with low R^2 values. Figure 28 also shows that the variations of sensor readings are well within the signal noise corresponding to the error bars.

Table 23: Effect of CO on 10 NO-B4_P1 sensors (sensor readings in volt), experimental results of 2016-05-20.

Sensors	Interc.	P(Interc.)	Slope	P(Slope)	R^2	RMSE	u(lof)
1_NILU_NOB4_P1	0.84035 ± 0.00001	0	-0.0000112 ± 0.0000025	0.045	0.9115	8.24e-06	2
2_KNMI_NOB4_P1	0.84206 ± 0.00003	0	-0.0000265 ± 0.0000045	0.028	0.9445	1.406e-05	2
3_52North_NOB4_P1	0.84058 ± 0.00003	0	-0.0000120 ± 0.0000051	0.144	0.7328	1.613e-05	2
4_INERIS_NOB4_P1	0.84114 ± 0.00001	0	-0.0000206 ± 0.0000014	0.005	0.9906	4.67e-06	2
5_VMM_NOB4_P1	0.83949 ± 0.00001	0	-0.0000043 ± 0.0000023	0.206	0.6307	7.36e-06	3
6_VITO_NOB4_P1	0.84063 ± 0.00001	0	-0.0000066 ± 0.0000020	0.081	0.845	6.72e-06	2
7_AEA_NOB4_P1	0.84009 ± 0.00001	0	-0.0000062 ± 0.0000018	0.075	0.8553	5.91e-06	2
8_GeonoVum_NOB4_P1	0.84060 ± 0.00001	0	-0.0000054 ± 0.0000014	0.066	0.8733	4.59e-06	2
9_AIRPARIF_NOB4_P1	0.84064 ± 0.00003	0	-0.0000070 ± 0.0000052	0.308	0.4792	1.537e-05	3
10_RIVM_NOB4_P1	0.83872 ± 0.00002	0	-0.0000013 ± 0.0000040	0.772	0.0522	1.285e-05	9
Means	0.84043 ± 0.00090		-0.0000101 ± 0.0000078		0.7315	0.0000096	
RSD	0.001		0.775				

4.2.4.2 Effect of NO_2

The NO-B4_P1 sensors show some NO_2 cross-sensitivity. The slopes of linear lines are generally significant but the interference is low. In fact, Figure 26 shows a kind of hysteresis effect on the sensor responses. Actually, the sensor response are well correlated with the small NO increase within the NO_2 ramp and it is likely that the sensor was measuring NO or a combination of NO and NO_2.

Table 25 and Figure 27 have been plotted to explain the effect of the low NO levels on the NO-B4 sensors. On average, the slope is 0.0002121 ± 0.0000186 V/ppb of NO, significantly higher than the sole NO calibration (0.0001398 ± 0.0000037V/ppb) that may indicate a remaining low NO_2 cross-sensitivity (0.0000723 V/ppb of NO x 3 ppb of NO / 100 ppb or 0.0000002169 V/ppb of NO_2). However this calculation is determined using the NO range between 1-3 ppb and hence with a lot of uncertainties if extrapolated to higher NO values.

Table 24: Effect of NO2 on 10 NO-B4_P1 sensors (sensor readings in volt), experimental results of 2016-05-20.

Sensors	Interc.	P(Interc.)	Slope	P(Slope)	R^2	RMSE	u(lof)
1_NILU_NOB4_P1	0.84016 ± 0.00014	0	0.0000030 ± 0.0000023	0.275	0.372	7.735e-05	23
2_KNMI_NOB4_P1	0.84178 ± 0.00017	0	0.0000029 ± 0.0000028	0.375	0.2645	9.974e-05	34
3_52North_NOB4_P1	0.84038 ± 0.00014	0	0.0000036 ± 0.0000023	0.217	0.4479	7.662e-05	22
4_INERIS_NOB4_P1	0.84095 ± 0.00015	0	0.0000034 ± 0.0000023	0.24	0.4157	7.642e-05	27
5_VMM_NOB4_P1	0.83947 ± 0.00008	0	0.0000038 ± 0.0000012	0.053	0.762	4.495e-05	16
6_VITO_NOB4_P1	0.84058 ± 0.00008	0	0.0000042 ± 0.0000013	0.048	0.7762	4.706e-05	15
7_AEA_NOB4_P1	0.83996 ± 0.00010	0	0.0000044 ± 0.0000016	0.068	0.7234	5.514e-05	17
8_GeonoVum_NOB4_P1	0.84056 ± 0.00010	0	0.0000037 ± 0.0000015	0.095	0.6588	5.354e-05	18
9_AIRPARIF_NOB4_P1	0.84055 ± 0.00008	0	0.0000046 ± 0.0000013	0.036	0.816	4.372e-05	13
10_RIVM_NOB4_P1	0.83872 ± 0.00008	0	0.0000035 ± 0.0000013	0.074	0.7069	4.615e-05	17
Means	0.84031 ± 0.00083		0.0000037 ± 0.0000006		0.5943	0.0000621	
RSD	0.001		0.153				

Table 25: Effect of NO on 10 NO-B4_P1 sensors (sensor readings in volt), experimental results of 2016-05-20.

Sensors	Interc.	P(Interc.)	Slope	P(Slope)	R^2	RMSE	u(lof)
1_NILU_NO-B4_P1	0.83993 ± 0.00005	0.000	0.0002129 ± 0.0000231	0.003	0.9658	5.3e-05	NA
2_KNMI_NO-B4_P1	0.84141 ± 0.00005	0.000	0.0002490 ± 0.0000236	0.002	0.9738	5.398e-05	NA
3_52North_NO-B4_P1	0.84016 ± 0.00003	0.000	0.0002184 ± 0.0000154	0.001	0.9853	3.528e-05	NA
4_INERIS_NO-B4_P1	0.84065 ± 0.00002	0.000	0.0002267 ± 0.0000091	0	0.9952	2.09e-05	NA
5_VMM_NO-B4_P1	0.83930 ± 0.00002	0.000	0.0001884 ± 0.0000092	0	0.9929	2.114e-05	NA
6_VITO_NO-B4_P1	0.84039 ± 0.00003	0.000	0.0002053 ± 0.0000134	0.001	0.9873	3.079e-05	NA
7_AEA_NO-B4_P1	0.83979 ± 0.00002	0.000	0.0002105 ± 0.0000096	0	0.9938	2.196e-05	NA
8_GeonoVum_NO-B4_P1	0.84034 ± 0.00002	0.000	0.0002089 ± 0.0000097	0	0.9936	2.216e-05	NA
9_AIRPARIF_NO-B4_P1	0.84038 ± 0.00003	0.000	0.0002178 ± 0.0000172	0.001	0.9816	3.94e-05	NA
10_RIVM_NO-B4_P1	0.83854 ± 0.00002	0.000	0.0001831 ± 0.0000091	0	0.9926	2.09e-05	NA
Means	0.84009 ± 0.00078		0.0002121 ± 0.0000186		0.9862	0.0000320	NA
RSD	0.001		0.088				NA

4.2.4.3 Effect of NO_2 and O_3 together

Although, the NO-B4 sensors were exposed to NO_2 (0-150 ppb) and O_3 (0-90 ppb) together it was shown before that NO_2 has likely little or no effect on NO-B4 sensors (see Table 24 and Table 25). Therefore, the variations in sensor readings in this experiment is attributed solely to O_3. Moreover, the estimation of the O_3 effect was unclear in the previous experiment (Table 12) as two groups of slope values were obtained. In this experiment, the NOB4_P1 sensors show an O_3 cross-sensitivity. The slopes of linear lines are highly significant. The extent of the effect shows substantial scattering with RSD of 14.6 % with mean slope value of -0.0000072 ± 0.0000011 V/ppb.

Table 26: Effect of NO_2 (0-150 ppb) and O_3 (0-90 ppb) together on 10 NOB4_P1 sensors versus O3 (sensor readings in volt versus O3 values in ppb or ppm), experimental results of 2016-05-20.

Sensors	Interc.	P(Interc.)	Slope	P(Slope)	R^2	RMSE	u(lof)
1_NILU_NOB4_P1	0.84006 ± 0.00004	0	-0.0000069 ± 0.0000007	0.011	0.9789	4.759e-05	5
2_KNMI_NOB4_P1	0.84154 ± 0.00005	0	-0.0000072 ± 0.0000008	0.013	0.9749	5.376e-05	5
3_52North_NOB4_P1	0.84028 ± 0.00004	0	-0.0000066 ± 0.0000007	0.011	0.979	4.565e-05	5
4_INERIS_NOB4_P1	0.84076 ± 0.00003	0	-0.0000073 ± 0.0000006	0.006	0.9875	3.848e-05	4
5_VMM_NOB4_P1	0.83939 ± 0.00005	0	-0.0000090 ± 0.0000008	0.009	0.9828	5.583e-05	4
6_VITO_NOB4_P1	0.84049 ± 0.00003	0	-0.0000072 ± 0.0000005	0.005	0.9905	3.327e-05	3
7_AEA_NOB4_P1	0.83990 ± 0.00005	0	-0.0000073 ± 0.0000008	0.012	0.9766	5.319e-05	5
8_GeonoVum_NOB4_P1	0.84043 ± 0.00003	0	-0.0000049 ± 0.0000005	0.010	0.9803	3.24e-05	3
9_AIRPARIF_NOB4_P1	0.84047 ± 0.00005	0	-0.0000074 ± 0.0000008	0.013	0.9745	5.604e-05	5
10_RIVM_NOB4_P1	0.83865 ± 0.00005	0	-0.0000081 ± 0.0000009	0.013	0.9737	6.242e-05	5
Means	0.84020 ± 0.00078		-0.0000072 ± 0.0000011		0.9799	0.0000479	4.4
RSD	0.001		0.146				

5 Effects of relative humidity (2016-05-15)

This experiment shows the effect of relative humidity on the CO/MF-200, NO2-B43F, NO-B4 and O3/M-5 sensors.

Table 27 below gives the reference values of all monitored parameters during the stable phase of the experiment. In this experiment each step was 30 minutes instead of one hour for all other experiments. We performed three ramps (increase, decrease and increase) of

relative humidity between 40 and 80 % with steps of 10 %. CO and O_3 were kept at constant values, 3 ppm and 60 ppb, respectively while SO_2, NO_2 and NO remained at about 0 ppb. Wind velocity was kept at about 2.5 m/s while atmospheric pressure changed about 10 hPa. The ambient pressure was the sole parameter that was not under control. In fact, we cannot completely distinguish between the effect of relative humidity and pressure (if any) in this experiment. Figure 32 shows the time series plot for all reference parameters.

Table 27: Reference values of all steps of experiments started on 2016-05-20.

Begin	End	O3, ppb	NO2, ppb	NO, ppb	CO, ppm	SO2, ppb	Temp., °C	RH, %	Pressure, hPa	Wind_Speed, m/s
2016-05-15 12:11	2016-05-15 13:10	60.0	0.2	0.1	2.956	-0.1	22.0	60.0	994	2.5
2016-05-15 14:02	2016-05-15 15:01	60.0	0.1	0.1	2.981	-0.1	22.0	40.1	995	2.5
2016-05-15 15:51	2016-05-15 16:50	60.0	0.1	0.1	2.989	-0.1	22.0	50.0	994	2.5
2016-05-15 17:34	2016-05-15 18:33	60.0	0.1	0.1	2.995	-0.1	22.0	60.0	994	2.5
2016-05-15 19:32	2016-05-15 20:31	60.0	0.1	0.1	2.997	-0.1	22.0	70.0	994	2.5
2016-05-15 21:54	2016-05-15 22:53	60.0	0.2	0.1	2.976	-0.1	21.9	80.0	997	2.5
2016-05-15 23:39	2016-05-16 00:38	60.0	0.1	0.1	2.989	-0.1	22.0	70.0	1000	2.5
2016-05-16 01:25	2016-05-16 02:24	60.0	0.1	0.1	2.991	-0.1	21.9	60.0	1002	2.5
2016-05-16 03:11	2016-05-16 04:10	60.0	0.0	0.1	2.995	-0.1	21.9	50.0	1003	2.5
2016-05-16 04:58	2016-05-16 05:57	60.0	0.0	0.0	2.995	-0.1	21.9	40.1	1004	2.5
2016-05-16 06:41	2016-05-16 07:40	60.0	0.0	0.1	2.996	-0.1	21.8	50.0	1004	2.5
2016-05-16 08:29	2016-05-16 09:28	60.0	0.0	0.1	2.998	-0.1	21.8	60.0	1005	2.5
2016-05-16 10:14	2016-05-16 11:13	60.0	0.0	0.1	2.991	-0.1	21.8	70.0	1004	2.5
2016-05-16 12:10	2016-05-16 13:09	60.0	0.1	0.1	2.999	-0.1	21.7	80.0	1003	2.5
2016-05-16 14:00	2016-05-16 14:59	60.0	0.0	0.1	2.992	-0.1	21.8	60.0	1002	2.5
2016-05-16 16:22	2016-05-16 17:21	62.1	0.1	0.1	3.110	-0.1	29.3	62.9	999	2.4

Table 28 shows the mean effect of relative humidity (sensor readings in volt versus relative humidity in %) on the 10 sensors of the four model types. The table gives the sensor model types, the reference gaseous compounds, the intercepts in V (Interc. ± s) and slopes in V/% (slope ± s) of the linear lines, the probability that the intercepts and slopes are different from 0 (any value > 0.05 indicates that these variables are significantly different from 0), the coefficients of determination (R^2) and the root mean square errors (RMSE) in V calculated using the residual degrees of freedom. The standard deviations of the intercepts and slopes are computed using the results of the 10 sensors.

The CO/MF-200 and O3/M-5 sensors are not linearly associated with relative humidity while the NO2-B-43F and NO-B4 sensors are linearly associated with the relative humidity with coefficients of determination (R^2) of about 0.85 and a probability of 0.001 that the slope of their calibration line is naught. The section below shows that these two sensors have a significant hysteresis effect due to relative humidity.

Moreover, the CO/MF-200 and O3/M-5 sensor values show a transient peak when relative humidity changes quickly while the NO2-B-43F and NO-B4 sensors show strong hysteresis effects.

Conversely to relative humidity, the CO/MF-200 and O3/M-5 sensors have a linear dependence on ambient pressure while the NO2-B-43F and NO-B4 sensor values do not appear to be dependent on pressure.

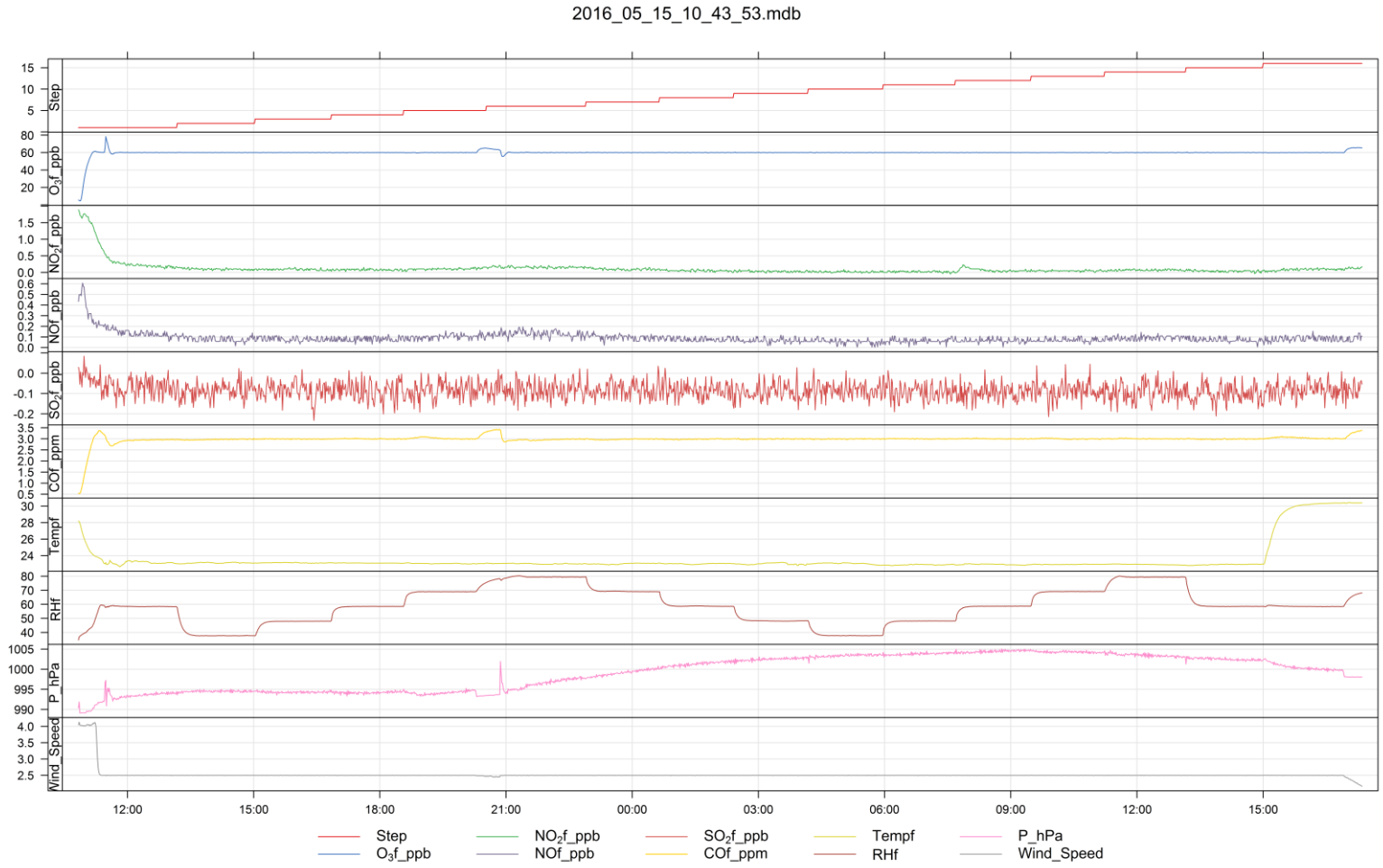

Figure 32: Time series plot of the reference parameters for the experiment started on 2016-05-15

Table 28: Effect of relative humidity on sensor readings, experimental results of 2016-05-15.

Sensors	Compounds	Interc.	P(Interc.)	Slope	P(Slope)	R^2	RMSE
CO/MF-200	Pressure	3.07710 ± 0.24786	0.000	-0.00176936 ± 0.00023026	0.000	0.7439	0.00137
CO/MF-200	Humidity	1.30068 ± 0.02028	0.000	0.00003967 ± 0.00002804	0.834	0.0094	0.00223
NO2-B43F	Pressure	2.13507 ± 0.00932	0.000	0.00001276 ± 0.00000918	0.793	0.0092	0.00019
NO2-B43F	Humidity	2.15073 ± 0.00092	0.000	-0.00004727 ± 0.00000446	0.000	0.8704	0.00009
NO-B4	Pressure	0.86131 ± 0.05126	0.000	-0.00001916 ± 0.00005052	0.794	0.0198	0.00038
NO-B4	Humidity	0.84772 ± 0.00098	0.000	-0.00009251 ± 0.00000505	0.001	0.8386	0.00019
O3/M-5	Pressure	2.28275 ± 0.03730	0.000	-0.00015273 ± 0.00003336	0.000	0.9120	0.00006
O3/M-5	Humidity	2.12901 ± 0.00473	0.000	0.00000954 ± 0.00000580	0.224	0.3137	0.00008

5.1 Scatter plots of effects of relative humidity

5.1.1 NO2-B43F sensor

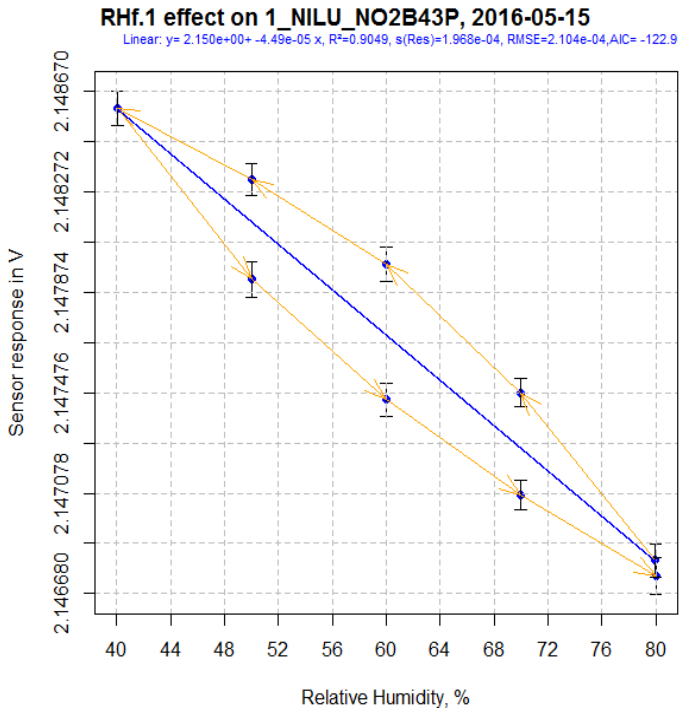

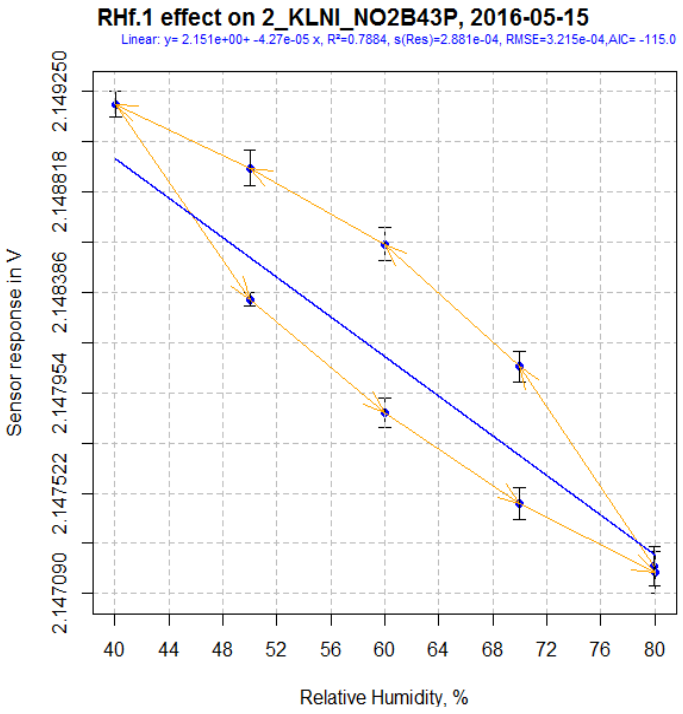

No data available because of connection error

No data available because the sensor channel was damaged

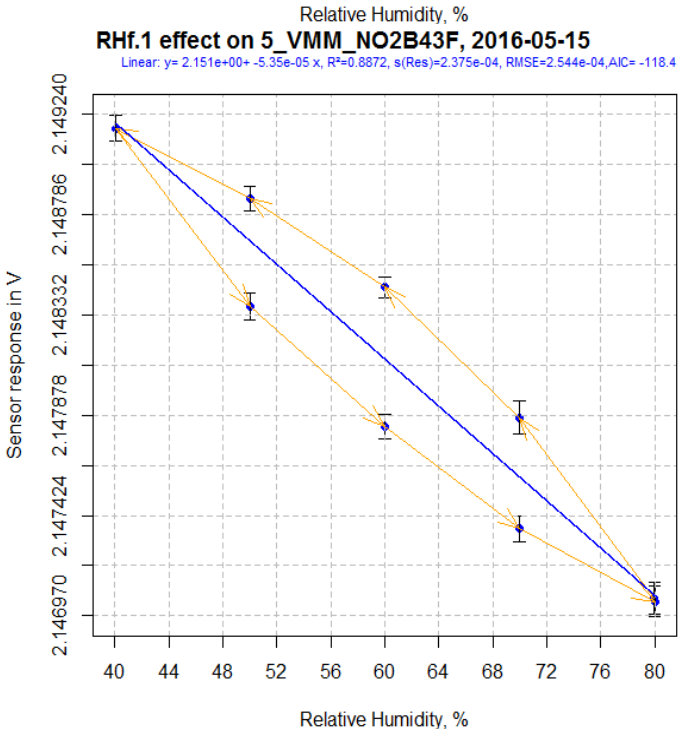

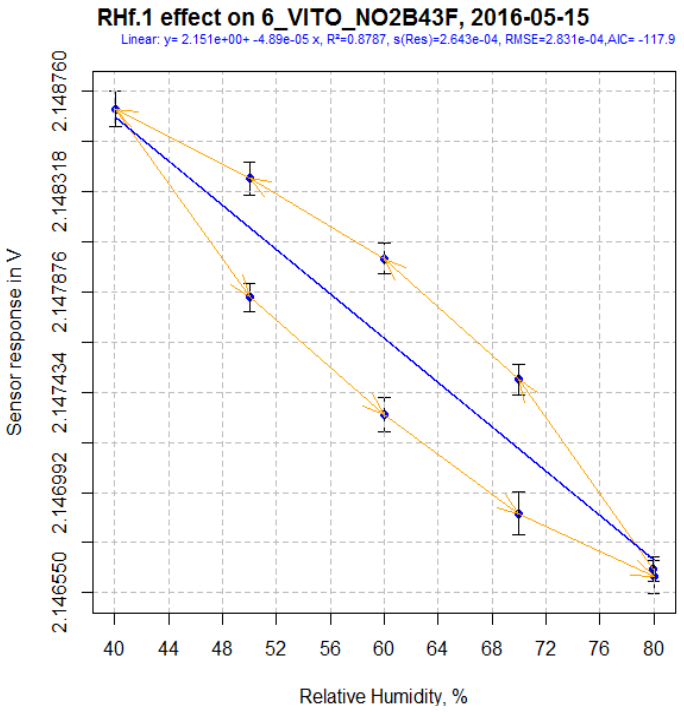

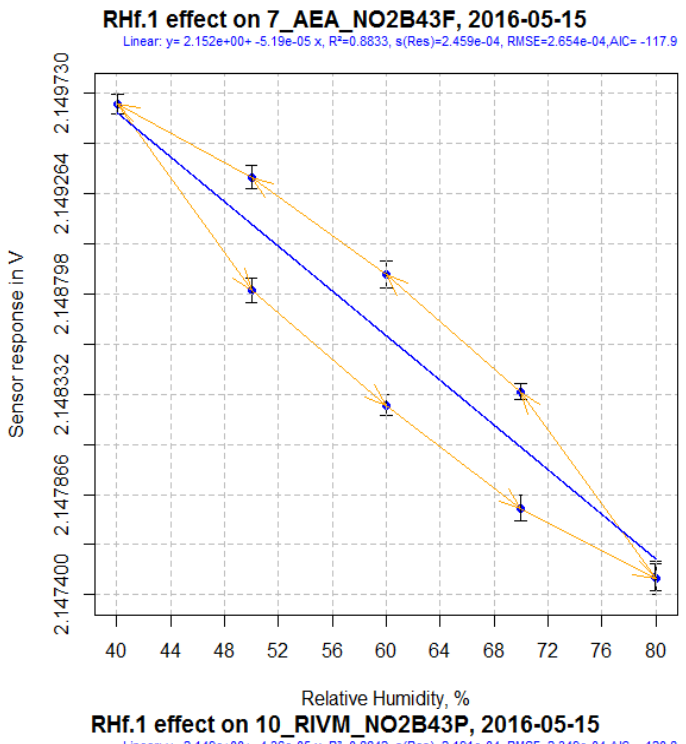

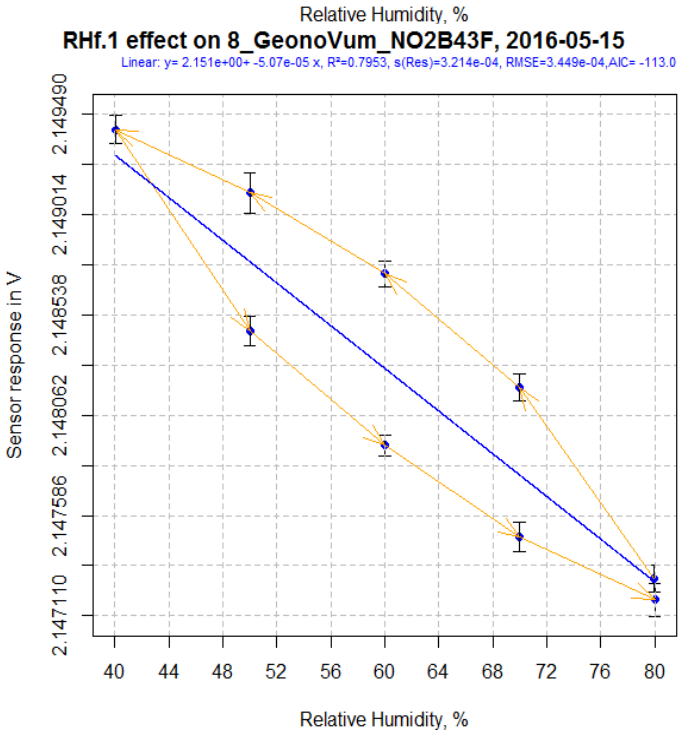

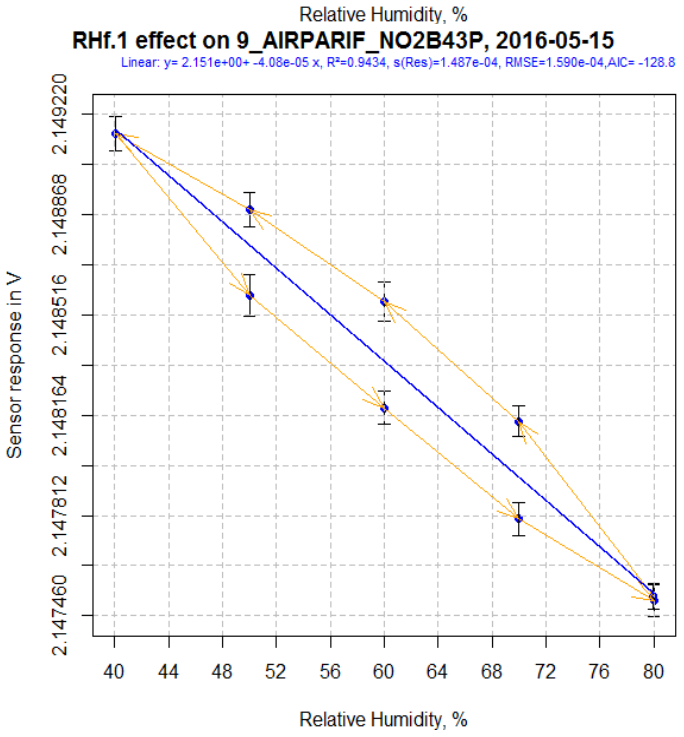

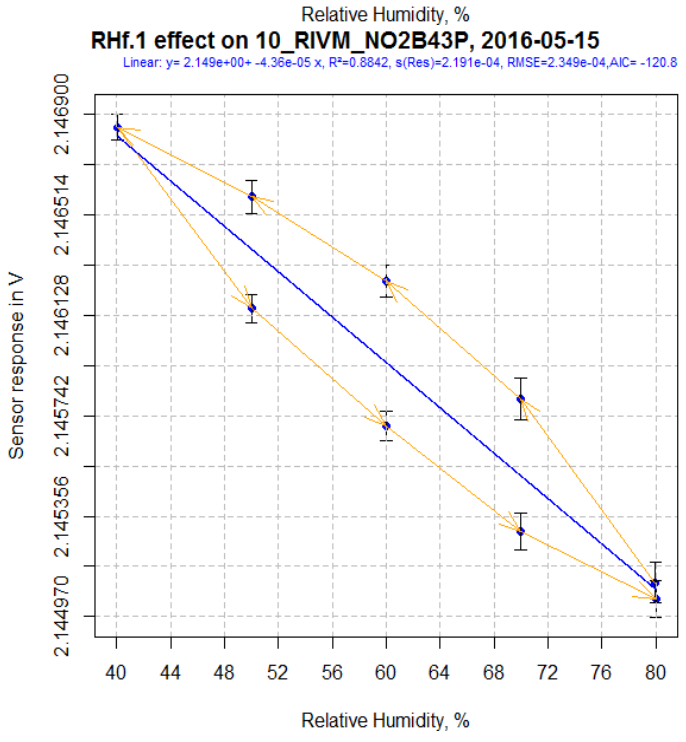

Figure 33:NO2-B43F relative humidity effect

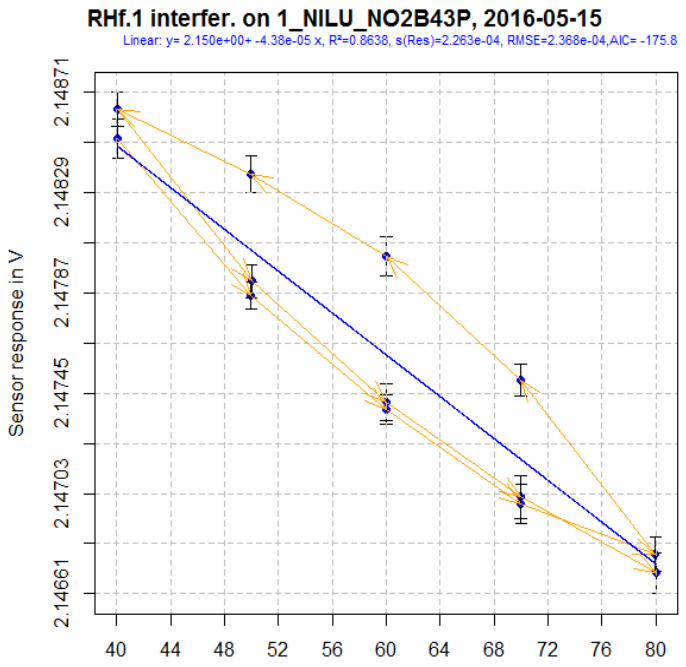

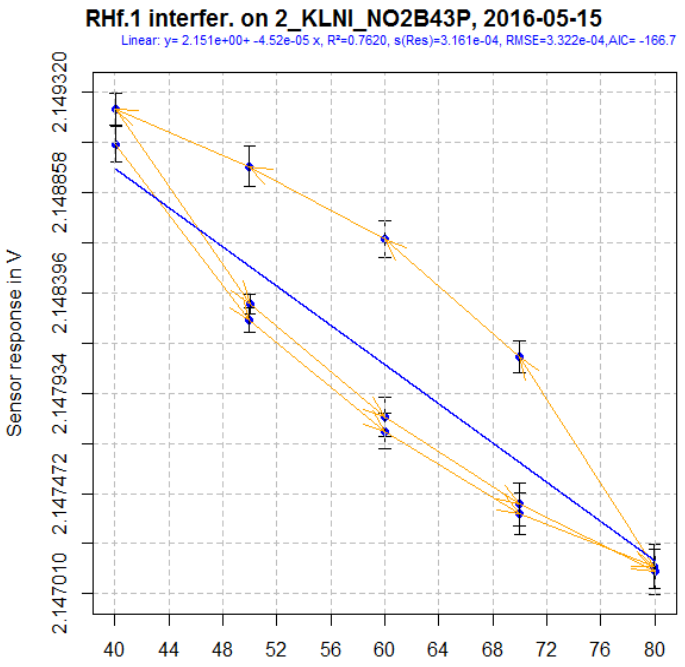

No data available because of connection error

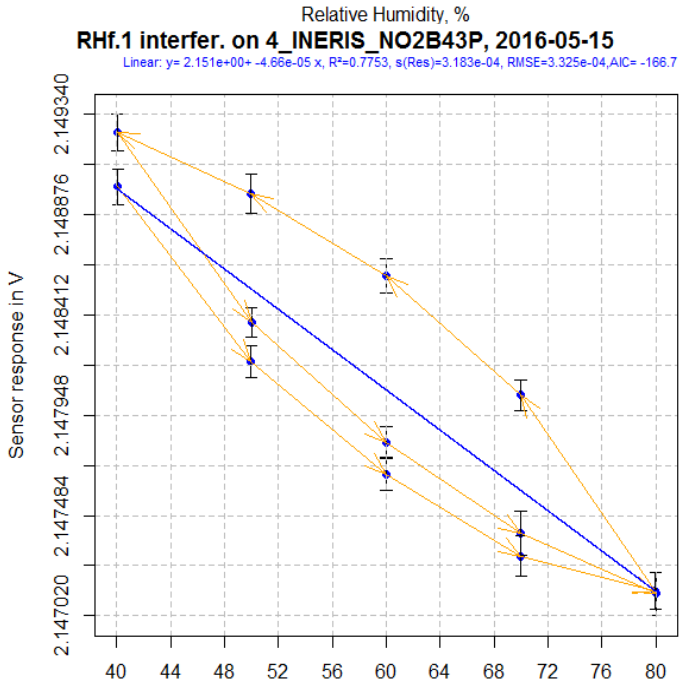

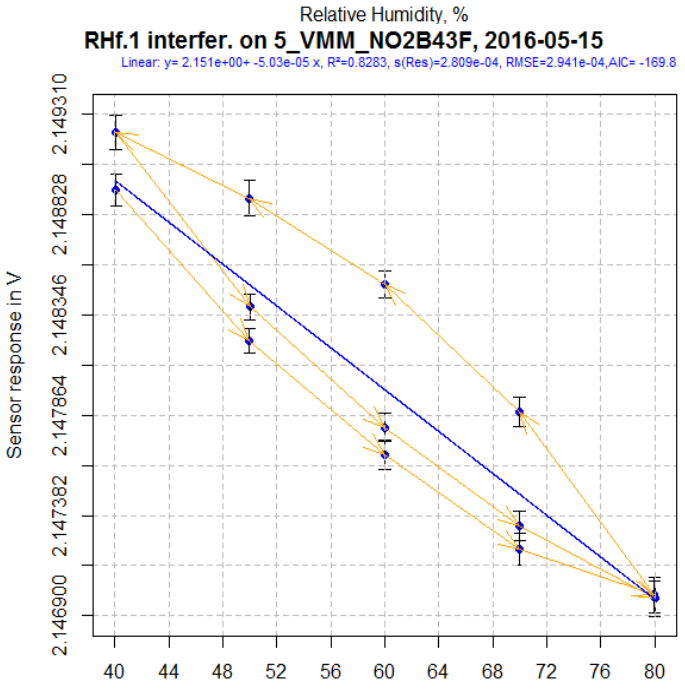

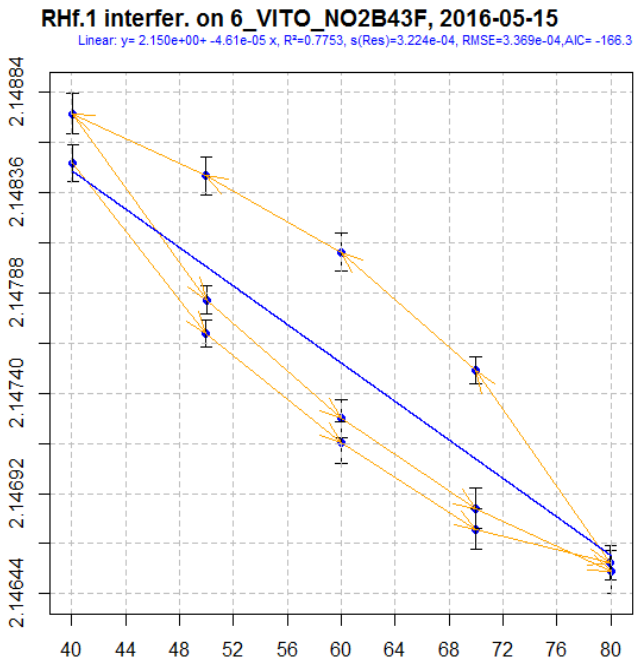

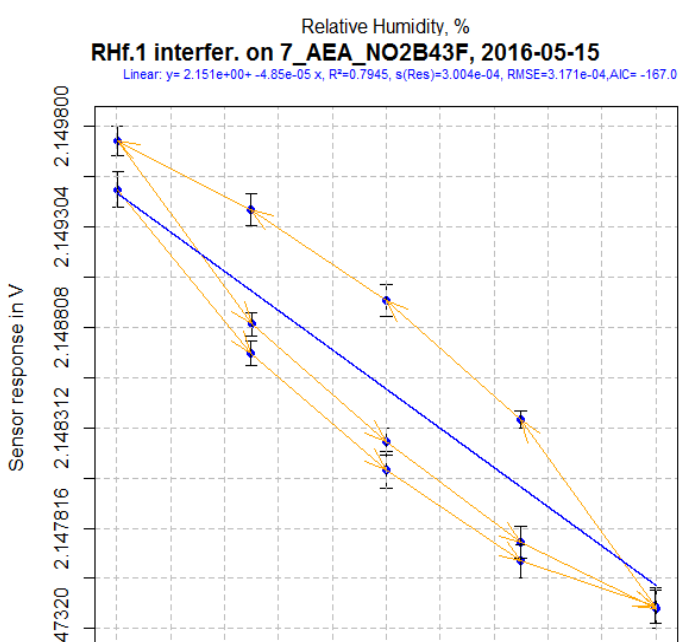

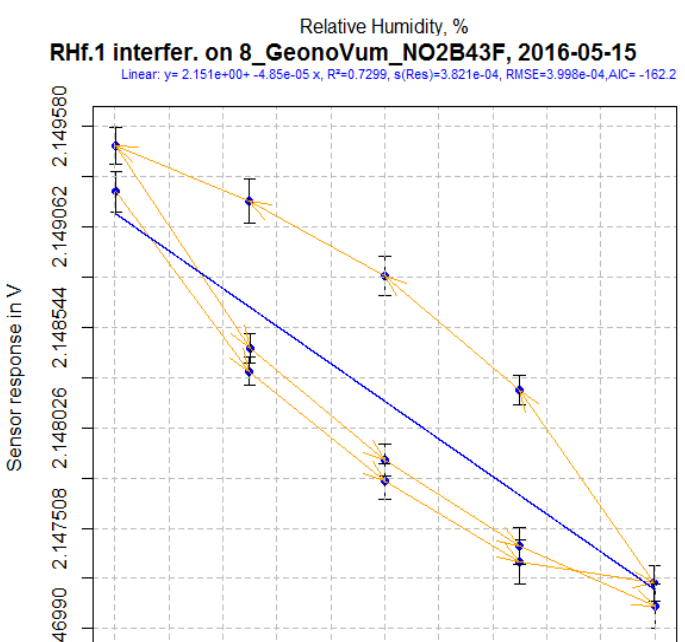

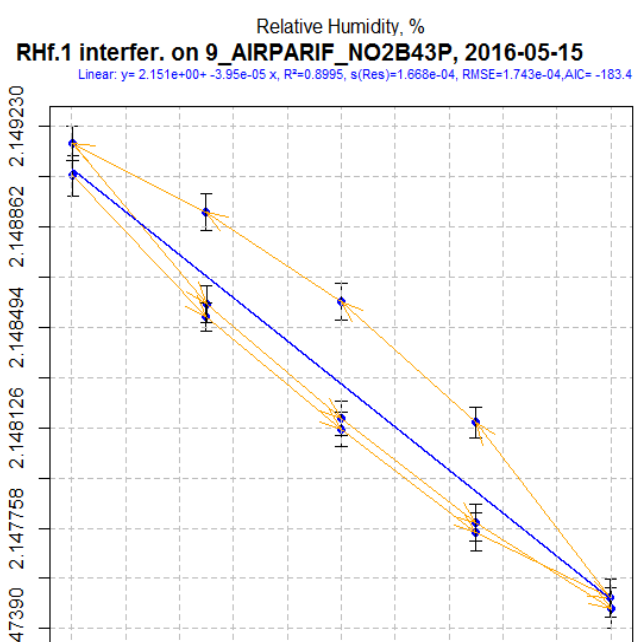

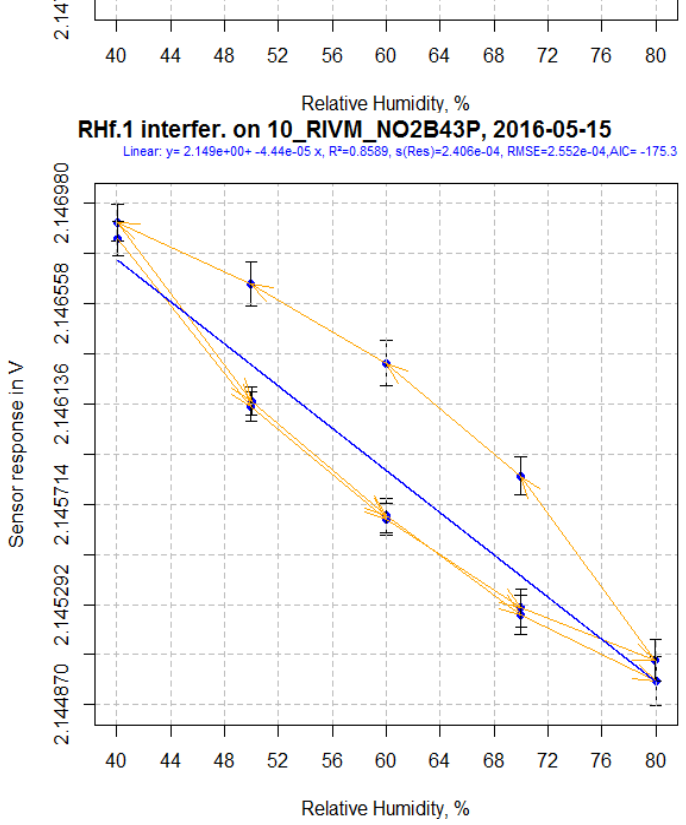

Figure 34:NO2-B43F relative humidity effect, all steps

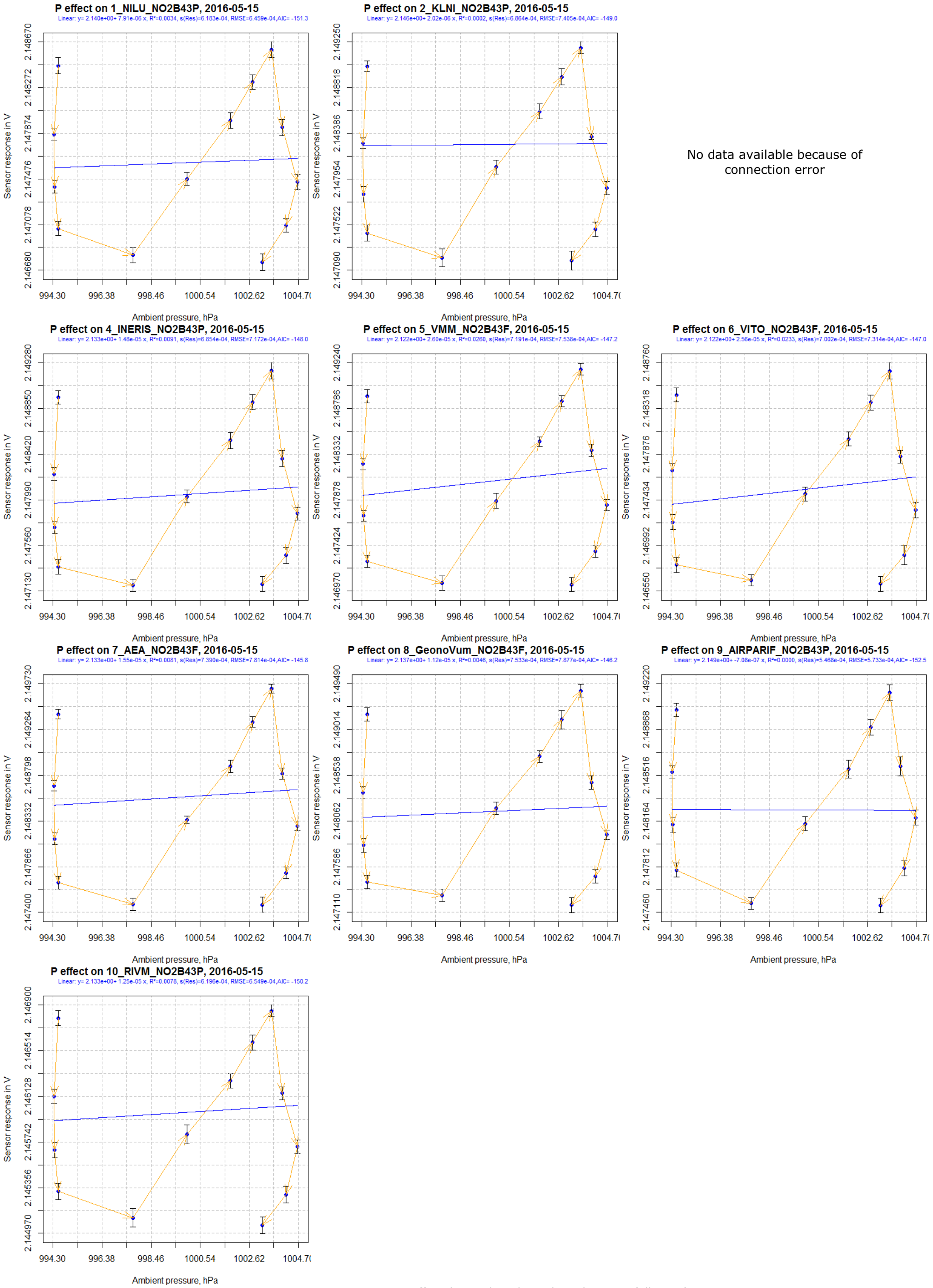

Figure 35: NO2-B43F, pressure effect during the relative humidity tests (all steps)

5.1.2 CO/MF-200 sensor

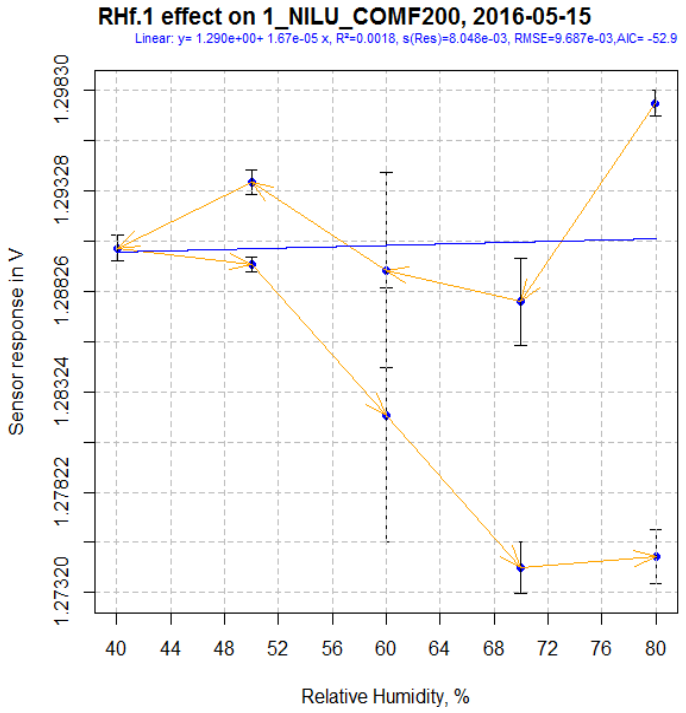

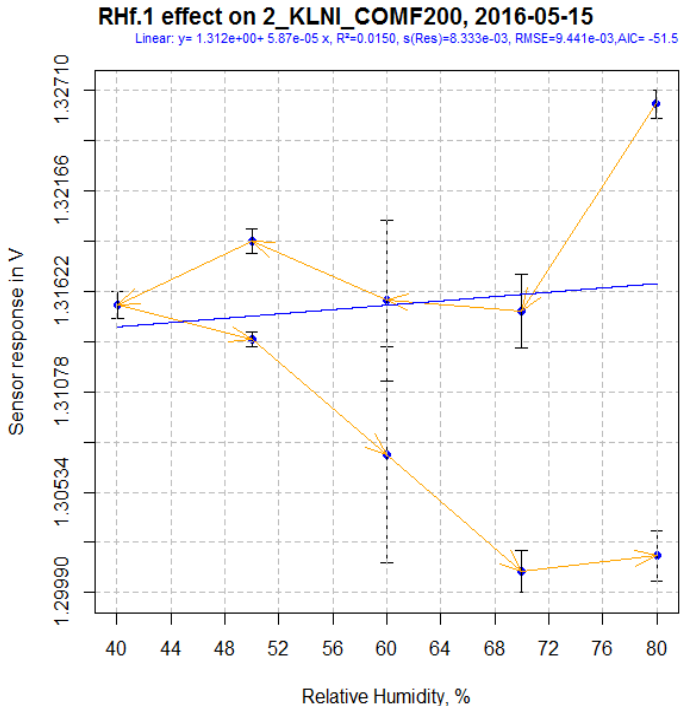

No data available because of connection error

No data available because the sensor channel was damaged

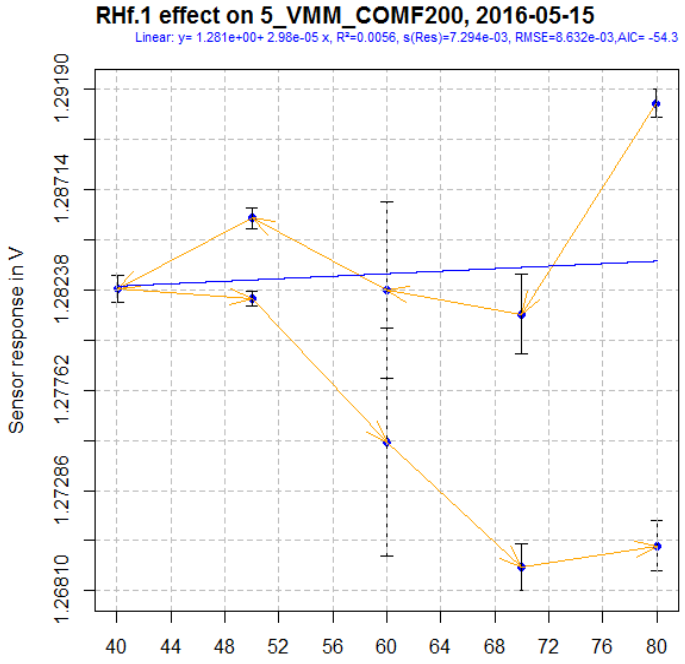

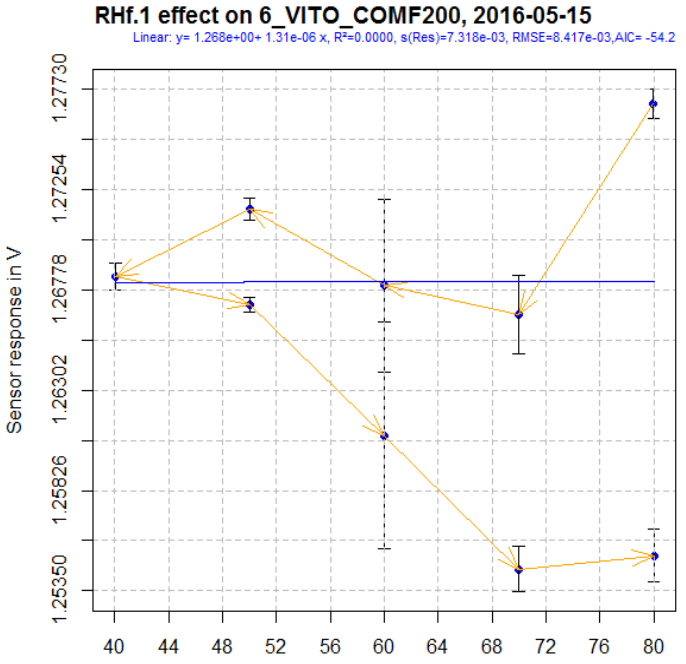

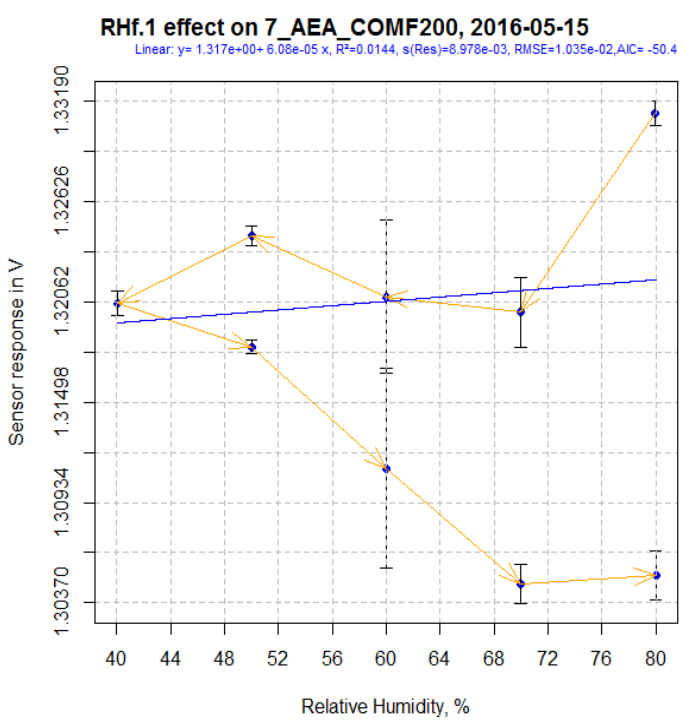

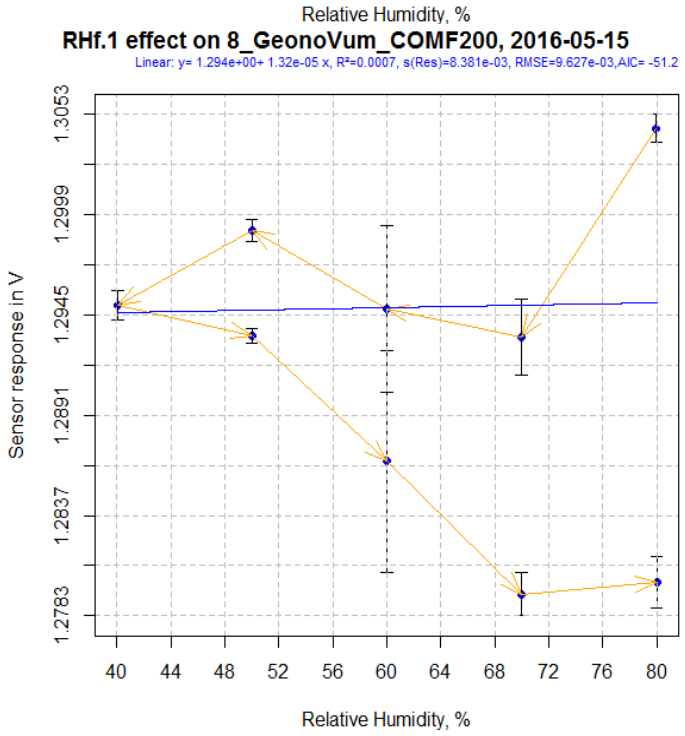

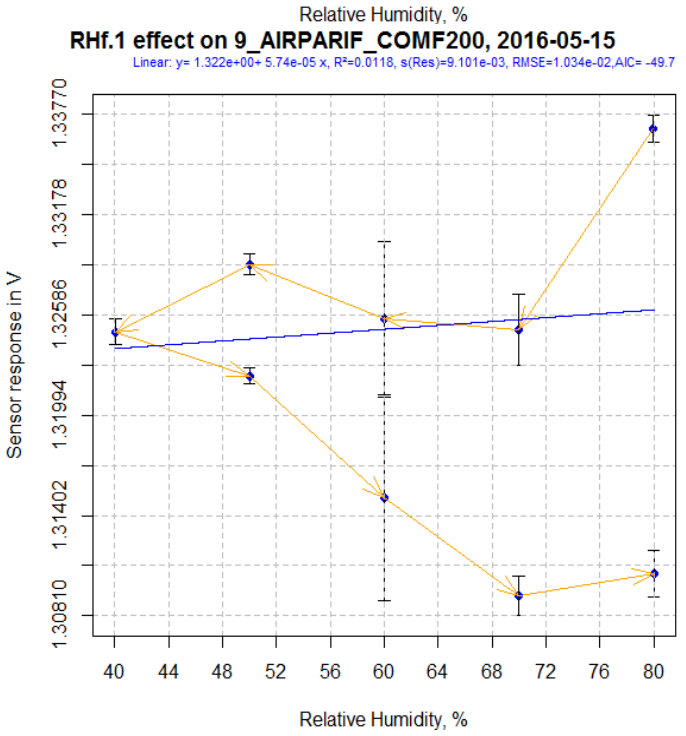

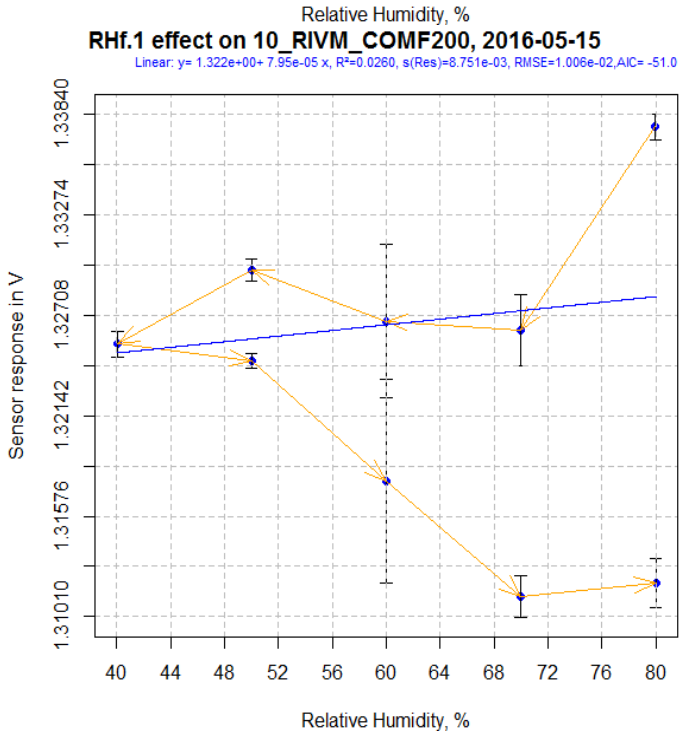

Figure 36: CO/MF-200, relative humidity effect

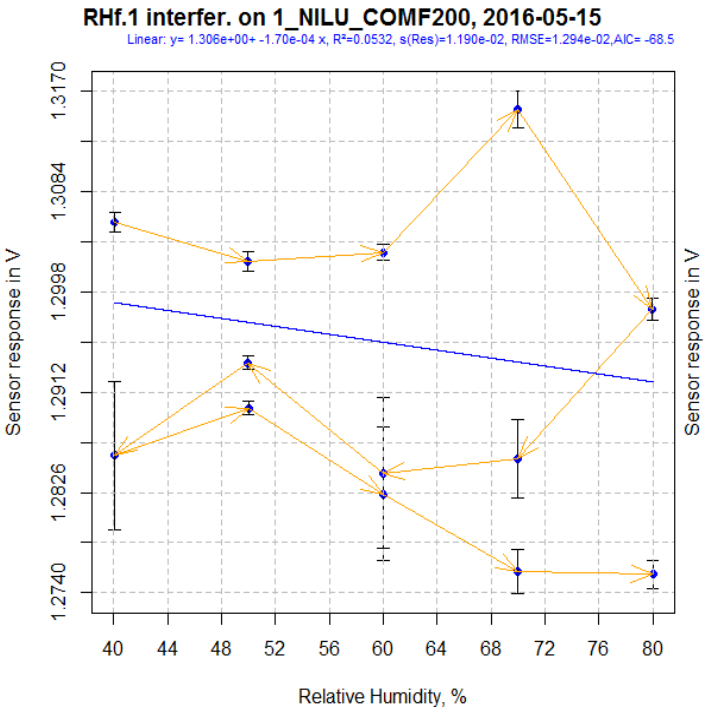

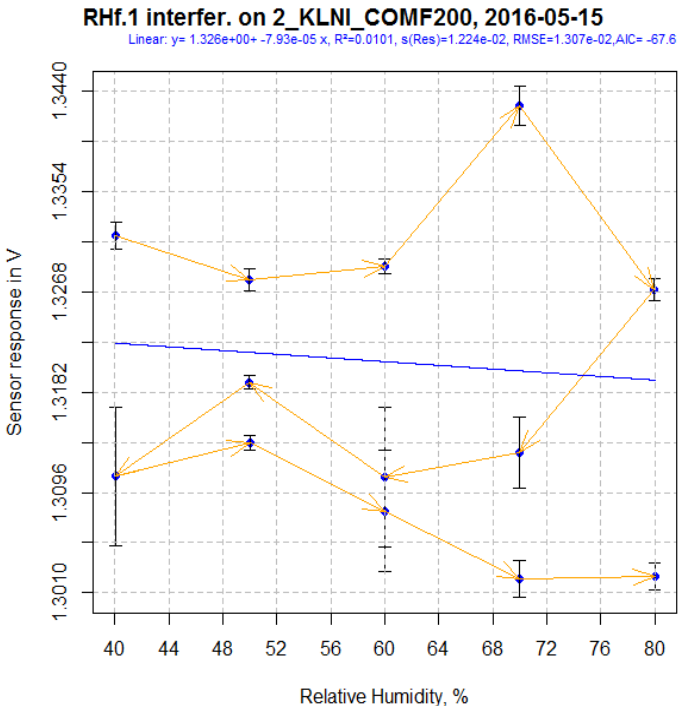

No data available because of connection error

No data available because the sensor channel was damaged

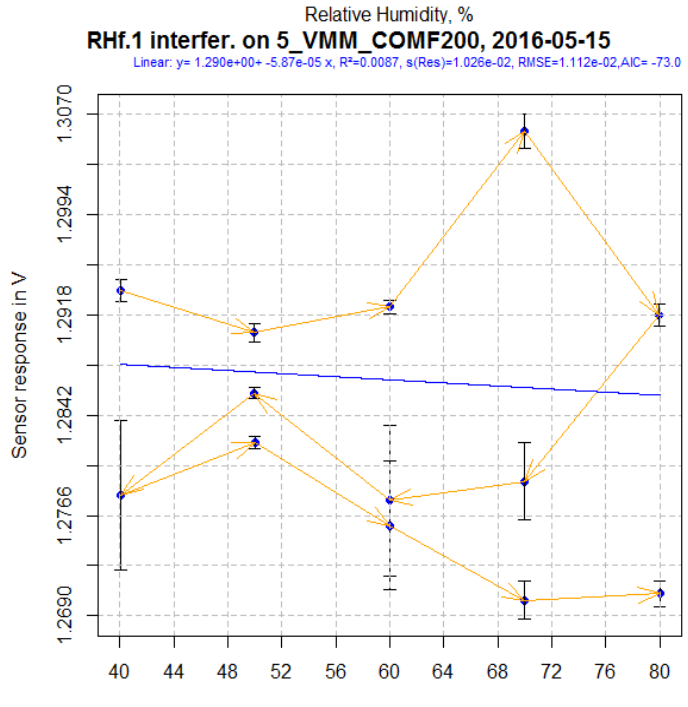

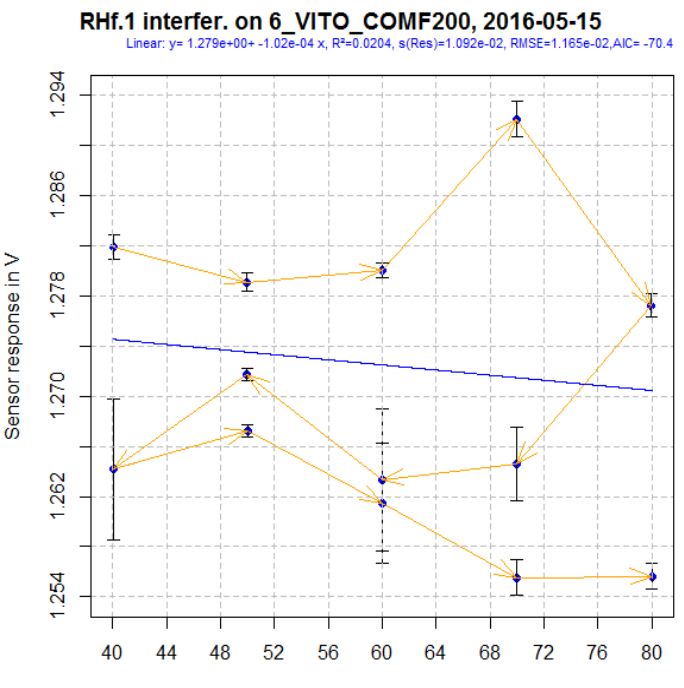

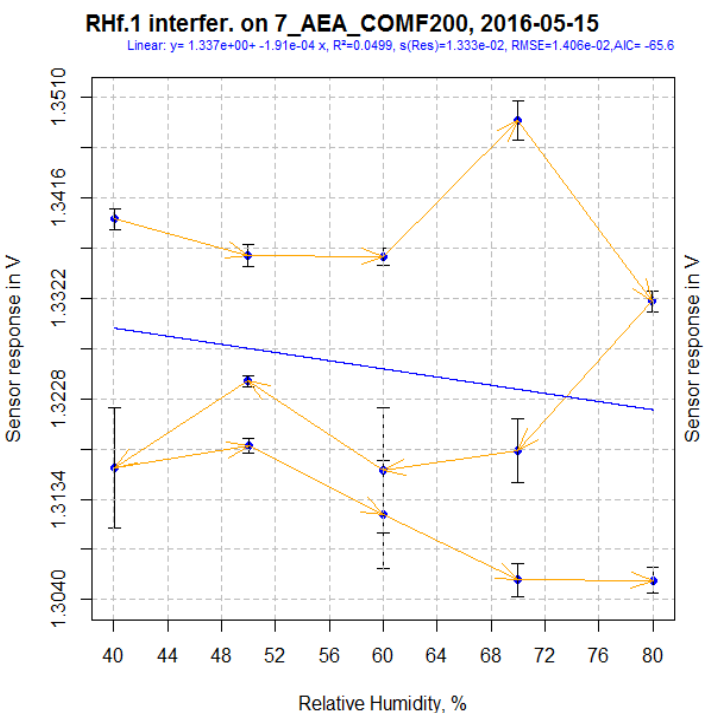

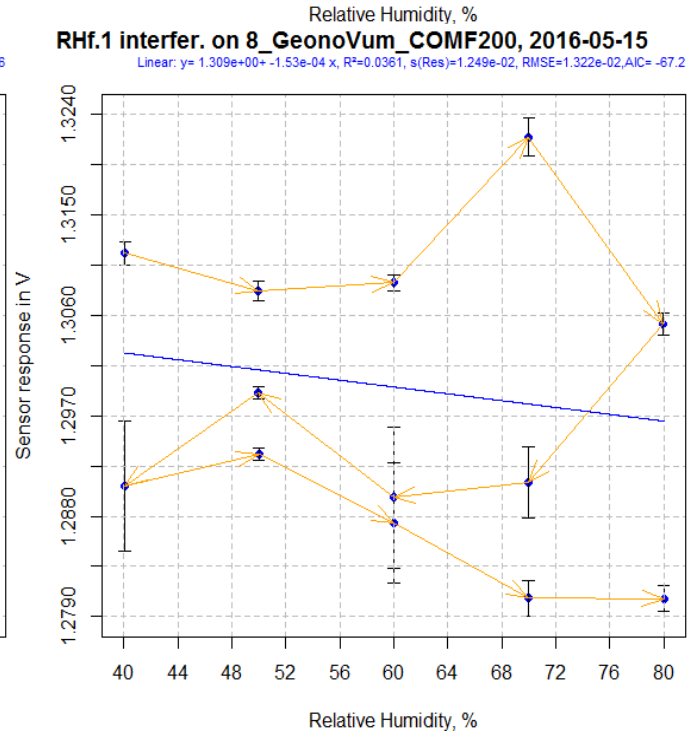

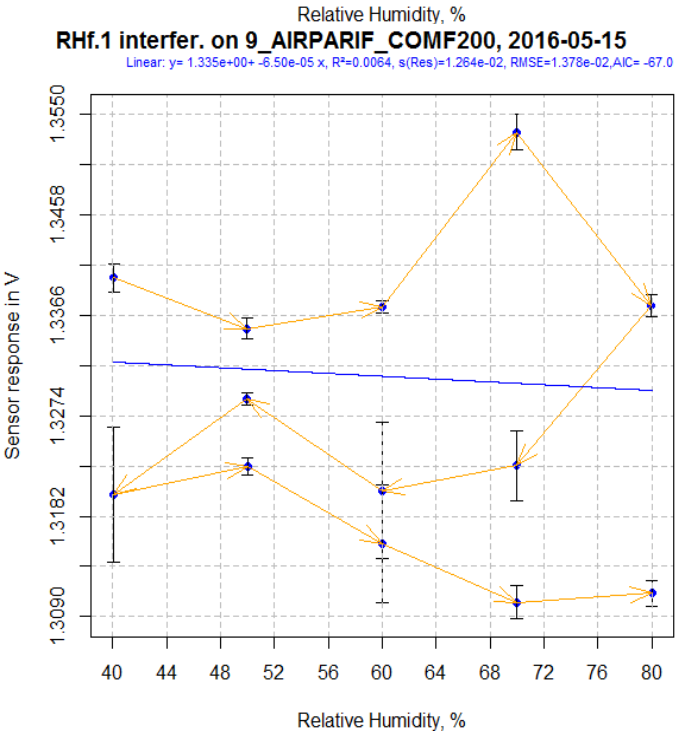

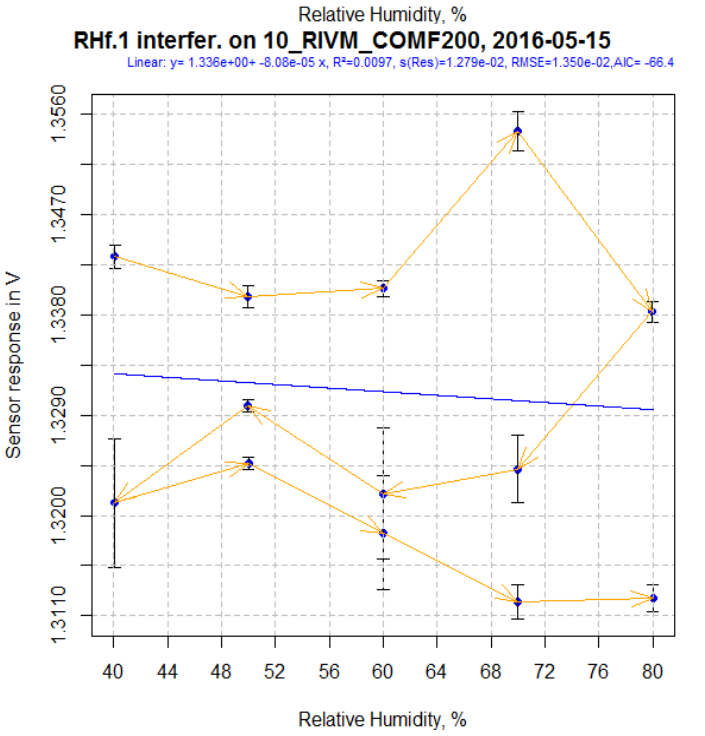

Figure 37: CO/MF-200, relative humidity effect (all steps)

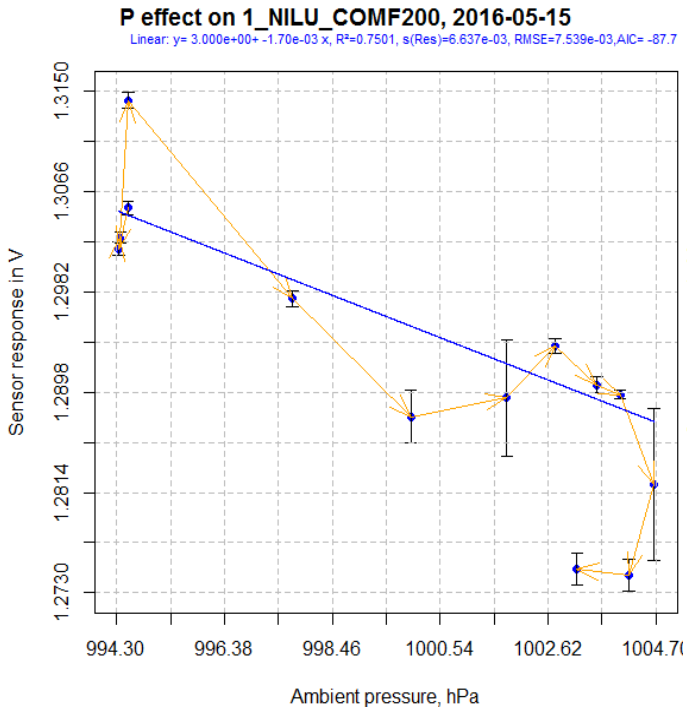

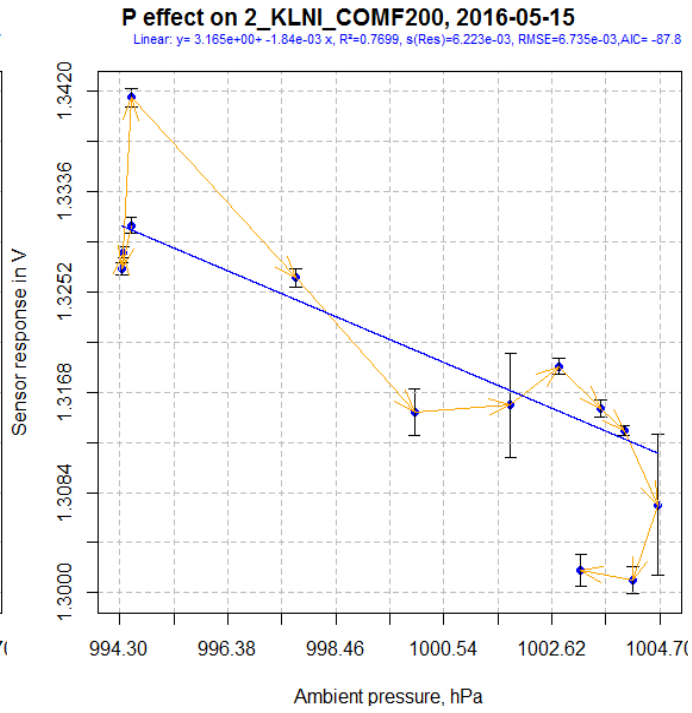

No data available because of connection error

No data available because the sensor channel was damaged

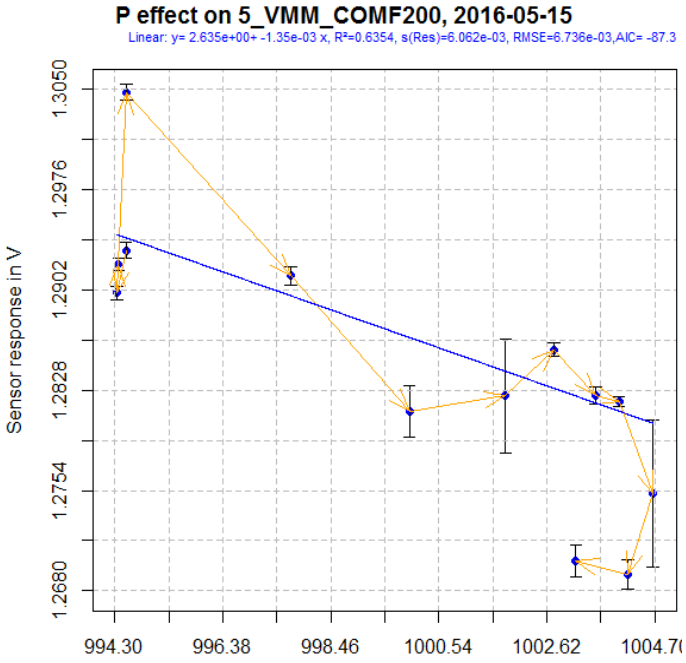

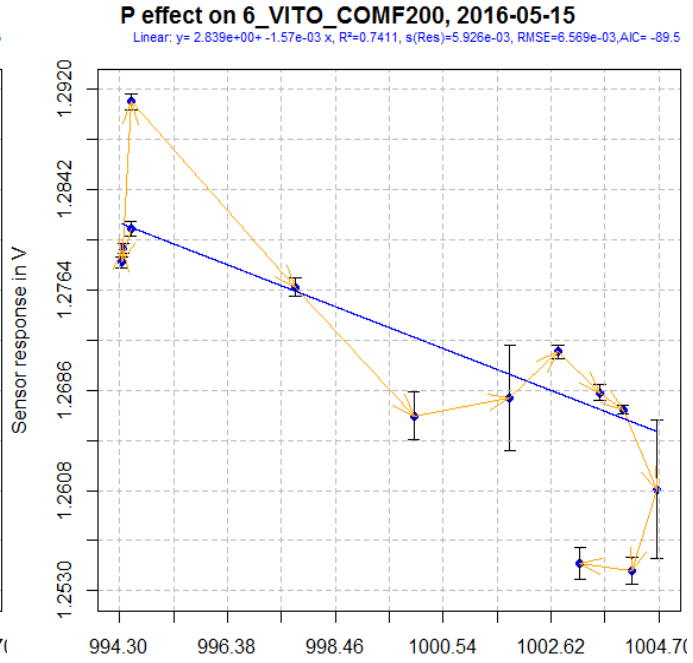

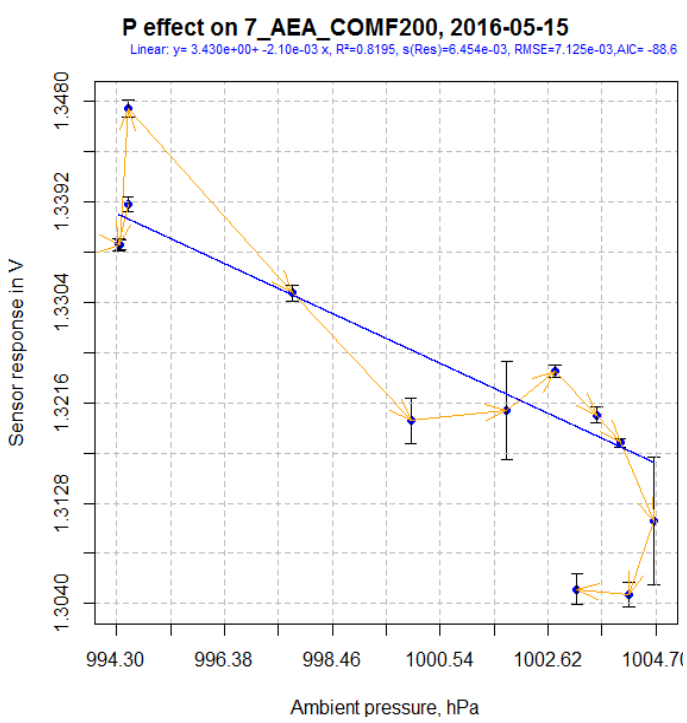

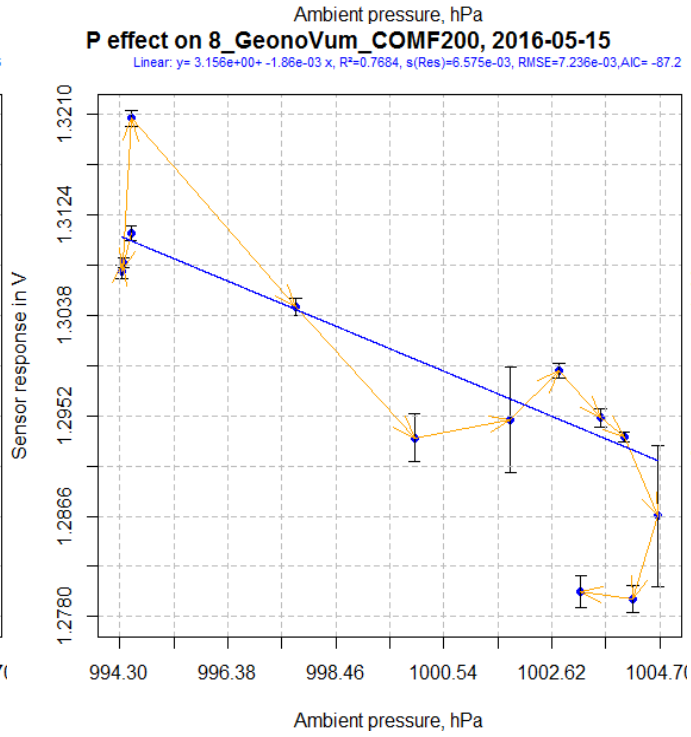

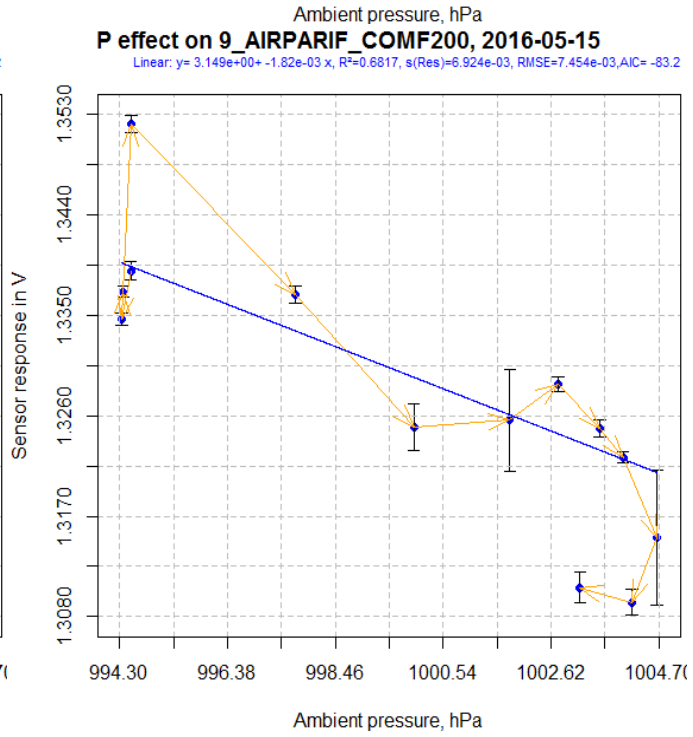

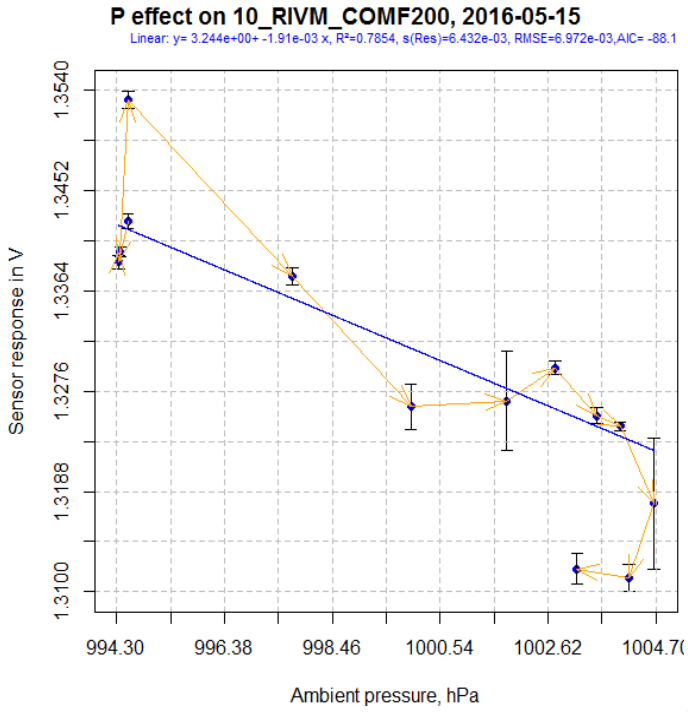

Figure 38: CO/MF-200, pressure effect during the relative humidity tests (all steps)

5.1.3 O3/M-5 sensor

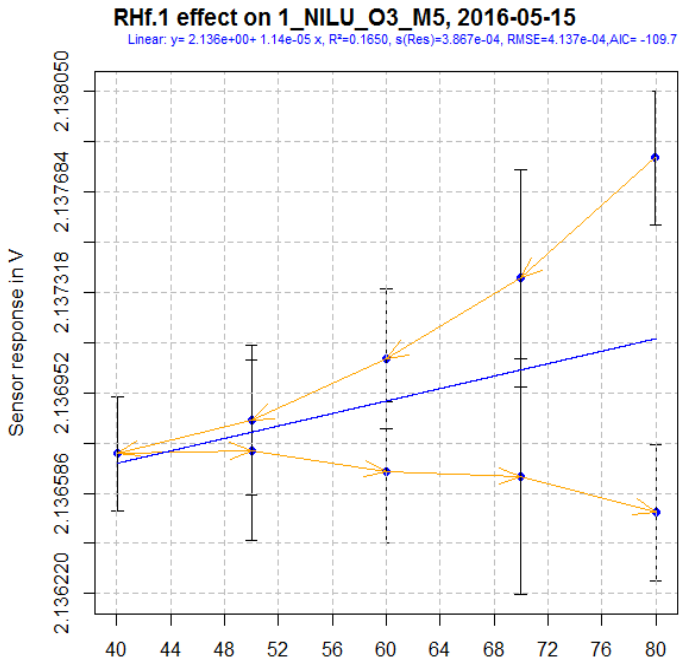

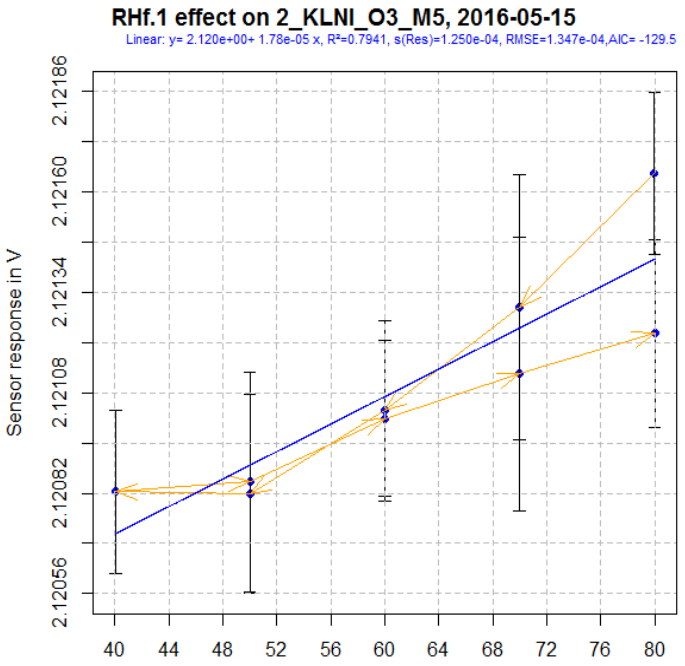

No data available because of connection error

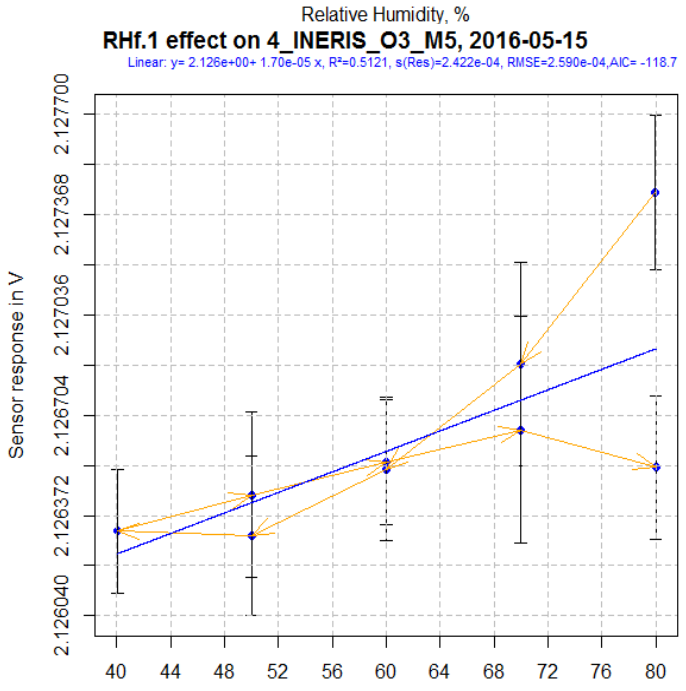

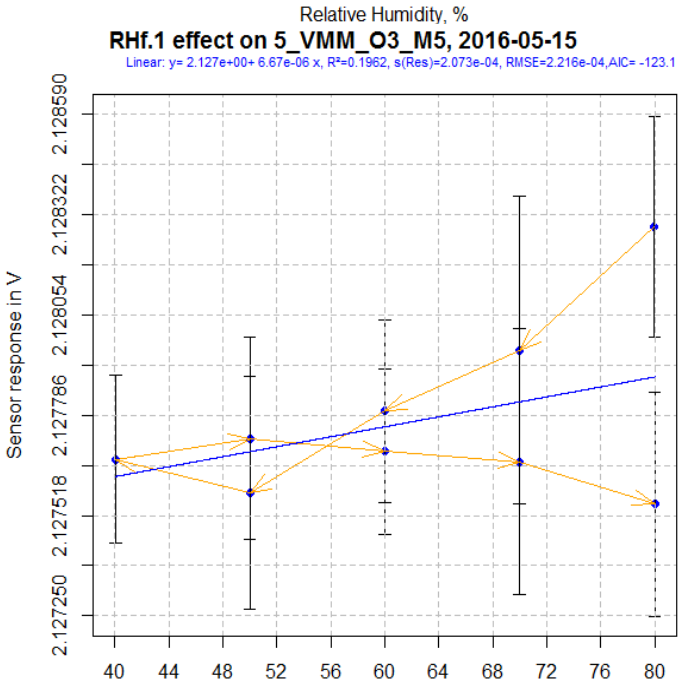

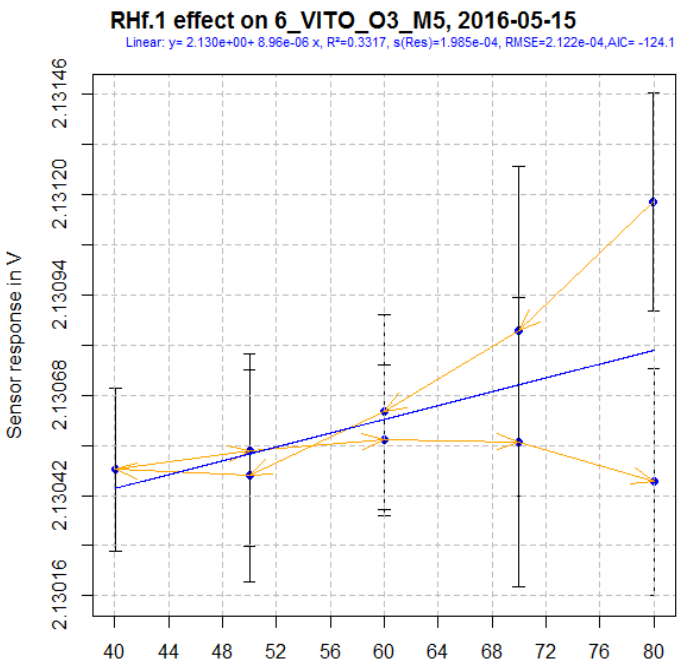

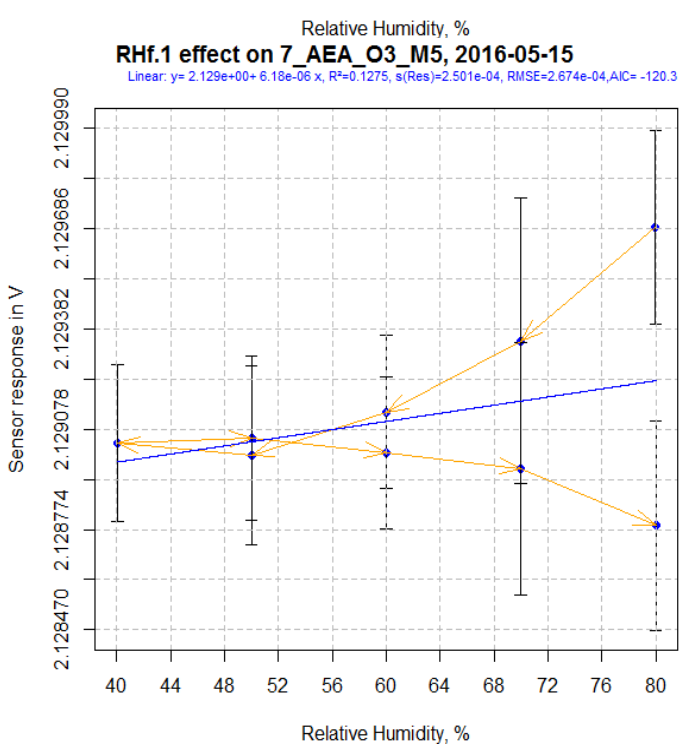

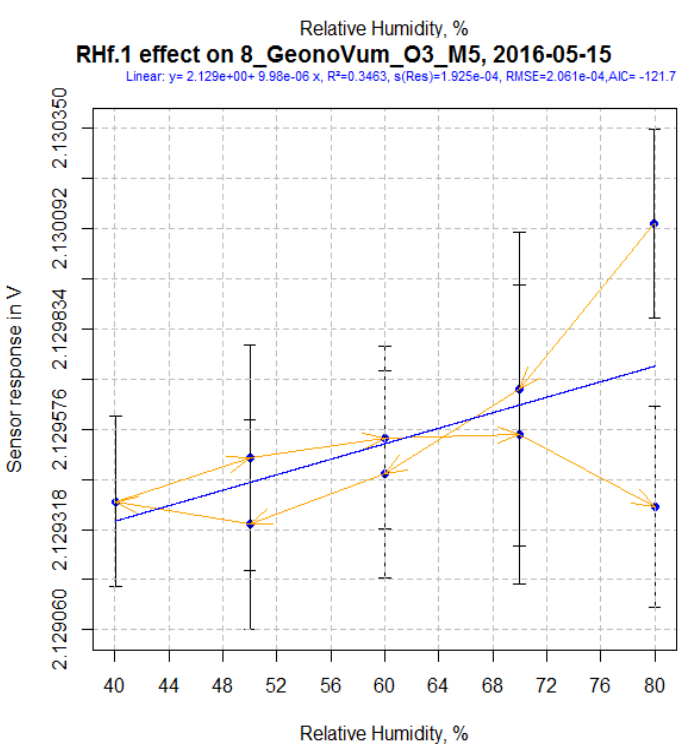

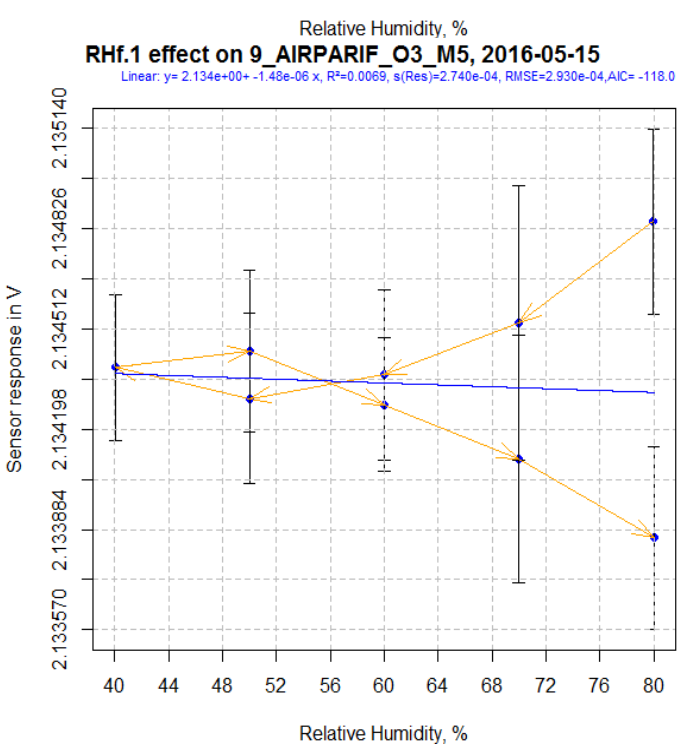

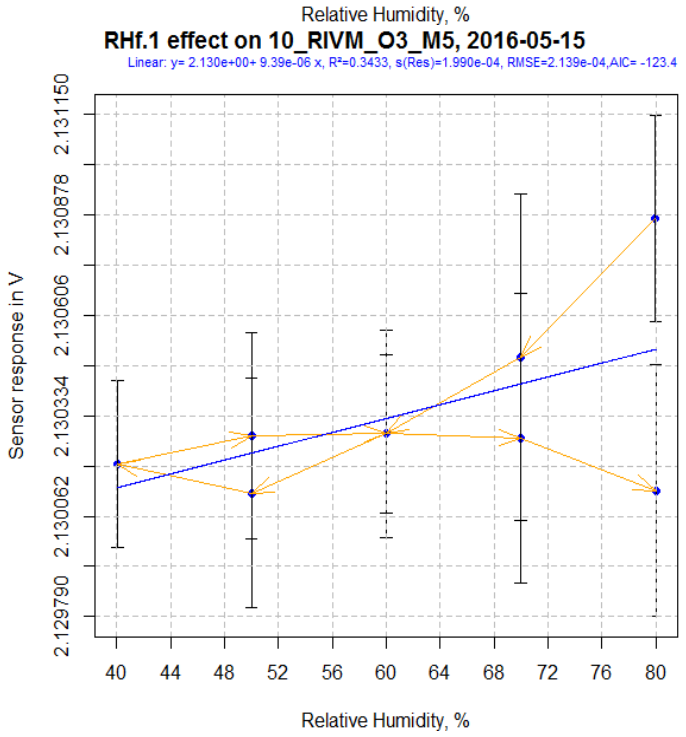

Figure 39: O3/M-5, relative humidity effect

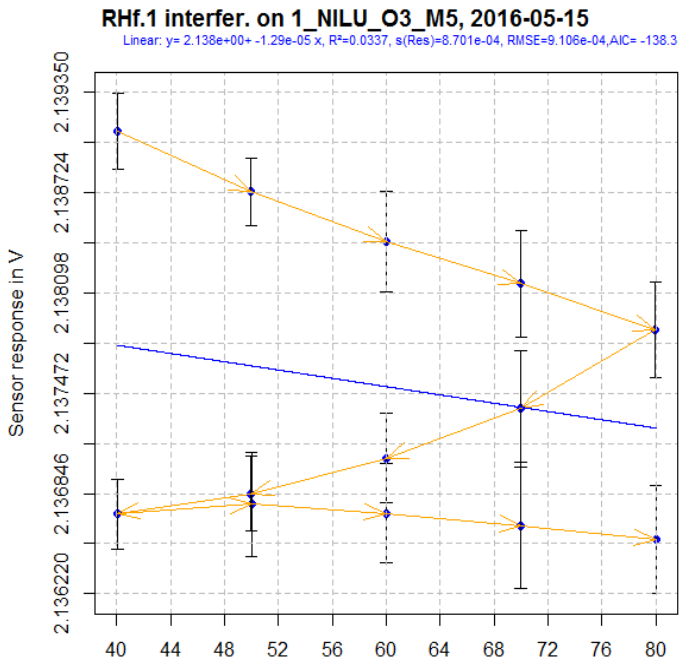

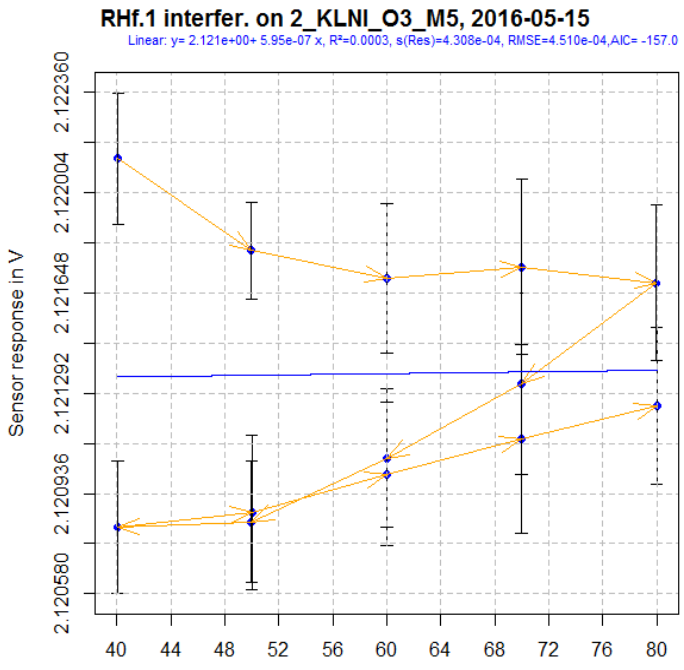

No data available because of connection error

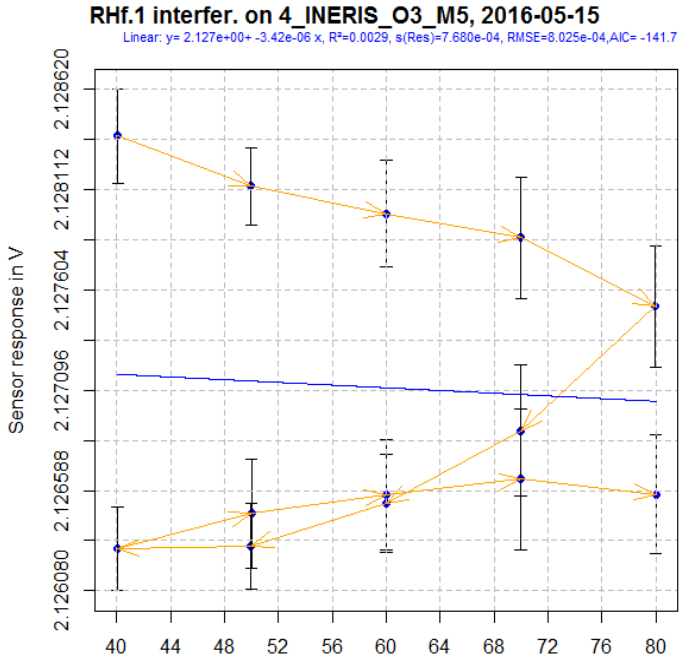

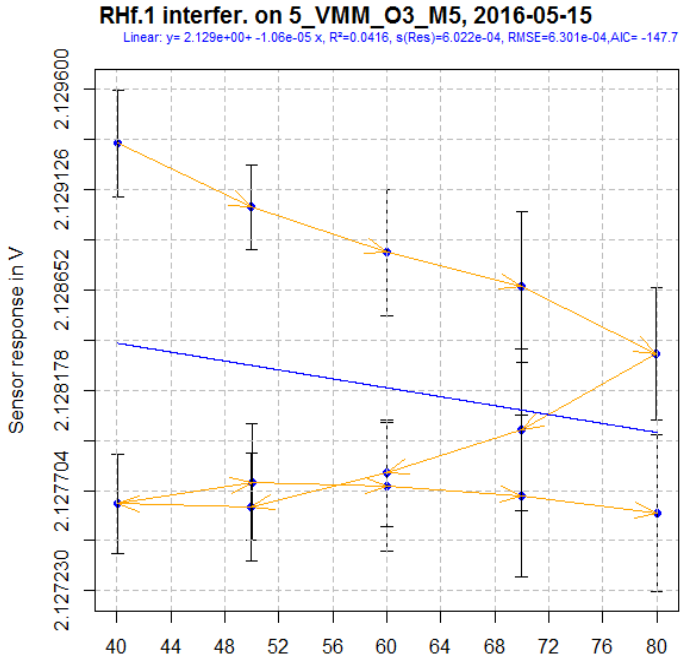

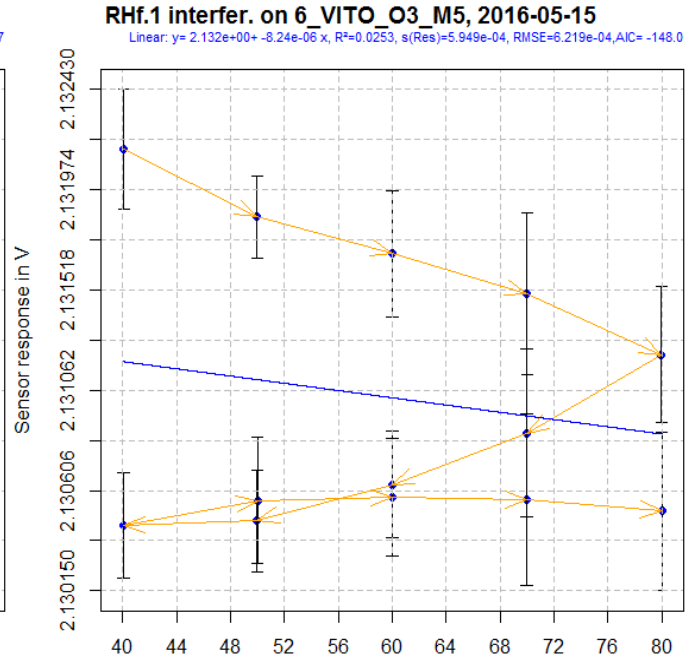

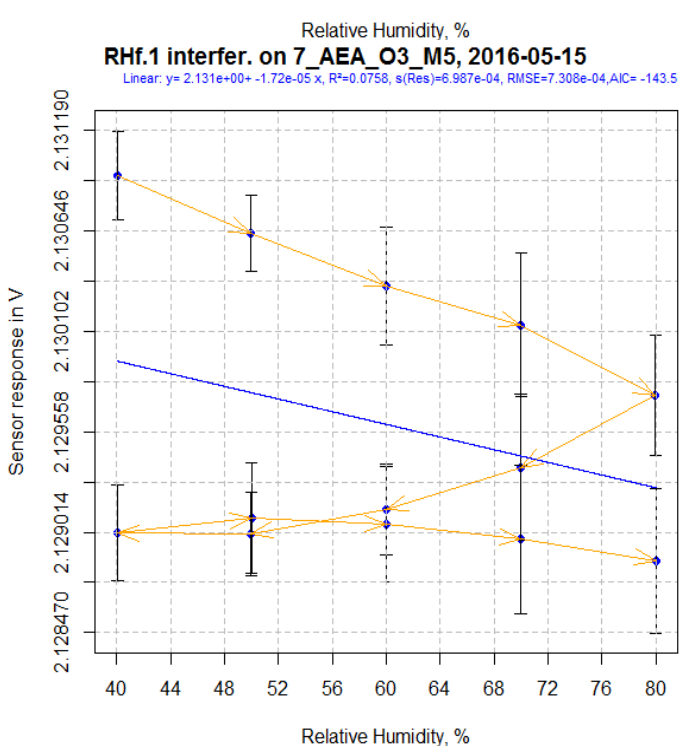

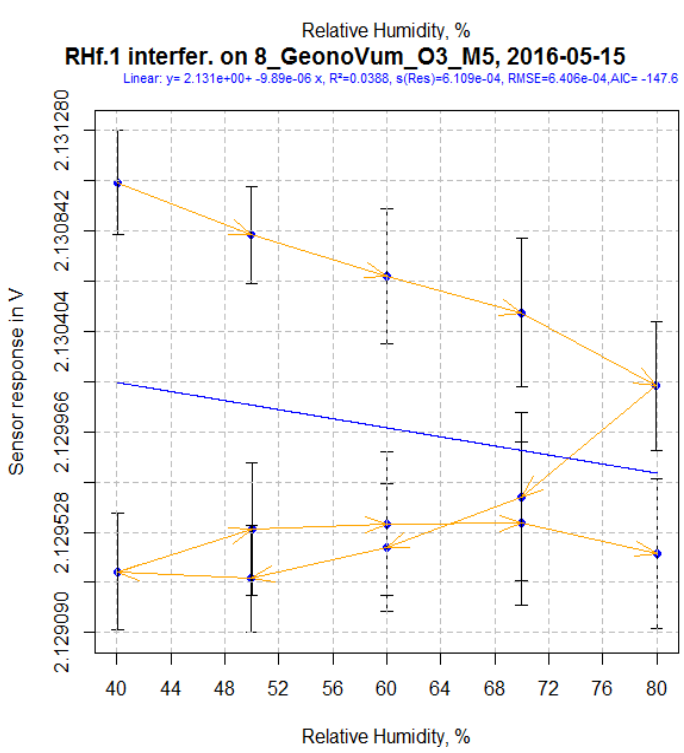

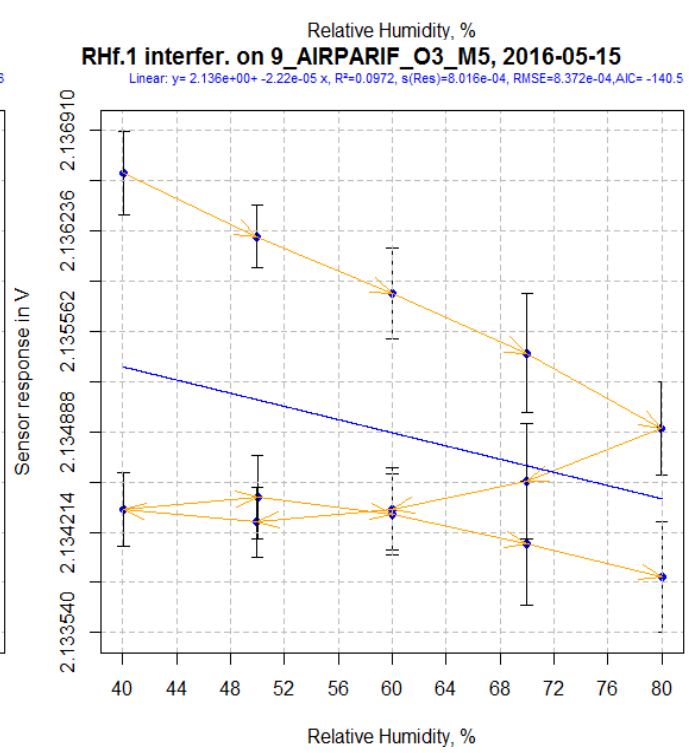

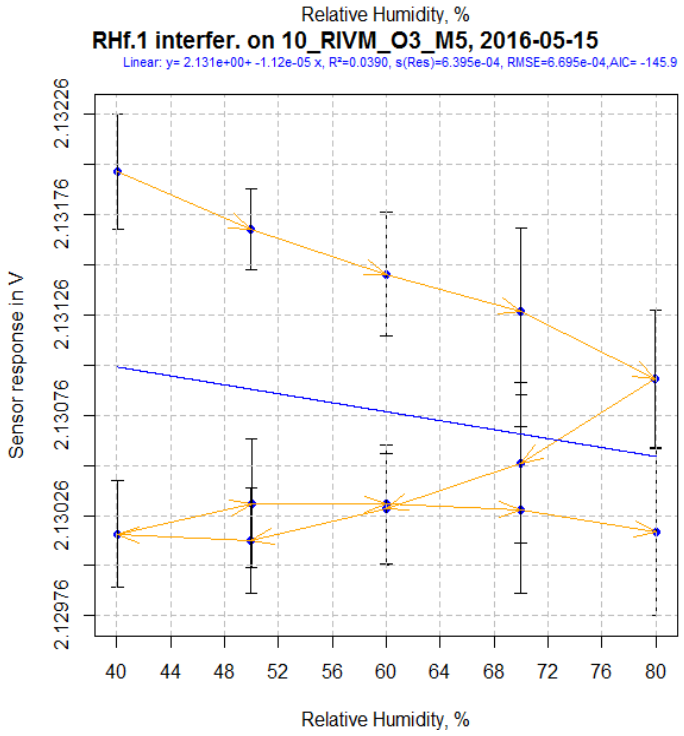

Figure 40: O3/M-5, relative humidity effect

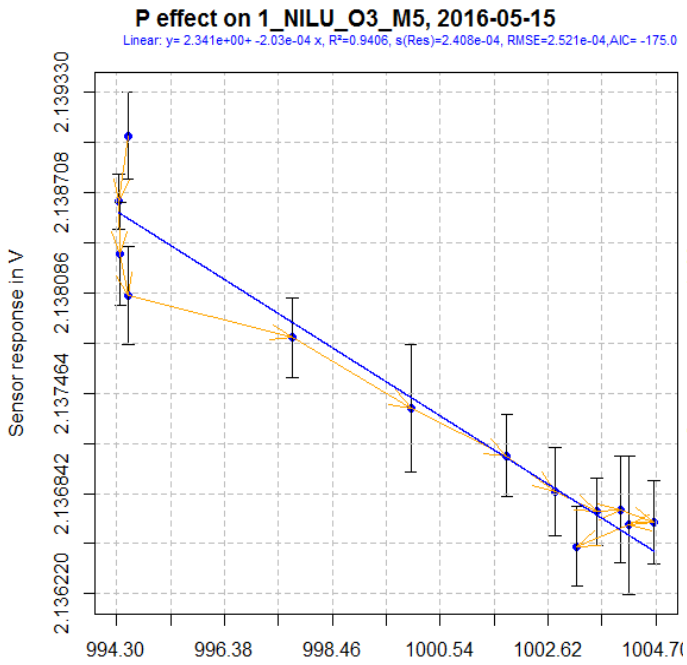

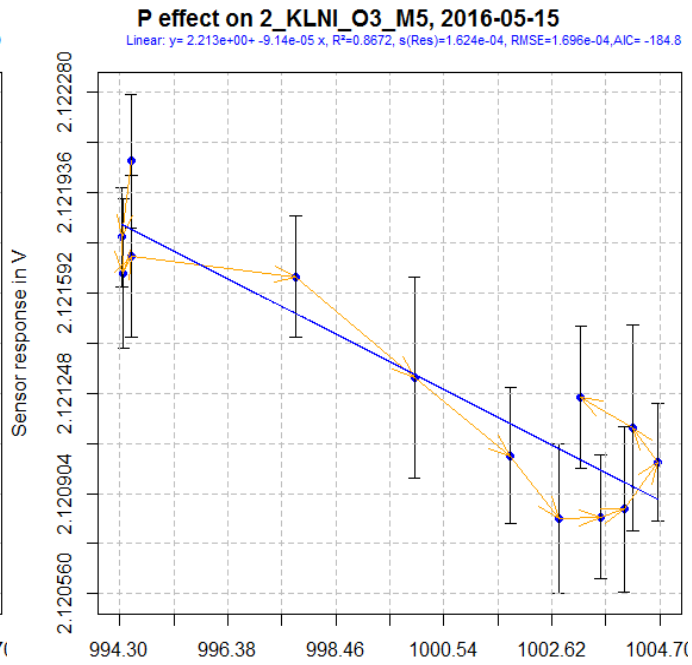

No data available because of connection error

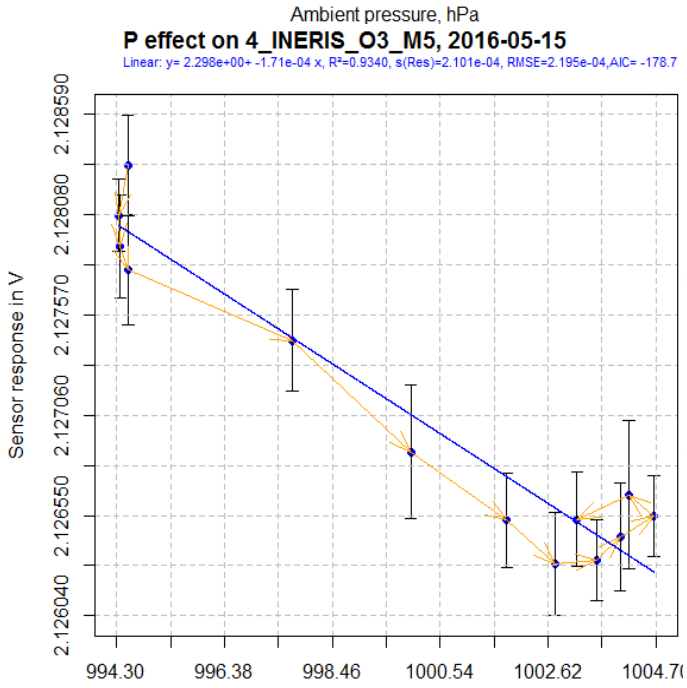

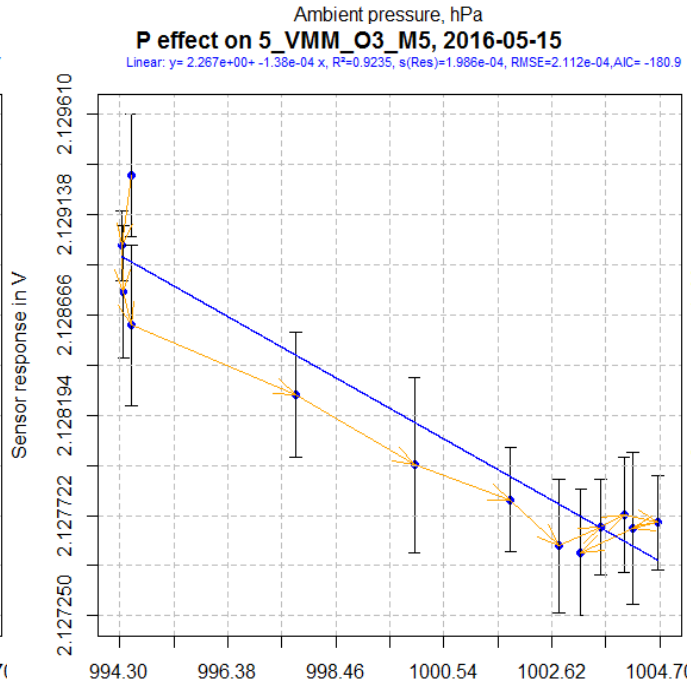

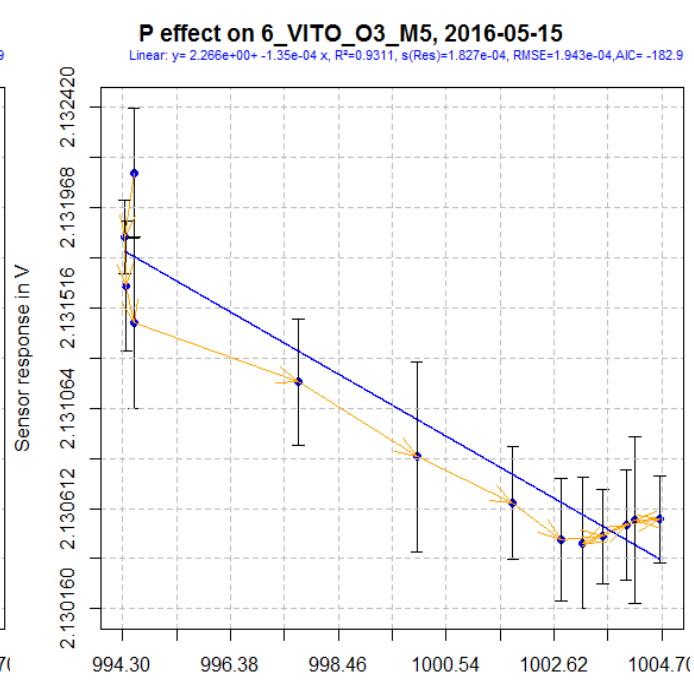

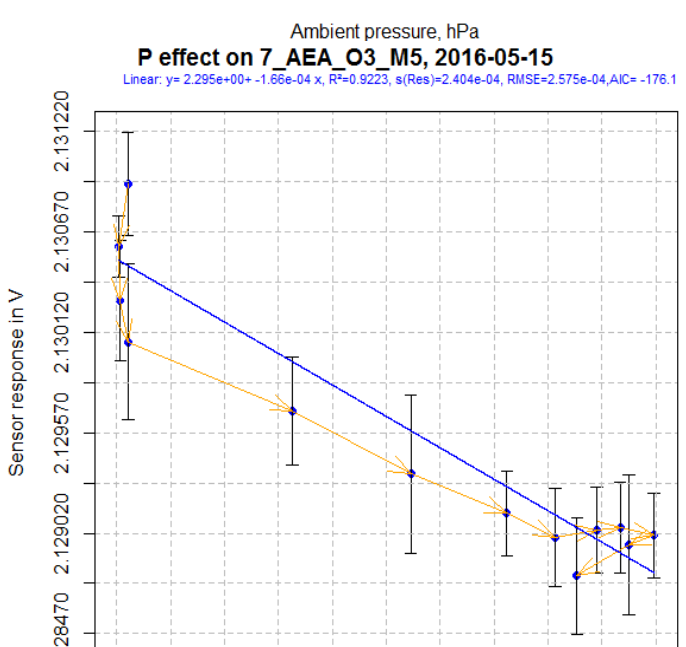

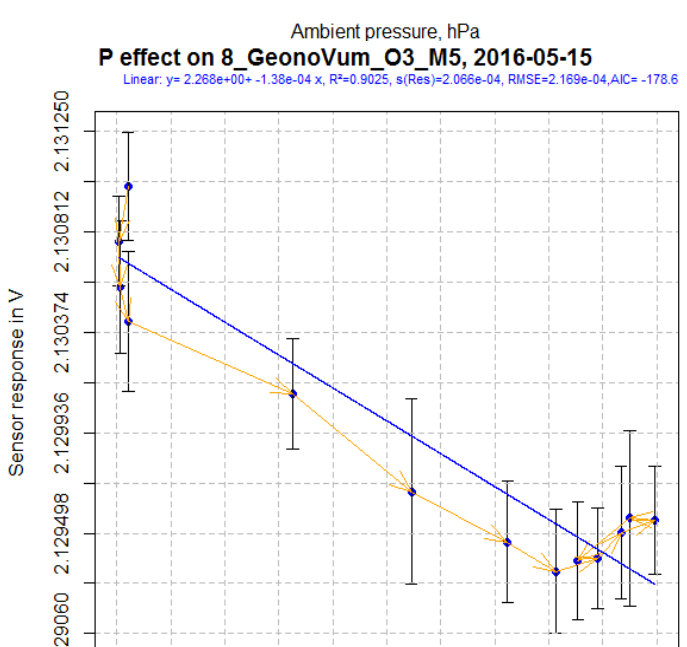

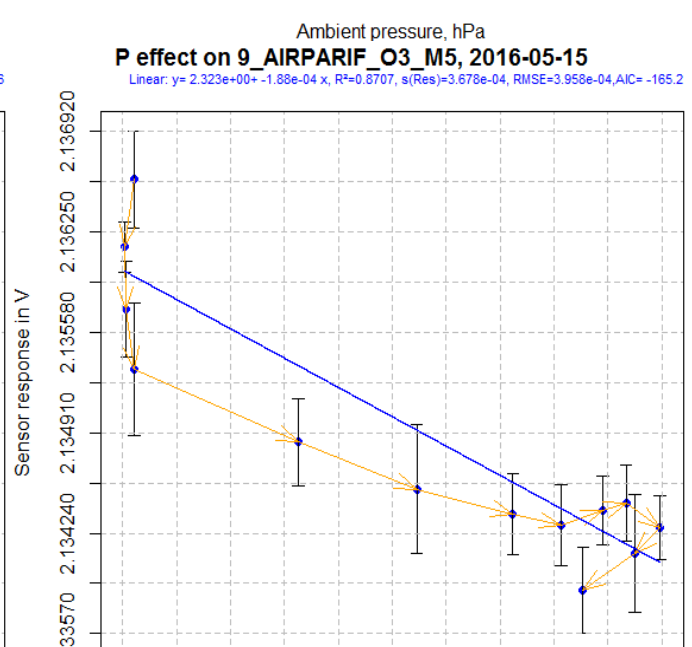

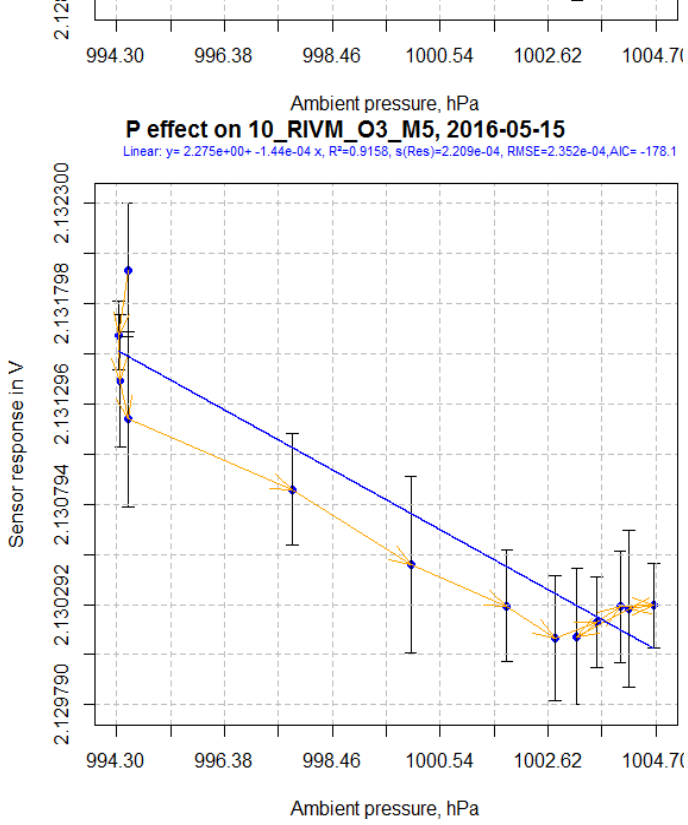

Figure 41: O3/M-5, pressure effect during the relative humidity tests (all steps)

5.1.4 NO-B4 sensor

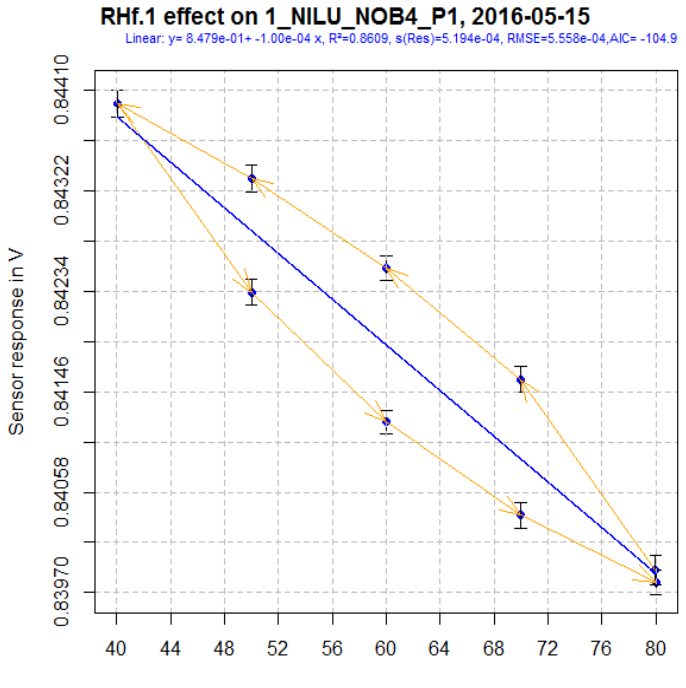

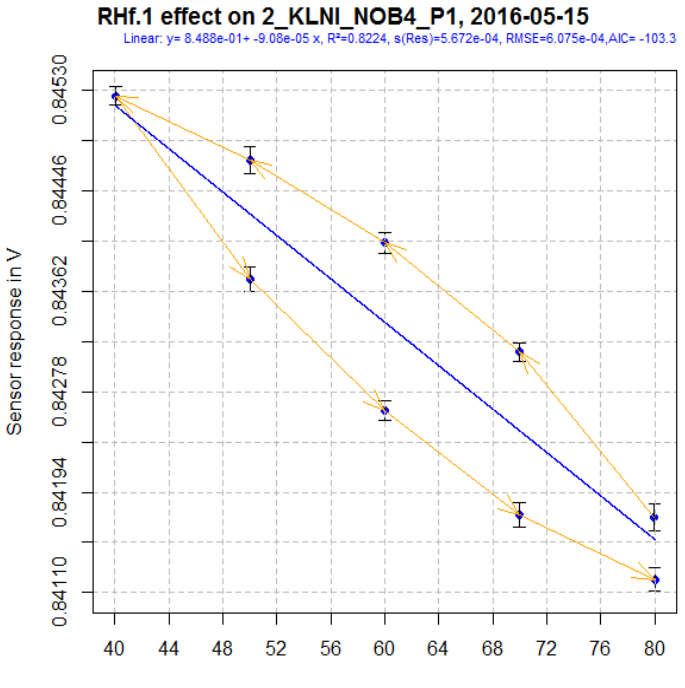

No data available because of connection error

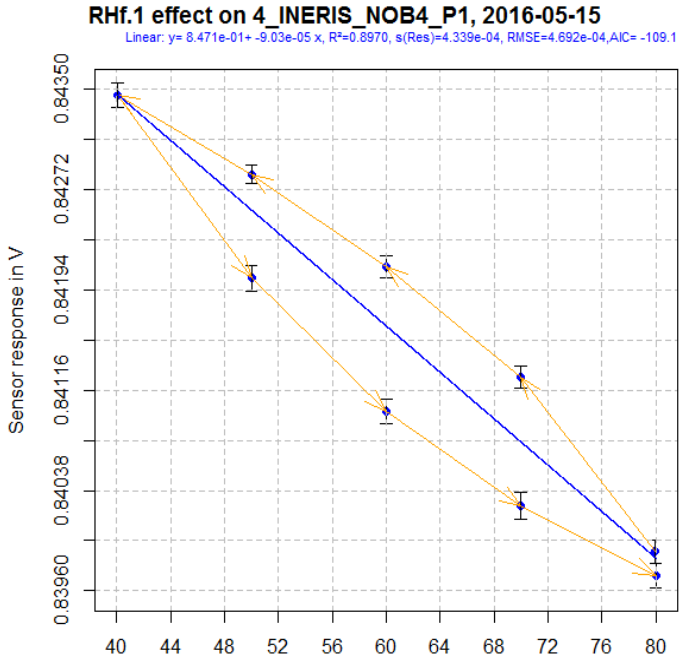

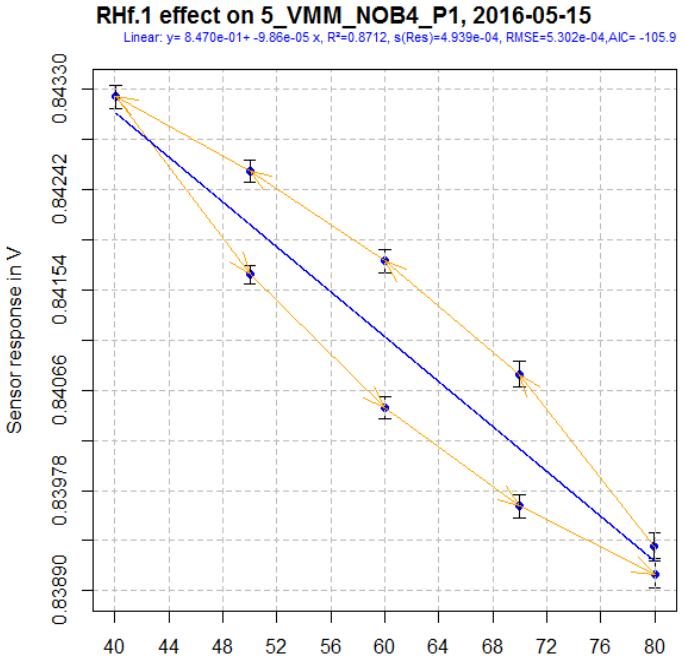

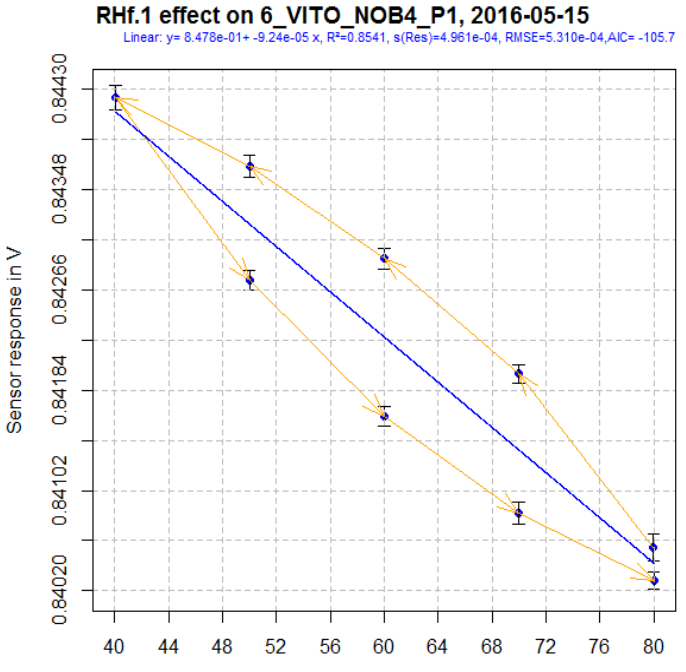

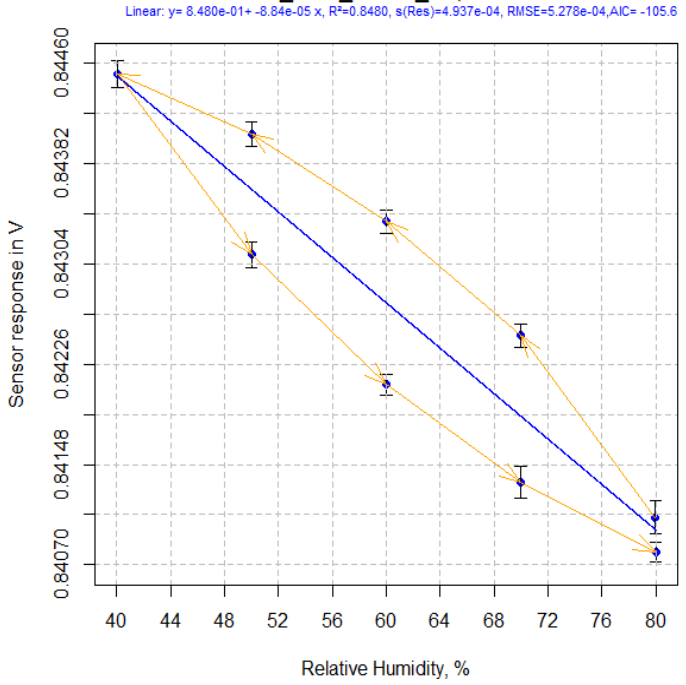

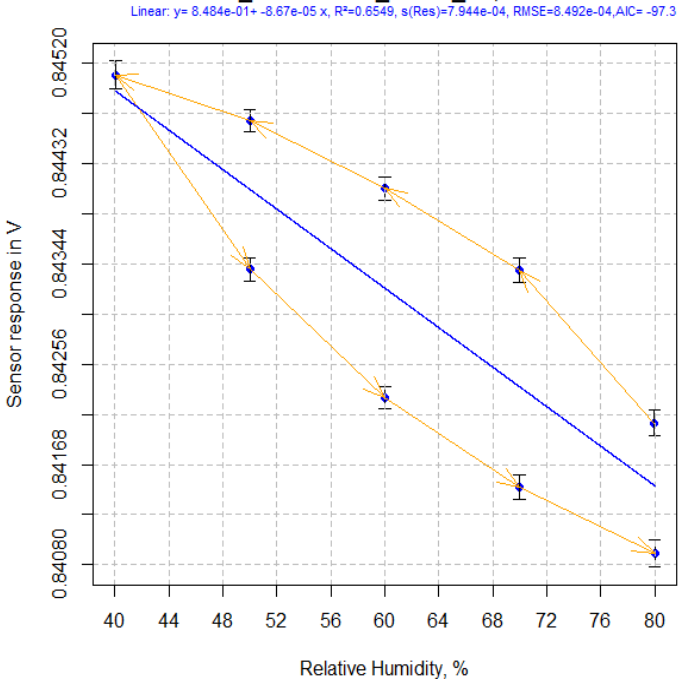

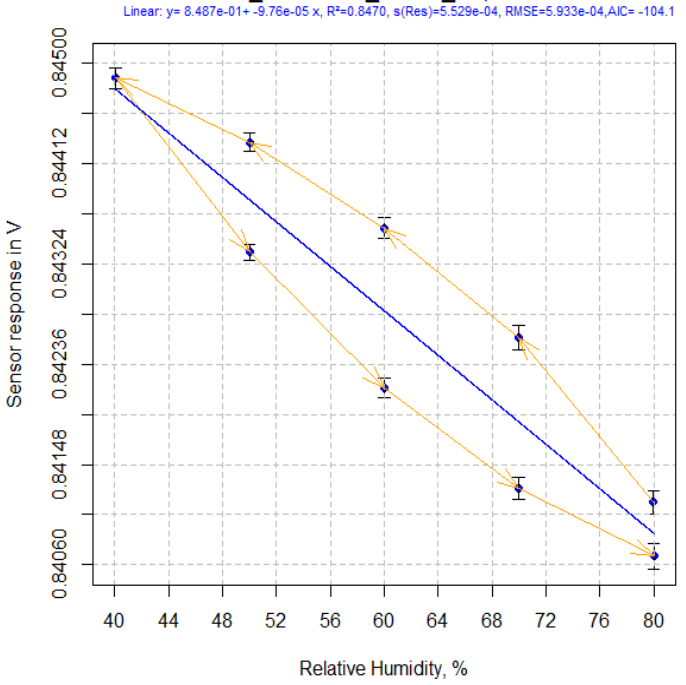

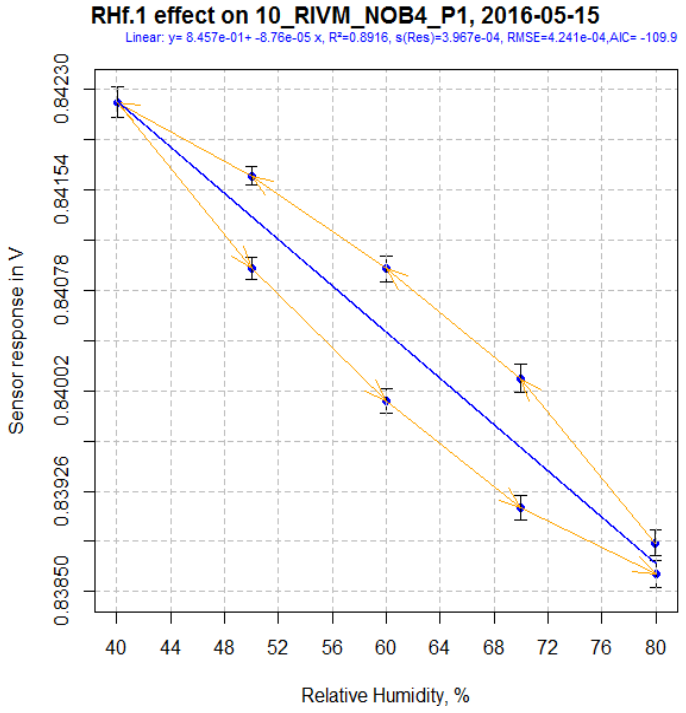

Figure 42: NO-B4, relative humidity effect

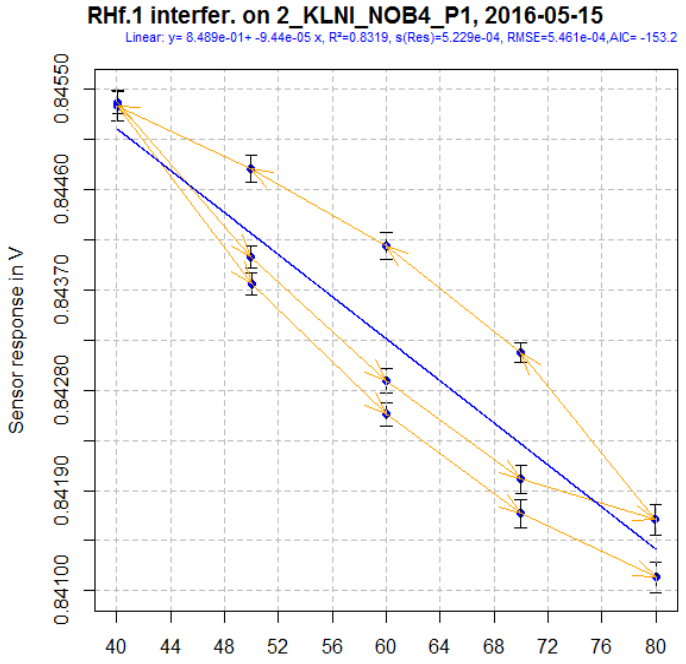

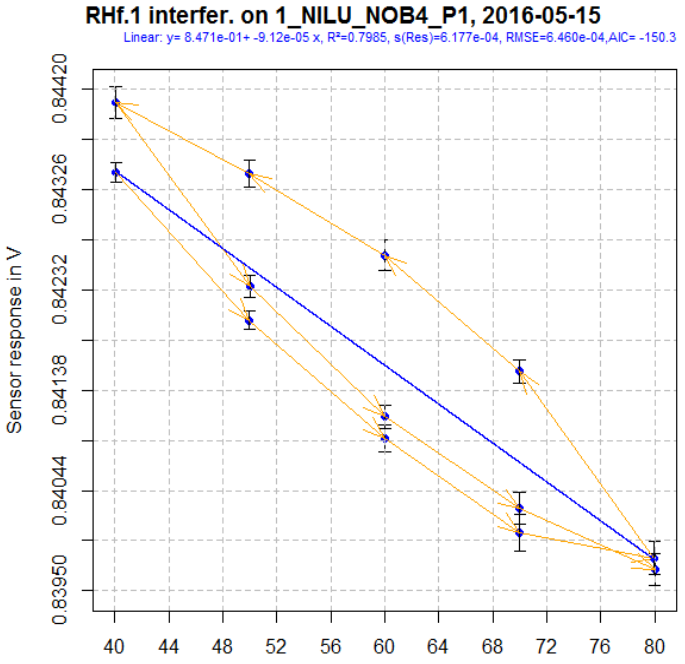

No data available because of connection error

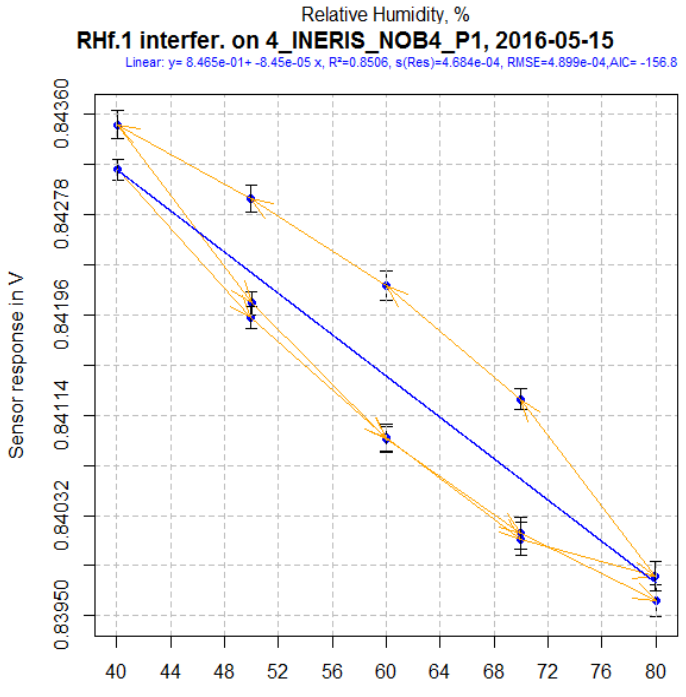

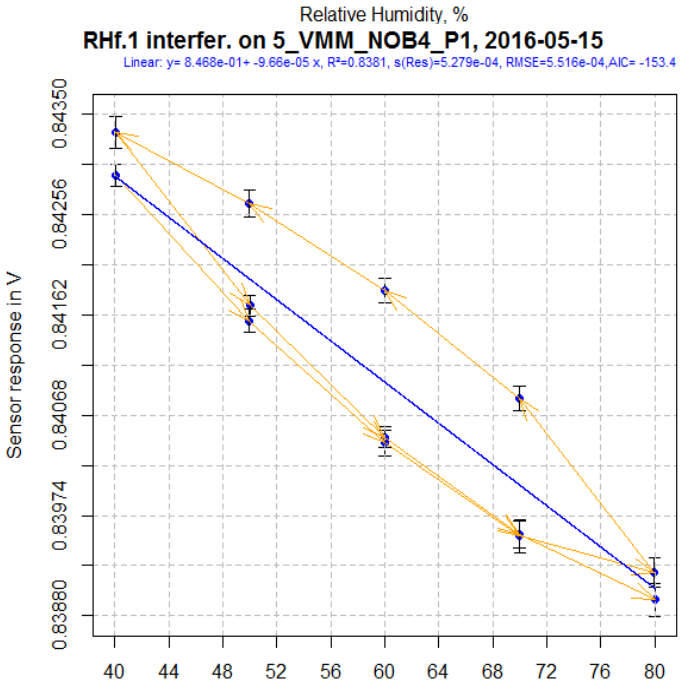

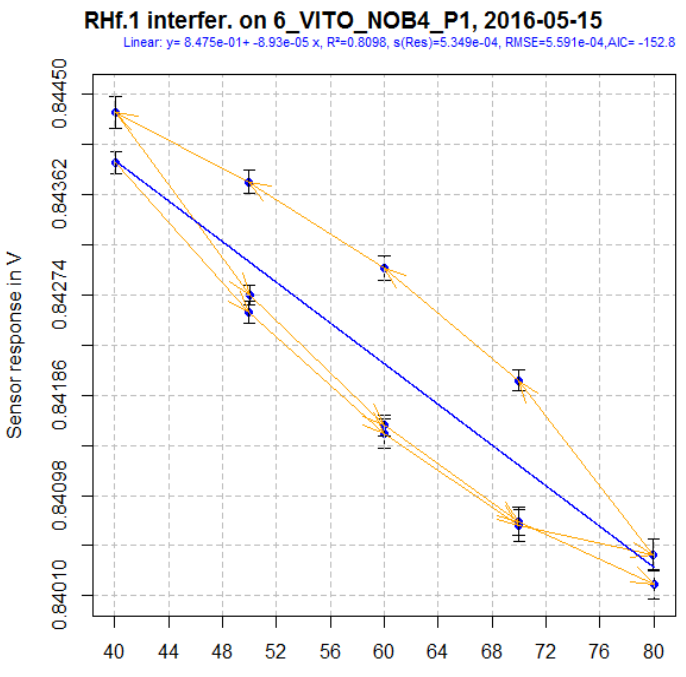

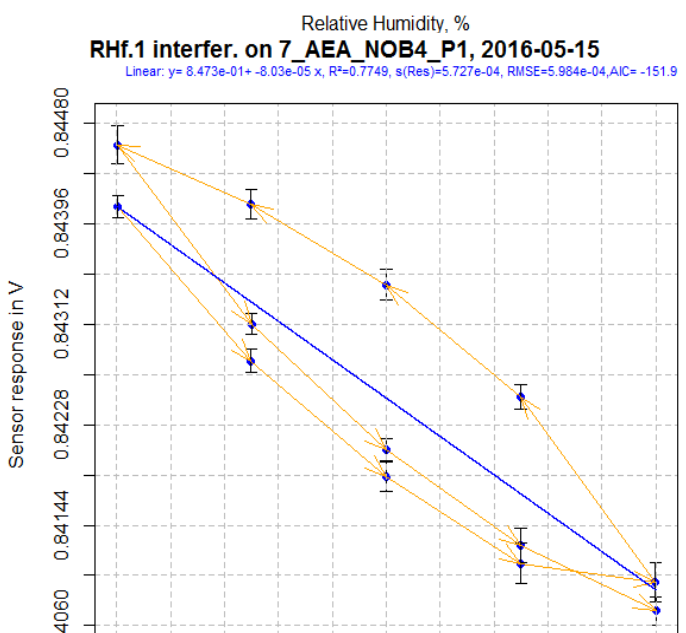

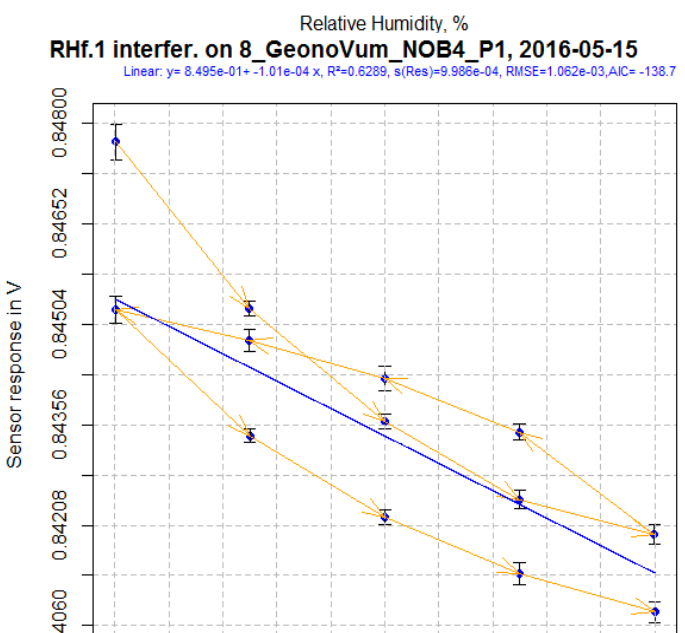

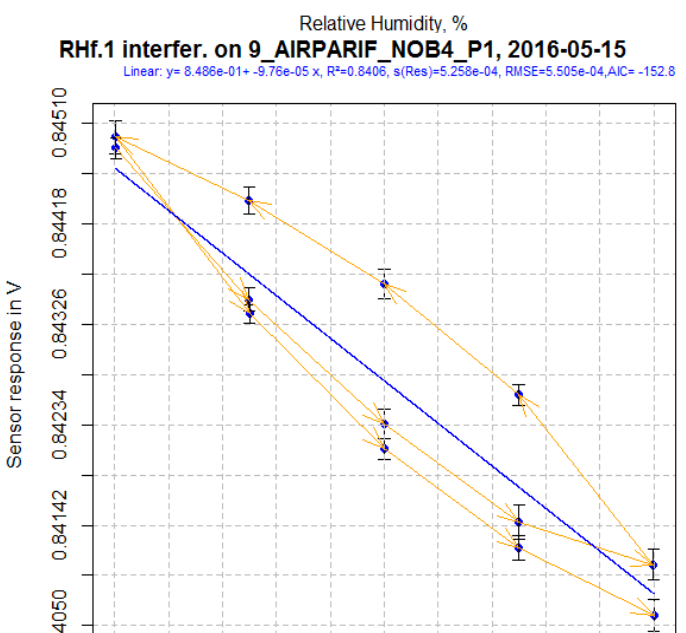

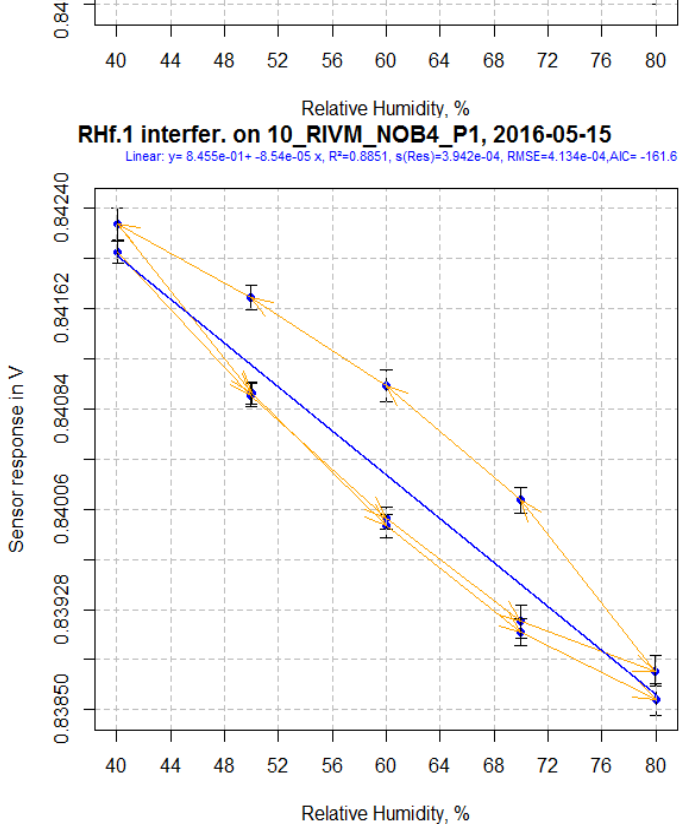

Figure 43: NO-B4, relative humidity effect

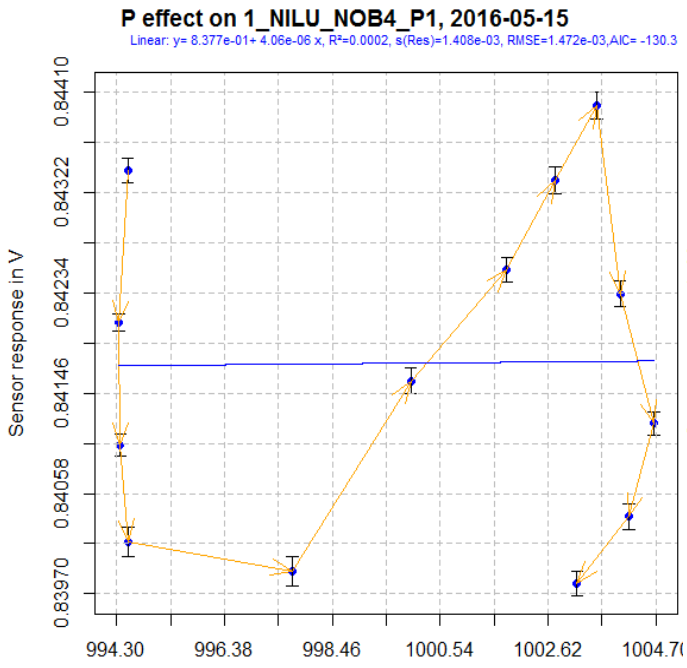

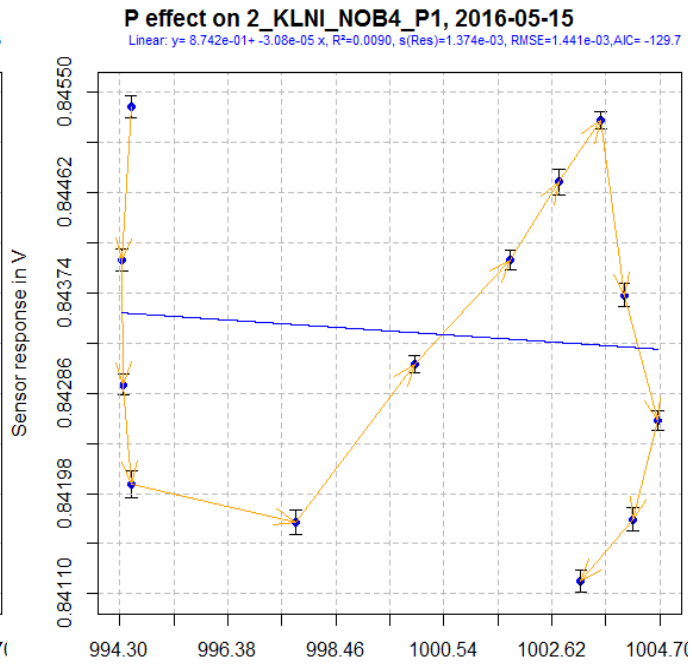

No data available because of connection error

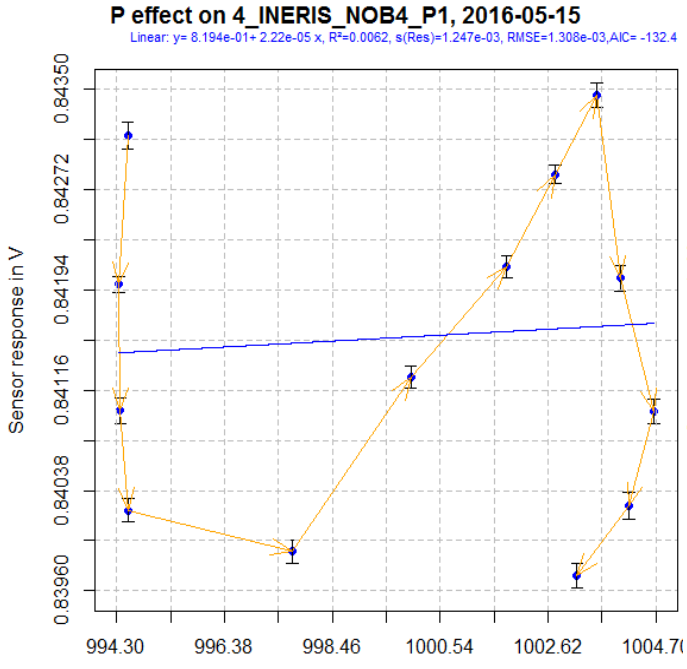

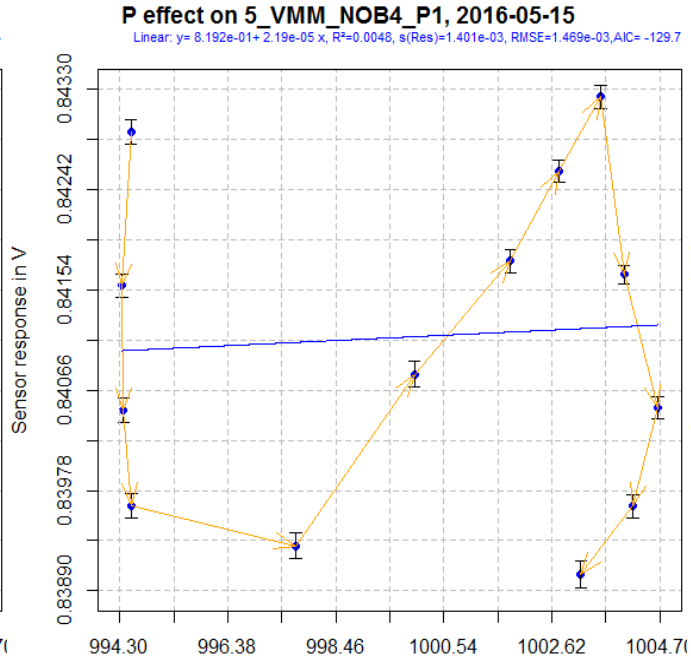

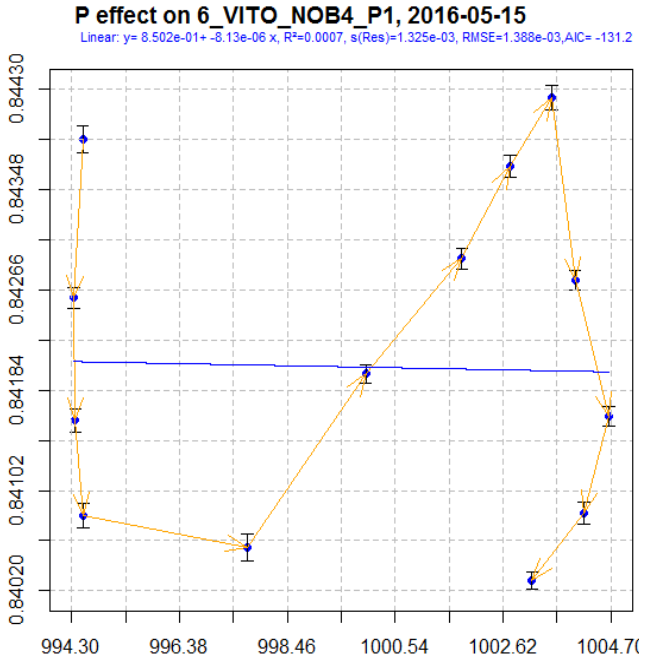

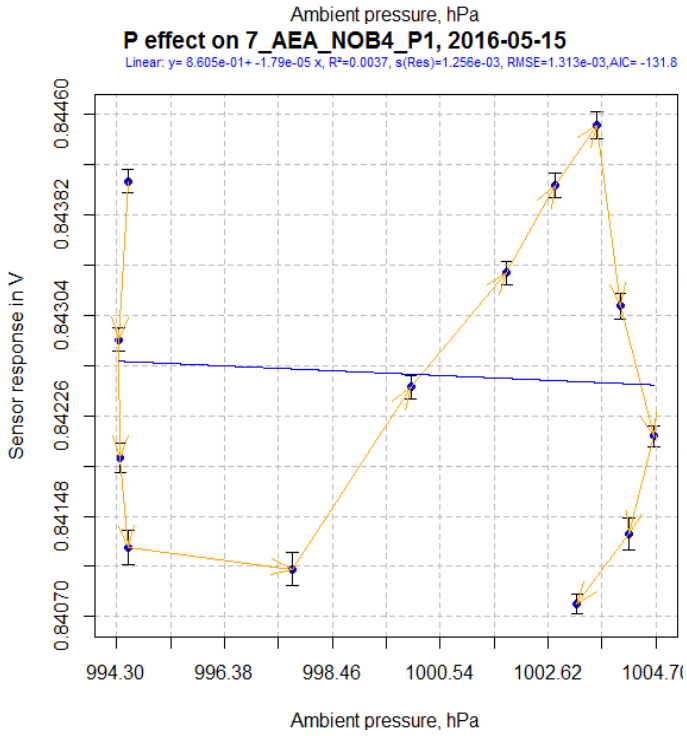

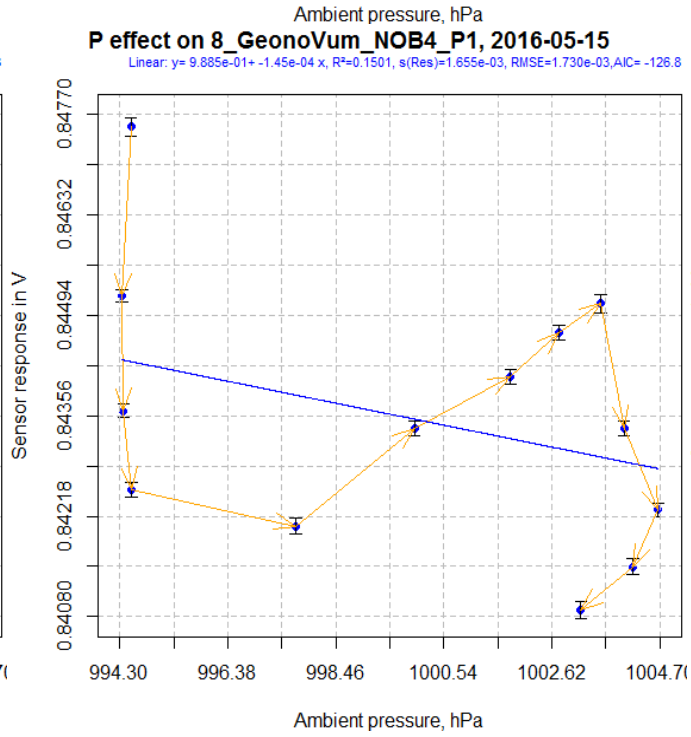

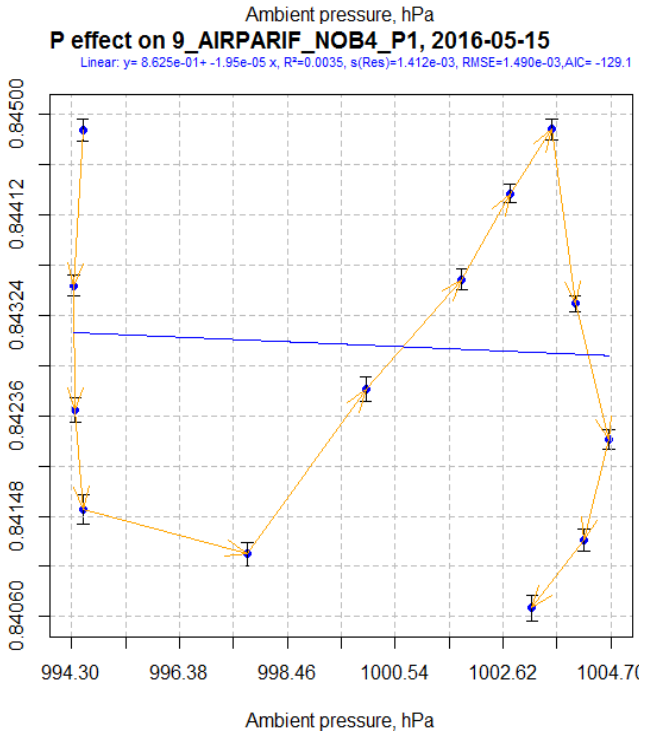

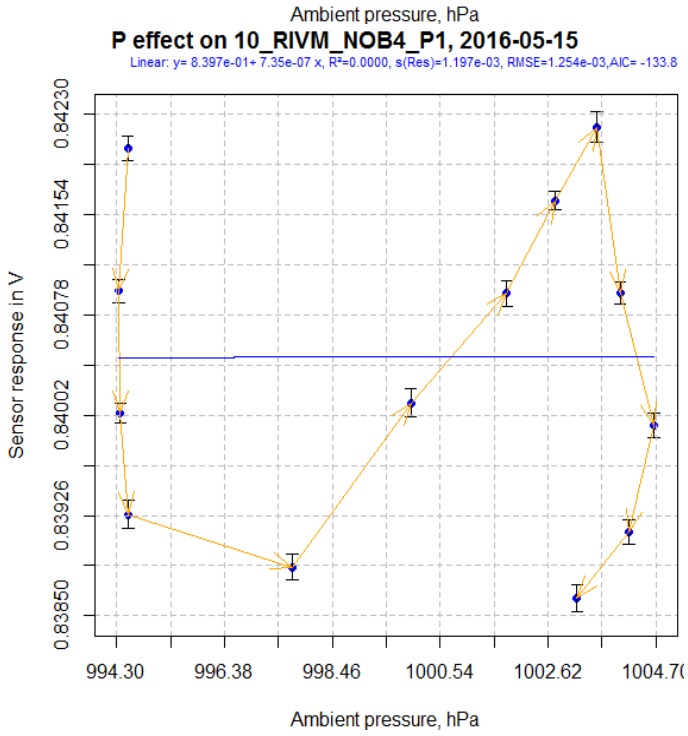

Figure 44: NO-B4, pressure effect during the relative humidity tests (all steps)

5.1.5 Selection of data steps within the experiment

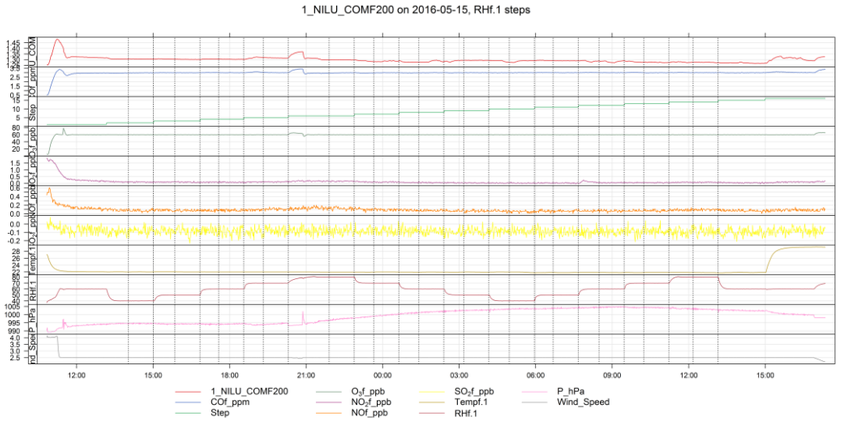

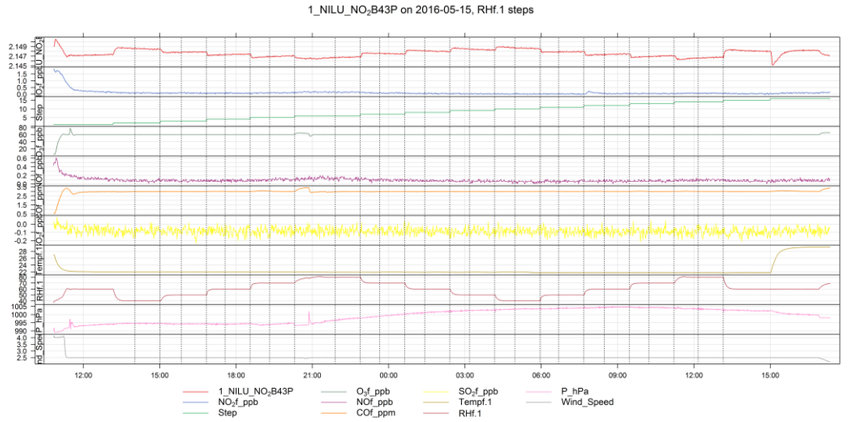

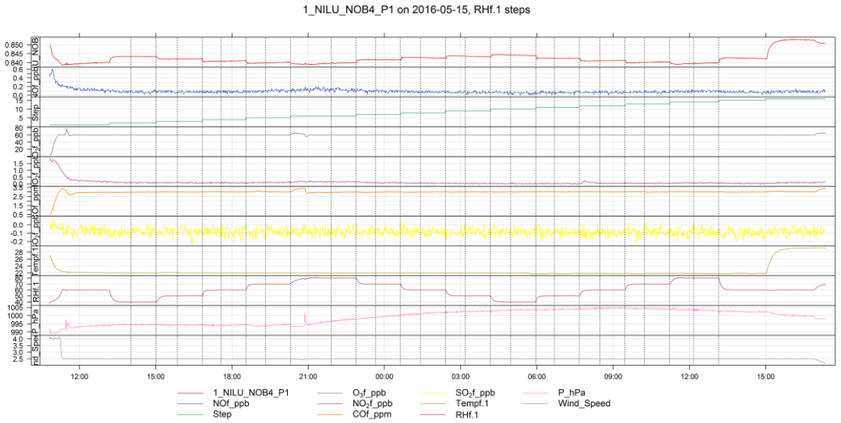

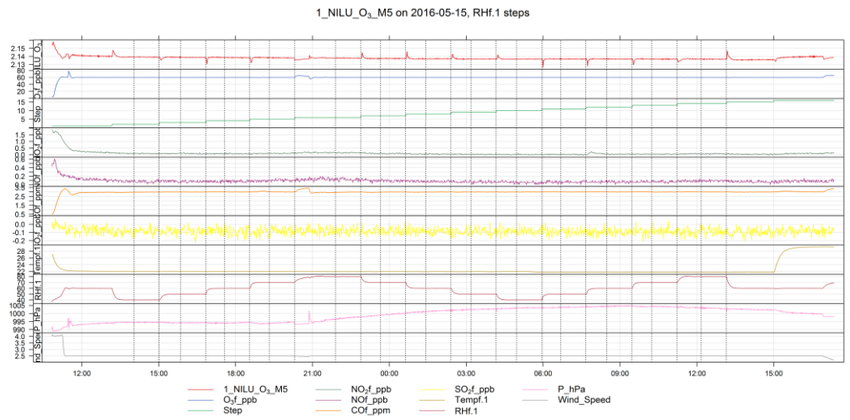

Figure 45: time series plots of CO, NO_2, NO and O_3 sensors of the 1st AirSensEUR shield, relative humidity experiment, 2016-05-15.
The vertical dotted lines correspond to the selection of the RH steps for the evaluation of the four sensors.

5.2 Relative humidity tests, tabulated results

The following tables give the effect of relative humidity on a set of 10 sensors (sensor readings in volt versus relative humidity in %) to estimate the scattering of sensor readings (see rows labelled Means and relative standard deviation (RSD). The tables give the sensor model types, the intercepts in V (Interc. ± s) and slopes in V/% (slope ± s) of the linear lines, the probability that the intercepts and slopes are different from 0 (any value > 0.05 indicates that these variables are significantly different from 0), the coefficients of determination (R^2), the root mean square errors (RMSE) in V calculated using the residual degrees of freedom and the lack of fit in % of the linear model calculated for the x axis u(lof). Figure 33 to Figure 44 gives the scatterplots of the experiments, sensors readings versus reference values.

During this experiment, the data acquisition system of the third shield (52North) was not correctly connected resulting in a lack of measurements being registered. The CO channel of the fourth AirSensEUR shield was damaged and it did not work correctly.

5.2.1 NO2-B43F sensor

The NO2-B43F sensor is sensitive to relative humidity. Additionally, the sensor suffers from a hysteresis effect. The slopes of linear lines are significant and the R^2 are high. The scattering of the slopes gives a RSD of 9.4 % with mean value -0.0000473 ± 0.0000045 V/% RH suggesting that the effect of relative humidity is repeatable. Figure 33 and Figure 34 also show that the sensors suffer from a hysteresis effect with different pattern or response when relative humidity increases and decreases. The RMSE can be used to evaluate the lack of fit of linear correction of humidity effect using the NO_2 sensitivity to evaluate the resulting RH effect: $2\,\frac{0.0000867}{0.0000877} = 2\,ppb$ between 40 and 80 % of relative humidity provided that the sensor readings are corrected for the relative humidity effect with the linear equations.

Table 29: Effect of relative humidity on NO2-B43F sensors (sensor readings in volt), experimental results of 2016-05-15.

Sensors	Interc.	P(Interc.)	Slope	P(Slope)	R^2	RMSE
1_NILU_NO2B43P	2.15040 ± 0.00035	0	-0.0000449 ± 0.0000055	0	0.9049	7.051e-05
2_KLNI_NO2B43P	2.15067 ± 0.00048	0	-0.0000426 ± 0.0000083	0.001	0.7884	9.723e-05
NA	NA ± NA	NA	NA ± NA	NA	NA	NA
4_INERIS_NO2B43P	2.15110 ± 0.00047	0	-0.0000485 ± 0.0000072	0	0.8678	9.243e-05
5_VMM_NO2B43F	2.15135 ± 0.00044	0	-0.0000536 ± 0.0000072	0	0.8872	8.953e-05
6_VITO_NO2B43F	2.15060 ± 0.00044	0	-0.0000489 ± 0.0000069	0	0.8787	9.202e-05
7_AEA_NO2B43F	2.15172 ± 0.00044	0	-0.0000519 ± 0.0000071	0	0.8833	9.054e-05
8_GeonoVum_NO2B43F	2.15133 ± 0.00062	0	-0.0000507 ± 0.0000097	0.001	0.7953	0.00011961
9_AIRPARIF_NO2B43P	2.15080 ± 0.00025	0	-0.0000408 ± 0.0000038	0	0.9434	5.022e-05
10_RIVM_NO2B43P	2.14856 ± 0.00036	0	-0.0000436 ± 0.0000060	0	0.8842	7.803e-05
Means	2.15073 ± 0.00092		-0.0000473 ± 0.0000045		0.8704	0.0000867
RSD	0.000		0.094			

5.2.2 CO/MF-200 sensor

5.2.2.1 Humidity effect

The CO/MF-200 sensor values do not show a linear relationship with relative humidity, see Figure 36 and Figure 37. The slopes of linear lines are not significant and the R^2 are low.

Table 30: Effect of relative humidity on CO/MF-200 sensors (sensor readings in volt), experimental results of 2016-05-15.

Sensors	Interc.	P(Interc.)	Slope	P(Slope)	R^2	RMSE
1_NILU_COMF200	1.28956 ± 0.00851	0	0.0000167 ± 0.0001505	0.915	0.0018	0.00199317
2_KLNI_COMF200	1.31195 ± 0.01017	0	0.0000587 ± 0.0001796	0.753	0.015	0.00230295
NA	NA ± NA	NA	NA ± NA	NA	NA	NA
NA	NA ± NA	NA	NA ± NA	NA	NA	NA
5_VMM_COMF200	1.28137 ± 0.00843	0	0.0000298 ± 0.0001498	0.848	0.0056	0.00189713
6_VITO_COMF200	1.26809 ± 0.00866	0	0.0000013 ± 0.0001552	0.993	0	0.00193137
7_AEA_COMF200	1.31702 ± 0.01067	0	0.0000608 ± 0.0001898	0.758	0.0144	0.00238043
8_GeonoVum_COMF200	1.29410 ± 0.01038	0	0.0000132 ± 0.0001828	0.944	7e-04	0.00232464
9_AIRPARIF_COMF200	1.32158 ± 0.01130	0	0.0000574 ± 0.0001985	0.781	0.0118	0.00262737
10_RIVM_COMF200	1.32179 ± 0.01043	0	0.0000795 ± 0.0001841	0.679	0.026	0.00238371
Means	1.30068 ± 0.02028		0.0000397 ± 0.0000280		0.0094	0.0022301
RSD	0.016		0.707			

5.2.2.2 Pressure effect

Figure 38 shows that the changes of CO sensor values are slightly associated with pressure changes. A possible explanation of this phenomena is that the transport of molecules at the entrance of the sensor is enhanced by an increase of pressure. This effect is likely higher for the sensor with high sensitivity in which the diameter of the capillary entrance is increased to be able to detect low concentration levels (see the ozone sensors).

Table 31: Effect of pressure on COMF200 sensors (sensor readings in volt), experimental results of 2016-05-15.

Sensors	Interc.	P(Interc.)	Slope	P(Slope)	R^2	RMSE
1_NILU_COMF200	2.99970 ± 0.29630	0	-0.0017044 ± 0.0002966	0	0.7501	0.00131661
2_KLNI_COMF200	3.16469 ± 0.30370	0	-0.0018444 ± 0.0003040	0	0.7699	0.00135993
NA	NA ± NA	NA	NA ± NA	NA	NA	NA
NA	NA ± NA	NA	NA ± NA	NA	NA	NA
5_VMM_COMF200	2.63469 ± 0.30758	0	-0.0013480 ± 0.0003079	0.001	0.6354	0.00136612
6_VITO_COMF200	2.83880 ± 0.27877	0	-0.0015661 ± 0.0002791	0	0.7411	0.00124905
7_AEA_COMF200	3.43004 ± 0.29747	0	-0.0021038 ± 0.0002977	0	0.8195	0.00131649
8_GeonoVum_COMF200	3.15553 ± 0.30671	0	-0.0018555 ± 0.0003071	0	0.7684	0.00136659
9_AIRPARIF_COMF200	3.14901 ± 0.37448	0	-0.0018196 ± 0.0003749	0.001	0.6817	0.00165815
10_RIVM_COMF200	3.24434 ± 0.30111	0	-0.0019130 ± 0.0003015	0	0.7854	0.00134101
Means	3.07710 ± 0.24786		-0.0017694 ± 0.0002303		0.7439	0.0013717
RSD	0.081		0.130			

5.2.3 O3/M-5 sensor

5.2.3.1 Humidity effect

The O3/M-5 sensors do not show a clear linear relationship with relative humidity. The slopes of linear lines are generally not significant and R^2 are low.

Additionally, Figure 45 at the bottom right shows transient sensors reading peaks when relative humidity changes. The signs of the peaks is determined by the sign of the relative humidity change either decreasing or increasing.

Table 32: Effect of relative humidity on O3/M-5 sensors (sensor readings in volt), experimental results of 2016-05-15.

Sensors	Interc.	P(Interc.)	Slope	P(Slope)	R^2	RMSE
1_NILU_O3_M5	2.13624 ± 0.00060	0	0.0000114 ± 0.0000097	0.278	0.165	0.00014092
2_KLNI_O3_M5	2.12000 ± 0.00022	0	0.0000178 ± 0.0000034	0.001	0.7941	4.761e-05
NA	NA ± NA	NA	NA ± NA	NA	NA	NA
4_INERIS_O3_M5	2.12557 ± 0.00039	0	0.0000170 ± 0.0000063	0.03	0.5121	8.645e-05
5_VMM_O3_M5	2.12736 ± 0.00031	0	0.0000067 ± 0.0000051	0.232	0.1962	6.779e-05
6_VITO_O3_M5	2.13008 ± 0.00029	0	0.0000090 ± 0.0000048	0.105	0.3317	6.322e-05
7_AEA_O3_M5	2.12873 ± 0.00037	0	0.0000062 ± 0.0000061	0.346	0.1275	7.878e-05
8_GeonoVum_O3_M5	2.12894 ± 0.00032	0	0.0000100 ± 0.0000052	0.096	0.3463	7.342e-05
9_AIRPARIF_O3_M5	2.13443 ± 0.00041	0	-0.0000015 ± 0.0000067	0.832	0.0069	8.908e-05
10_RIVM_O3_M5	2.12976 ± 0.00030	0	0.0000094 ± 0.0000049	0.097	0.3433	6.569e-05
Means	2.12901 ± 0.00473		0.0000095 ± 0.0000058		0.3137	0.0000792
RSD	0.002		0.608			

5.2.3.2 Pressure effect

The O3/M-5 sensor is sensitive to pressure. The slopes of linear lines are significant and the R^2 are high. The scattering of the slopes is with RSD of 21.8 % with mean value of -0.0001527 ± 0.0000334. The RMSE can be used to evaluate the lack of fit of linear pressure correction dividing it by the O_3 sensor sensitivity after applying the linear equation $(2\frac{0.0000599}{-0.0003670} = -0.4\ ppb)$.

Table 33: Effect of pressure on O3/M-5 sensors (sensor readings in volt versus pressure in hPa), experimental results of 2016-05-15.

Sensors	Interc.	P(Interc.)	Slope	P(Slope)	R^2	RMSE
1_NILU_O3_M5	2.34087 ± 0.01541	0	-0.0002034 ± 0.0000154	0	0.9406	6.513e-05
2_KLNI_O3_M5	2.21269 ± 0.01078	0	-0.0000914 ± 0.0000108	0	0.8672	4.562e-05
NA	NA ± NA	NA	NA ± NA	NA	NA	NA
4_INERIS_O3_M5	2.29772 ± 0.01368	0	-0.0001707 ± 0.0000137	0	0.934	5.796e-05
5_VMM_O3_M5	2.26664 ± 0.01202	0	-0.0001385 ± 0.0000120	0	0.9235	5.189e-05
6_VITO_O3_M5	2.26555 ± 0.01104	0	-0.0001345 ± 0.0000110	0	0.9311	4.762e-05
7_AEA_O3_M5	2.29525 ± 0.01449	0	-0.0001657 ± 0.0000145	0	0.9223	6.195e-05
8_GeonoVum_O3_M5	2.26794 ± 0.01367	0	-0.0001380 ± 0.0000137	0	0.9025	5.799e-05
9_AIRPARIF_O3_M5	2.32309 ± 0.02187	0	-0.0001882 ± 0.0000219	0	0.8707	9.382e-05
10_RIVM_O3_M5	2.27496 ± 0.01318	0	-0.0001442 ± 0.0000132	0	0.9158	5.692e-05
Means	2.28275 ± 0.03730		-0.0001527 ± 0.0000334		0.9120	0.0000599
RSD	0.016		0.218			

5.2.4 NO-B4 sensor

The NO-B4 sensor is sensitive to relative humidity. Additionally, the sensor suffers from a hysteresis effect. The slopes of linear lines are highly significant and the R^2 are high. The scattering of the slopes is with RSD of 5.5 % with mean value -0.0000925 ± 0.0000050 V/% suggesting that the effect of relative humidity is repeatable. Figure 43 and Figure 44 also show that the sensors suffer from a hysteresis effect with different pattern or response when relative humidity increases and decreases. The RMSE can be used to evaluate the lack of fit of linear correction of humidity effect using the NO sensitivity to

evaluate the resulting RH effect: $2.\frac{0.0001916}{0.0001398} = 2.7\ ppb$ between 40 and 80 % of relative humidity provided that the sensor readings are corrected for the relative humidity effect with the provided linear equations.

Table 34: Effect of relative humidity on NO-B4 sensors (sensor readings in volt), experimental results of 2016-05-15.

Sensors	Interc.	P(Interc.)	Slope	P(Slope)	R^2	RMSE
1_NILU_NOB4_P1	0.84788 ± 0.00096	0	-0.0001001 ± 0.0000152	0	0.8609	0.00019184
2_KLNI_NOB4_P1	0.84881 ± 0.00100	0	-0.0000908 ± 0.0000160	0.001	0.8224	0.00020743
NA	NA ± NA	NA	NA ± NA	NA	NA	NA
4_INERIS_NOB4_P1	0.84708 ± 0.00073	0	-0.0000903 ± 0.0000116	0	0.897	0.00015106
5_VMM_NOB4_P1	0.84704 ± 0.00088	0	-0.0000986 ± 0.0000143	0	0.8712	0.00018004
6_VITO_NOB4_P1	0.84782 ± 0.00093	0	-0.0000924 ± 0.0000144	0	0.8541	0.00018152
7_AEA_NOB4_P1	0.84804 ± 0.00090	0	-0.0000884 ± 0.0000141	0	0.848	0.00018086
8_GeonoVum_NOB4_P1	0.84843 ± 0.00150	0	-0.0000867 ± 0.0000238	0.008	0.6549	0.00029104
9_AIRPARIF_NOB4_P1	0.84869 ± 0.00096	0	-0.0000976 ± 0.0000157	0	0.847	0.00019783
10_RIVM_NOB4_P1	0.84572 ± 0.00072	0	-0.0000876 ± 0.0000115	0	0.8916	0.0001429
Means	0.84772 ± 0.00098		-0.0000925 ± 0.0000050		0.8386	0.0001916
RSD	0.001		0.055			

6 Effects of Temperature (2016-05-17)

This experiment tested the effect of temperature on the CO/MF-200, NO2-B43F, NO-B4 and O3/M-5 sensors. Table 35 below gives the reference values of all monitored parameters during the stable steps of the experiment. We performed three ramps (increase, decrease and increase) of temperature between 12 and 37 ºC with steps of 7 ºC. CO and O_3 were kept at constant values, 3 ppm and 60 ppb respectively while SO_2, NO_2 and NO remained at about 0 ppb. Wind velocity was kept at about 2.5 m/s while atmospheric pressure changed about 10 hPa. Figure 46 shows the time series plot for all reference parameters. Unfortunately, the experiment was interrupted due to malfunctioning during a temperature decrease at T = 22 ºC. The experiment was resumed after about 4 hours. It is likely that this interruption had an effect with sensors being allowed to return to their initial values in particular for the CO sensors and a few of the NO sensors.

Table 36 shows the mean effect of temperature (sensor readings in volt versus temperature in ºC) on the 10 sensors of the 4 model types. The table gives the sensor model types, the reference gaseous compounds, the intercepts in V (Interc. ± s) and slopes in V/ºC (slope ± s) of the linear lines, the probability that the intercepts and slopes are different from 0 (any value > 0.05 indicates that these variables are significantly different from 0), the coefficients of determination (R^2) and the root mean square errors (RMSE) in V calculated using the residual degrees of freedom. The standard deviations of the intercepts and slopes are computed using the results of the 10 sensors. A few outliers are identified in the presentation of detailed tests, thus more accurate values are given in the following tables.

Table 35: Reference values of all steps of experiments started on 2016-05-17.

Begin	End	O3, ppb	NO2, ppb	NO, ppb	CO, ppm	SO2, ppb	Temp., °C	RH, %	Pressure, hPa	Wind_Speed, m/s
2016-05-17 02:40	2016-05-17 03:39	60.0	0.0	0.1	3.000	-0.1	22.1	60.0	1001	2.5
2016-05-17 07:24	2016-05-17 08:23	60.0	0.2	0.1	2.993	-0.1	30.1	60.0	1000	2.5
2016-05-17 08:45	2016-05-17 09:44	59.9	0.3	0.1	3.128	-0.1	36.6	60.1	998	2.5
2016-05-17 10:19	2016-05-17 11:18	60.0	0.2	0.1	2.955	-0.1	37.9	60.0	1000	2.5
2016-05-17 12:16	2016-05-17 13:15	60.0	0.1	0.1	2.969	-0.1	29.4	60.0	1001	2.5
2016-05-17 15:18	2016-05-17 16:17	61.4	0.0	0.1	3.092	-0.1	21.8	61.3	1001	2.3
2016-05-17 23:16	2016-05-18 00:15	60.1	0.2	0.1	2.906	-0.1	22.3	59.9	1001	3.9
2016-05-18 01:16	2016-05-18 02:15	60.0	0.1	0.1	2.959	-0.1	15.4	60.0	1004	3.7
2016-05-18 03:42	2016-05-18 04:41	60.0	0.0	0.1	2.989	-0.1	9.1	60.0	1004	3.6
2016-05-18 05:24	2016-05-18 06:23	60.0	0.1	0.1	3.020	-0.1	15.3	60.0	1003	3.7
2016-05-18 09:51	2016-05-18 10:50	1.7	0.0	0.1	2.461	-0.1	22.0	60.0	999	3.8
2016-05-18 13:57	2016-05-18 14:56	60.0	0.0	0.1	2.990	-0.1	22.0	60.0	1001	3.8
2016-05-17 02:40	2016-05-17 03:39	60.0	0.0	0.1	3.000	-0.1	22.1	60.0	1001	2.5
2016-05-17 07:24	2016-05-17 08:23	60.0	0.2	0.1	2.993	-0.1	30.1	60.0	1000	2.5
2016-05-17 08:45	2016-05-17 09:44	59.9	0.3	0.1	3.128	-0.1	36.6	60.1	998	2.5
2016-05-17 10:19	2016-05-17 11:18	60.0	0.2	0.1	2.955	-0.1	37.9	60.0	1000	2.5

Table 36: Effect of temperature on sensor readings, experimental results of 2016-05-15.

Sensors	**Compounds**	**Interc.**	**P(Interc.)**	**Slope**	**P(Slope)**	**R^2**	**RMSE**
CO/MF-200	Pressure	16.86940 ± 1.13842	0.000	-0.01551439 ± 0.00112144	0.001	0.9338	0.00260
CO/MF-200	Temperature	1.25656 ± 0.01922	0.000	0.00331365 ± 0.00040471	0.001	0.8205	0.00398
NO2-B43F	Pressure	0.24505 ± 6.41305	0.081	0.00188877 ± 0.00636720	0.213	0.3547	0.03454
NO2-B43F	Temperature	2.13393 ± 0.04235	0.000	0.00014049 ± 0.00033503	0.158	0.5703	0.03467
NO-B4	Pressure	4.53109 ± 0.78860	0.040	-0.00368096 ± 0.00078533	0.068	0.4985	0.00231
NO-B4	Temperature	0.81996 ± 0.00502	0.000	0.00106271 ± 0.00024318	0.002	0.8475	0.00121
O3/M-5	Pressure	2.27515 ± 0.94621	0.082	-0.00014630 ± 0.00094016	0.253	0.2852	0.00045
O3/M-5	Temperature	2.12756 ± 0.00136	0.000	0.00005194 ± 0.00024653	0.160	0.4828	0.00033

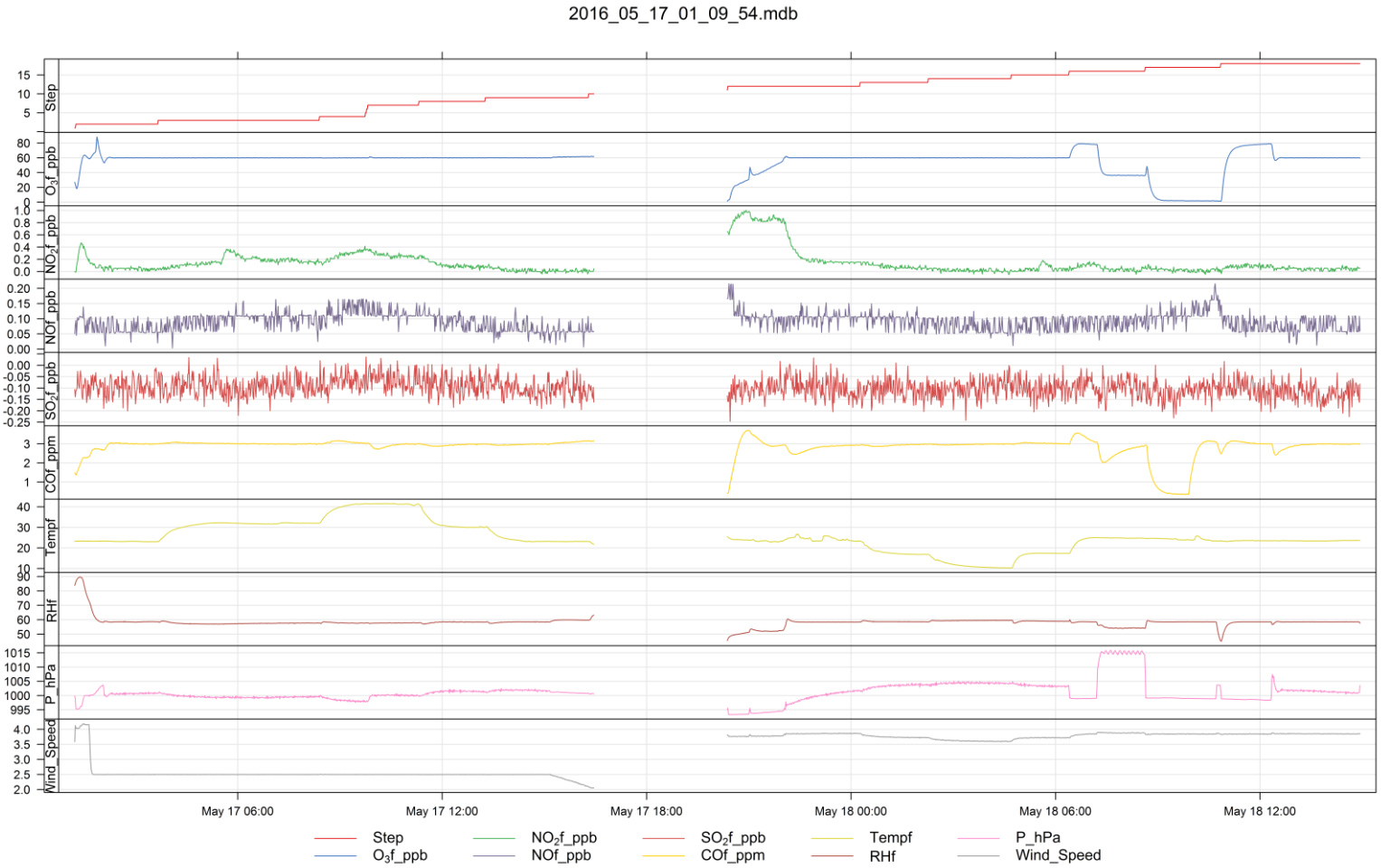

Figure 46: Time series plot of the reference parameters for the experiment started on 2016-05-17

The CO/MF-200 and O3/M-5 sensors do not show any linear relationship with temperature while the NO2-B43F and NO-B4 sensors are linearly associated with coefficients of determination (R^2) of about 0.85 and a probability of 0.001 that the slope of their calibration line is naught. Below, it is also shown that these two sensors have a significant hysteresis effect.

6.1 Scatter plots of effects of temperature

6.1.1 NO2-B43F sensor

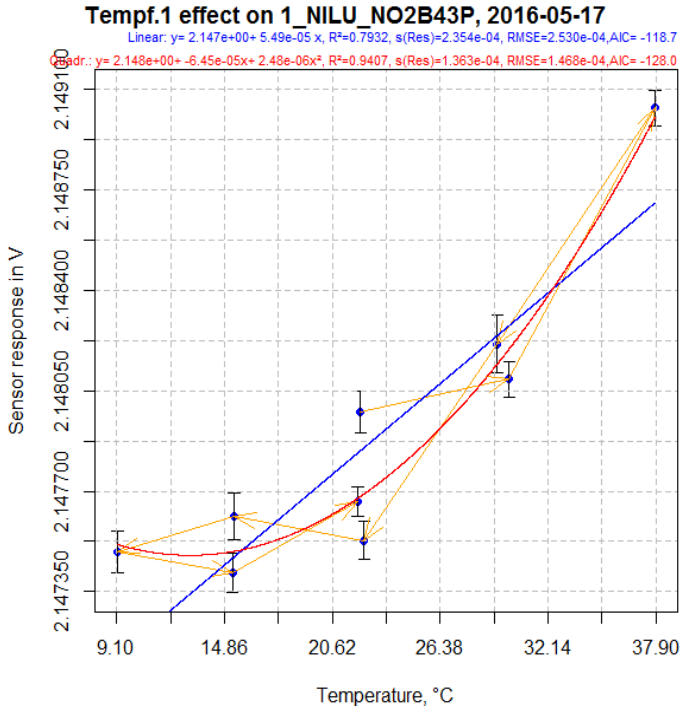

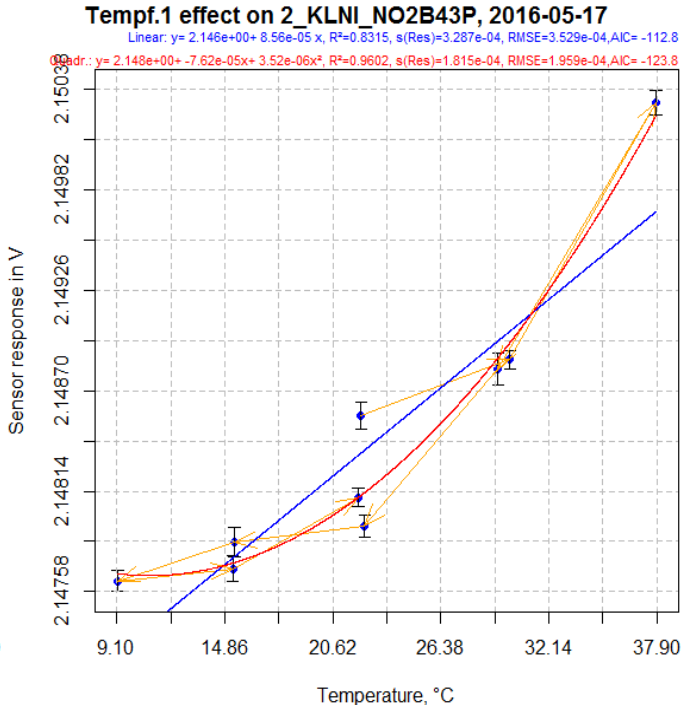

No data available because of connection error

No data available because the sensor channel was damaged

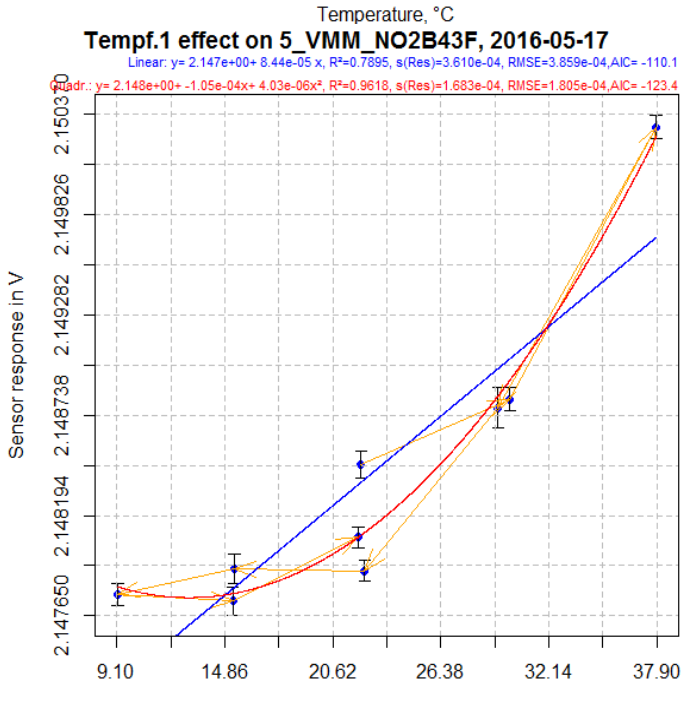

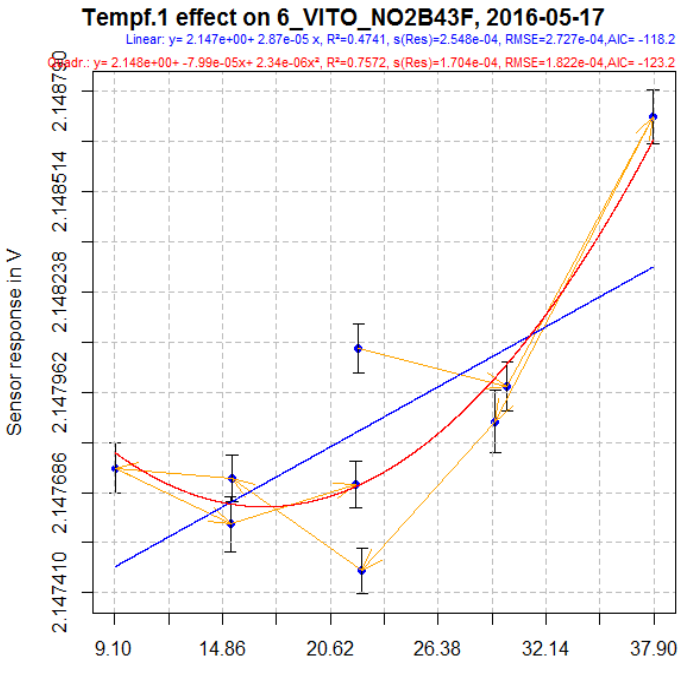

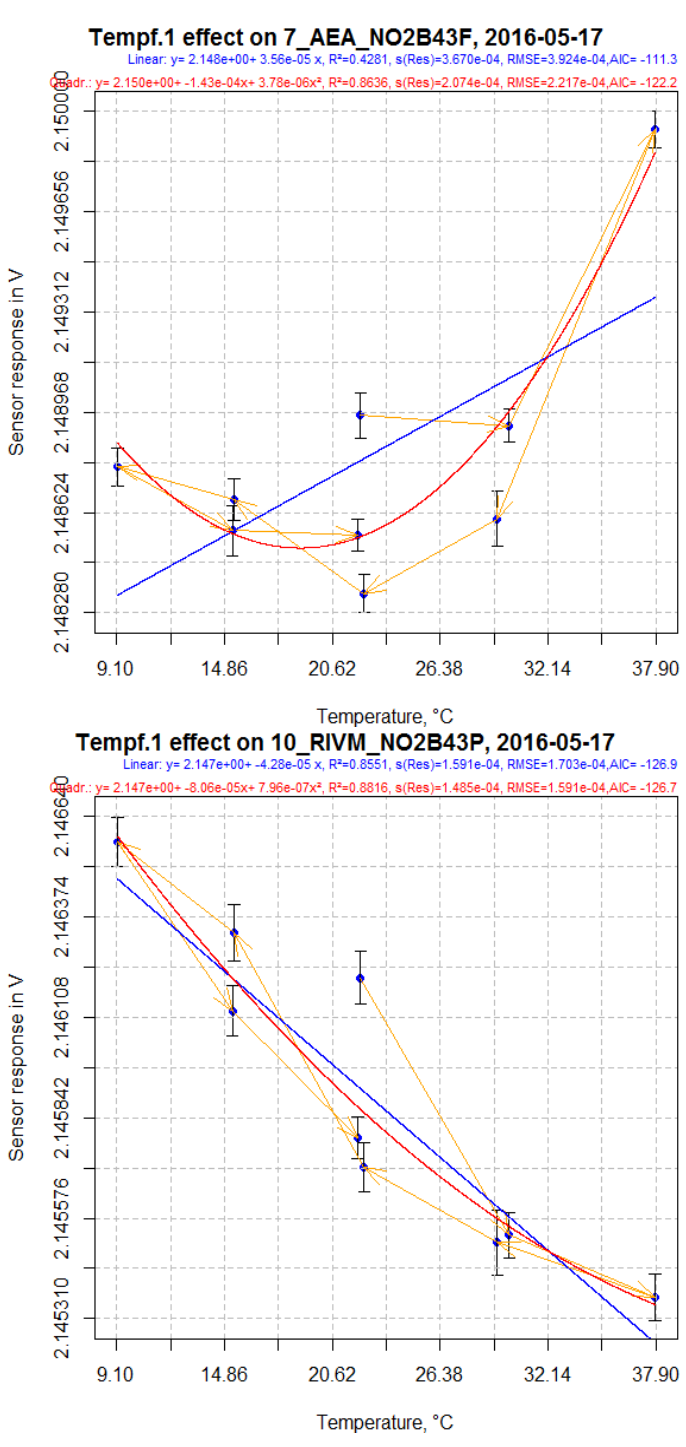

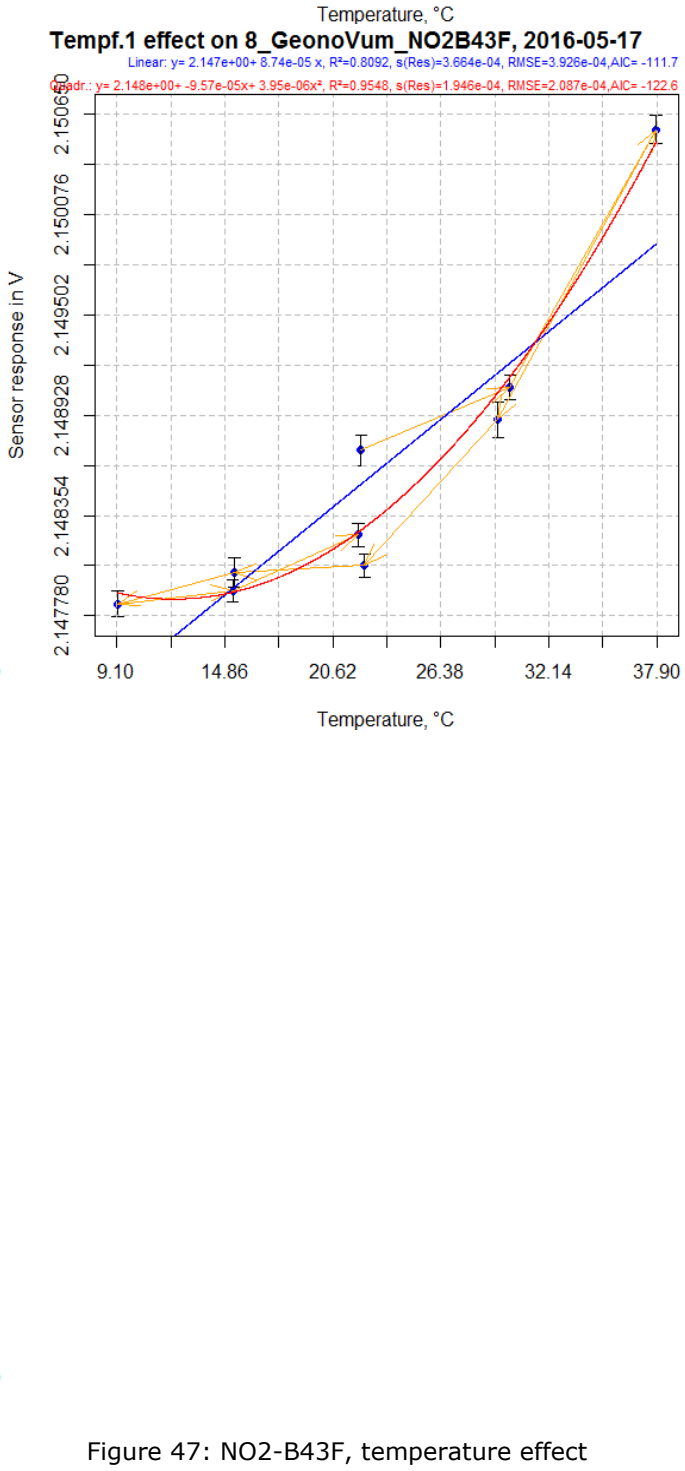

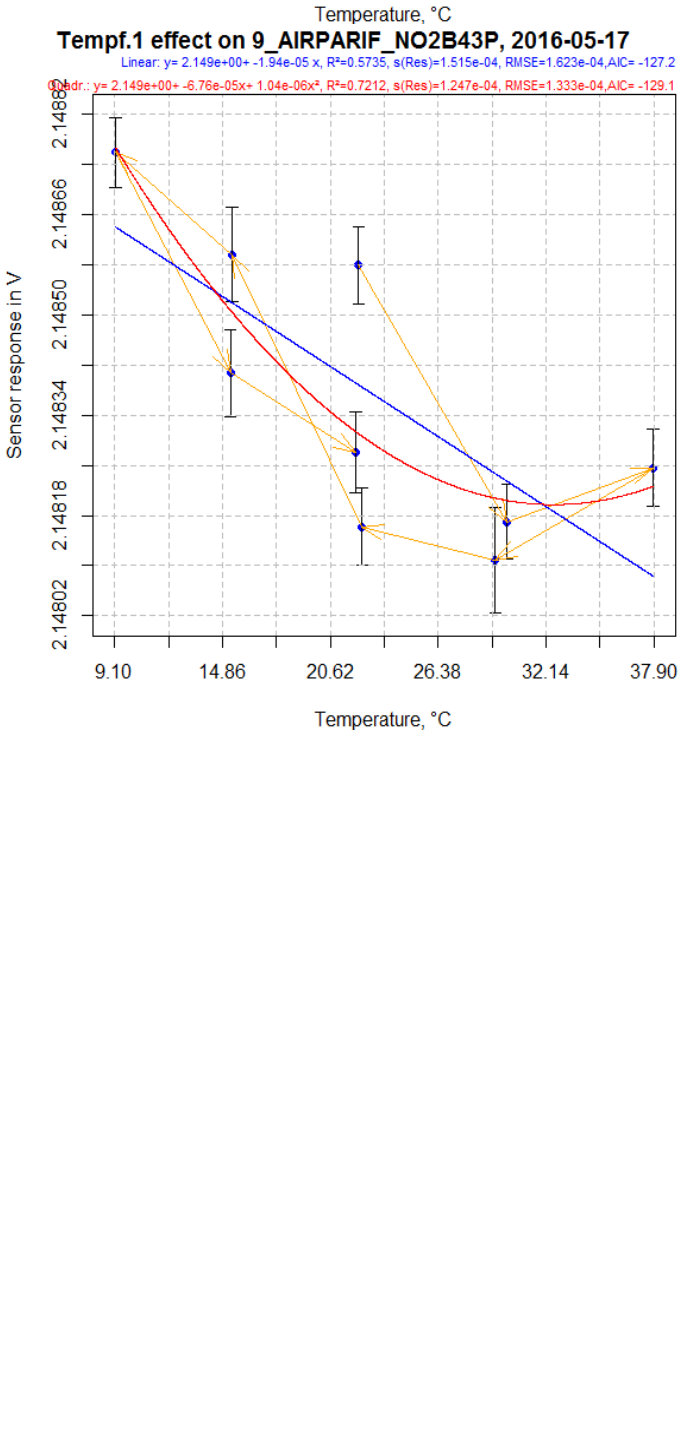

Figure 47: NO2-B43F, temperature effect

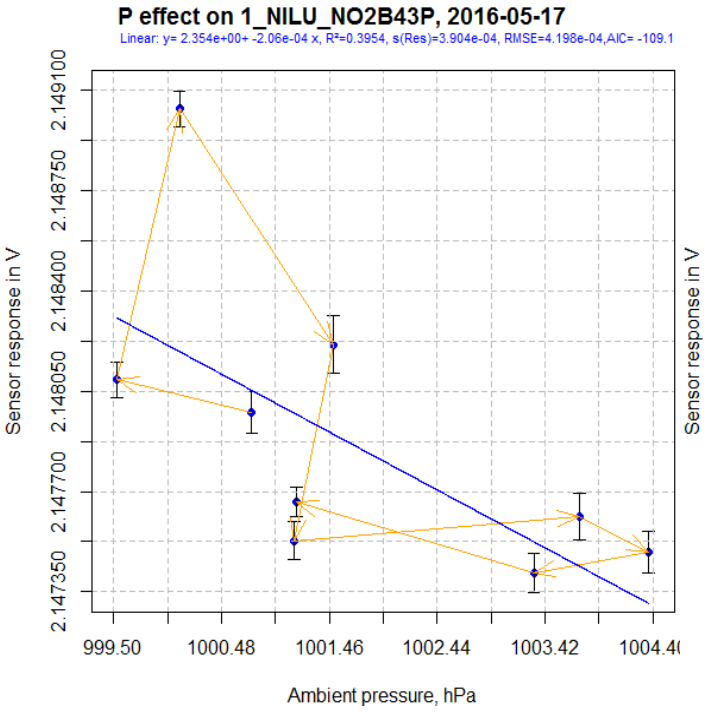

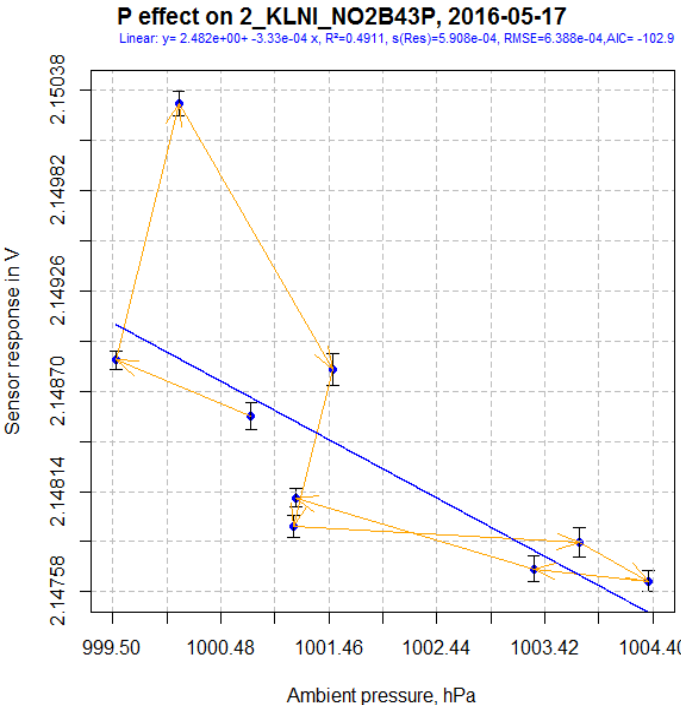

No data available because of connection error

No data available because the sensor channel was damaged

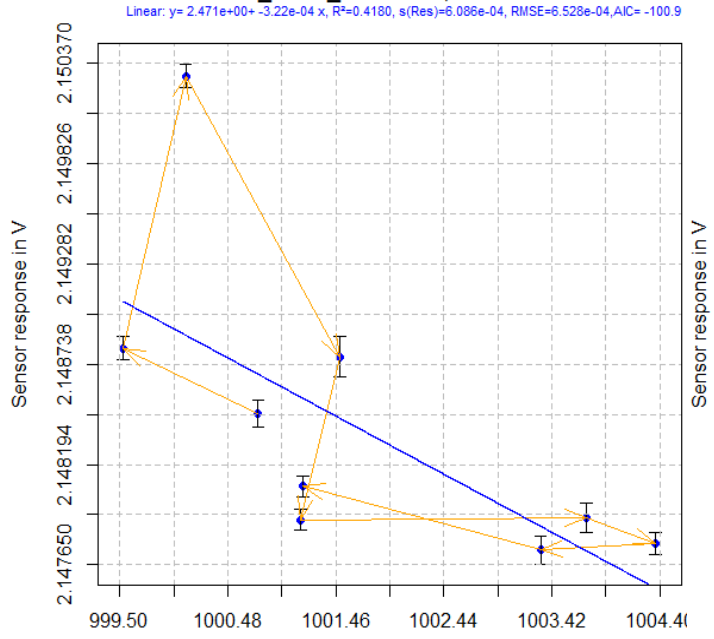

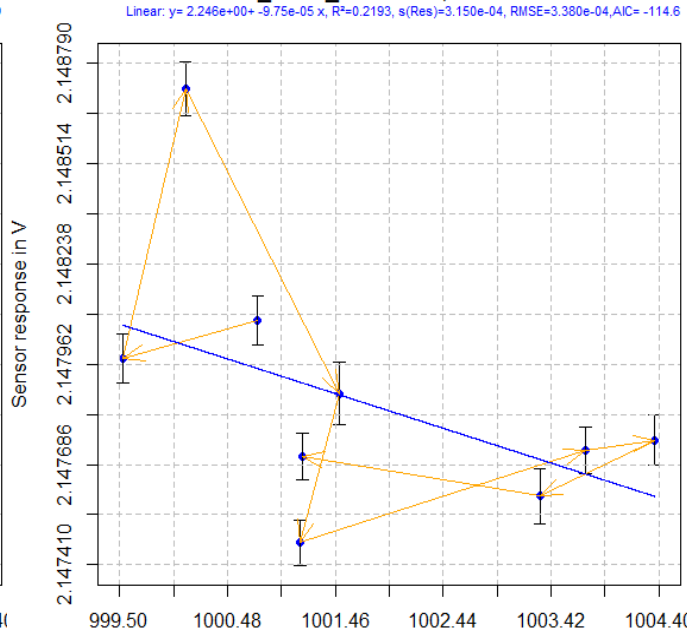

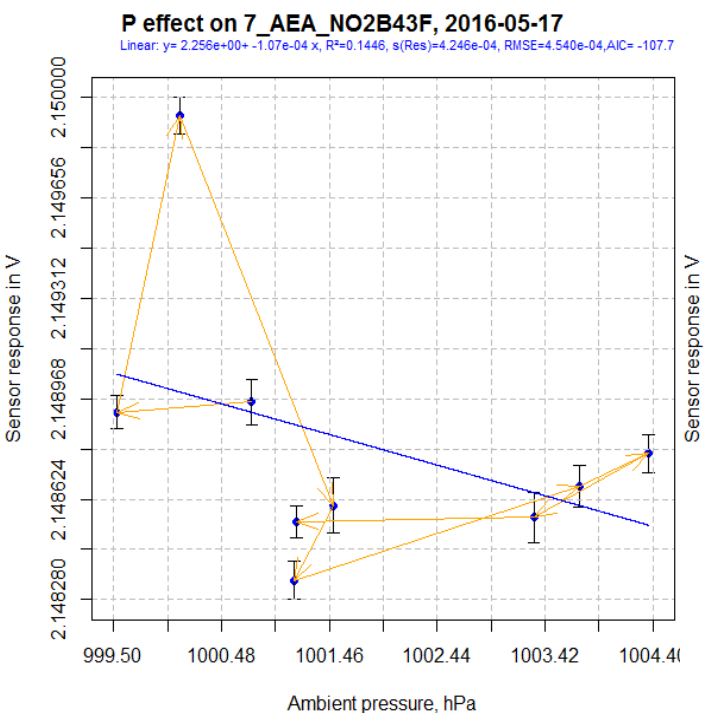

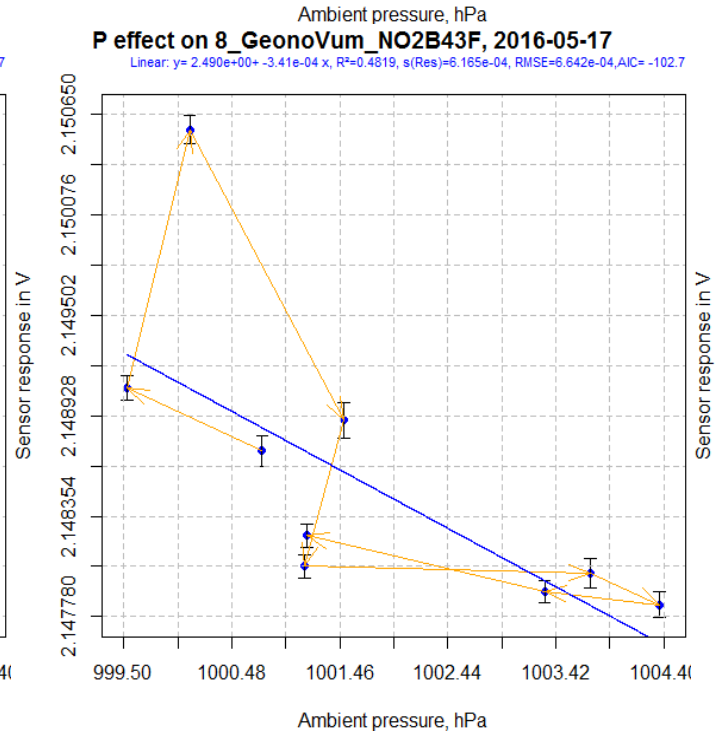

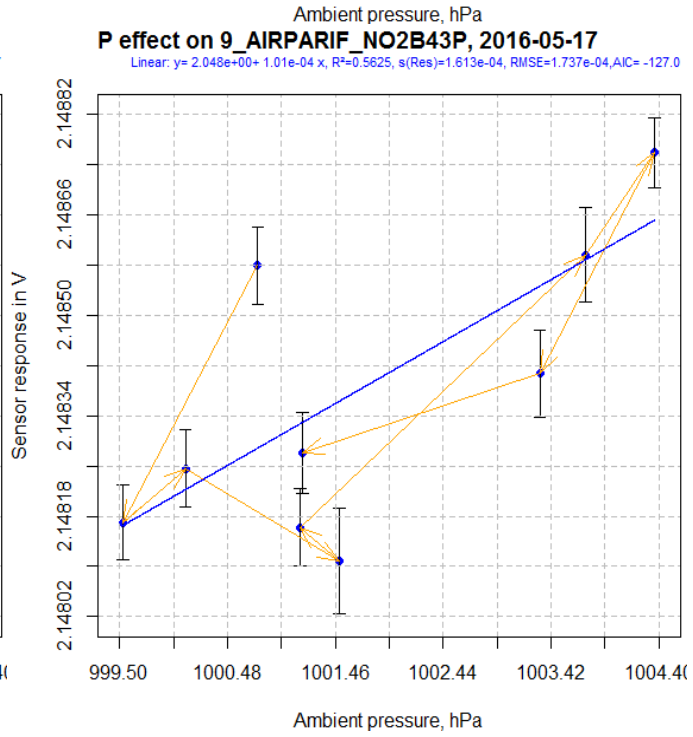

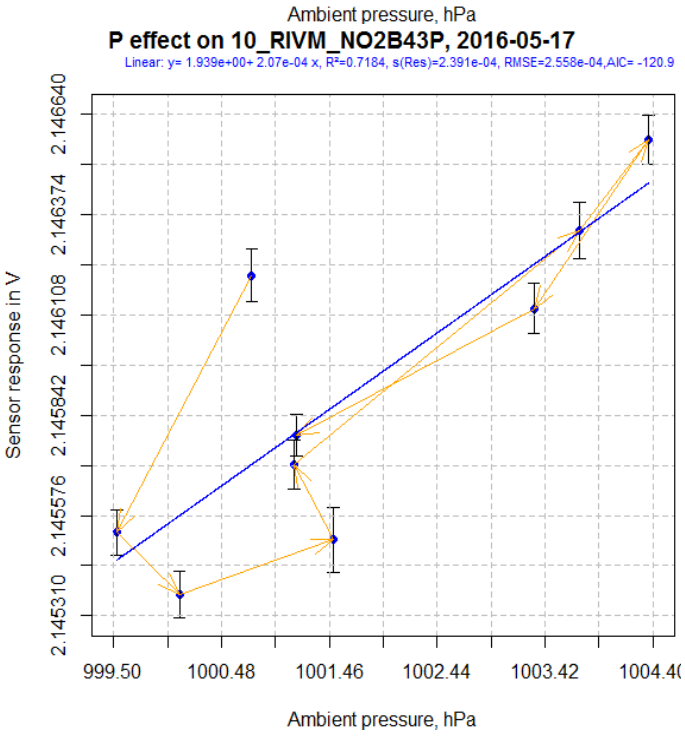

Figure 48: NO2-B43F, pressure effect

6.1.2 CO/MF-200 sensor

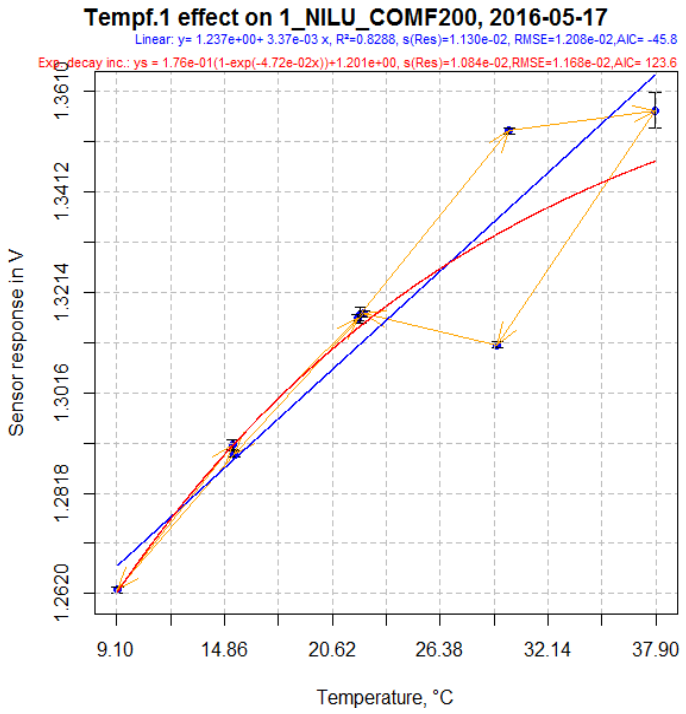

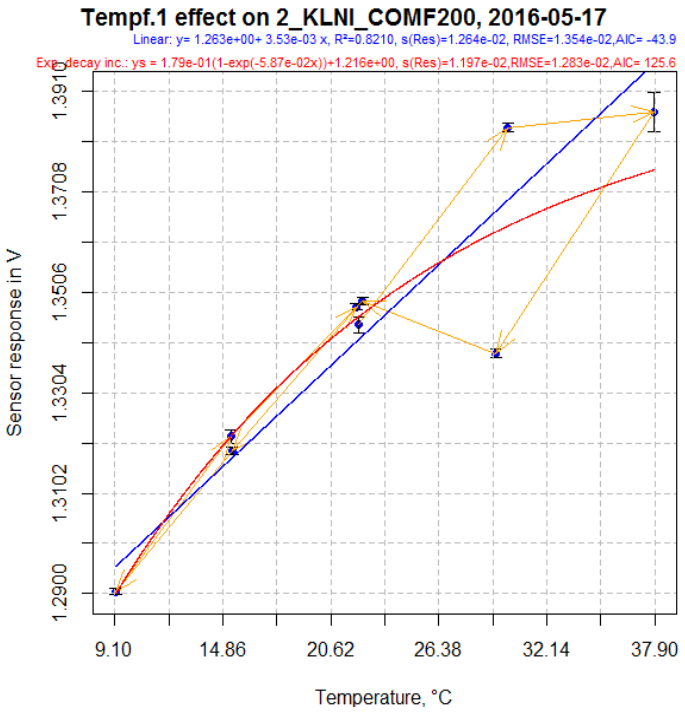

No data available because of connection error

No data available because the sensor channel was damaged

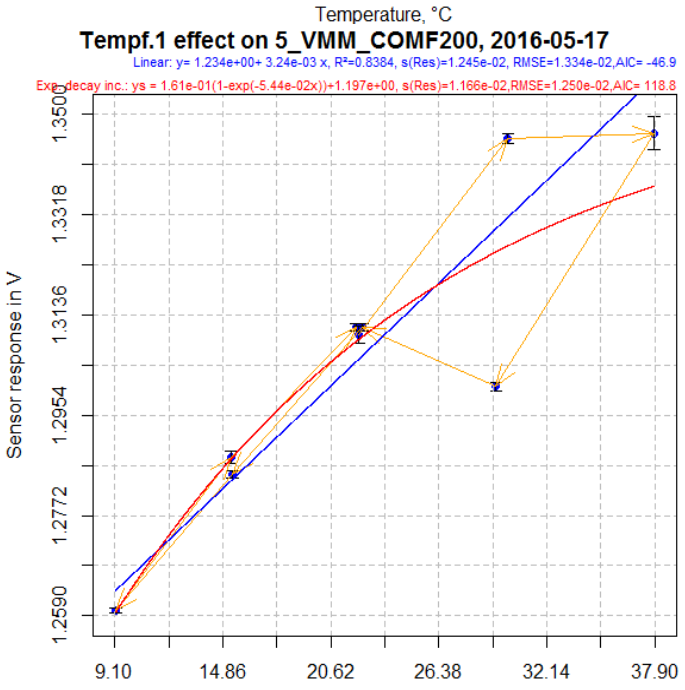

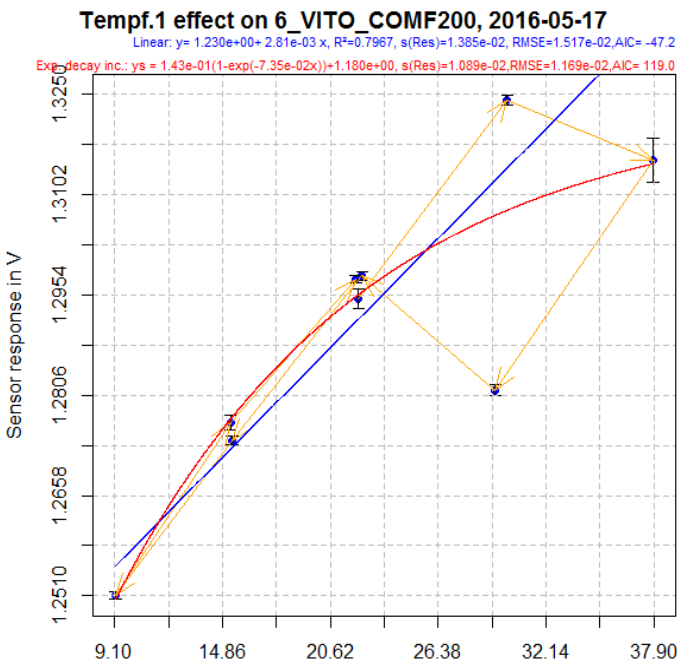

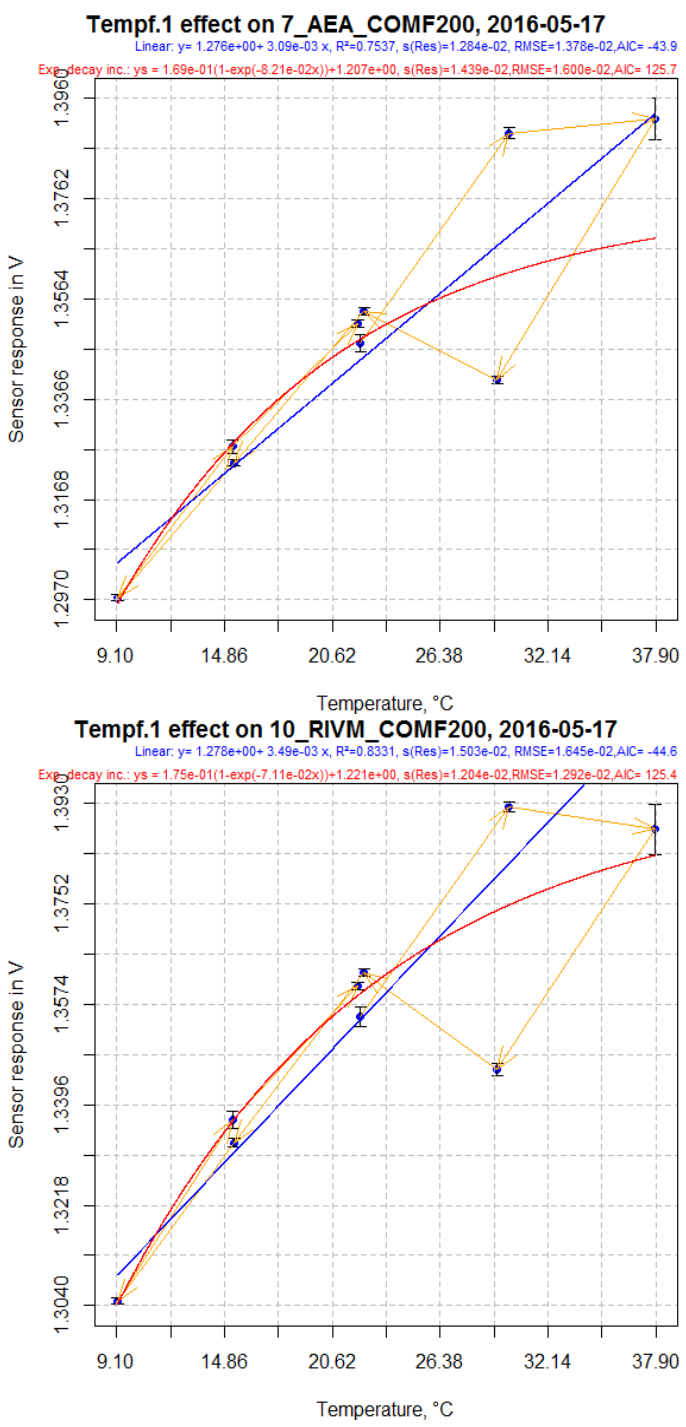

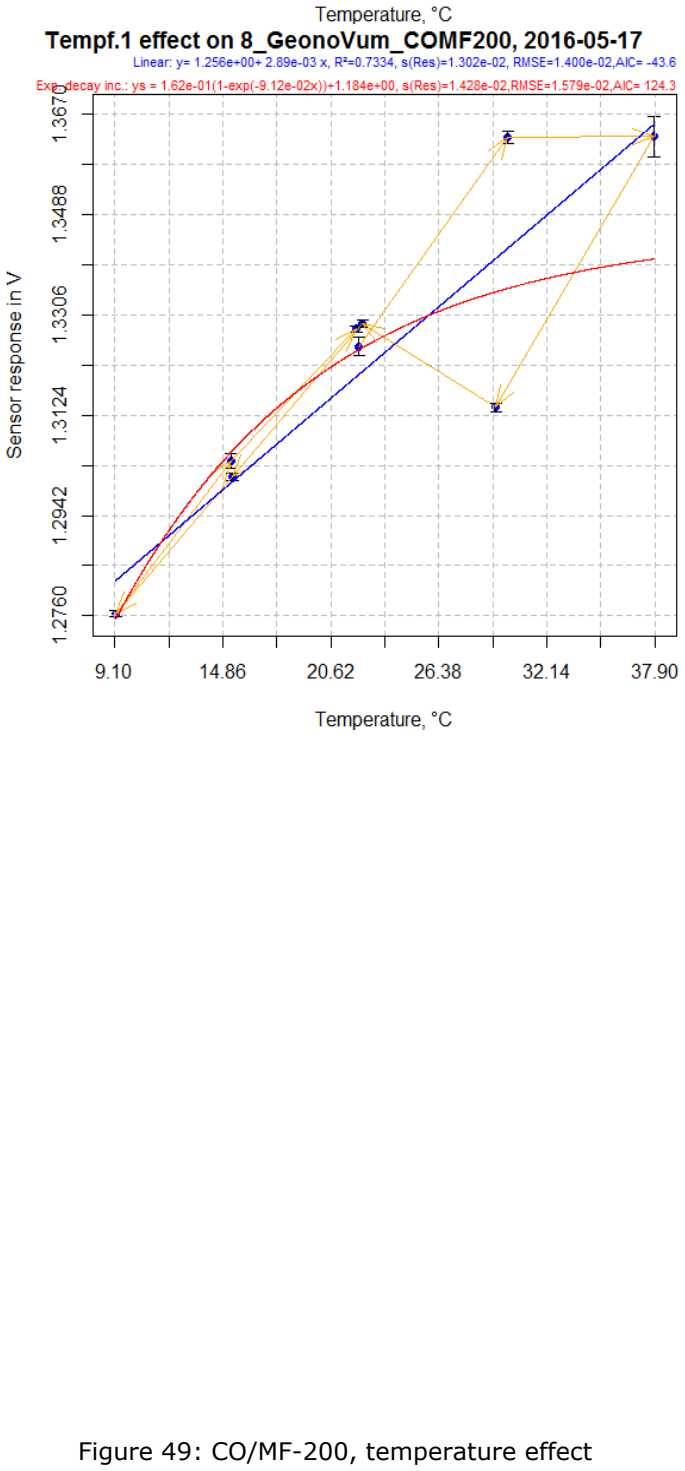

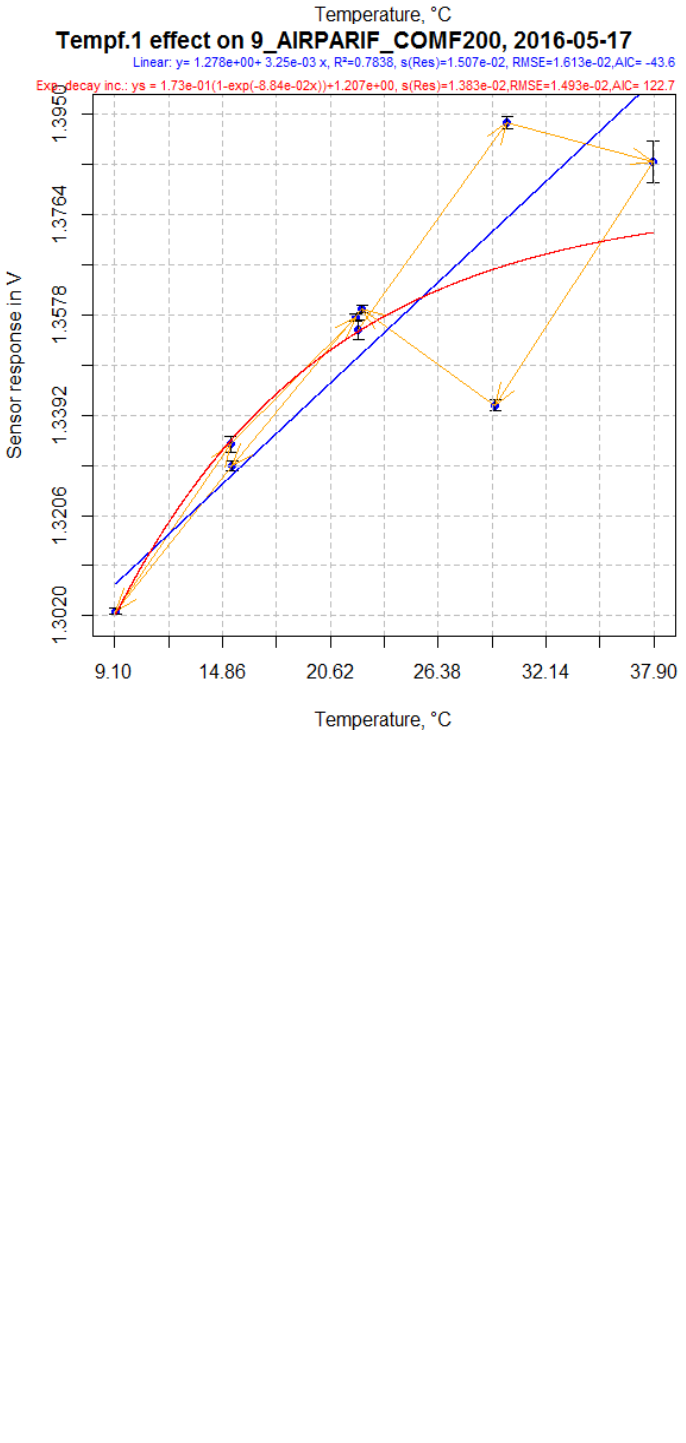

Figure 49: CO/MF-200, temperature effect

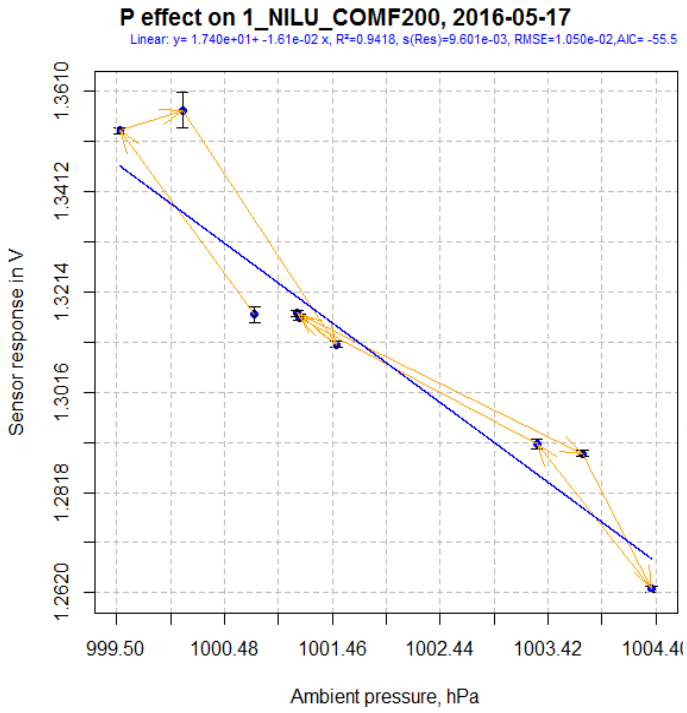

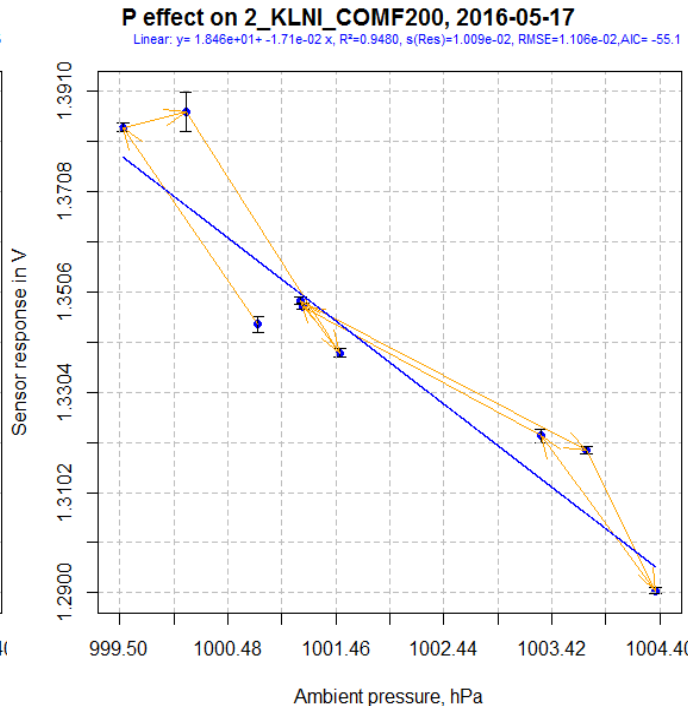

No data available because of connection error

No data available because the sensor channel was damaged

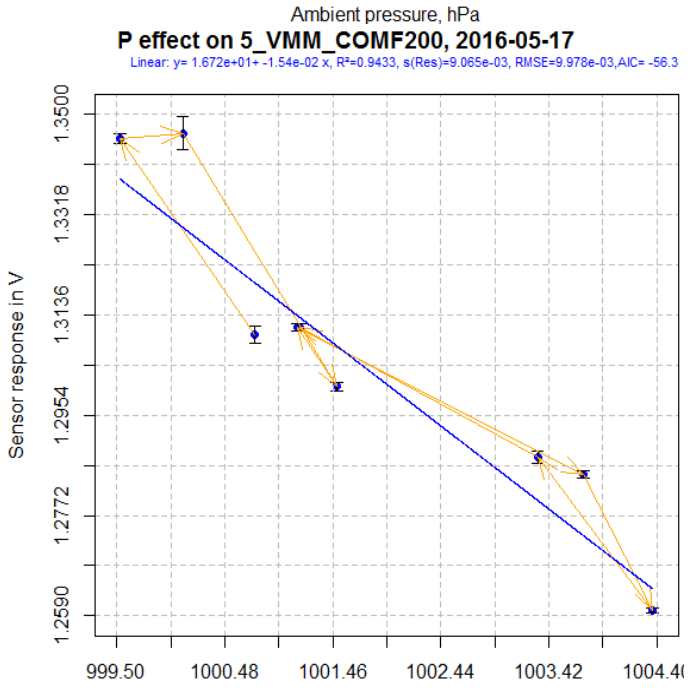

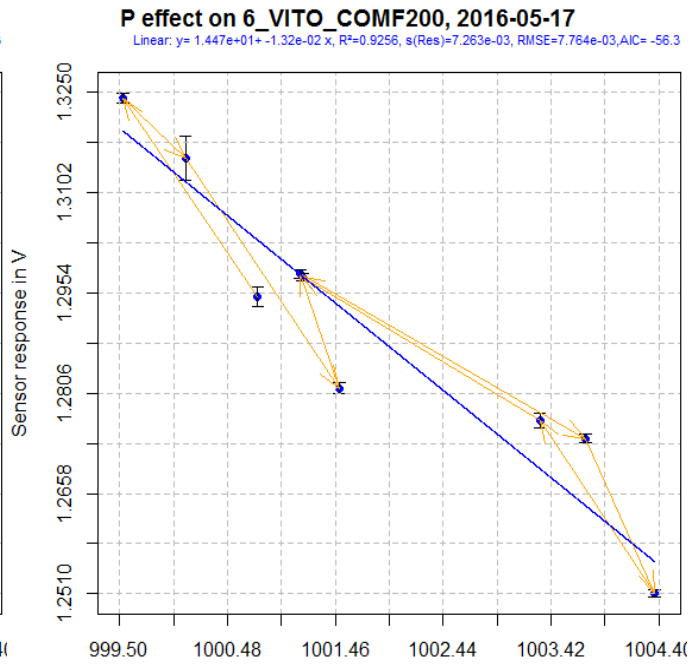

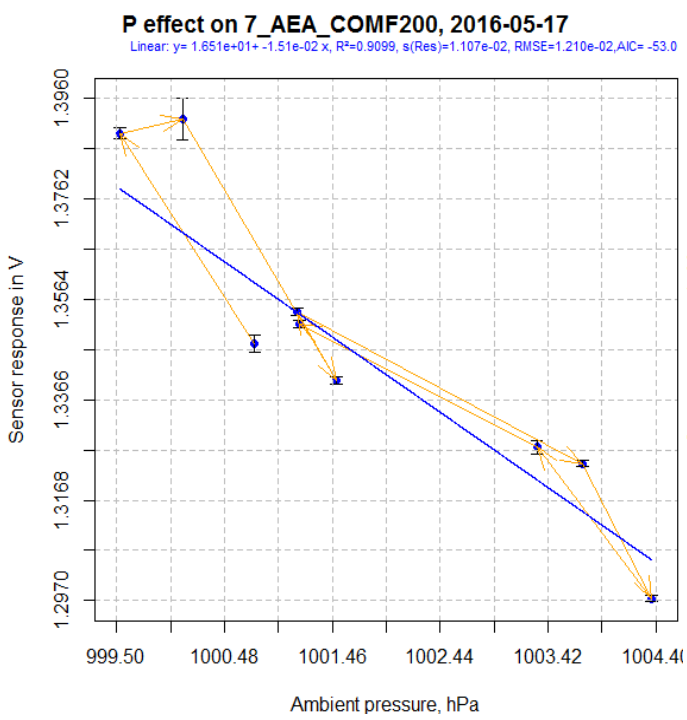

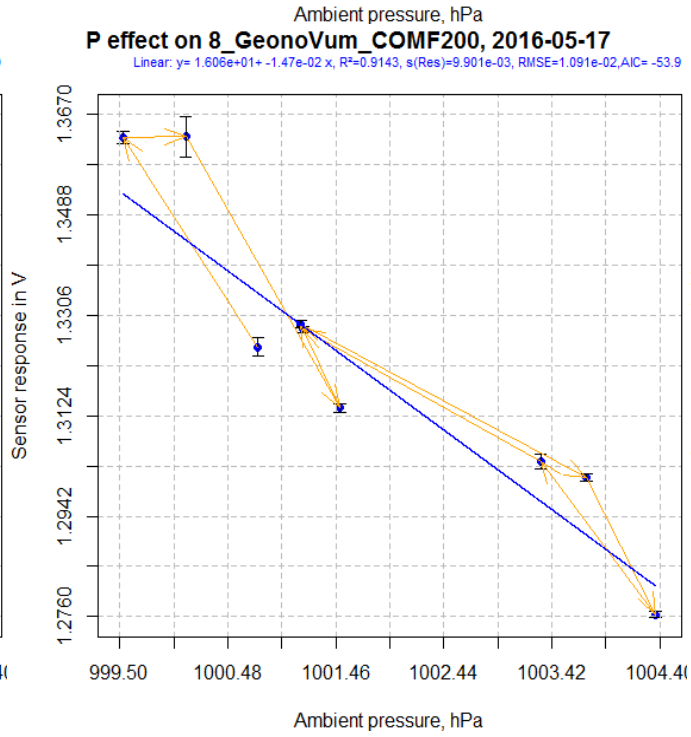

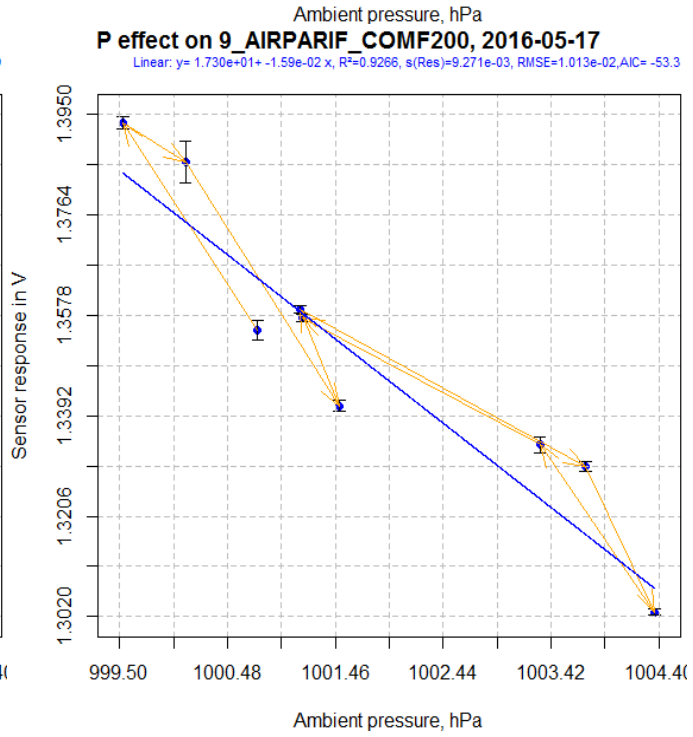

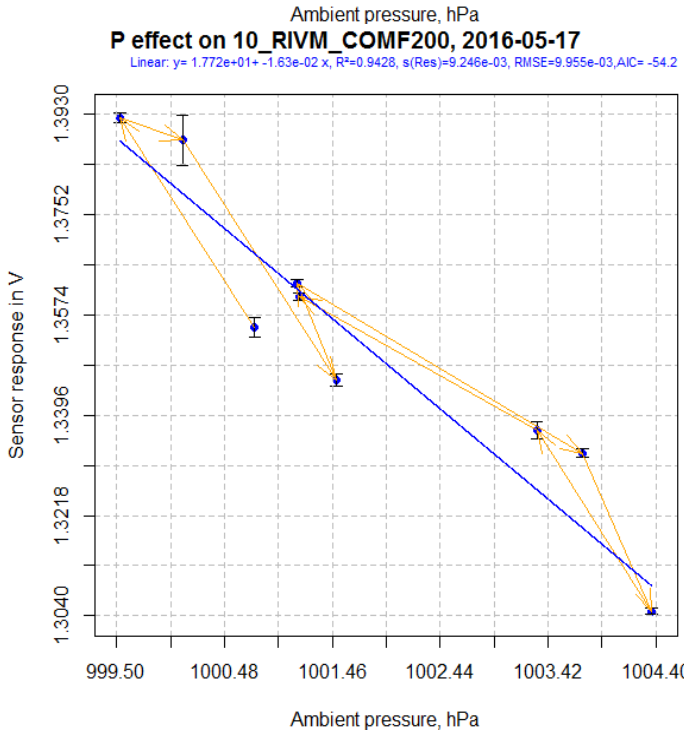

Figure 50: CO/MF-200, pressure effect

6.1.3 O3/M-5 sensor

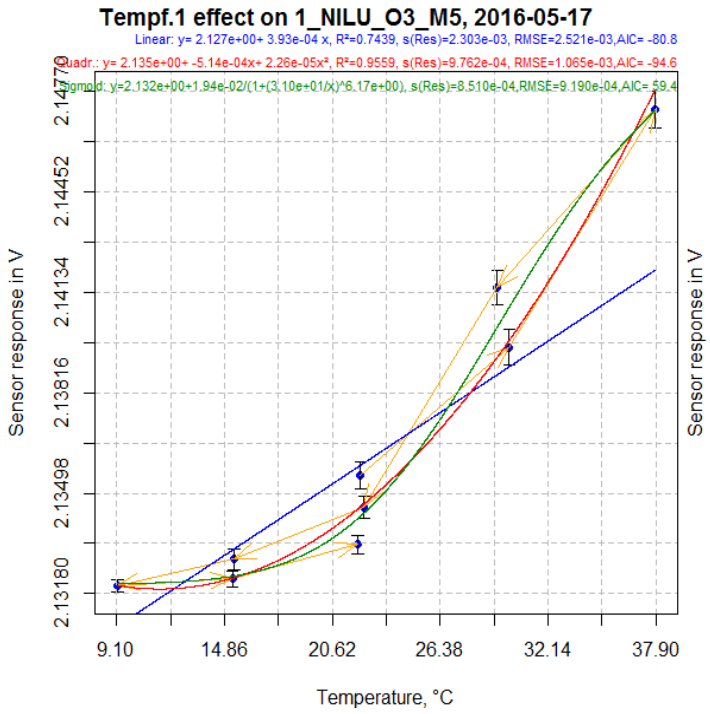

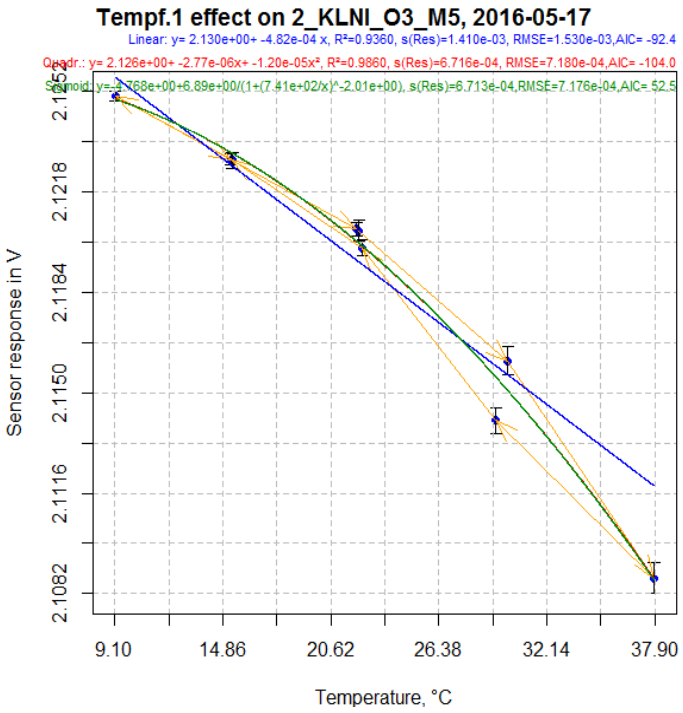

No data available because of connection error

No data available because the sensor channel was damaged

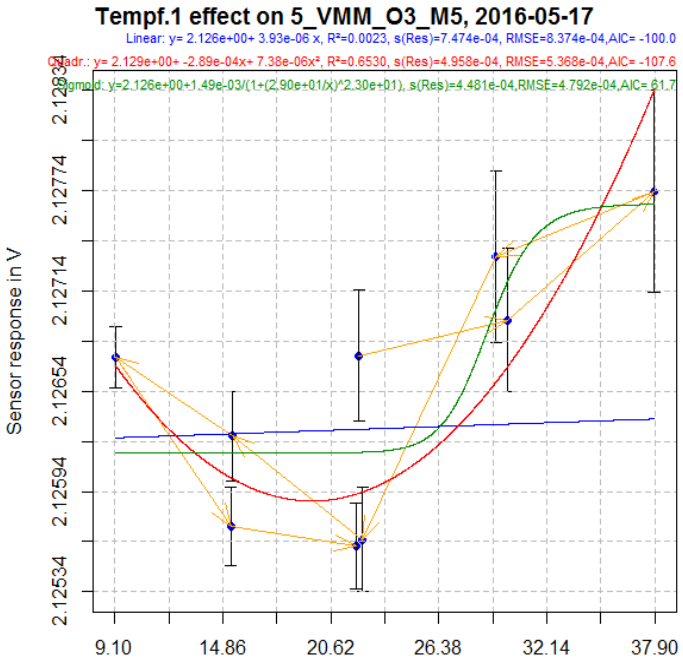

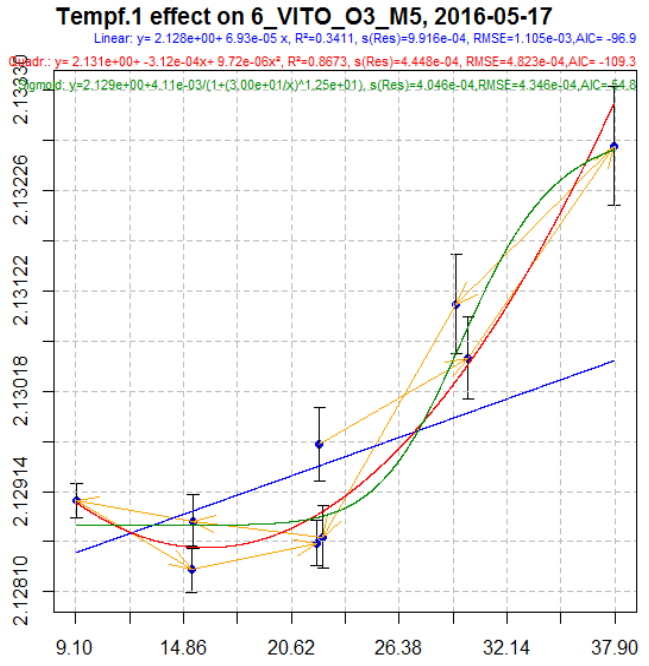

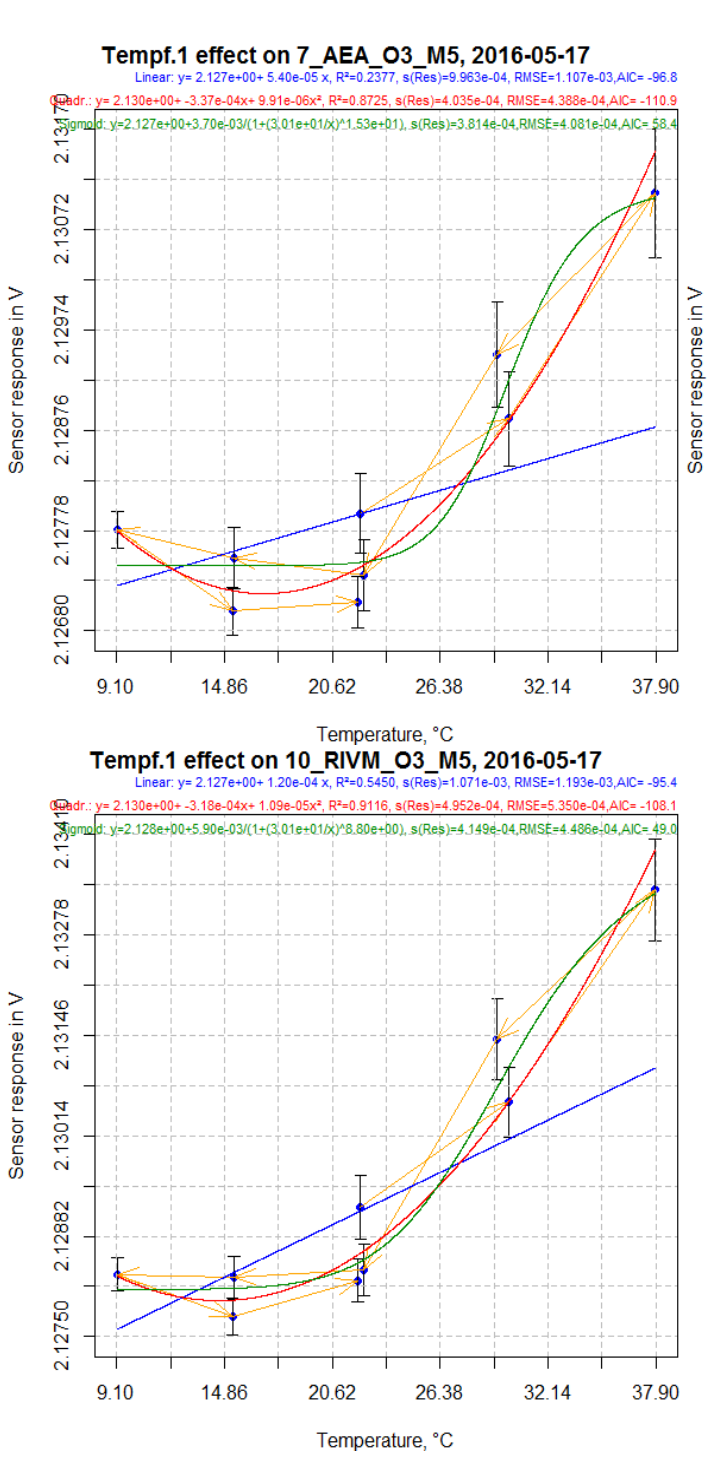

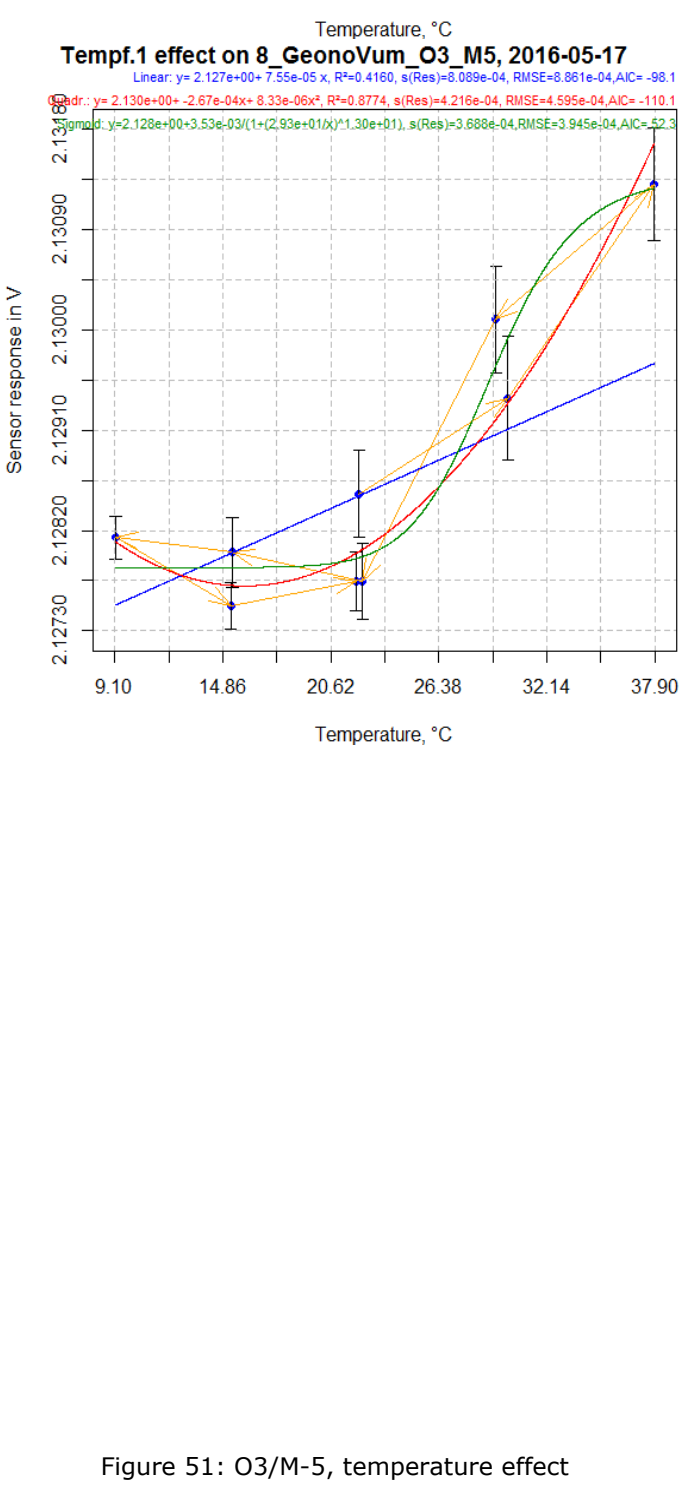

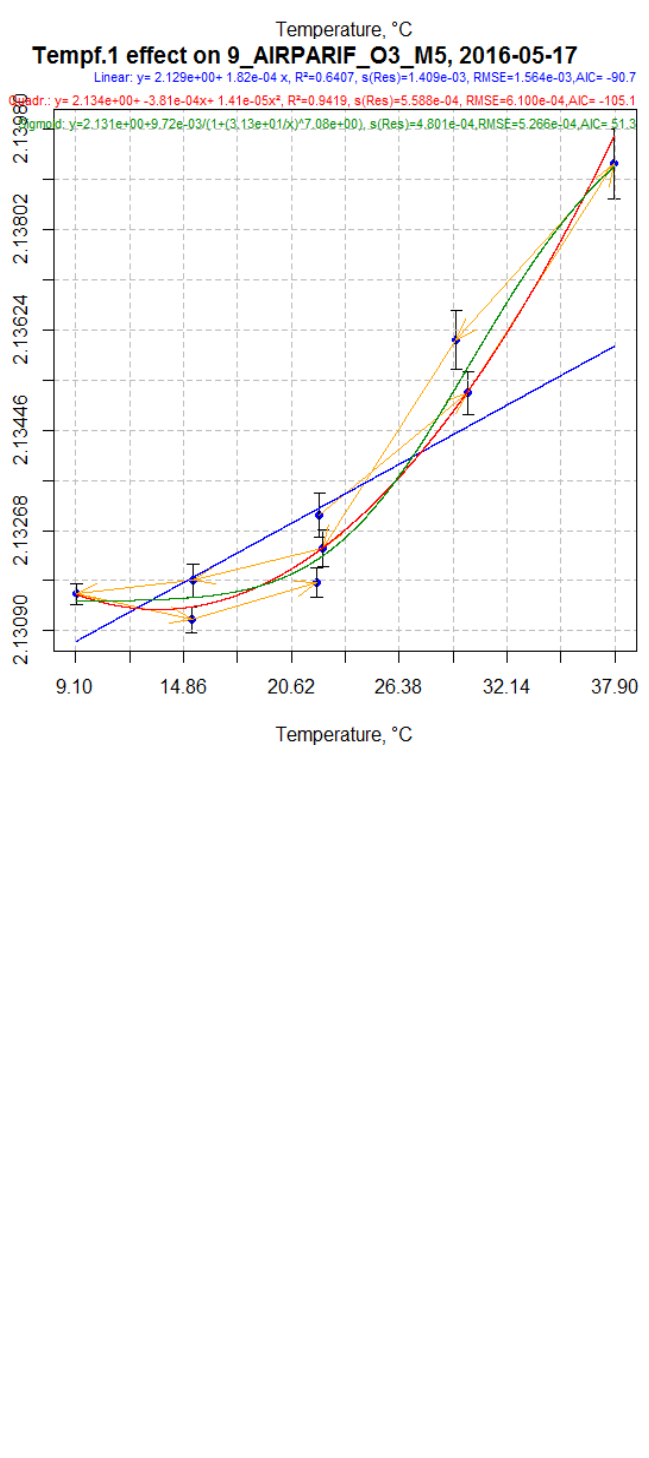

Figure 51: O3/M-5, temperature effect

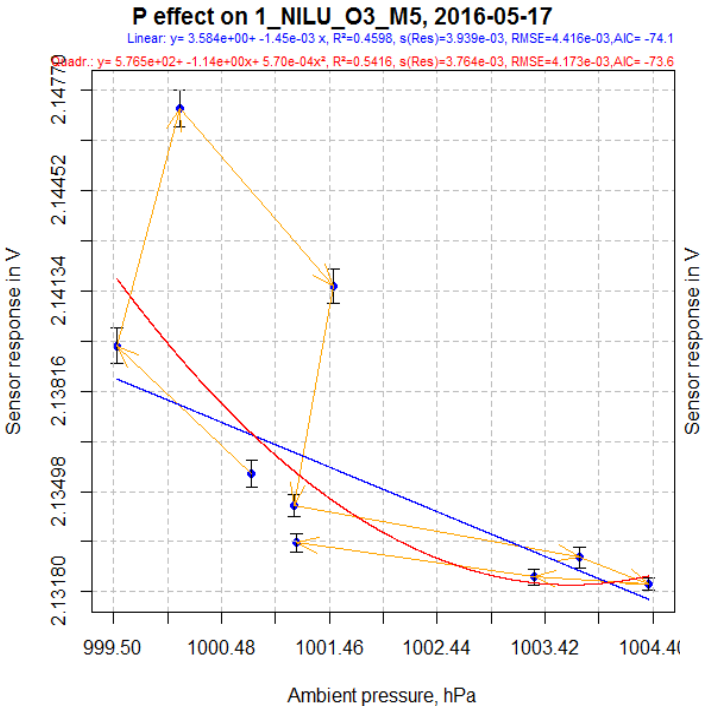

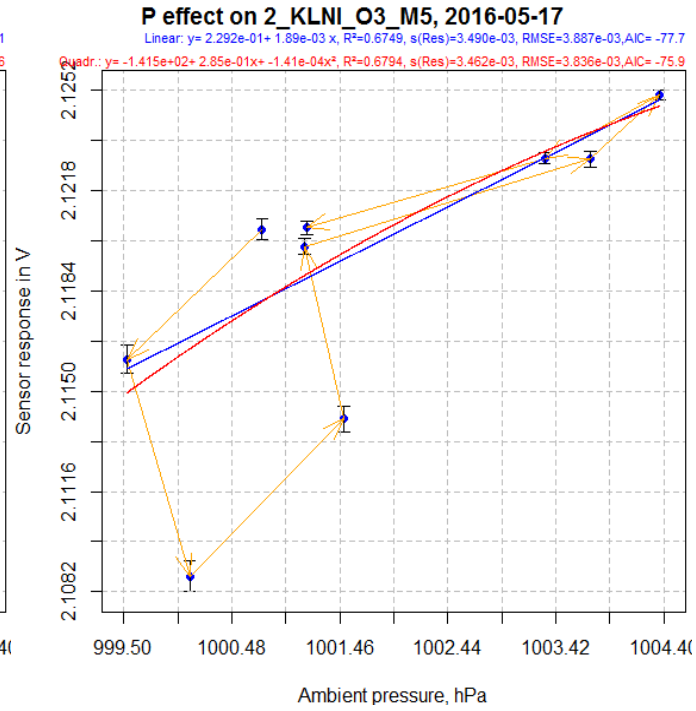

No data available because of connection error

No data available because the sensor channel was damaged

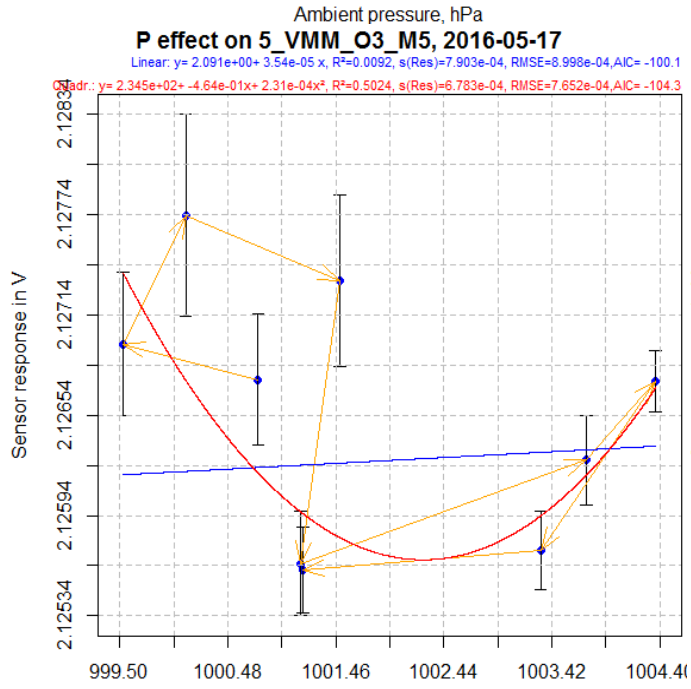

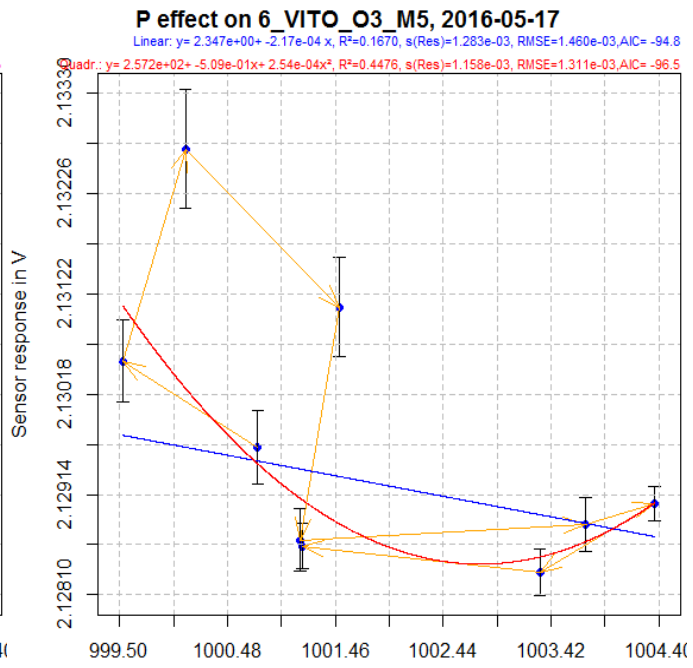

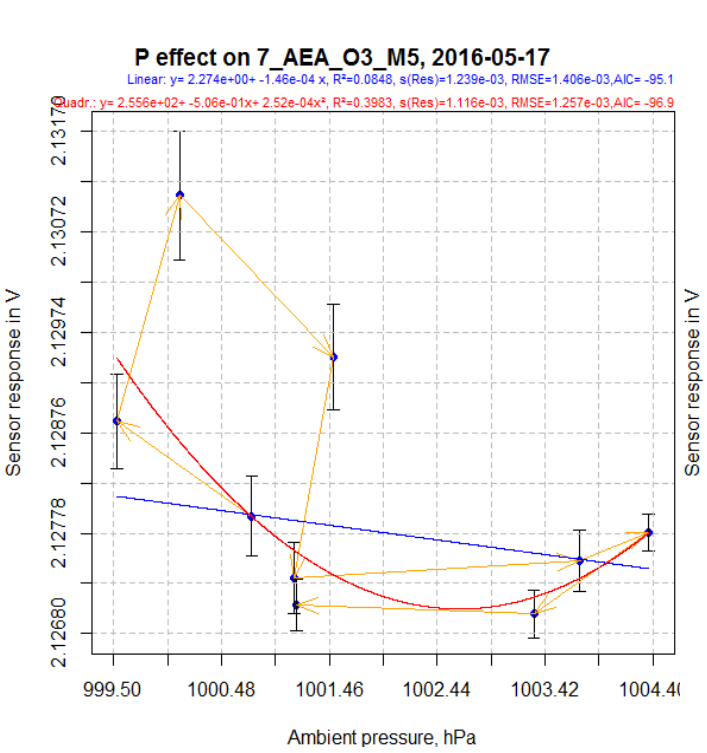

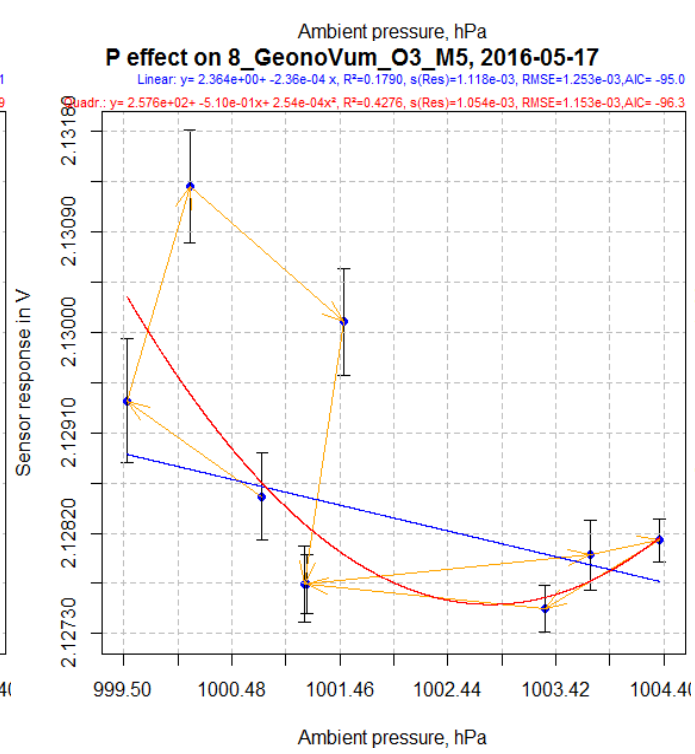

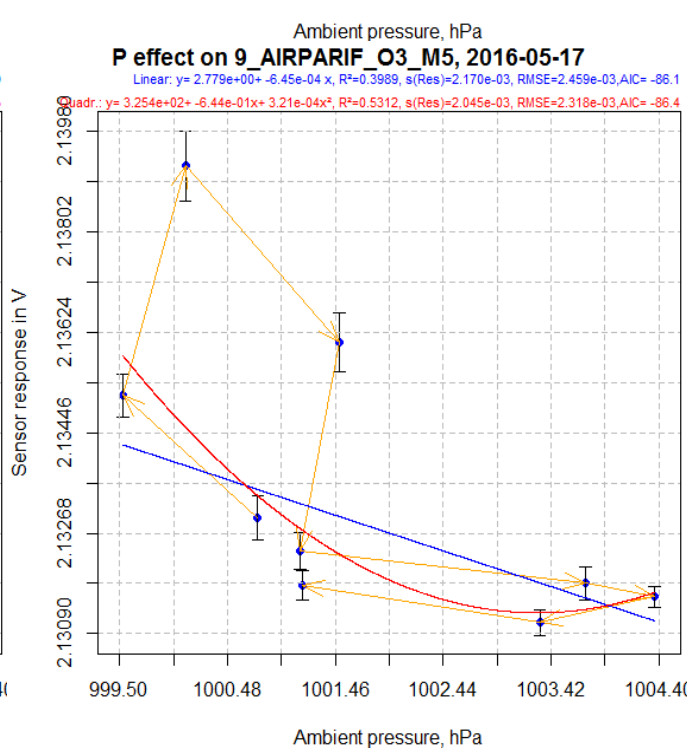

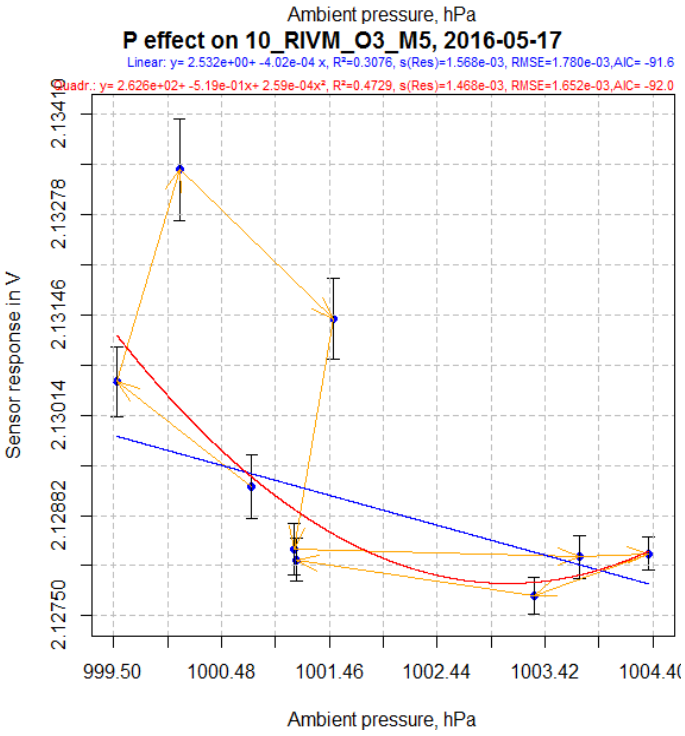

Figure 52: O3/M-5, pressure effect

6.1.4 NO-B4 sensor

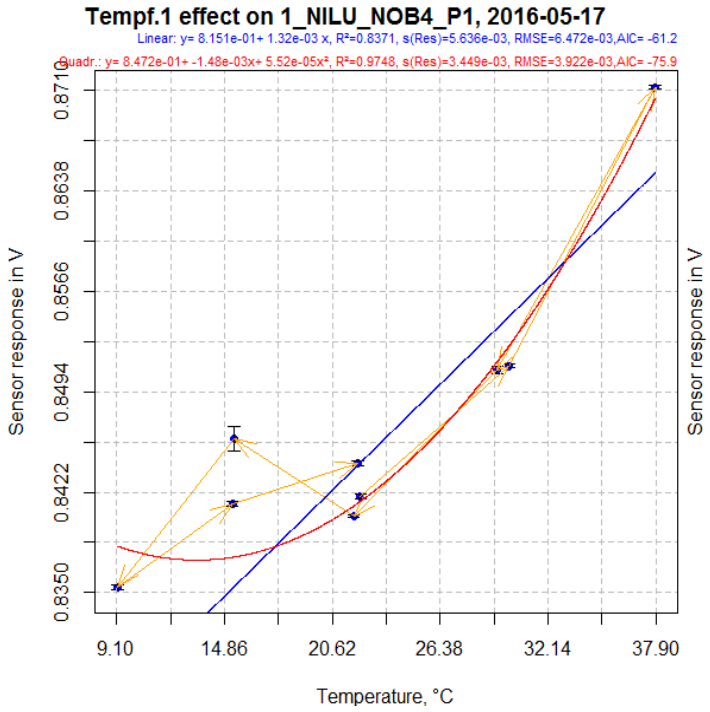

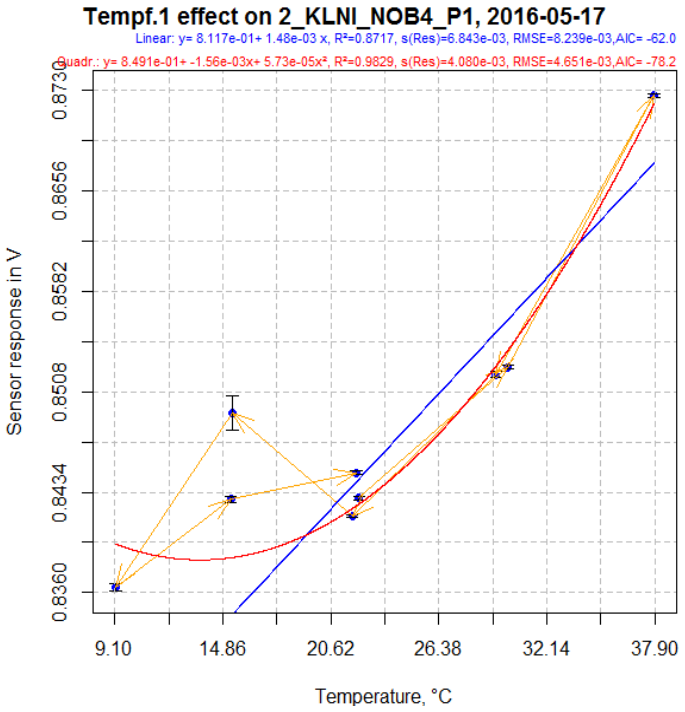

No data available because of connection error

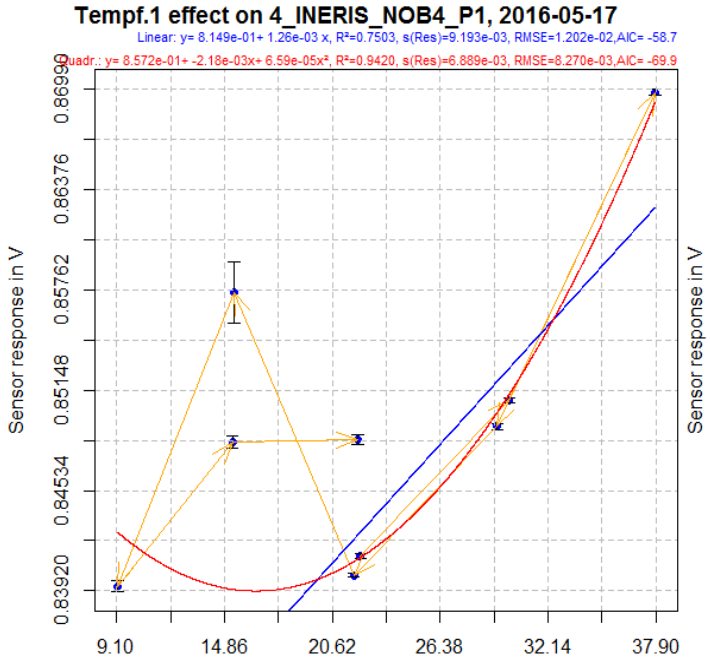

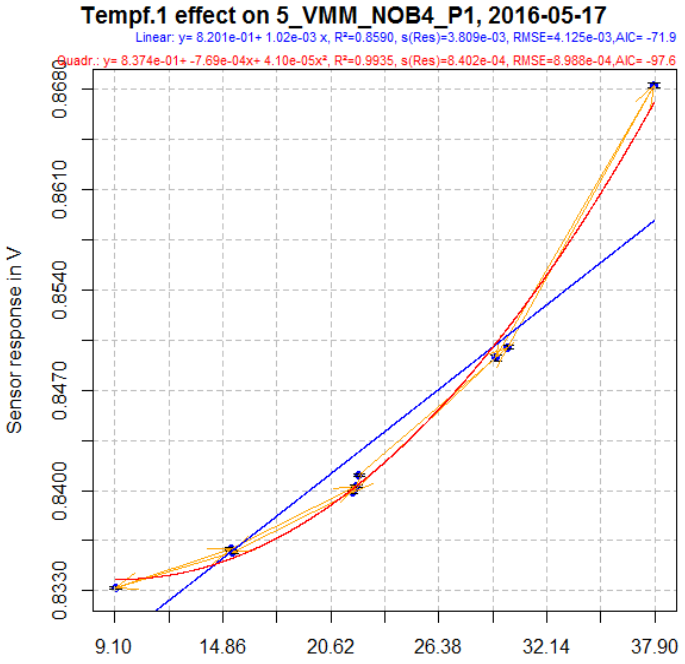

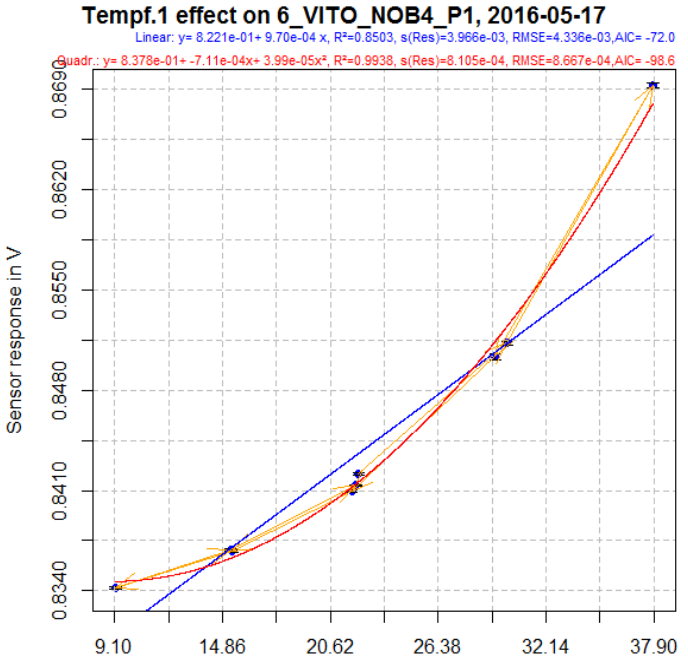

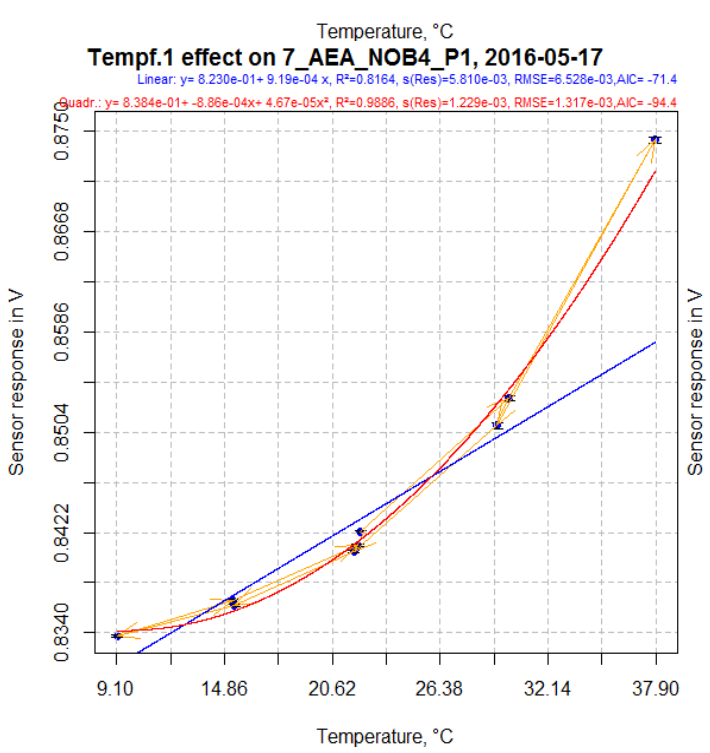

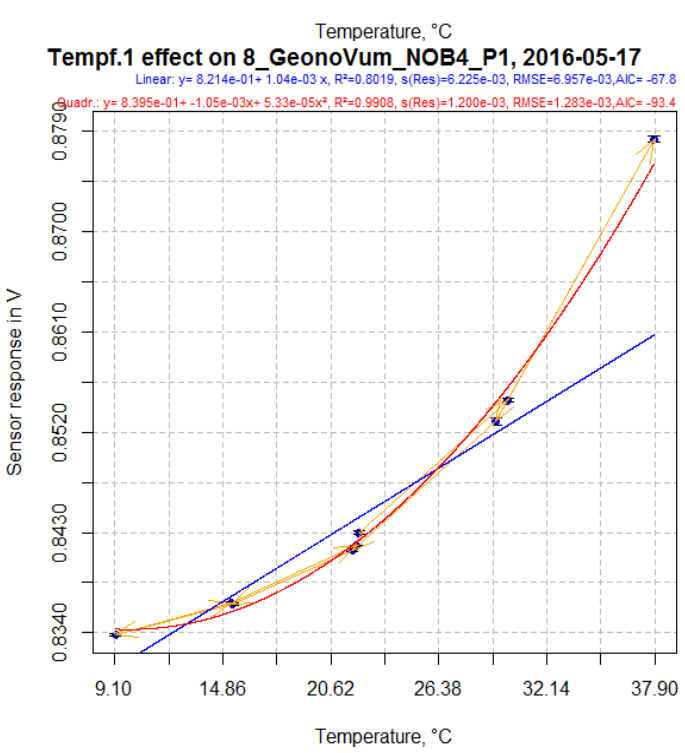

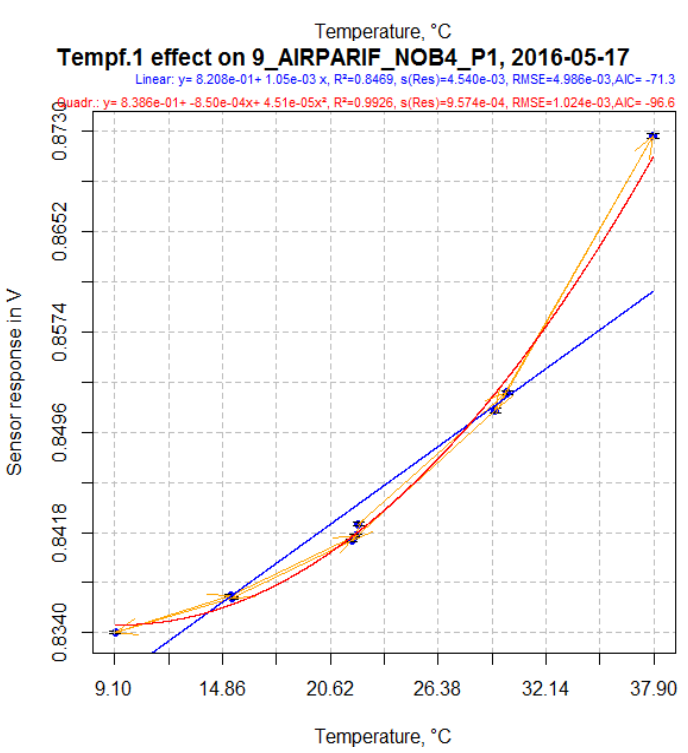

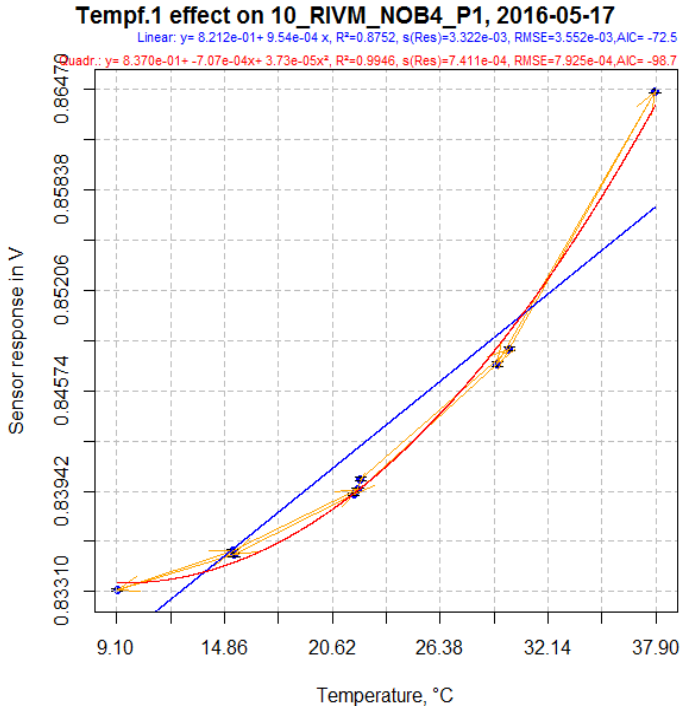

Figure 53: NO-B4, temperature effect

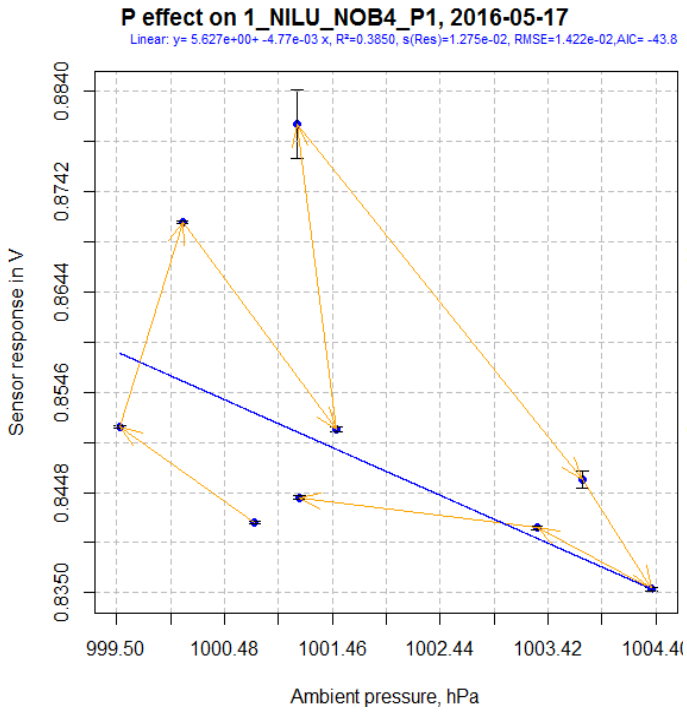

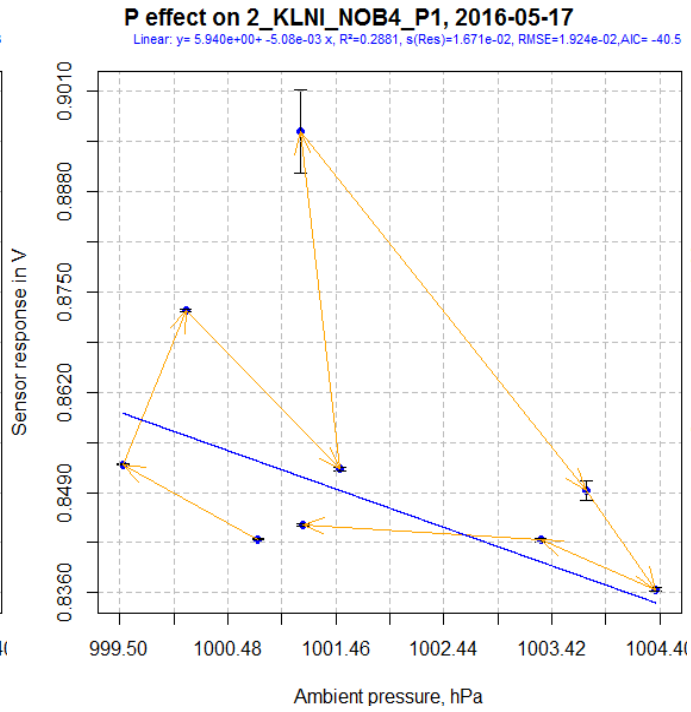

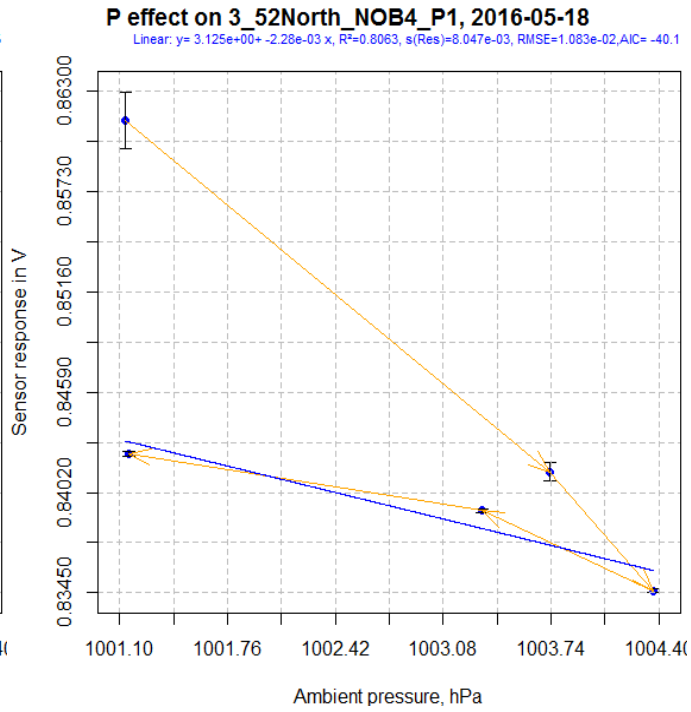

No data available because the sensor channel was damaged

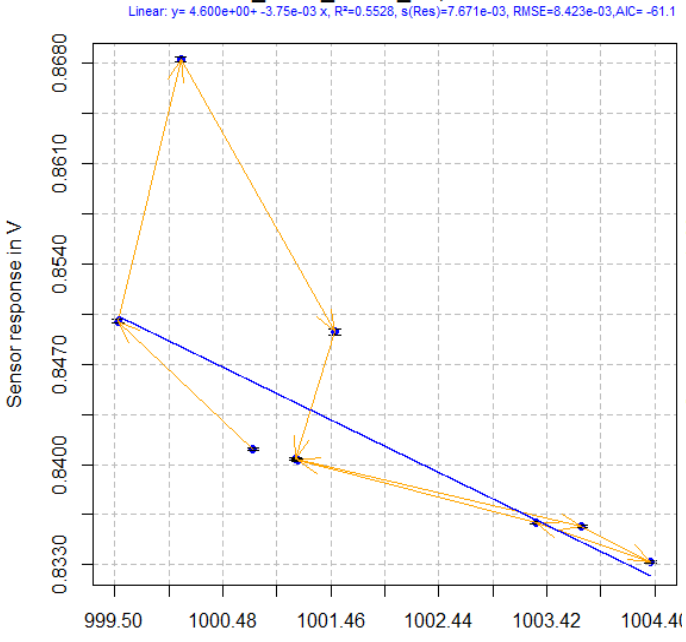

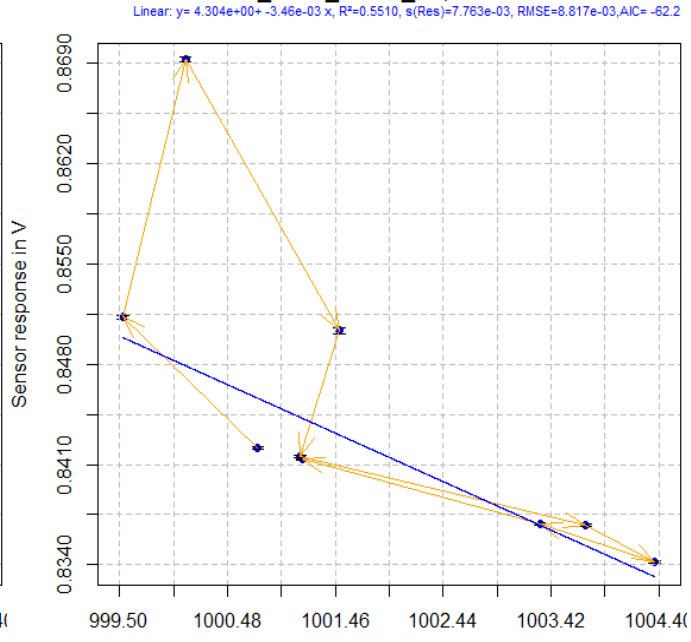

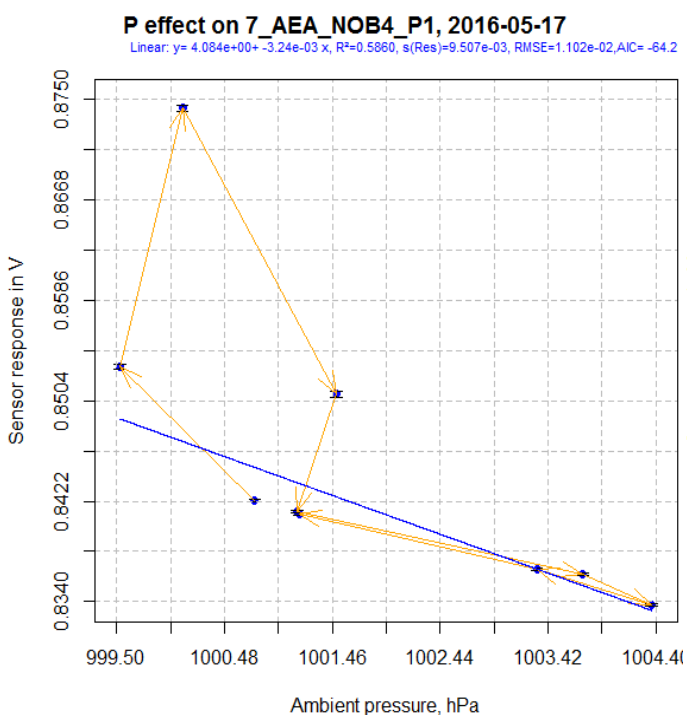

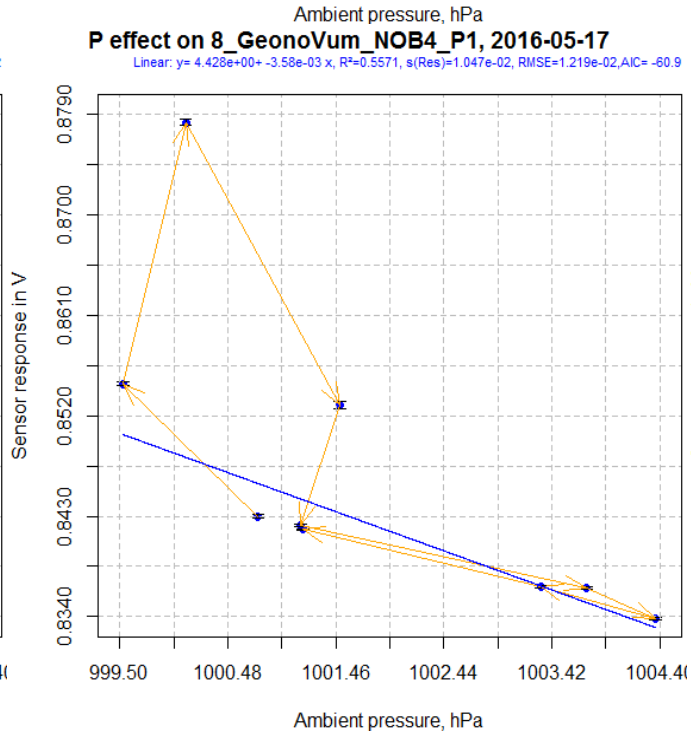

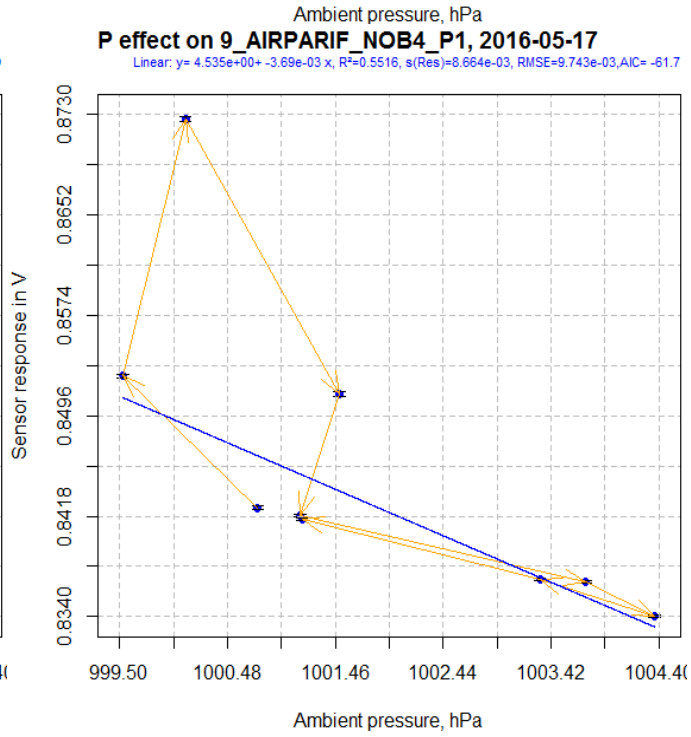

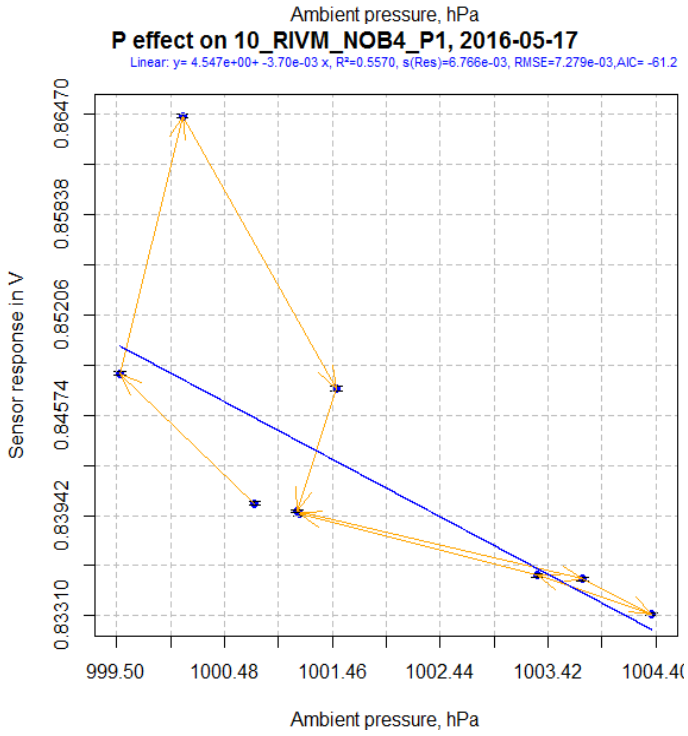

Figure 54:NO-B4, pressure effect

6.2 Temperature tests, tabulated results

The following tables give the effect of temperature on the set of 10 sensors (sensor readings in volt versus relative humidity in %) to estimate the scattering of sensor readings (see rows labelled means and relative standard deviation (RSD). The tables give the sensor model types, the intercepts in V (Interc. ± s) and slopes in V/% or V/hPa (slope ± s) of the linear lines, the probability that the intercepts and slopes are different from 0 (any value > 0.05 indicates that these variables are significantly different from 0), the coefficients of determination (R^2), the root mean square errors (RMSE) in V calculated using the residual degrees of freedom and the lack of fit in % of the linear model calculated for the x axis u(lof). Figure 47 to Figure 54 gives the scatterplots of the experiments, sensor readings versus reference values.

During this experiment, the data acquisition system of the third shield (52North) was not correctly connected resulting in a lack of measurements being registered. The CO channel of the fourth AirSensEUR shield was damaged and it did not work correctly.

Unfortunately, temperature and pressure were not independent in the experiment. Therefore, it is not possible to distinguish between the effects of both of them in order to conclude on the true effect.

6.2.1 NO2-B4F sensor

Six sensors show the same behaviour and pattern of sensor values, both for temperature and pressure while sensors 9 and 10 are completely different. We have no explanation for this discrepancy.

6.2.1.1 Temperature effect

The NO2-B43F sensor is affected by temperature. The slopes of linear lines are significant and the R^2 are high. The scattering of the slopes is high with RSD of 42.5% with mean value of 0.0000628 ± 0.0000267suggesting that the effect of temperature is not repeatable. The RMSE can be used to evaluate the lack of fit of linear correction of pressure using the NO_2 sensitivity to evaluate the remaining lack of fit of the pressure correction provided that the sensor readings are corrected for the pressure effect with the provided linear equations.

Table 37: Effect of Temperature on NO2B43F sensors (sensor readings in volt), experimental results of 2016-05-17. 3_52North_NO2B43P, 4_INERIS_NO2B43P, 9_AIRPARIF_NO2B43P, 10_RIVM_NO2B43P discarded for computing the means, mean SDs and RSDs

Sensors	Interc.	P(Interc.)	Slope	P(Slope)	R^2	RMSE
1_NILU_NO2B43P	2.14663 ± 0.00026	0.000	0.0000549 ± 0.0000106	0.001	0.7932	8.694e-05
2_KNMI_NO2B43P	2.14646 ± 0.00035	0.000	0.0000856 ± 0.0000146	0.001	0.8315	0.00011991
3_52North_NO2B43P	2.14877 ± 0.00013	0.000	0.0000051 ± 0.0000071	0.523	0.1478	3.414e-05
4_INERIS_NO2B43P	2.01342 ± 0.33401	0.001	0.0010854 ± 0.0138618	0.94	9e-04	0.34589321
5_VMM_NO2B43F	2.14651 ± 0.00040	0.000	0.0000844 ± 0.0000165	0.001	0.7895	0.0001399
6_VITO_NO2B43F	2.14722 ± 0.00027	0.000	0.0000287 ± 0.0000114	0.04	0.4741	9.126e-05
7_AEA_NO2B43F	2.14802 ± 0.00038	0.000	0.0000356 ± 0.0000155	0.056	0.4281	0.00013107
8_GeonoVum_NO2B43F	2.14660 ± 0.00037	0.000	0.0000874 ± 0.0000160	0.001	0.8092	0.00012969
9_AIRPARIF_NO2B43P	2.14882 ± 0.00015	0.000	-0.0000194 ± 0.0000063	0.018	0.5735	5.504e-05
10_RIVM_NO2B43P	2.14687 ± 0.00016	0.000	-0.0000428 ± 0.0000067	0	0.8551	5.602e-05
Means	2.14691 ± 0.00061		0.0000628 ± 0.0000267		0.6876	0.0001165
RSD	0.000		0.425			

6.2.1.2 Pressure effect

The NO2-B43F sensor seems to be slightly affected by pressure. The slopes of linear lines are rarely significant and the R^2 are rather low. The scattering of the slopes is high with RSD of 48.4 % with mean value of -0.0002344 ± 0.0001135.

Table 38: Effect of pressure on NO2B43F sensors (sensor readings in volt versus relative pressure in hPa), experimental results of 2016-05-17. 3_52North_NO2B43P, 4_INERIS_NO2B43P, 9_AIRPARIF_NO2B43P, 10_RIVM_NO2B43P, discarded for computing the means, mean SDs and RSDs

Sensors	Interc.	P(Interc.)	Slope	P(Slope)	R^2	RMSE
1_NILU_NO2B43P	2.35441 ± 0.09652	0.000	-0.0002062 ± 0.0000964	0.07	0.3954	0.00014866
2_KNMI_NO2B43P	2.48174 ± 0.12824	0.000	-0.0003328 ± 0.0001280	0.035	0.4911	0.00020839
3_52North_NO2B43P	2.16476 ± 0.02677	0.000	-0.0000159 ± 0.0000267	0.594	0.1053	3.498e-05
4_INERIS_NO2B43P	-17.99911 ± 72.45207	0.811	0.0200025 ± 0.0723268	0.79	0.0108	0.34416954
5_VMM_NO2B43F	2.47086 ± 0.14382	0.000	-0.0003219 ± 0.0001436	0.06	0.418	0.00023262
6_VITO_NO2B43F	2.24553 ± 0.06966	0.000	-0.0000975 ± 0.0000695	0.204	0.2193	0.00011119
7_AEA_NO2B43F	2.25610 ± 0.09862	0.000	-0.0001071 ± 0.0000985	0.313	0.1446	0.0001603
8_GeonoVum_NO2B43F	2.49016 ± 0.13389	0.000	-0.0003410 ± 0.0001336	0.038	0.4819	0.00021371
9_AIRPARIF_NO2B43P	2.04751 ± 0.03363	0.000	0.0001007 ± 0.0000336	0.02	0.5625	5.575e-05
10_RIVM_NO2B43P	1.93856 ± 0.04906	0.000	0.0002070 ± 0.0000490	0.004	0.7184	7.809e-05
Means	2.38313 ± 0.11382		-0.0002344 ± 0.0001135		0.3584	0.0001791
RSD	0.048		0.484			

6.2.2 CO/MF-200 sensor

All sensors show the same behaviour and pattern of sensor values, both for temperature and pressure.

6.2.2.1 Temperature effect

The COM/F200 sensor is affected by temperature. The slopes of linear lines are significant and the R^2 are fairly high. The scattering of the slopes is low with RSD of 8.2 % and mean value of 0.0033137 ± 0.0004047 V/ºC suggesting that the effect of temperature is repeatable. The RMSE can be used to evaluate the lack of fit of linear correction of temperature resulting from applying the linear correction ($2\frac{0.004366}{0.08117} = 0.1\ ppm$).

Table 39: Effect of temperature on COMF200 sensors (sensor readings in volt), experimental results of 2016-05-17. 3_52North_COMF200 discarded for computing the means, mean SDs and.

Sensors	Interc.	P(Interc.)	Slope	P(Slope)	R^2	RMSE	u(lof)
1_NILU_COMF200	1.23673 ± 0.01252	0	0.0033708 ± 0.0005791	0.001	0.8288	0.0042003	4
2_KNMI_COMF200	1.26322 ± 0.01338	0	0.0035257 ± 0.0006222	0.001	0.821	0.00463494	5
3_52North_COMF200	1.25742 ± 0.00281	0	0.0041678 ± 0.0001536	0	0.9959	0.00089184	1
NA	NA ± NA	NA	NA ± NA	NA	NA	NA	NA
5_VMM_COMF200	1.23400 ± 0.01096	0	0.0032386 ± 0.0005374	0.001	0.8384	0.00398128	5
6_VITO_COMF200	1.22977 ± 0.01089	0	0.0028067 ± 0.0005359	0.001	0.7967	0.00384452	6
7_AEA_COMF200	1.27610 ± 0.01380	0	0.0030883 ± 0.0006672	0.002	0.7537	0.00454309	5
8_GeonoVum_COMF200	1.25602 ± 0.01360	0	0.0028857 ± 0.0006576	0.003	0.7334	0.00468153	5
9_AIRPARIF_COMF200	1.27825 ± 0.01290	0	0.0032479 ± 0.0006447	0.001	0.7838	0.00468538	6
10_RIVM_COMF200	1.27751 ± 0.01212	0	0.0034915 ± 0.0005907	0.001	0.8331	0.00435697	6
Means	1.25645 ± 0.02055		0.0032069 ± 0.0002645		0.7986	0.0043660	5.2
RSD	0.016		0.082				

6.2.2.2 Pressure effect

The COMF200 sensor is affected by pressure. The slopes of the linear fits are significant and the R^2 are high. The scattering of the slopes is low with RSD of 7.2 % with mean value of -0.0155144 ± 0.0011214 V/hPa suggesting that the Pressure effect is repeatable. The RMSE can be used to evaluate the lack of fit of linear correction of pressure resulting from applying the linear correction ($2\frac{0.0025984}{0.08117} = 0.1\ ppm$). The effect of pressure in this experiment is about 10 times more than the one observed during the humidity/pressure experiment (see 5.2.2.2 Pressure effect). Therefore, it is likely that the changes of sensor values are rather due to a temperature effect.

Table 40: Effect of P on COMF200 sensors (sensor readings in volt), experimental results of 2016-05-17.

Sensors	Interc.	P(Interc.)	Slope	P(Slope)	R^2	RMSE	u(lof)
1_NILU_COMF200	17.39890 ± 1.51250	0.000	-0.0160602 ± 0.0015094	0	0.9418	0.00244931	1
2_KNMI_COMF200	18.46106 ± 1.51580	0.000	-0.0170914 ± 0.0015127	0	0.948	0.00249788	1
3_52North_COMF200	17.16659 ± 2.05769	0.004	-0.0157982 ± 0.0020527	0.005	0.9518	0.00307446	1
NA	NA ± NA	NA	NA ± NA	NA	NA	NA	NA
5_VMM_COMF200	16.72340 ± 1.42958	0.000	-0.0153924 ± 0.0014263	0	0.9433	0.00235818	1
6_VITO_COMF200	14.47178 ± 1.41286	0.000	-0.0131586 ± 0.0014096	0	0.9256	0.00232485	1
7_AEA_COMF200	16.51482 ± 1.80475	0.000	-0.0151437 ± 0.0018006	0	0.9099	0.00274708	1
8_GeonoVum_COMF200	16.06169 ± 1.70714	0.000	-0.0147160 ± 0.0017032	0	0.9143	0.00265467	1
9_AIRPARIF_COMF200	17.30226 ± 1.69764	0.000	-0.0159256 ± 0.0016936	0	0.9266	0.00272936	0
10_RIVM_COMF200	17.72408 ± 1.52430	0.000	-0.0163435 ± 0.0015209	0	0.9428	0.0025497	1
Means	16.86940 ± 1.13842		-0.0155144 ± 0.0011214		0.9338	0.0025984	0.9
RSD	0.067		0.072				

6.2.3 O3/M-5 sensor

The effect of temperature on the O3/M-5 is unclear. There is significant variation between the results and the second sensor (KNMI) has a different behaviour (decrease with temperature) than all the other sensors and we do not know the reason. The same sensor

also shows pressure effects that are opposite to the other sensors. It is difficult to conclude on a significant temperature effect because of the variation of the results.

6.2.3.1 Temperature effect

The O3/M-5 sensor seems to be affected by temperature although not consistently. In general, the sensor readings increase with increasing temperature. The relationship between the sensor values and temperature is not linear, rather quadratic, although we use a linear relationship for comparison purposes. The slopes of linear fits are generally not significant and the R^2 are generally low. The scattering of the slopes shows a RSD of 86% with a mean value of 0.0001489 ± 0.0001282 V/°C.

Table 41: Effect of Tempf.1 on O3/M-5 sensors (sensor readings in volt), experimental results of 2016-05-17. 2_KNMI_O3/M-5, 5_VMM_O3/M-5 discarded for computing the means, mean SDs and RSDs

Sensors	Interc.	P(Interc.)	Slope	P(Slope)	R^2	RMSE
1_NILU_O3/M-5	2.12718 ± 0.00164	0	0.0003927 ± 0.0000871	0.003	0.7439	0.00064605
2_KNMI_O3/M-5	2.13008 ± 0.00089	0	-0.0004816 ± 0.0000476	0	0.936	0.0003367
NA	NA ± NA	NA	NA ± NA	NA	NA	NA
NA	NA ± NA	NA	NA ± NA	NA	NA	NA
5_VMM_O3/M-5	2.12623 ± 0.00059	0	0.0000039 ± 0.0000311	0.903	0.0023	0.00022223
6_VITO_O3/M-5	2.12787 ± 0.00068	0	0.0000693 ± 0.0000364	0.099	0.3411	0.0002617
7_AEA_O3/M-5	2.12675 ± 0.00068	0	0.0000540 ± 0.0000365	0.183	0.2377	0.00026332
8_GeonoVum_O3/M-5	2.12684 ± 0.00064	0	0.0000755 ± 0.0000338	0.061	0.416	0.00024757
9_AIRPARIF_O3/M-5	2.12905 ± 0.00099	0	0.0001823 ± 0.0000516	0.01	0.6407	0.00037533
10_RIVM_O3/M-5	2.12651 ± 0.00079	0	0.0001195 ± 0.0000413	0.023	0.545	0.00029106
Means	2.12737 ± 0.00095		0.0001489 ± 0.0001282		0.4874	0.0003475
RSD	0.000		0.861			

6.2.3.2 Pressure effect

As for temperature, the effect of pressure on the O3/M-5 is difficult to demonstrate with a lot of scattering of results. The slopes of the linear fits are generally not significant and the R^2 are low.

The dependence of the O3/M-5 sensors on pressure was not clearly demonstrated. In fact, the observed relationship did not match the linear relationship found before in the experiment of relative humidity/pressure. The scattering of the slopes gave a RSD of 0.950 with mean value of -0.0005155 V/hPa corresponding to about 140 % of the sensor sensitivity to O_3 (-0.0003670 V/ppb).

Table 42: Effect of pressure on O3/M-5 sensors (sensor readings in volt), experimental results of 2016-05-17. 2_KLNI_O3_M5, 5_VMM_O3_M5 discarded for computing the means, mean SDs and RSDs

Sensors	Interc.	P(Interc.)	Slope	P(Slope)	R^2	RMSE
1_NILU_O3_M5	3.58438 ± 0.59424	0.001	-0.0014465 ± 0.0005927	0.045	0.4598	0.00093825
2_KLNI_O3_M5	0.22921 ± 0.49642	0.658	0.0018874 ± 0.0004951	0.007	0.6749	0.00075896
NA	NA ± NA	NA	NA ± NA	NA	NA	NA
NA	NA ± NA	NA	NA ± NA	NA	NA	NA
5_VMM_O3_M5	2.09076 ± 0.13970	0.000	0.0000354 ± 0.0001393	0.807	0.0092	0.00022147
6_VITO_O3_M5	2.34699 ± 0.18393	0.000	-0.0002173 ± 0.0001834	0.275	0.167	0.00029425
7_AEA_O3_M5	2.27420 ± 0.18199	0.000	-0.0001461 ± 0.0001815	0.447	0.0848	0.00028852
8_GeonoVum_O3_M5	2.36445 ± 0.19128	0.000	-0.0002357 ± 0.0001908	0.257	0.179	0.00029354
9_AIRPARIF_O3_M5	2.77935 ± 0.30025	0.000	-0.0006454 ± 0.0002995	0.068	0.3989	0.00048548
10_RIVM_O3_M5	2.53188 ± 0.22865	0.000	-0.0004022 ± 0.0002281	0.121	0.3076	0.00035903
Means	2.64688 ± 0.49361		-0.0005155 ± 0.0004899		0.2662	0.0004432
RSD	0.186		0.950			

6.2.4 NO-B4 sensor

6.2.4.1 Temperature effect

The NO-B4_P1 sensor is sensitive to temperature. The relationship between the sensor values and temperature is quadratic, although for comparison purpose, linear regression has been used hereafter. The slopes of the linear fits are highly significant and the R^2 are high. The variation between the slopes is low with RSD of 17.4 % with mean value of 0.0011135 ± 0.0001937 V/°C suggesting that the effect of temperature is repeatable. The RMSE can be used to evaluate the lack of fit of linear correction of pressure resulting from applying the linear correction ($2\frac{0.0012998}{0.0001398} = 19\,ppb$).

Table 43: Effect of Temperature on NO_B4 sensors (sensor readings in volt), experimental results of 2016-05-17. 3_52North_NOB4_P1 discarded for computing the means, mean SDs and RSDs.

Sensors	Interc.	P(Interc.)	Slope	P(Slope)	R^2	RMSE
1_NILU_NOB4_P1	0.81514 ± 0.00568	0	0.0013197 ± 0.0002201	0.001	0.8371	0.00170421
2_KNMI_NOB4_P1	0.81165 ± 0.00566	0	0.0014797 ± 0.0002146	0	0.8717	0.00152406
3_52North_NOB4_P1	0.82948 ± 0.00128	0	0.0006056 ± 0.0000796	0.017	0.9666	0.00038635
4_INERIS_NOB4_P1	0.81487 ± 0.00697	0	0.0012630 ± 0.0002754	0.003	0.7503	0.00168063
5_VMM_NOB4_P1	0.82005 ± 0.00332	0	0.0010246 ± 0.0001569	0	0.859	0.00112065
6_VITO_NOB4_P1	0.82213 ± 0.00321	0	0.0009698 ± 0.0001538	0	0.8503	0.00107447
7_AEA_NOB4_P1	0.82298 ± 0.00314	0	0.0009186 ± 0.0001646	0.001	0.8164	0.00106318
8_GeonoVum_NOB4_P1	0.82135 ± 0.00373	0	0.0010403 ± 0.0001954	0.001	0.8019	0.00126602
9_AIRPARIF_NOB4_P1	0.82077 ± 0.00344	0	0.0010513 ± 0.0001690	0	0.8469	0.00113581
10_RIVM_NOB4_P1	0.82118 ± 0.00301	0	0.0009544 ± 0.0001362	0	0.8752	0.00112888
Means	0.81890 ± 0.00397		0.0011135 ± 0.0001937		0.8343	0.0012998
RSD	0.005		0.174			

6.2.4.2 Pressure effect

The NOB4_P1 sensor seems to be slightly sensitive to pressure. The slopes of the linear fits are not significant for all sensors and the R^2 are generally low. The scattering of the slopes is low with RSD of 16.9 % with mean value of -0.0038367 ± 0.0006488 V/hPa.

Table 44: Effect of pressure on NO-B4 sensors (sensor readings in volt), experimental results of 2016-05-17. 3_52North_NOB4_P1 discarded for computing the means, mean SDs and RSDs

Sensors	Interc.	P(Interc.)	Slope	P(Slope)	R^2	RMSE
1_NILU_NOB4_P1	5.62662 ± 2.28146	0.043	-0.0047705 ± 0.0022791	0.075	0.385	0.00361797
2_KNMI_NOB4_P1	5.93989 ± 3.02231	0.090	-0.0050830 ± 0.0030200	0.136	0.2881	0.00385897
3_52North_NOB4_P1	3.12478 ± 0.64690	0.017	-0.0022791 ± 0.0006449	0.039	0.8063	0.00079988
4_INERIS_NOB4_P1	4.12147 ± 2.94331	0.204	-0.0032694 ± 0.0029409	0.303	0.1501	0.0034109
5_VMM_NOB4_P1	4.59957 ± 1.27797	0.009	-0.0037510 ± 0.0012752	0.022	0.5528	0.0020636
6_VITO_NOB4_P1	4.30417 ± 1.18142	0.008	-0.0034559 ± 0.0011791	0.022	0.551	0.00184812
7_AEA_NOB4_P1	4.08444 ± 1.03091	0.005	-0.0032370 ± 0.0010284	0.016	0.586	0.0015813
8_GeonoVum_NOB4_P1	4.42782 ± 1.20903	0.008	-0.0035792 ± 0.0012062	0.021	0.5571	0.00182351
9_AIRPARIF_NOB4_P1	4.53546 ± 1.25894	0.009	-0.0036862 ± 0.0012561	0.022	0.5516	0.00193684
10_RIVM_NOB4_P1	4.54672 ± 1.24917	0.008	-0.0036984 ± 0.0012466	0.021	0.557	0.00210959
Means	4.68735 ± 0.65188		-0.0038367 ± 0.0006488		0.4643	0.0024723
RSD	0.139		0.169			

7 Discussion and conclusions

The results of all the tests are summarized in the Table 45 with the following conclusions:

7.1 Alphasense NO_2 sensor NO2-B43F

The sensor was found highly linear when calibrating against NO_2 with a sensitivity of -0.0000877 V/ppb ± 2.9 %, the quoted value being the Relative Standard Deviation (RSD). User may consider the use of this sensor without pre-calibration if they accept the scattering of the sensitivity, the 95 % confidence interval of sensor sensitivity being ± 6.8 %. The corresponding sensitivity is -0.0000877/350 kΩ*1000 = -251 nA/ppm compared to the manufacturer claim of a range between -175 and -450 nA/ppm.

The O_3 filter placed on top of the sensor appeared to be effective. A slight O_3 dependence remained, with an O_3 sensitivity of about 6.6 % of the NO_2 sensitivity (with 20 % of scattering). One outlier sensor showed an O_3 sensitivity of 18 %. When sensing a mixture of NO_2 and O_3, the O_3 cross-sensitivity remained the same as for O_3 alone. Moreover, the efficiency of the O_3 filtering over time should be checked to test any drifting of the efficiency of O_3 filtering, but was not done here.

The NO2-B43F sensors showed a slight NO cross-sensitivity: for 1 ppb of NO the sensor would sense as for 0.027 ppb of NO_2. The low and fluctuating CO cross-sensitivity (1 ppm CO corresponds to about 0.05 ppb of NO_2) is not significant in the range of ambient air concentration up to 20 ppm CO.

The NO2-B43F sensor was linearly dependent to relative humidity with coefficients of determination (R^2) of about 0.87 and a probability of 0.001 that the slope of their calibration line was zero. The sensor also demonstrate a clear hysteresis effect of humidity while it seemed to be independent to changes of ambient pressure similar to what is observed outdoors.

The temperature tests gave scattered values for the NO2-B43F sensors. Conversely to the other sensors, two NO2-B43F gave decreasing readings associated with increases of

temperature. The reason for this discrepancy was not identified. The conclusions of the temperature experiments are thus not robust. The relationship between the sensor readings and temperature seemed to be quadratic, while for simplification and comparisons purposes we used linear regression. Using the linear line, the effect of a 15 ºC change corresponded to about -17.9 % of the sensor signal for 100 ppb of NO_2. The NO2-B43F sensor generally seemed not to be affected by changes of pressure during this experiment.

7.2 Membrapor CO sensor CO/MF-200

The sensor was found highly linear when calibrating against CO and with high sensitivity, 0.0812 V/ppm ± 7.7%, the quoted value being the RSD. User may consider the use of this sensor without pre-calibration if they accept the scattering of the sensitivity, the 95 % confidence interval of sensor sensitivity being ± 17.8 %. The corresponding sensitivity is 0.0812/350 kΩ = 232 nA/ppm compared to the manufacturer claim of 500 ± 100 nA/ppm.

In a mail exchange about this difference, the Membrapor representative confirmed that according to their quality control tests, the sensitivity of the CO/MF-200 sensor is found to be 455 nA/ppm in the range 0 to 150 ppm. Repeated tests of our reference analyser (TECO 48C) could not identify an important problem with the reference value. The maximum linearity deviation of the analyser was found to be 1 % between 1 and 10 ppm. Temperature, the other important parameter affecting the performance of the analyser gives an increase of 50 ppb per degree of the CO value. These two parameters cannot explain the 100 % difference found in the sensitivity. Also the homogeneity of the gas sample is likely not causing problems because of the 2.5 to 3 m/s wind velocity in the chamber preventing any stratification/depletion of the gas sample. Another explanation may be the absorption or reaction of CO molecules on the wall of the sensor or the AirsensEUR electronic boards. We have no robust explanation for the important difference in sensitivity. For the time being we should take into account a possible change of sensitivity between high and low CO concentration levels.

NO gaseous interferents affected the CO/MF-200 sensor. The interference is relevant only at high NO and low CO values. The NO sensor sensitivity was -0.0000287 V/ppb ± 16.1 %. Because of the low NO sensitivity, there is no necessity to test it for each sensor.

The effect of NO_2 was found to be extremely low while O_3 was not found to be significant. Some scattering was observed with changes of O_3. However, we think the experiment may be misleading as CO was not completely stable (change of 20 ppb during concentration steps), temperature changed by 0.2ºC and pressure changed by 5 hPa. The scattering, in particular the one of the sensor base line, was likely a combination of these 3 parameters. We assume that changes of pressure was the main driver of the sensor response changes.

The CO/MF-200 sensor did not show a linear dependence on relative humidity while the changes in sensor values during the humidity test were largely associated with pressure changes. The sensitivity to the pressure effect was -0.0017694 V/hPa ± 13 %, leading to pressure changes of 10 hPa giving sensor response corresponding to 218 ppb of CO. This effect is important and should be further investigated.

Temperature affected the CO/MF-200 sensor values. We could not clearly establish if the relationship is linear or quadratic. During the temperature test, pressure was not controlled and it changed in addition to the temperature changes. The sensor readings appeared to be more associated with pressure than with temperature. The sensitivity of the sensor to temperature was 0.0032069 V/ºC ± 8.2 % and that to pressure was -0.0155144 V/hPa ± 7.2 %. However, the sensitivity to pressure was about 10 times higher in this temperature experiment than the one estimated during the previous experiment on humidity, which appears unrealistic. Consequently, this observation suggests that for the experiment on temperature/pressure changes, the main effect came from temperature and not from pressure. Anyhow this experiment shows that a major shortcoming of the sensor values was either temperature or pressure interference. More tests are needed to identify the origin of the shortcoming.

7.3 Membrapor O_3 sensor O3/M-5

The O3/M-5 sensor was found to have a linear dependence on O_3. The slopes of the linear fits were highly significant with a RSD of 4.8 % (-0.0003670 ± 0.0000176 V/ppb). Users may consider the use of this sensor without pre-calibration if they accept the scattering of the sensitivity, the 95 % confidence interval of sensor sensitivity being ± 11.3 %. The corresponding sensitivity is -0.0003670/350 kΩ * 1000 = -1048 nA/ppm compared to the manufacturer claim of -1000 ± .350 nA/ppm.

This sensor was affected by an important NO_2 cross-sensitivity, the sensor would sense 0.79 ppb of O_3 for 1 ppb of NO_2. This interference remained constant when sensing mixtures of NO_2 (between 0 and 150 ppb) and O_3 (between 0 and 90 ppb).

The CO cross-sensitivity was not clearly demonstrated and could be neglected for CO up to 20 ppm. The NO cross-sensitivity was low, giving a response of 0.015 ppb of O_3 for 1 ppb of NO. Normally, simultaneous high NO and O_3 levels are rarely observed in ambient air. The major impact of the NO cross-sensitivity would be if O_3 is measured near traffic NO emission, and even in this case O_3 would be 'consumed' by NO.

The O3/M-5 sensor did not show a linear dependence on relative humidity. Conversely, the changes of sensor values during the humidity test were fairly associated with pressure changes. The sensitivity to the pressure effect was -0.0001527 ± 21.8 % giving for a 10 hPa variation of pressure, a change in sensor signal equal to 6.9 % of the signal for 60 ppb O_3. After correcting the sensor readings for pressure with the estimated linear equation, the residual lack of fit was on average 0.4 ppb. Additionally, an important transient peak of the sensor signal appeared when relative humidity changed quickly.

The results of the temperature tests on the O3/M-5 sensor were not fully conclusive because of scattered results and because one sensor, conversely to the others, showed decreased values with increasing temperature. Nevertheless, the O3/M-5 sensor appeared to be affected by temperature. The relationship (sensor readings versus temperature) seems to be quadratic, with in general, the sensor readings increasing with increasing temperature. Nevertheless, we use linear relationship for comparison purposes. The slopes of linear lines are generally not significant and the R^2 are generally low. The scattering of the slopes was high with RSD of 86% and a mean value of 0.0001489 V/ºC corresponding to about -41 % of the sensor sensitivity to O_3 (-0.0003670 V/ppb). During the temperature test, the pressure in the exposure chamber was not controlled and it changed in addition to the temperature changes without the possibility to distinguish between the two effects.

The dependence of the O3/M-5 sensors on pressure was not clearly demonstrated either. In fact, this observed relationship did not match the linear relationship found before in the experiment of humidity/pressure. The slopes of linear lines were generally not significant and the R^2 were low. The scattering of the slopes gave a RSD of 95 % with mean value of -0.0005155 V/hPa corresponding to about 140 % of the sensor sensitivity to O_3 (-0.0003670 V/ppb).

7.4 Alphasense NO sensor NO-B4

The NO-B4 sensors were found highly linear when calibrating against NO. Both the intercepts and slopes of the linear fits are highly significant. The scattering of these two parameters is low with RSD of 0.1 % for the intercepts and 2.6 % for the slopes (0.000140 ± 2.6 %) suggesting that the sensor could be used without previous calibration. The corresponding sensitivity in nA/ppm is -0.000140/350 kΩ*1000 = 400 nA/ppm compared to the manufacturer claim of a range between 500 and 850 nA/ppm.

There was likely little or no NO_2 cross-sensitivity for the NO Sensors. During the NO_2 experiment, the NO sensors showed some minor sensor reading changes caused by minimal NO changes in the exposure chamber.

The O_3 cross-sensitivity was on average -0.0000098 V/ppb ± 6.7 %, giving for 1 ppb of O_3 a signal equal to 7.0 % of 1 ppb of NO. Two groups of sensor responses were characterised

by different behaviours at low concentrations. This has been attributed to a local alteration of the air composition around the sensors.

The CO cross-sensitivity was low, giving for 1 ppm of CO a sensor response equal to 0.07 ppb of NO. Ambient situations with high CO levels and without NO are unrealistic.

The NO-B4 sensor was linearly associated with relative humidity with coefficients of determination (R^2) of 0.84 and a probability of 0.001 that the slope of their calibration line was zero. The sensor also presented a clear hysteresis effect for humidity while it seemed to be independent to changes in ambient pressure similar to what is observed outdoors.

Finally, the NO-B4 showed a high dependence on temperature. However, the tests produced scattered response values. Three NO-B4 sensors had surprising readings at low temperatures although the relationship between the sensor readings and temperature was shown to be quadratic. However, for simplification and comparison purposes we used a linear regression. Using the linear fit, the effect of a 15 ºC change corresponds to a sensor response to 119 ppb of NO. The NO-B4 sensor seemed not to be dependent on changes of pressure during this experiment.

7.5 Summary of test results

Table 45: Summary of test results of sensors giving the sensitivity of sensors on several parameters based on linear regression analysis

Experiment	2		1		2	3		4	
Sensors	**CO, V/ppm**	**NO_2, V/ppb**	**NO, V/ppb**	**O_3, V/ppb**	**NO_2 (0-150) and O_3 (0-90 ppb) together**	**Humidity, V/%**	**Pressure, V/hPa, evaluated with the humidity test**	**Temperature, V/°C**	**Pressure, V/hPa, evaluated with the temperature test**
NO2-B43F	-0.0000041 ± 57.2 %, R^2=0.624 2 ppm CO ⇔ <0.1% of 100 ppb NO2 RMSE = 0.0000057 V Lack of fit = 0.6 ppb (2 RMSE/S)	-0.0000877 ± 2.9 %, R^2=0. 9992 RMSE = 0. 0000503 V	-0.0000024 ± 8.0 %, R^2 = 0.6664 100 ppb NO ⇔ 2.7 % of 100 ppb NO_2 RMSE = 0.0000416 V Lack of fit = 1 ppb (2 RMSE/S)	-0.0000058 ± 22.5 % R^2 = 0.9012, 60 ppb O_3 ⇔ 4.0 % of 100 ppb NO_2 RMSE = 0.0000382 V Lack of fit = 0.9 ppb (2 RMSE/S)	Same O_3 cross-sensitivity as O_3 alone	-0.0000473 ± 9.4 % R^2 = 0.8704 40 % RH ⇔ 21.6 % of 100 ppb NO_2 RMSE = 0.0000867V Lack of fit = 2.0 ppb (2 RMSE/S) due to hysteresis	No effect observed	0.0000628 ± 42.5 % R^2 = 0.6876 15 ºC ⇔ -17.9 % of 100 ppb NO_2 RMSE = 0.0000267 V Lack of fit = 0.6 ppb (2 RMSE/S)	Little to no pressure effect -0.0002344 ± 48.4 % R^2 = 0. 0.3584 10 hPa ⇔ 44.5 % of 100 ppb NO_2 RMSE = 0.0001791 V Lack of fit = 4.1 ppb (2 RMSE/S)
CO/MF-200	0.08117327 ± 7.7 % R^2=0.997 RMSE = 0.0023636 V	Likely no cross-sensitivity 0.0000339 ± 37.9 % R^2=0.158 100 ppb NO2 ⇔ 2.5 % of 2 ppm CO RMSE = 0.0014496 V Lack of fit = 0.037 ppm (2 RMSE/S)	-0.0000287 ± 16.1 % R^2 = 0.8993 100 ppb NO ⇔ -1.8 % of 2 ppm CO RMSE = 0.0000416 V Lack of fit = 0.000 ppm (2 RMSE/S)	Likely no cross-sensitivity 0.0000424 ± 36.9 % R^2 = 0.1013 60 ppb O_3 ⇔ 1.6 % of 2 ppm CO RMSE = 0.0030246 V Lack of fit = 0.075 ppm (2 RMSE/S)	As for the NO_2 and O_3 test alone, no cross-sensitivities	No relative humidity effect on hourly values and no transient peak with rapid humidity changes. Sensor signal changes is attributed to pressure effect	-0.0017694 ± 13.0 % R^2 = 0.7439 10 hPa ⇔ -10.9 % of 2 ppm CO RMSE = 0.0013717V Lack of fit = 0.034 ppm (2 RMSE)	0.0032069 ± 8.2 % R^2 = 0. 7986 15 ºC ⇔ 29.6 % of 2 ppm CO RMSE = 0.004366 V Lack of fit = 0.108 ppm (2 RMSE/S)	-0.015514 ± 7.2 % R^2 = 0. 9338 10 hPa ⇔ -95.6 % of 2 ppm CO RMSE = 0. 0025984 V Lack of fit = 0.064 ppm (2 RMSE/S). Likely a temperature effect.
O3/M-5	No or low cross-sensitivity 0.0000058 ± 485 % R^2 = 0.609 2 ppm CO ⇔ <0.1 % of 60 ppb O_3 RMSE = 0.00000270 V Lack of fit = 0.0 ppb (2 RMSE/S)	-0.0002881 ± 3.6 % R^2=0.998 100 ppb NO_2 ⇔ 131 % of 60 ppb O_3 RMSE = 0.0002154 V Lack of fit = 1.2 ppb (2 RMSE/S)	-0.0000057 ± 25.2 %, R^2 = 0. 8224, 100 ppb NO ⇔ 2.6 % of 60 ppb O_3 RMSE = 0.0000615 V	-0.0003670 ± 4.8 %, R^2 = 0.9995 RMSE = 0.000127 V	The effect of NO_2 and O_3 together is the sum of the single sensitivities of O_3 and NO_2	No relative humidity effect on hourly values while transient peaks were observed. Sensor signal changes is attributed to pressure	-0.0001527 ± 21.8 % R^2 = 0.9120 10 hPa ⇔ 6.9 % of 60 ppb O_3 RMSE = 0.0000599 V Lack of fit = -0.3 ppb (2 RMSE)	0.0001489 ± 86.1 % R^2 = 0.4874 15 ºC ⇔ 10.1 % 60 ppb O_3 RMSE = 0.0003475 V Lack of fit = 1.9 ppb (2 RMSE/S)	-0.0005155 ± 95.0% R^2 = 0. 2662 10 hPa ⇔ 23.4 % of 60 ppb O_3 RMSE = 0.0004432V Lack of fit = 2.4 ppb (2 RMSE/S)
NO-B4	-0.0000101 ± 77.5 %, R^2=0.735 2 ppm CO ⇔ 0.1 % of 100 ppb NO RMSE = 0. 0000096 V Lack of fit = 0.1 ppb (2 RMSE/S)	Likely no NO_2 cross-sensitivity. Sensor changes due to NO between 0 and 3 ppb. 0.0002121 ± 8.8% R^2 = 0.9862 RMSE = 0.0000320 V Lack of fit = 0.5 ppb (2 RMSE/S)	0.0001398 ± 2.6 %, R^2 = 0.9981 RMSE = 0.0001337 V	2 groups of sensors -0.0000098 ± 6.7 %, R^2 = 0.9927, 60 ppb O3 ⇔ 4.1 % of 100 ppb NO RMSE = 0.000021 V Lack of fit = 3 ppb (2 RMSE/S)	O_3 cross-sensitivity -0.0000072 ± 14.6 % R^2 = 0.9799 60 ppb O_3 ⇔ 3 % of 100 ppb NO RMSE = 0.0000479 V Lack of fit = 0.7 ppb (2 RMSE/S)	-0.0000925 ± 5.5 % R^2 = 0.8386 40 % RH ⇔ -26.4 % of 100 ppb NO RMSE = 0.0001916V Lack of fit = 2.7 ppb (2 RMSE/S) due to hysteresis!	No effect observed	0.0011135 ± 17.4 % R^2 = 0.8343 15 ºC ⇔ 119 % of 100 ppb NO RMSE = 0.0012998 V Lack of fit = 18.6 ppb (2 RMSE/S) – quadratic!	Little to no pressure effect -0.0038367 ± 16.9 % R^2 = 0.4643 10 hPa ⇔ -274 % of 100 ppb NO RMSE = 0.0024723 V Lack of fit = 35.4 ppb (2 RMSE/S)

Annex 1: Setup of the Exposure chamber for sensors at the Joint Research Centre

The gas sensors were evaluated in an exposure chamber. This chamber allows the control of test gases and other gaseous interfering compounds, temperature, relative humidity and wind velocity. The exposure chamber is an "O"-shaped ring-tube system, covered with dark insulation material. The exposure chamber can accommodate the micro-sensors directly inside the "O"-shaped ring-tube system.

A special Labview software was developed for controlling the exposure chamber and for easy programming of a set of experiments under different controlled conditions: temperature, humidity, wind velocity, test gases and gaseous interfering compounds. It allowed setting criteria for the stability of each parameter and for the duration of each step. The software was also able to manage data acquisition and all results (exposure conditions and sensors responses) were collected in Access databases for later data treatment. The data acquisition system had a frequency of acquisition of 100 Hz and averages over one minute were stored.

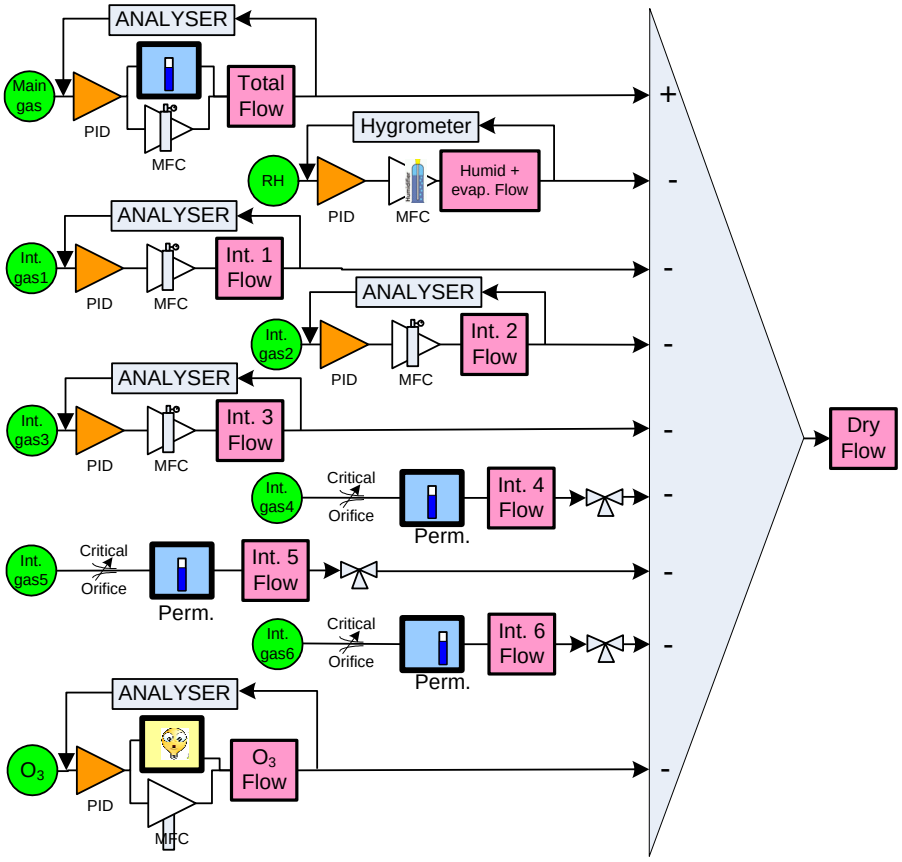

Figure 55: Feedback loops of the exposure chamber control system

During experiments, an automatic system (feed-back loop) used the reference measurements of gaseous compounds, temperature, humidity and wind speed to auto-correct the gas mixture generation system, temperature controlling cryostat and wind velocity to reach the target conditions (see the logical graph in Figure 55).

Gas mixture generation system

For generating test gases and gaseous interferences MicroCal 5000 Umwelttechnik MCZ Gmbh (G) O_3 generators were used, high concentration cylinders were dynamically diluted and in house designed permeation systems were used.

For the response time experiment, the controlled conditions in the exposure chamber shall be established after a few minutes. Seen the internal volume of the exposure chamber (about 120 L), it was decided to use the automatic bench that ERLAP uses for the European inter-comparison exercises of the National Reference Laboratories of Air Pollution [2] that can generated mixtures with a flow of about 100 L/min.

Reference methods of measurements

- O_3 was monitored using a Thermo Environment TEI 49C UV-photometer. The analyser was calibrated before the experiments using an O_3 primary standard. It consists of a TEI Model 49 C Primary Standard, Thermo Environmental Instruments cross-checked against a long-path UV photometer (National Institute of Standards and Technology, reference photometer n° 42, USA).

- NO/NOx/NO_2: Thermo Environment 42 C chemiluminescence analyser, calibrated against a permeation system for NO_2 and a NO working standard consisting of a gas cylinder at low concentration (down to 50 nmol/mol) certified against a Primary Reference Material of NMI VSL - NL

- SO_2: Environment SA AF 21 M, calibrated with a working standard consisting of gas cylinder at low concentration (down to 50 nmol/mol) certified against a Primary Reference Material of NMI VSL - NL. The calibration of the analyser was confirmed by cross-checking with a permeation method.

- CO: Thermo Environment 48 C NDIR analyser, calibrated with a CO working standard consisting of a gas cylinder at low concentration (down to 1 µmol/mol) certified against a Primary Reference Material of NMI VSL - NL.

The sampling line of each gas analyser was equipped with a Nafion dryer to avoid interference from water vapour on O_3, NOx, SO_2 and CO analyser.

In addition, some other parameters were recorded and/or controlled using:

- Three refrigerating/heating circulators were used to regulate the temperature of the exposure chamber. One cryostat (Julabo (G) Model SP-FP50) was used to control the temperature inside the exposure chamber, another one (Julabo (G) Model HE-FP50) for the surface of the O-shaped glass tube and the last one (Julabo (G) Model HE-FP50) was devoted to the control of temperature of the humid and dry air flows. These cryostats used a laboratory calibrated pt-100 probe placed inside the exposure chamber.

- Two KZC 2/5 certified sensors (TERSID-It) were used to control temperature and relative humidity. One sensor was used to monitor in real-time using our Labview software, the second one was used to register these parameter.

- One Testo 445 sensor (Testoterm – G) with a temperature and relative humidity probe was used as a control interface to check values inside the chamber.

2 M. Barbiere and F. Lagler, Evaluation of the Laboratory Comparison Exercise for SO2, CO, O3, NO and NO2, 11th-14th June 2012, EUR 25536, ISBN 978-92-79-26844-1, ISSN 1831-9424, doi:10.2788/52649 , ftp://ftp_erlap_ro:3rlapsyst3m@s-jrciprvm-ftp-ext.jrc.it/ERLAPDownload.htm

- One Testo 452 sensor (Testoterm – G) with a temperature and relative humidity probe was used as a reference sensor and to monitor temperature and relative humidity.
- One wind velocity probe based on hot-wire technology was used to monitor wind velocity during tests.
- One pressure gauge DPI 261 from Druck (G) was used to monitor pressure inside the exposure chamber
- Fan ventilator placed inside the chamber, Papst (G) model, DV6224, 540 m^3/hr.

An in-house developed permeation system able to accommodate 8 permeation cells with carrier flows about 200 ml/min with critical orifices (Calibrage SA, F). Each permeation cell was dipped in a water bath (Haake-GE W26 Thermostatic Circulating Water Bath with Haake E8 Controller). The temperature of each cell was set at 40 °C. The permeation tubes were weighed every three weeks. The permeation cells were filled with NO_2, SO_2 permeation tubes manufactured by KinTec (G) and Calibrage (F).

Annex 2: Table of figures

Europe Direct is a service to help you find answers to your questions about the European Union.

Freephone number (*)**:**

00 800 6 7 8 9 10 11

(*) The information given is free, as are most calls (though some operators, phone boxes or hotels may charge you).

More information on the European Union is available on the internet (http://europa.eu).

HOW TO OBTAIN EU PUBLICATIONS

Free publications:

- one copy:
  via EU Bookshop (http://bookshop.europa.eu);
- more than one copy or posters/maps:
  from the European Union's representations (http://ec.europa.eu/represent_en.htm);
  from the delegations in non-EU countries (http://eeas.europa.eu/delegations/index_en.htm);
  by contacting the Europe Direct service (http://europa.eu/europedirect/index_en.htm) or
  calling 00 800 6 7 8 9 10 11 (freephone number from anywhere in the EU) (*).

  (*) The information given is free, as are most calls (though some operators, phone boxes or hotels may charge you).

Priced publications:

- via EU Bookshop (http://bookshop.europa.eu).

KJ-NA-28601-EN-N

JRC Mission

As the science and knowledge service of the European Commission, the Joint Research Centre's mission is to support EU policies with independent evidence throughout the whole policy cycle.

EU Science Hub
ec.europa.eu/jrc

@EU_ScienceHub
EU Science Hub - Joint Research Centre
Joint Research Centre
EU Science Hub

Publications Office

doi:10.2760/548327
ISBN 978-92-79-68830-0